JPL PUBLICATION 84-3

The SIR-B Science Investigations Plan

SIR-B Science Team

July 1, 1984

NASA
National Aeronautics and
Space Administration

Jet Propulsion Laboratory
California Institute of Technology
Pasadena, California

The SIR-B Science Investigations Plan

Overleaf: SIR-B in the Shuttle's payload bay

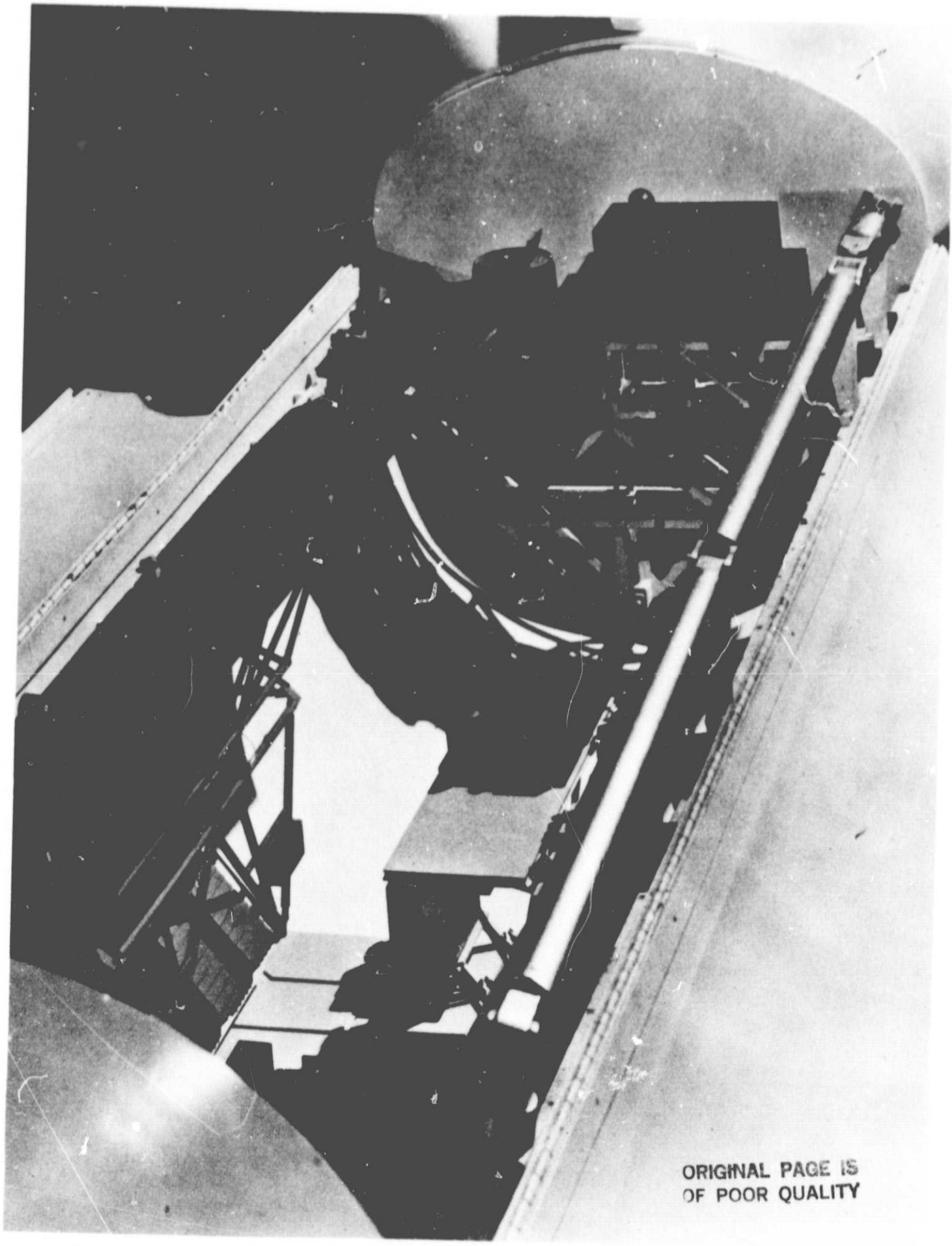

JPL PUBLICATION 84-3

The SIR-B Science Investigations Plan

SIR-B Science Team

July 1, 1984

NASA
National Aeronautics and
Space Administration

Jet Propulsion Laboratory
California Institute of Technology
Pasadena, California

This publication was prepared by the Jet Propulsion Laboratory, California Institute of Technology, under a contract with the National Aeronautics and Space Administration.

Preface

The Shuttle Imaging Radar-B (SIR-B) is the second major step in an evolutionary NASA radar remote-sensing research program leading to the development of the research capability for a long-term orbiting radar sensor such as the Earth Observation System (EOS)/Space Station. The SIR-B science team consists of 43 scientists and engineers from leading research institutions around the world. They will conduct scientific investigations in geology, renewable resources, oceanography, and calibration techniques. This document includes brief descriptions of the planned investigations as well as a description of the SIR-B sensor and data processing system.

Acknowledgment

All the team members contributed to this document. In addition, a number of people from the SIR-B team at JPL provided significant contributions: Steve Pravdo, JoBea Cimino, John Curlander, and Annie Holmes. Special acknowledgment goes to Steve Pravdo who, in addition to his contribution, was responsible for putting the whole document together.

Charles Elachi, Ph.D.
SIR-B Principal Investigator

Abstract

Shuttle Imaging Radar (SIR) B is the second synthetic-aperture radar (SAR) to be flown on the National Aeronautics and Space Administration's Space Transportation System (Shuttle). It is the first spaceborne SAR to feature an antenna that allows acquisition of multiincidence-angle imagery. An international team of scientists will use SIR-B to conduct investigations in a wide range of disciplines. This work describes SIR-B: the radar, the mission, and the investigations.

Acronyms

AVHRR	Advanced Very High Resolution Radiometer
BER	bit error rate
bits/s (in.)	bits per second (inch)
bps	bits per sample
CCT	computer-compatible tape
CMD	command
CZCS	Coastal Zone Color Scanner (Nimbus)
DDHS	digital data handling subsystem
DFVLR	Deutsche Forschungs– und Versuchsanstalt für Luft– und Raumfahrt
DTM	digital topographic map
EISCAT	European Incoherent Scatterer
ESA	European Space Agency
FFT	fast Fourier transform
GPC	general-purpose computer
GSFC	Goddard Space Flight Center
HCMM	Heat-Capacity Mapping Mission
HDDR	high-density digital recorder
HDDT	high-density digital tape
HF	high frequency
IFDN	image-film duplicate negative
IFMP	image-film master positive
IFON	image-film original negative
IPL	image processing laboratory
IR	infrared
JASIN	Joint Air-Sea Interaction
JSC	Johnson Space Center
MRS	mobile radar scatterometer
MSS	Multispectral Scanner (Landsat)
NASA	National Aeronautics and Space Administration
NOAA	National Oceanographic and Atmospheric Administration
OPS	operations
OR	optical recorder
OSTA	Office of Space and Terrestrial Applications
RBV	Return Beam Vidicon (Landsat)
RCS	radar cross section
RF	radio frequency
SAR	synthetic-aperture radar
SFMP	signal-film master positive
SFON	signal-film original negative
SIR	Shuttle imaging radar
SLAR	side-looking airborne radar
SNR	signal-to-noise ratio
STS	Space Transportation System
TDRS	Tracking and Data Relay Satellite
TLM	telemetry
TM	Thematic Mapper (Landsat)
UV	ultraviolet

Contents

References

Tables

Figures

Section I
Introduction

With the launch of SIR-B, the National Aeronautics and Space Administration (NASA) will take the next step in an evolutionary radar program that leads toward a final multifrequency, multiincidence angle, multipolarization imaging radar system. The program began in 1978 with the launch of Seasat: a free-flying, Earth-orbiting, synthetic-aperture radar. This instrument provided the first synoptic radar imagery of the Earth's surface. Not only was the experiment a success technologically, but the imagery returned provided a new means of studying and observing the Earth's surface.

The radar program continued in 1981 with the launch of the second Space Shuttle. Aboard that Shuttle was the first Office of Space and Terrestrial Applications (OSTA) payload, which contained SIR-A, the first Shuttle-based imaging radar, among other Earth-observing instruments. The main objective of the SIR-A experiment was to acquire radar data over a variety of geologic regions to further our understanding of the radar signatures of geologic features. A complimentary objective was to assess the capability of the Shuttle as a scientific platform for Earth observations.

The SIR-A sensor operated nominally and the full data-acquisition capacity of the optical recorder was used. Ten-million square kilometers were imaged over all continents except Antarctica. One of the most exciting results of this experiment was the imaging of buried dry-river channels in hyperarid regions of southern Egypt. These channels are buried under 1 to 3 m of sand cover and are not visible on Landsat images or from the ground.

Seasat and SIR-A were fixed-parameter sensors acquiring images at constant look angles (measured from nadir) of 20 and 47 deg, respectively. A comparison of imagery acquired over the same area by each of these sensors demonstrates that image intensity is a function of the incidence angle of the radar beam at the surface. In general, the response of the radar is controlled by topography at lower incidence angles and surface roughness (or average size of rocks and vegetation) at larger incidence angles. If it were possible to acquire imagery at a variety of incidence angles, a new means of classifying surface features could be developed.

This was the inspiration for SIR-B: a multilook-angle radar system. The SIR-B instrument is an upgraded version of SIR-A that has the additional capability of tilting the antenna mechanically to acquire data at incidence angles that vary from 15 to 60 deg. Like Seasat and SIR-A, SIR-B will be an L-band (23-cm) HH polarized radar. The variable-incidence-angle capability will allow several new experiments. A specific area may be imaged with a variety of incidence angles on successive days. These images can then be registered and used to produce curves of backscatter as a function of incidence angle for various terrain types. These curves can be used ultimately to characterize the terrain. Stereoimaging may also be done in the multiple-incidence-angle mode. In addition, large areas may be imaged and mosaicked together with only slight variations in incidence angle with each swath.

The SIR-B experiment will be launched in the fall of 1984 on the Space Shuttle into a nominally circular orbit at an inclination of 57 deg and an average altitude of 352 km for the first day, 274 km for the next day, and 225 km for the balance of the mission; the duration of the entire mission is presently set at 8.3 days. At the 225-km altitude, the ground

track repeats with a 1-day cycle, but with a westward drift. This will allow SIR-B to image a given site at several different incidence angles, one angle each day.

The investigations using these unique capabilities will be conducted by a science team selected by NASA on the basis of science proposals. Table 1-1 lists the team members and their investigations.

The SIR-B investigations include areas of geology, hydrology, vegetation, oceanography, and cartography, as well as studies of the characteristics of the radar system itself. These investigations were selected primarily on their scientific merit and ability to take advantage of the unique characteristics of the SIR-B radar. Of those chosen, 13 are from foreign countries including Japan, Australia, Sweden, New Zealand, the Netherlands, the Federal Republic of Germany, the United Kingdom, and Canada. In addition, many of the experiments by United States team members will be carried out in foreign countries with the cooperation of collaborators from those countries, which include Egypt, Indonesia, Turkey, Argentina, Bangladesh, Botswana, India, Peru, Brazil, and Saudi Arabia. Also, two investigations will be carried out in foreign oceans—one along the Agulhas Current off the southeast coast of Africa and the other in the South Atlantic Ocean off the coast of Antarctica.

In the area of geology, a number of experiments will be done to assess the capability of multiple-incidence-angle SAR data for lithologic mapping (Farr and Parr) and the delineation of textural and structural features (Kaupp). Areas of primary interest for these studies include Hawaii, the Western United States, and the Isle of Skye in Europe. SIR-B data will also be used to delineate subtle boundaries between geologic regions in Argentina, where the boundary between active and inactive volcanism will be mapped (Bloom), and in the Canadian Shield where the boundary between the Churchill, Superior, and Grenville Provinces will be clarified (Lowman). Radar imagery over a very large, nonvegetated, flat dry playa lake—Lake Eyre in Central Australia—will be used to assess the degree of detectability and identification of salts and clays (Honey). The extent of Wisconsinan glaciation in Illinois, Indiana, and Ohio (Johnson) and Pleistocene glaciation in Argentina (Bloom) will be investigated, and impact craters in the Canadian Shield will be mapped (Head). The radar signatures of exposed craters will be used to further characterize poorly exposed craters. More rugged terrain will be imaged by SIR-B in Turkey, where the imagery will be used to map the extensions of the North and East Anatolian faults (Toksoz). In New Zealand, the Alpine Fault along the boundary between the Pacific and the Indian-Australian Plates will be mapped with better accuracy than is possible from the ground because of extremely dense vegetation (Collins). In Africa, a large part of the Great Rift valley will be mapped to investigate some of its subtle structural features (Elachi).

The exciting discovery with SIR-A of the buried dry-river channels in Egypt has focused interest upon the characterization of this radar-penetration phenomenon. The SIR-B experiment will place great emphasis on the extension of such coverage to more of the western deserts of Egypt and Sudan, as well as other hyperarid areas including southwest Africa, India, the western coasts of Peru, China, and central Australia (Schaber). The penetration studies will extend east of the Nile (Dixon) to the Precambrian Shield, where frequent outcrops of basement rocks will provide landmarks for coregistration of the SIR-B data with Landsat data. Receivers will be buried at different depths to measure the actual penetration of the radar energy. Penetration will be studied in the more semiarid regions of the United States along the Nevada/California border (Taranik), in California's Mojave desert (Elachi), and in central Australia at Fowlers Gap, Pooncarie, and the Amadeus Basin (Richards). The relative effects of vegetation cover, surface-cover characteristics, and soil moisture will be assessed. Penetration is also expected in a limestone plain called the "Great Alvar" on the island of Öland in the Baltic Sea (Ulriksen). Potential penetration sites will be measured with an impulse radar system to verify the penetration. In addition, penetration studies will be extended to Saudi Arabia where the SIR-B data will be used as surface indicators for groundwater prospecting in the Arabian Shield (Berlin).

SIR-B investigations in vegetation will include studies of both forests and agriculture. Equatorial rain forests in Sumatra, Kalimantan, and Colombia will be imaged (Ford) in an attempt at geologic mapping of these cloud-shrouded, inaccessible areas. The multiple-incidence-angle data over Sumatra and Kalimantan, along with multiple-incidence data over Bangladesh (Imhoff), will be used to quantify the signatures of tropical rain forests as a function of imaging geometry and assess penetration of the dense vegetation canopies. Results of the study over Bangladesh will be used also to assess the potential in spaceborne radar data for delineation of malaria-mosquito breeding areas. In the more tame forests of the United States, two team members will assess the radar signatures of forested areas as a function of incidence angle. In the Klamath National Forest of northern California, a coniferous forest canopy will be studied (Simonett), and several well-defined, operationally managed deciduous forest stands outside of Jacksonville, Florida, will be assessed (Hoffer) in an attempt at identifying and characterizing forest-cover types and condition classes. Clear cutting in the Amazon forest is difficult to monitor on the ground, but easily traced on radar imagery. The forests around the Amazon in central Brazil are a primary target for a quantitative assessment of the potential

in multiple-incidence-angle imagery for determining the location, areal extent, and rate of deforestation (Bryan).

Several very extensive investigations of the radar signatures of agricultural areas are planned as part of the overall SIR-B experiment. Large crews at two "supersites" in Kansas (Ulaby) and near Freiburg, Germany, (Sieber) will collect extensive ground-truth data as SIR-B images the sites. The agricultural supersite in Kansas will also be imaged simultaneously by the Jet Propulsion Laboratory's (JPL's) aircraft imaging radar and scatterometer. A site in the Central Valley of California will be used to study both agriculture (Paris) and soil moisture (Wang). Several fields will be irrigated to different extents during the SIR-B mission. In addition, agricultural lands in Western Australia will be imaged by SIR-B in an attempt at delineating areas affected by secondary salinity (Honey).

Other hydrology experiments that will be carried out during the SIR-B mission deal primarily with rivers and deltas. The dynamics of floodplains in wet tropical ecosystems and river channel changes will be assessed using imagery acquired over the Amazon River in Brazil (Bryan). SIR-B data acquired over deltas will also be used to map land/water interfaces of deltas over an entire tidal cycle and to characterize the diverse range of salt- and fresh-water vegetation located on the stable portion of deltas (Head). Tidal erosion and sedimentation along the Waddensea coast of northern Netherlands cause continual change in the ocean bottom configuration and constant remodeling of the coastal regions. SIR-B data will be collected at several intervals during the tidal cycle to monitor these effects (Koopmans).

Oceanography experiments are concentrated in the waters around Europe in the North Atlantic, the North Sea, the Mediterranean, and off the coasts of Chile and South Africa. Two team members from England (Keyte and Allan) will investigate a number of ocean features including internal waves, currents, bathymetric features, and surface gravity waves; they will use ships, buoys, and satellites to monitor the sea surface during the SIR-B overflights. The characteristics of ocean-surface-wave imagery will be studied in the North Sea off the coast of Germany (Alpers). During the SIR-B overflight, directional ocean-wave spectra will be acquired simultaneously by ships and the German North Sea Research Platform.

Two investigations (Fugono and Alpers) are designed to determine the radar signatures of oil spills created during the SIR-B mission by dropping frozen olyl alcohol into the ocean from airplanes.

Two United States team members will conduct extensive oceanography experiments. One investigation will be of the Agulhas Current, which runs along the southeast tip of Africa (Beal). This region has long been notorious for extreme waves that reach heights greater than 20 m and threaten ships. Swell systems will be tracked as they propagate northward and encounter the south-flowing Agulhas Current. The ocean wave directional spectrum will be monitored and assessed as a function of incidence angle. The second United States ocean experiment will be conducted off the New York Bight in the Atlantic Ocean (Winokur). The basic hydrodynamic mechanisms responsible for internal waves will be investigated. Theories and models used to predict internal-wave signatures from ocean and radar parameters will be tested.

The Seasat SAR demonstrated the potential of spaceborne imaging radar for monitoring ocean ice. Two team members will further assess this capability with emphasis on feature identification as a function of illumination geometry. Sea ice in the transition zone between compact pack and the ice edge in the Weddell Sea off Antarctica will be studied (Carsey). Pack morphology, ice-drift speed, and ice deformation will be assessed. Iceberg detectability and reconnaissance will be assessed as a function of ocean condition off the east coast of Canada along the Grand Banks, the Scotian Shelf, and the Laborador Coast (Gray). The all-weather capability of imaging radar makes it very useful for monitoring ice in regions where offshore structures for fossil-fuel resource exploration are located.

Investigations to be conducted with SIR-B are not limited to the surface of the Earth. The utility of SIR-B data for the detection and measurement of rainfall events and the potential application of spaceborne radar imagery to improvements of existing rainfall models will be investigated (Garofalo).

Multiple-incidence-angle radar imagery can be used in a stereo mode for cartographic, topographic, and thematic mapping. Two investigations (Kobrick and Ramapriyan) will assess the optimum radar illumination geometry for stereoscopic analysis and for future radar mapping missions. High-resolution elevation can also be measured using interferometric techniques. The surface relief of featureless plains and gentle slopes of alluvial fans are difficult to detect using stereo techniques but they can be easily observed with interferometric methods. Radar signals from separate passes that cross at very shallow angles will be used to provide the equivalent of an interferometer (Goldstein).

A step toward a fully calibrated radar system will be taken with a number of calibration experiments conducted during the SIR-B mission. As part of one experiment (Held), a calibrator that will provide a reference signal has been added to the SIR-B hardware. Such variables as antenna pattern, spacecraft attitude, transmitter power, receiver gain, system linear-

ity, and SAR correlator effects will be considered. The calibration will then be verified with ground-truth measurements, the aircraft SAR, and the Mobile Radar Scatterometer from the University of Kansas.

To further verify the calibration of SIR-B, an airborne scatterometer will underfly SIR-B, and surface-parameter estimations will be validated using in-situ data collection in a well-controlled reclaimed land area or polder in the Netherlands (Attema).

Knowledge of the antenna pattern is essential to any calibration experiment. This pattern will be measured using the radar data collected along a swath that crosses the Amazon forest in Brazil—a relatively uniform area (Moore). Corner reflectors will also be used in an attempt to calibrate the SIR-B radar. Corner reflectors located along an airstrip of northern Japan and large antennas at the Kashima Radio Research Laboratories near Tokyo will be used to establish the relationship between image intensity and radar backscatter, and then to evaluate the resolution characteristics of SIR-B and to investigate the side-lobe characteristics (Fugono). Several very large corner reflectors placed in Australia will be used to calibrate the radar and to provide a surveyed point target for reference in a number of other investigations (Bryans).

It is generally believed that the ionosphere has very little effect on radar imagery acquired at the SIR-B operating frequency. To assess this theory more thoroughly, the effects of ionospheric irregularities on SAR processing and information extraction will be investigated (Szuszczewicz). A worldwide network of ground radar will be used to measure the state of the ionosphere at the times of SIR-B imaging.

The following sections describe the SIR-B experiment (Section II), the observing plan (Section III), and the expected data (Section V). A brief description of each SIR-B investigation is found in Section IV.

Table 1-1. Team members and their investigations

Name and affiliation	Investigation
C. Elachi, SIR-B Team Leader and Principal Investigator Jet Propulsion Laboratory, California Institute of Technology Pasadena, California	
T. Allan Institute of Oceanographic Sciences Surrey, United Kingdom	"The Interpretation of SIR-B Imagery of Surface Waves and Other Oceanographic Features Using In-Situ, Meteorological Satellite, and Infrared Satellite Data"
W. Alpers Max-Planck-Institut and Universität Hamburg Federal Republic of Germany	"SAR Imaging Mechanisms of Ocean Surface Waves"
E. P. W. Attema Delft University of Technology Delft, Netherlands	"ROVE Calibration and Inverse Scattering Experiment"
R. C. Beal The Johns Hopkins Applied Physics Laboratory Laurel, Maryland	"The Spatial Evolution of the Directional Wave Spectrum in the Southern Ocean: Its Relation to Extreme Waves in the Agulhas Current"
G. L. Berlin U.S. Geological Survey Flagstaff, Arizona	"Application of SIR-B Data for Groundwater Exploration in the Arabian Shield and Sand-Drift Monitoring in the An Nafud and Al Jafurah Fringe Areas, Kingdom of Saudi Arabia"
A. L. Bloom Cornell University Ithaca, New York	"Tectonic, Volcanic, and Climatic Geomorphology Study of the Sierras Pampeanas Andes, Northwestern Argentina"
M. L. Bryan Jet Propulsion Laboratory Pasadena, California	"Deforestation, Floodplain Dynamics, and Carbon Biogeochemistry in the Amazon Basin"
N. L. Bryans Defence Research Centre Salisbury Adelaide, Australia	"Investigations Involving Corner-Reflector Arrays, Signal Processing, and Oceanographic Studies"
F. Carsey Jet Propulsion Laboratory Pasadena, California	"Southern Ocean Sea-Ice Morphology and Kinematics"
M. A. Collins Department of Scientific and Industrial Research Lower Hutt, New Zealand	"New Zealand SIR-B Science Investigations"
T. H. Dixon Jet Propulsion Laboratory Pasadena, California	"SIR-B Analysis of the Precambrian Shield of Sudan and Egypt: Penetration Studies and Subsurface Mapping"
T. G. Farr Jet Propulsion Laboratory Pasadena, California	"Quantitative Use of Multiincidence-Angle SAR for Geologic Mapping"
J. P. Ford Jet Propulsion Laboratory Pasadena, California	"Geologic Mapping of Indonesian Rain Forest With Analysis of Multiple SIR-B Incidence Angles"

Table 1-1. (Cont)

Name and affiliation	Investigation
N. Fugono Radio Research Laboratories Tokyo, Japan	"Remote Sensing of Rice Fields and Sea Pollution by SIR-B"
D. Garofalo Earth Satellite Corporation Chevy Chase, Maryland	"Evaluation of SIR-B Data for Identifying Rainfall Event Occurrence and Intensity"
R. M. Goldstein Jet Propulsion Laboratory Pasadena, California	"SIR-B Interferometric Topography"
A. L. Gray Canada Centre for Remote Sensing Ottawa, Canada	"Use of SIR-B Multiincidence-Angle Imagery to Study Iceberg Detectability and Offshore Ocean Feature Extraction"
J. W. Head III Brown University Providence, Rhode Island	"Geological, Structural, and Geomorphological Analyses From SIR-B"
D. N. Held Jet Propulsion Laboratory Pasadena, California	"Amplitude Calibration Experiment for SIR-B"
R. M. Hoffer Purdue University West Lafayette, Indiana	"Microwave and Optical Remote Sensing of Forest Vegetation"
F. R. Honey Commonwealth Scientific and Industrial Research Organization Wembley, Australia	"Evaluation of SIR-B Imagery for Geologic and Geomorphic Mapping, Hydrology, and Oceanography in Australia"
M. L. Imhoff Goddard Space Flight Center Greenbelt, Maryland	"The Use of Digital Spaceborne SAR Data for the Delineation of Surface Features Indicative of Malaria Vector Breeding Habits"
W. H. Johnson University of Illinois Urbana, Illinois	"Interlobate Comparison of Glacial-Depositional Style as Evidenced by Small-Relief Glacial Landscape Features in Illinois, Indiana, and Ohio, Utilizing SIR-B"
V. H. Kaupp University of Arkansas Fayetteville, Arkansas	"Evaluation of the L-Band Scattering Characteristics of Volcanic Terrain in Aid of Lithologic Identification, Assessment of SIR-B Calibration, and Development of Planetary Geomorphic Analogs"
G. E. Keyte Royal Aircraft Establishment Farnborough, United Kingdom	"The Investigation of Selected Oceanographic Applications of Spaceborne Synthetic-Aperture Radar"
M. Kobrick Jet Propulsion Laboratory Pasadena, California	"SIR-B Cartography and Stereo Topographic Mapping"
B. N. Koopmans International Institute for Aerial Survey and Earth Sciences Enschede, Netherlands	"Monitoring of the Tidal Dynamics of the Dutch Waddensea by SIR-B"

Table 1-1. (Cont)

Name and affiliation	Investigation
P. D. Lowman, Jr. Goddard Space Flight Center Greenbelt, Maryland	"Structural Investigation of the Canadian Shield by Orbital Radar and Landsat" "Structural Investigation of the Grenville Province by Radar and Other Imaging and Nonimaging Sensors"
R. K. Moore University of Kansas Center for Research, Inc. Lawrence, Kansas	"Studies of Coastal Mesoscale Winds Using SIR-B" "Information for Space-Radar Designers: Required Dynamic Range vs Resolution and Antenna Calibration Using the Amazon Rain Forest"
J. F. Paris Jet Propulsion Laboratory Pasadena, California	"Development and Evaluation of Techniques for Using Combined Microwave and Optical Image Data for Vegetation Studies"
J. T. Parr The Analytic Sciences Corporation Reading, Massachusetts	"Investigation of SIR-B Images for Lithologic Mapping"
H. K. Ramapriyan Goddard Space Flight Center Greenbelt, Maryland	"Automatic Terrain Elevation Mapping and Registration"
J. A. Richards University of New South Wales Kensington, Australia	"Australian Multiexperimental Assessment of SIR-B (AMAS)"
G. G. Schaber U.S. Geological Survey Flagstaff, Arizona	"Application and Calibration of the Subsurface Mapping Capability of SIR-B in Desert Regions"
A. J. Sieber Deutsche Forschungs– und Versuchsanstalt für Luft– und Raumfahrt Federal Republic of Germany	"German Radar Observation Shuttle Experiment (ROSE)"
D. S. Simonett University of California Santa Barbara, California	"The Extension of an Invertible Coniferous Forest Canopy Reflectance Model Using SIR-B and Landsat Data"
E. P. Szuszczewicz Naval Research Laboratory Washington, D.C.	"An Investigation of Ionospheric Irregularity Effects on SIR-B Image Processing and Information Extraction"
J. V. Taranik University of Nevada Reno, Nevada	"Analysis of SIR-B Radar Illumination Geometry for Depth of Penetration and Surface Feature and Vegetation Detection, Nevada and California"
M. N. Toksoz Massachusetts Institute of Technology Cambridge, Massachusetts	"Delineation of Major Geologic Structures in Turkey Using SIR-B Data"
F. T. Ulaby University of Kansas Center for Research, Inc. Lawrence, Kansas	"Evaluation of the Radar Response to Land Surfaces and Volumes: Examination of Theoretical Models, Target Statistics, and Applications"
P. Ulriksen Lund University of Technology Lund, Sweden	"Ground Truth for SIR-B Images Obtained by SIR System 8 Impulse Radar"

Table 1-1. (Cont)

Name and affiliation	Investigation
J. R. Wang Goddard Space Flight Center Greenbelt, Maryland	"Remote Sensing of Soil Moisture"
R. S. Winokur Office of Naval Research Arlington, Virginia	"SAR Internal Wave Signature Experiment"

Section II
Experiment Description

A. Summary

SIR-B will be the second of the synthetic-aperture radar experiments to fly on the Shuttle. As such, the hardware owes much to its predecessor, SIR-A (Ref. 2-1), although several new features have been incorporated. The antenna and the radar sensor are subsystems carried over from SIR-A to SIR-B with some modifications. The optical recorder (OR) is unchanged from that used in SIR-A. Important new elements in SIR-B are antenna electronics that allow selectable look angles, a digital data handling subsystem (DDHS), increased bandwidth, a calibrator, and a digital data processor on the ground. Table 2-1 is a list of the SIR-B characteristics.

Radio-frequency (RF) pulses at 1.28 GHz (L-band) are generated in the transmitter portion of the sensor and radiated by the antenna. The RF signals are reflected from the Earth, collected by the antenna, and sent to the receiver portion of the sensor where they are beaten down to baseband to form the offset video output. This output is then sent to either the OR, the DDHS, or both.

The OR will store 8 h of selected data with 6-MHz bandwidth on about 1100 m of signal film, which will be unloaded after the Shuttle lands. The DDHS will handle about 65 h of digital data, a large majority of which (>95%) will be routed to the Shuttle Ku-band system for transmission to the Tracking and Data Relay Satellite (TDRS) and retransmission to the ground receiving station at White Sands, New Mexico. (Some digital data will be temporarily stored on high-density digital tapes (HDDTs) onboard the Shuttle for later transmission through TDRS.) These data then will be sent from White Sands via the DOMSAT satellite to Goddard Space Flight Center (GSFC) in Greenbelt, Maryland, and recorded at GSFC on HDDTs. The permanent onboard storage capacity for digital data is limited to about 20 min on each of four to seven tapes, which will be unloaded after the mission. All data will be shipped back to JPL where signal film from the OR will be processed into film images with an optical correlator, and data from the HDDTs will be processed into digital images with a software correlator. SIR-B digital images will feature a factor-of-two better range resolution than either the SIR-A or SIR-B optically-correlated images because of the increased SIR-B bandwidth.

Figure 2-1 illustrates the end-to-end system block diagram for SIR-B. The following sections describe in more detail some of these subsystems.

B. Antenna

The SIR-B antenna (Fig. 2-2) consists of an array of eight component panels seven of which constituted the SIR-A antenna. The SIR-B antenna, with a total length of 10.7 m, is thus longer than that of SIR-A; the width, 2.16 m, is the same. The increased antenna area results in a slightly larger signal-to-noise ratio (SNR) for a given observation, especially important at large look angles.

During launch, the antenna will be folded in three pieces along two hinges and stored in the Shuttle payload bay. The inner leaf is 2.7 m long and the outer leaf is 4.0 m long. In orbit, the payload bay doors will be opened and the antenna deployed. The antenna will remain deployed for observations throughout the mission except during Shuttle maneuvers that

involve large altitude changes. Two such maneuvers are planned; at these times the antenna will again be stowed.

The most significant new feature of the SIR-B antenna subsystem is the antenna array tilt mechanism. This consists of a third hinge and its associated mechanism and electronics. The antenna can be commanded to tilt to angles between 15 and 60 deg in approximately 1-deg steps. A posteriori determination of the look angle will be accurate to ±0.1 deg. At a command from the ground, the antenna will move from one orientation to another at the rate of approximately 1 deg per second of time.

C. Electronics

The transmitter forms a linearly swept, frequency-modulated pulse with a minimum peak power of 1122 W, a 30.4-μs pulse length, and a 12-MHz bandwidth. This bandwidth results in a range resolution of between 14 and 46 m. There are 16 selectable pulse-repetition frequencies (PRFs) with values between 1248 pulses/s and 1824 pulses/s. A particular PRF value will be chosen for each observation to insure that neither a transmit event nor a nadir return occurs in the data acceptance window for the reflected signal. This data acceptance window also will be chosen for each observation and will begin at one of the 64 data-window positions that equally divide the interpulse period. The temporal length of the data window determines the width in the cross-track or range dimension of the area imaged on the ground (the "swath") and is based on a number of experiment parameters discussed below.

The receiver has eight useable gain-control levels that range from about 70 to 100 dB. Selection of the level for each observation will be based upon the expected backscatter intensity and the required saturation margin. The DDHS samples the offset video output at 30 MHz and converts this analog signal into digital output, quantized with 3 to 6 bits per sample (bps). The bps value chosen for a given observation will reflect a trade-off between a larger data-rate-limited swath for smaller bps, and a larger dynamic range and system SNR for larger bps. The DDHS outputs a stream of serial data that consists of the digitized backscatter signals, housekeeping, and other data used in image processing on the ground. When the OR is in use, the DDHS also provides annotation for the signal film.

The data rate for SIR-B digital data differs depending upon whether the DDHS sends data directly to TDRS or to the onboard recorder. In the direct-to-TDRS case, the data rate is 45.6 Mbits/s; in the other case, the data rate is 30.4 Mbits/s.

The data rate is one of the experiment parameters that determines the swath width. For the higher data rate, the swath width will be 50% larger. Other parameters that affect swath width are the bps, the PRF, and the look angle. That portion of the swath in which the data exceed a minimum SNR is called the SNR-limited swath. It depends, in addition to the above parameters, on radar backscatter intensity. Figure 2-3 shows the SNR-limited swath widths for both high (360-km) and low (225-km) Shuttle operations, for both data rates, and for two minimum SNR limits, 3 and 8 dB. An average backscatter curve is assumed with $\sigma_0 = (-8 - 0.25\,\theta)$ dB, where θ is the incidence angle in degrees. For most of the operating range, the 3-dB swath widths are between 40 and 60 km, while the 8-dB swath widths are between 30 and 50 km. These SNR limits are deemed necessary for either mapping an area (3 dB) or obtaining a fully calibrated image (8 dB).

Image calibration will be performed with the aid of the onboard SIR-B calibrator. The calibrator generates a single-frequency "cal tone" that is injected into the offset video output at one of four selectable power levels. These levels have been accurately measured in preflight tests. The calibrator will be turned on for all observations that use 5 or 6 bps. The cal-tone level is chosen to be the highest level below the expected radar return.

D. Data Processor

1. Introduction

The raw echo data collected during the SIR-B mission will be of two general types: optical and digital. The optical data will be recorded onboard via film by the same optical recorder used in SIR-A. The digital data may be either recorded onboard by an Odetics high-density digital recorder (HDDR) and subsequently transmitted to the ground receiving station via TDRS, or transmitted directly to TDRS, bypassing the HDDR.

2. Optical Processing

Two types of optical imagery will be produced from the SIR-B data (Fig. 2-4). The flight recorder data (8 h) will be processed to the same quality and resolution (approximately 40 m, 6 looks) as that for SIR-A. In addition, all digitally collected data will be converted to signal film via a laser beam recorder and processed in the "survey" mode on the optical correlator. This survey-mode data will provide team members with the capability of validating the digital data over their sites and accurately locating the swath. To expedite the processing of these data, minor ambiguities will not be corrected and the image quality will be somewhat degraded (50 m, 4 looks) from the onboard recorder products.

The bandwidth limitations of the optical correlator will reduce the range resolution by a factor of two relative to the

digital data. Thus, the optical imagery will have a ground-range resolution of 30 to 100 m depending on the incidence angle. All optical products will be annotated with date and time-of-acquisition marks, but no image location or radiometric calibration will be performed on these products. The imagery will be in a slant-range presentation of approximately 500,000:1 in scale (Note: onboard recorder products are required to meet scale requirements within 5%). The current production schedule calls for all data to be processed optically within one year of the mission. This assumes 65 h of digital data converted to film and 8 h of onboard OR data.

3. Digital Processing

The SIR-B digital processor, which performs both range and azimuth compression in the frequency domain, is an upgraded version of the Seasat processor. The SIR-B processor, however, is more flexible, having incorporated the capability of handling data of 3, 4, 5, or 6 bps with a full range of synthetic-aperture lengths that result from the variable look angles (15 to 60 deg). In addition, as a result of the instability of the Shuttle as an imaging platform and the high look angles (up to 60 deg), range migration of the target across many range bins during the imaging period required incorporation of a new azimuth-compression algorithm to maintain the required SNR levels.

Figure 2-5 shows the digital processor block diagram, which illustrates the set of supporting software modules developed to provide better data quality control and to simplify operation for maximum throughput. The input processor controls the data transfer, evaluates the bit error rate (BER), detects and fills any missing range lines, and decodes header information to set up the image processing. This module produces range spectra and histograms of the raw data input.

The input processor also determines the initial Doppler parameters (Doppler frequency f_d and Doppler frequency rate change $\dot{f}_d$) for the preprocessor. This module has been upgraded to reduce the effects of local terrain variation by performing a regression analysis across the swath. An additional feature has been added to detect and correct azimuth ambiguities resulting from large pointing errors. The image formation processor is shown functionally in Fig. 2-6. The rectification and output formatting processor (Fig. 2-5) performs geometric and radiometric correction on the image product and determines the absolute location of the image center.

The geometric correction converts a slant-range presentation to a ground-range presentation (exclusive of local terrain distortion) and removes the skew that results from Earth rotation during the data collection period. The accuracy of the algorithm relative to terrain and spacecraft ephemeris error is specified to be less than 0.1% relative misregistration across the swath. Output spacing is 12.5 m in both directions and image size is 25 to 60 km across-track and 90 to 110 km along-track, dependent on the imaging mode (i.e., look angle, PRF, bps, and data rate).

The radiometric compensation is designed to produce a relative uniformity in the image presentation independent of imaging mode or target location across the swath. No attempt will be made to relate the image gray level (8-bit magnitude) to the backscatter coefficient. The processor uses prelaunch test data in conjunction with in-flight sensor data (in header of raw data) to compensate for the following data characteristics: (1) transmitter output-power variation; (2) elevation antenna-pattern modulation; (3) variable slant range both across swath and at different look angles; (4) receiver gain fluctuation; and (5) along-track Doppler drift. It is estimated that a relative calibration of approximately 2 dB will be maintained over the digital data set.

The image data will have an azimuth resolution of 20 to 30 m, depending on PRF and side-lobe weighting, and a range resolution of 14 to 46 m depending on look angle. The peak side-lobe response will be more than 25 dB below the main response and the integrated side-lobe ratio less than −21 dB. The dynamic range for distributed targets will vary between 15 and 30 dB, depending on receiver gain and bps.

Reference

2-1. Cimino, J. B., and C. Elachi, *Shuttle Imaging Radar-A (SIR-A) Experiment*, Publication 82-77. Jet Propulsion Laboratory, Pasadena, California, December 15, 1982.

Table 2-1. SIR-B experiment characteristics

Description	Value
Orbital altitudes	352, 274, 225 km
Orbital inclination	57 deg
Mission length	8.3 days
Wavelength	23.5 cm
Frequency	1.28 GHz
Polarization	HH
Pulse length	30.4 μs
Bandwidth	12 MHz
Optical recorder bandwidth	6 MHz
Minimum peak power	1.12 kW
Antenna dimensions	10.7 × 2.16 m
Antenna gain	33.2 dB
Look angles	15 to 60 deg
Swath width	20 to 50 km
Range resolution	14 to 46 m
Azimuth resolution	20 to 30 m (4-look)
Digital data rate	45.6 and 30.4 Mbits/s
Total digital data	65 h
Total optical data	8 h

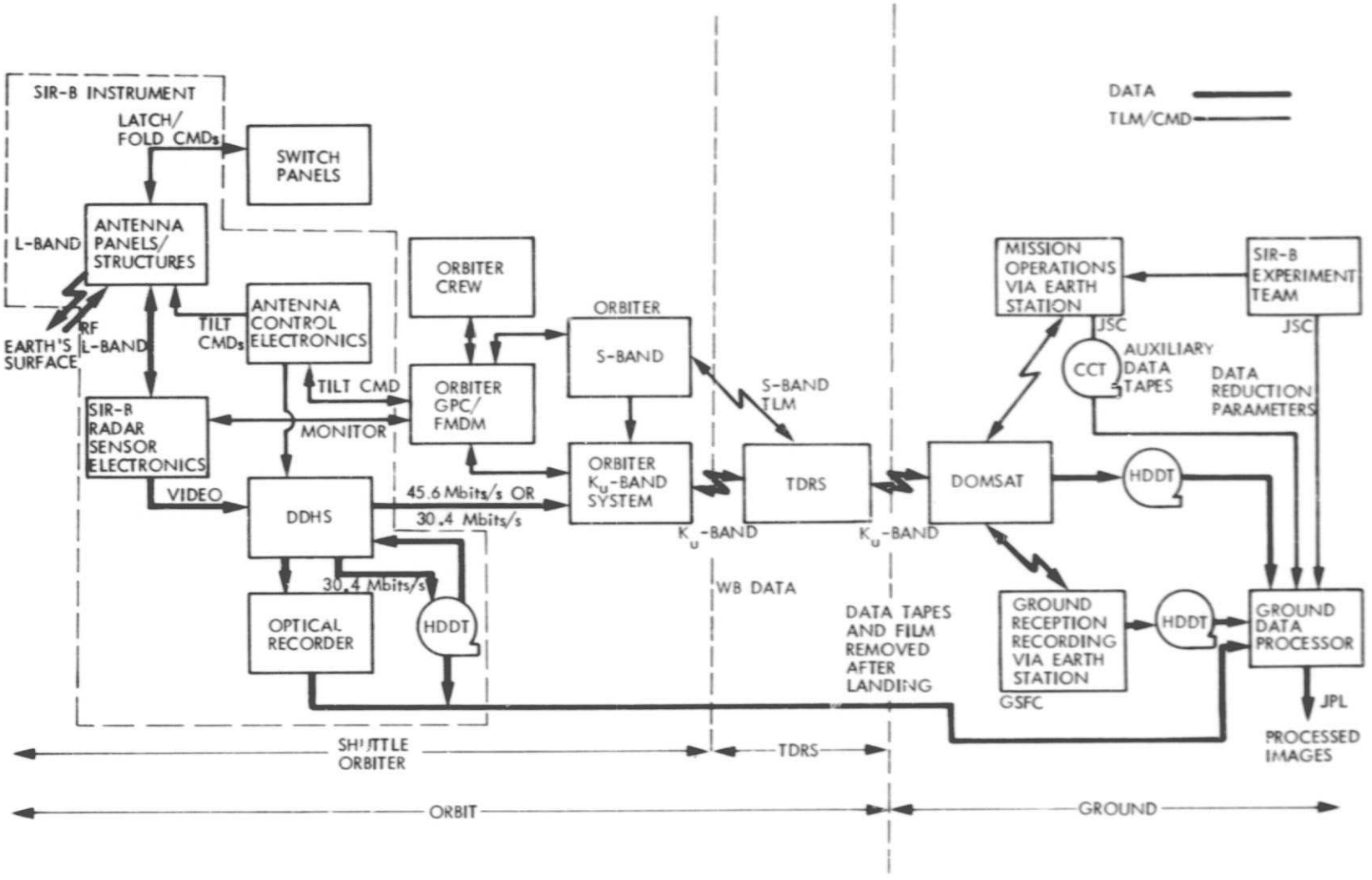

Fig. 2-1. SIR-B end-to-end system block diagram

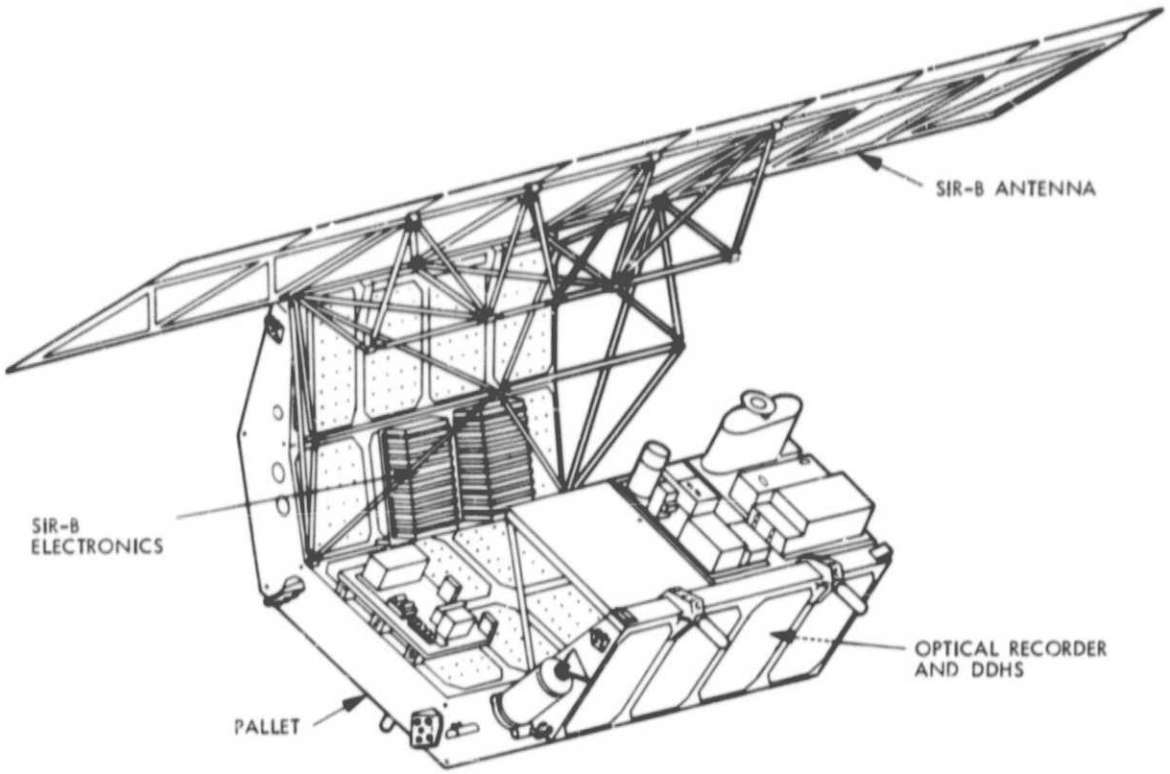

Fig. 2-2. SIR-B experiment package

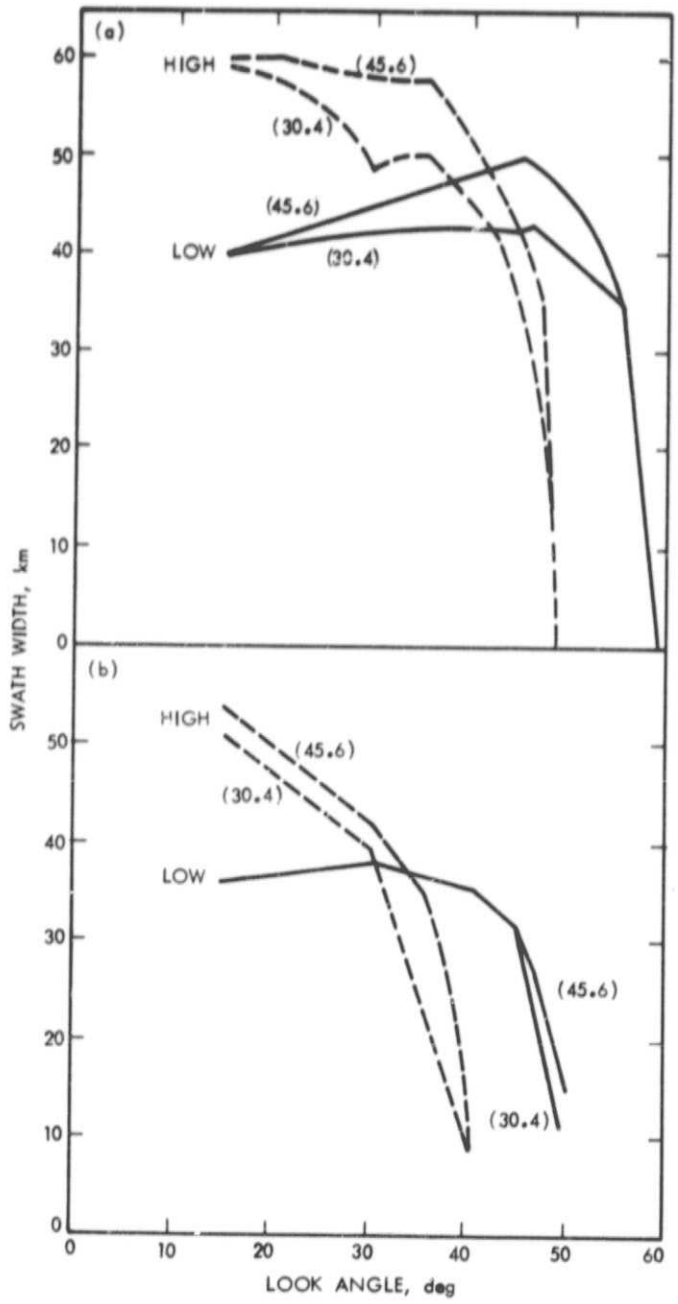

Fig. 2-3. Signal-to-noise limited SIR-B swath widths for high (360-km) and low (225-km) altitudes and high and low data rates: (a) 3-dB minimum SNR; (b) 8-dB minimum SNR

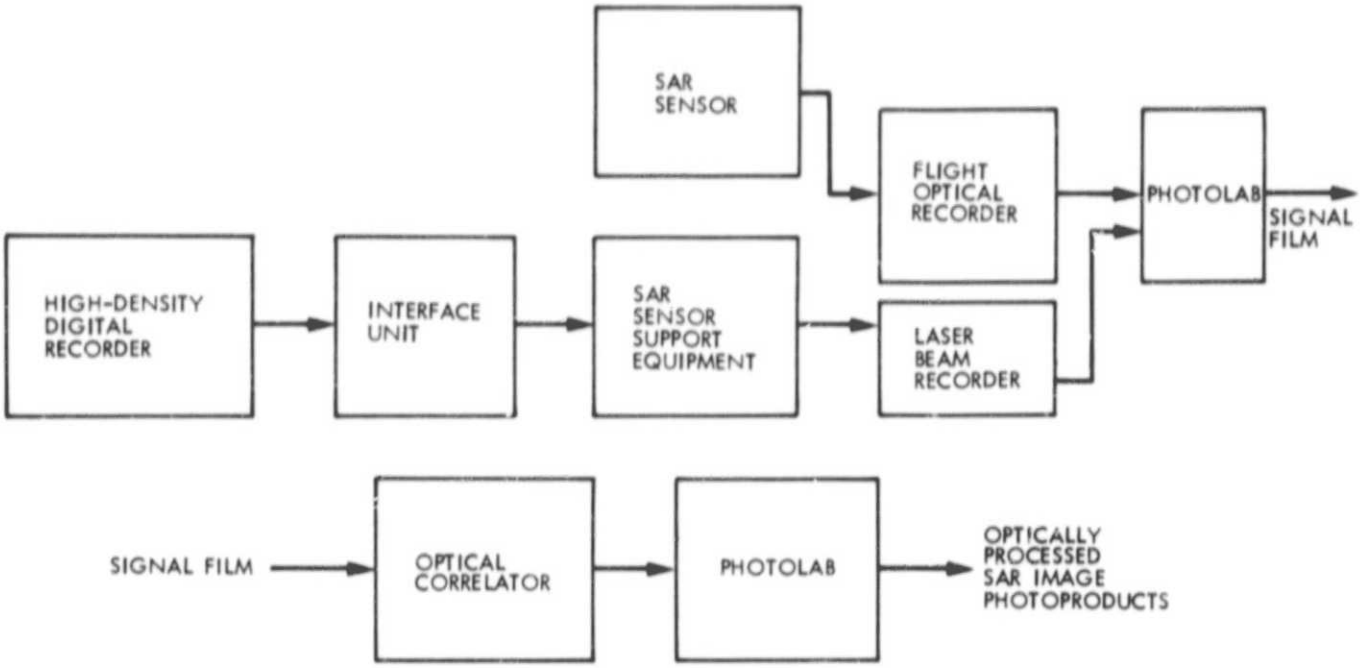

Fig. 2-4. Optical processor block diagram

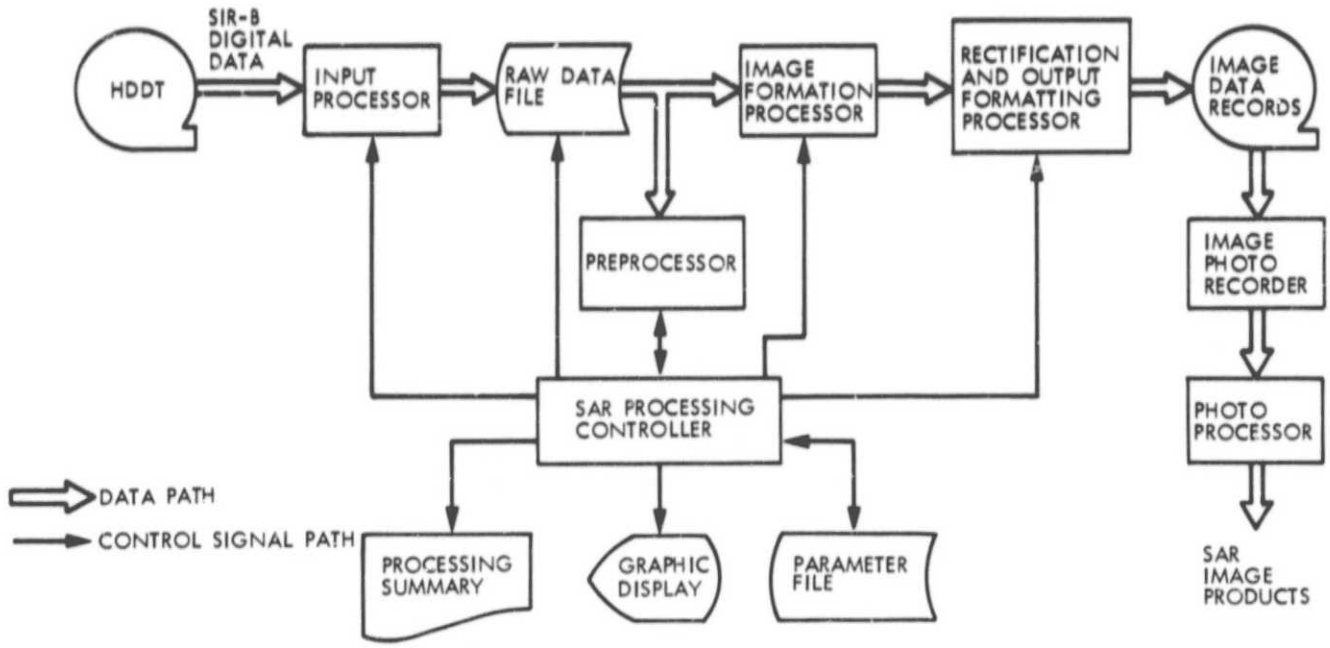

Fig. 2-5. SIR-B digital processor block diagram

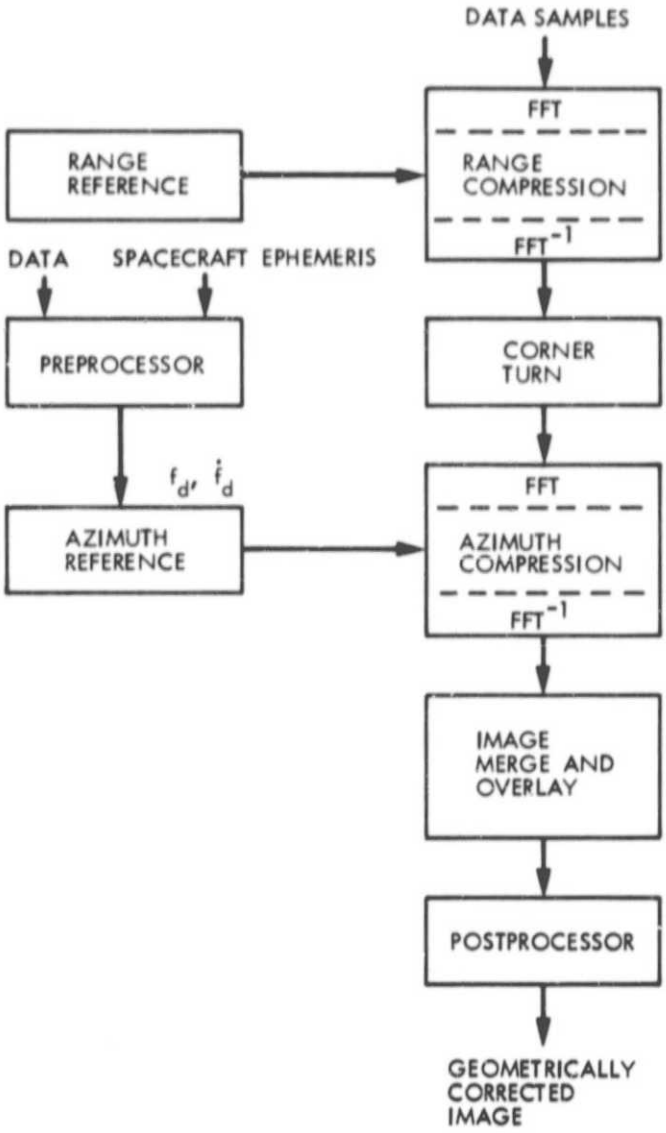

Fig. 2-6. Functional block diagram of SAR digital correlation algorithm

Section III
SIR-B Coverage

A. Overview

In this section, the planned coverage with SIR-B is described in detail. A total of about 60-million km^2 of coverage will be acquired including 50 h of TDRS data and 8 h of optically recorded data. In general, data will be acquired directly through TDRS whenever possible; however, because of certain constraints imposed by having just one TDRS in orbit during the time of this mission, many digitally taped data takes will be required. (Each separate SIR-B observation is designated as a "data take.") Optical data takes will be taken only over sites that cannot be acquired either directly through TDRS or on a digital tape. It is important to note that, although a digital data take may be acquired at any time during the mission, it will be necessary to dump that data take through TDRS at some later time, or replace the tape onboard the Shuttle with another blank tape.

B. Shuttle Attitudes and Constraints

The Shuttle-TDRS link enables a large quantity of data to be transmitted to the ground. Only a small fraction of these data can be stored onboard the Shuttle (Section II.A). In addition, the real-time use of TDRS enhances data quality because the higher data rate results in a larger swath width (Section II.C).

The Shuttle's flexibility in orientation increases the line-of-sight access to the TDRS (Fig. 3-1). In the nominal spacecraft attitude where the payload bay faces Earth (-ZLV attitude) and the nose forward, the SIR-B antenna images north of the Shuttle ground track. With a 90-deg roll, the antenna images south of the ground track. A yaw maneuver of 180 deg reverses the coverage of either of these nose-forward attitudes.

Shuttle maneuvers, however, do introduce some constraints. First and foremost, crew safety must be assured. Shuttle maneuvers are limited during crew sleep periods or extravehicular activities. The requirements of other onboard experiments (for example, maintaining a particular attitude) affect operation of SIR-B. Finally, the fuel available for maneuvering is limited by supply.

C. Explanation of Maps

The coverage to be acquired by SIR-B is shown on the maps (Figs. 3-2 through 3-9) on pages 3-5 to 3-12. The world has been divided into eight sections to present the coverage in more detail. Each section (map) shows the SIR-B test sites for that part of the world. The number at each site corresponds to a number in Table 3-1, which lists the team member and the target.

The maps also show the data takes to be acquired in a nominal SIR-B mission. The tracks shown for each data take represent the center of the radar swath (no Shuttle ground tracks are shown).

Each data take is labeled with one or two letters that indicate a series of data takes over approximately the same area. Each data take in a series is acquired during one of the low-altitude days. Data takes acquired during the first 20 orbits (the high-altitude portion of the mission) are labeled HH; data takes acquired during orbits 21 through 33 (the medium-altitude portion of the mission) are labeled MM.

Table 3-1. Preliminary SIR-B sites

Number	Investigator	Site name
1	Allan	Ligurian Sea
2	Allan	Forties
3	Allan	Lima
4	Allan	Channel
5	Allan	Data Buoy, No. 2
6	Allan	Data Buoy, No. 3
7	Allan	Dowsing
8	Allan	Fred Russel
9	Allan	Seven Stones
10	Allan	UCNW
11	Allan	Waverider
12	Allan	West Sole
13	Alpers	Corsica
14	Alpers	North Sea Platform
15	Alpers	North Sea
16	Attema	Flevoland, Netherlands
17	Beal	Agulhas Current
18	Beal	Southern Ocean off Chile
19	Berlin	Al Jawf, Saudi Arabia
20	Berlin	Al Hisma, Saudi Arabia
21	Berlin	Ha'il, Saudi Arabia
22	Bloom	Argentina, No. 1
23	Bloom	Argentina, No. 2
24	Bloom	Argentina, No. 3
25	Bloom	Argentina, No. 4
26	Bryan	Deforestation, Brazil
27	Bryan	Deforestation, Brazil
28	Bryan	Deforestation, Brazil
29	Bryan	Deforestation, Brazil
30	Bryan	Floodplain, Brazil
31	Bryan	Amazon River, Brazil
32	Bryan	Amazon River, Brazil
33	Bryan	Amazon River, Brazil
34	Bryan	Amazon River, Brazil
35	Bryan	Amazon River, Brazil
36	Bryans	Maree, Australia
37	Collins	Alpine Fault, New Zealand
38	Collins	Canterbury, New Zealand
39	Collins	Kaingaroa, New Zealand
40	Collins	Auckland, New Zealand
41	Collins	Wairarapa, New Zealand
42	Collins	Taupo Volcanic Region, New Zealand
43	Dixon	Precambrian Shield, Egypt and Sudan
44	Elachi	Rift Valley, Africa
45	Elachi	Rio Pico, Argentina
46	Elachi	Ubar, Saudi Arabia
47	Elachi	Altyn-Tagh, China
48	Elachi	Karlik-Tagh, China
49	Elachi	Ganshu, China
50	Elachi	Kunlin, China
51	Elachi	Karakum, China
52	Elachi	Red River, China
53	Farr	Death Valley, California
54	Farr	Mauna Loa, Hawaii
55	Farr	Pisgah Crater, California
56	Farr	Snake River, Idaho
57	Ford	Colombia
58	Ford	Sumatera
59	Ford	East Borneo
60	Ford	West Borneo
61	Fugono	Akita Airport, Japan
62	Fugono	Echigo Plains, Japan
63	Fugono	Hokkaido, Japan
64	Fugono	Kashima, Japan
65	Fugono	Kagoshima, Japan
66	Fugono	Kuroshio Current, Japan
67	Fugono	Oogata Mura, Japan
68	Fugono	Sendai Plains, Japan
69	Fugono	Suigo, Japan
70	Fugono	Toyohashi, Japan
71	Fugono	Tsukushi Plains, Japan
72	Fugono	Ishikari Plains, Japan
73	Gray	Labrador Coast
74	Head	Amazon Delta, Brazil
75	Head	Danube Delta, Romania
76	Head	Ganges Delta, Bangladesh
77	Head	Mississippi Delta, Mississippi
78	Head	Niger Delta, Nigeria
79	Head	Nile Delta, Egypt
80	Head	Volga Delta, USSR
81	Head	Carswell Crater, Canada
82	Head	Charlevoix Crater, Canada
83	Head	Clearwater Crater, Canada
84	Head	Manicouagan Crater, Canada
85	Head	Martin Crater, Canada
86	Head	Mistastin Crater, Canada
87	Head	Sudbury Crater, Canada
88	Herd	Illinois
89	Hoffer	Jacksonville, Florida
90	Honey	West Salinity Site, Australia
91	Honey	Archean, Australia
92	Honey	Bass Strait, Australia
93	Honey	Canberra, Australia
94	Honey	Paleo River, Australia
95	Honey	Davenport Downs, Australia
96	Honey	Eden, Australia
97	Honey	Great Barrier Reef
98	Honey	Hamersley, Australia
99	Honey	Argyle, Australia
100	Honey	Lake Eyre, Australia
101	Honey	Lake Eyre South, Australia
102	Honey	Lake Frome, Australia
103	Honey	Leeuwin Current, Australia
104	Honey	Melbourne, Australia
105	Honey	Mount Isa, Australia
106	Honey	Perth, Australia
107	Honey	East Salinity Site, Australia
108	Honey	Weipa, Australia
109	Honey	Brisbane, Australia
110	Honey	Hobart, Australia
111	Imhoff	Bangladesh
112	Johnson	Illinois
113	Kaupp	Cascades, California
114	Kaupp	Kilauea, Hawaii
115	Keyte	Bathymetry, United Kingdom
116	Keyte	North Atlantic
117	Kobrick	Lubbock, Texas
118	Kobrick	Shasta, California
119	Kobrick	Sydney, Australia
120	Koopmans	Waddensea, Netherlands

Table 3-1 (contd)

Number	Investigator	Site name
121	Lowman	Bancroft, Canada
122	Moore	Hawaii
123	Moore	Falklands
124	Moore	Jamaica
125	Moore	Lesser Antilles
126	Moore	Puerto Rico
127	Moore	Aleutian Islands
128	Paris	Central Valley, California
129	Paris	New England
130	Paris	Raisin City, California
131	Parr	Helvetia, Arizona
132	Parr	Silver Bell, Arizona
133	Ramapriyan	Illinois
134	Ramapriyan	Sydney, Australia
135	Ramapriyan	Shasta, California
136	Richards	Adelaide, Australia
137	Richards	Amadeus Basin, Australia
138	Richards	Canberra, Australia
139	Richards	Cane Fields, Australia
140	Richards	Fowler's Gap, Australia
141	Richards	Melbourne, Australia
142	Richards	NSW Wheat Belt, Australia
143	Richards	Perth, Australia
144	Richards	Pooncarie, Australia
145	Richards	Sydney, Australia
146	Richards	Brisbane, Australia
147	Schaber	Augrabies Falls, South Africa
148	Schaber	Aus, South Africa
149	Schaber	Lake Dow, South Africa
150	Schaber	Molopo, South Africa
151	Schaber	Walnes Bay, South Africa
152	Schaber	Confluence, Egypt
153	Schaber	Saf Saf, Egypt
154	Schaber	Selima Sandsheet, Egypt
155	Schaber	Terfawi, Egypt
156	Schaber	Mongolia
157	Schaber	Wuwei, China
158	Schaber	Peru Coast
159	Sieber	Botswana
160	Sieber	Freiburg, Germany
161	Sieber	Köln, Germany
162	Simonett	Cascades, California
163	Szuszczewicz	Peru
164	Taranik	Beatty, Western U.S.
165	Taranik	Fish Lake, Western U.S.
166	Taranik	Goldfield, Western U.S.
167	Taranik	Long Valley, Western U.S.
168	Taranik	Mount Grant, Western U.S.
169	Taranik	Walker Lane, Western U.S.
170	Taranik	Pahrump Valley, Western U.S.
171	Taranik	Tonopah, Western U.S.
172	Taranik	White Mtns., Western U.S.
173	Toksoz	East Turkey
174	Toksoz	Northwest Turkey
175	Toksoz	Western Turkey
176	Ulaby	Illinois
177	Ulrickson	Öland
178	Wang	Fresno, California
179	Winokur	New York Bight
180	Winokur	NOSC Tower, California

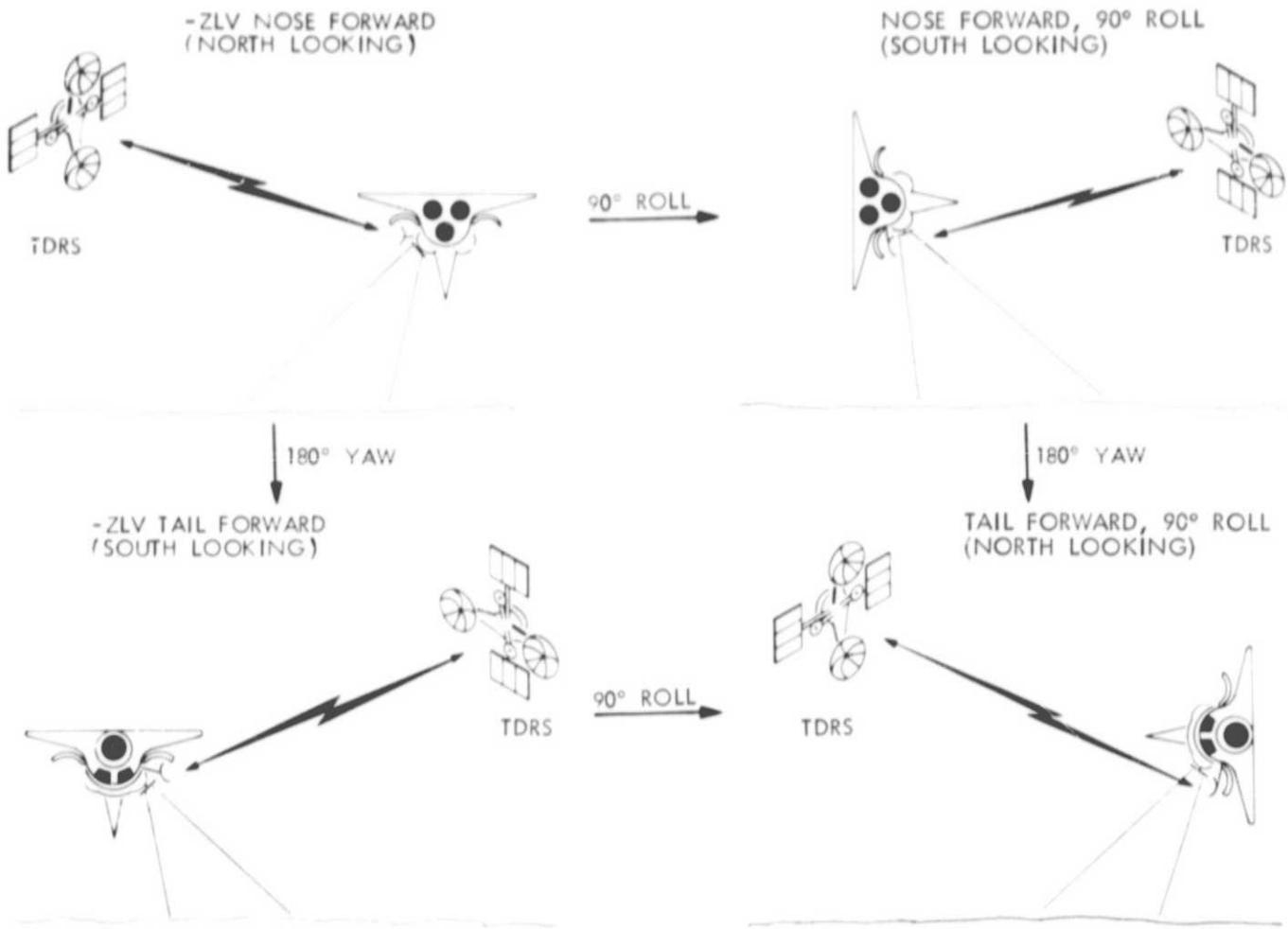

Fig. 3-1. Shuttle orientations for SIR-B observations; shuttle velocity vector is into page

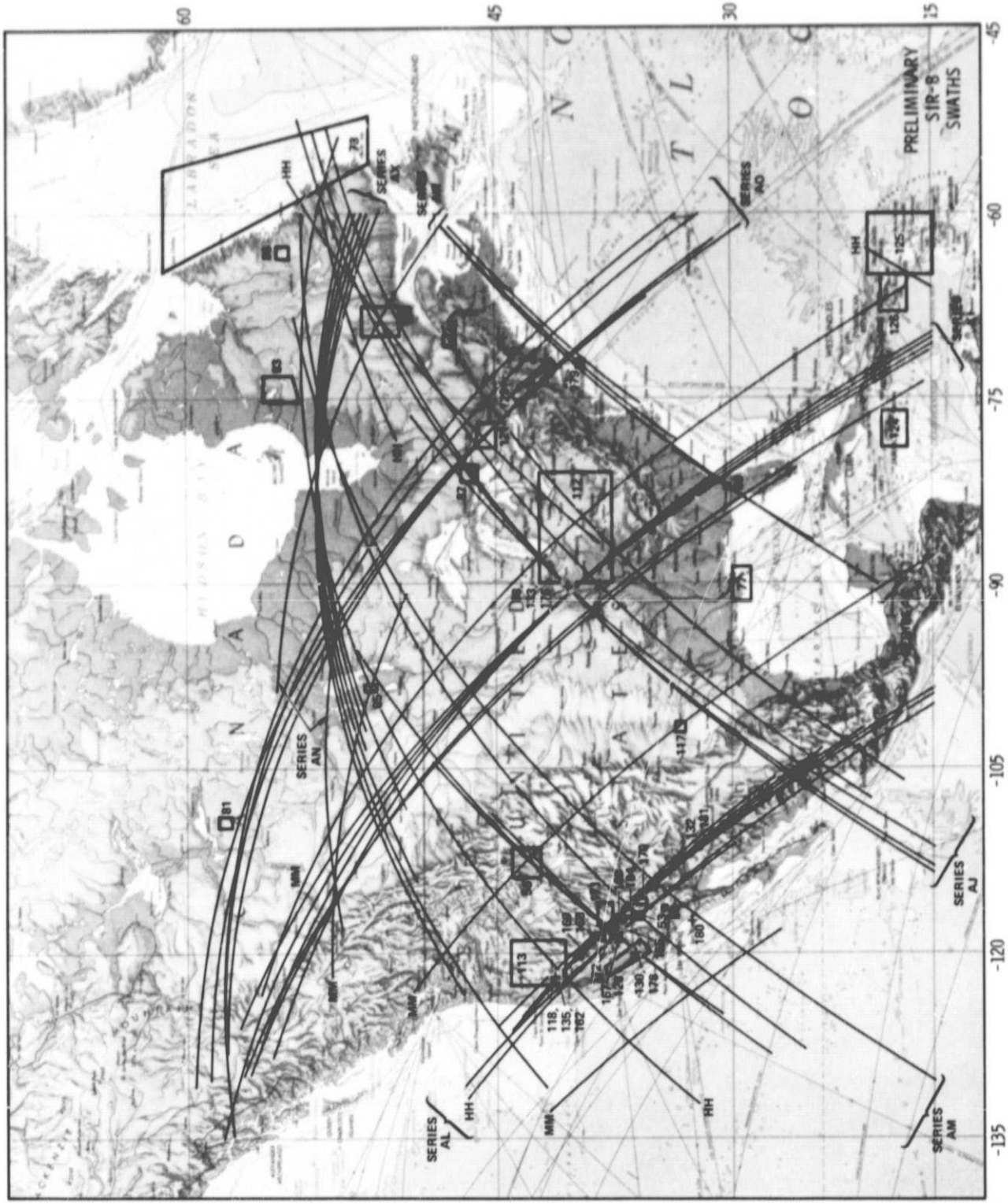

Fig. 3-2. United States and Canada: preliminary SIR-B swaths

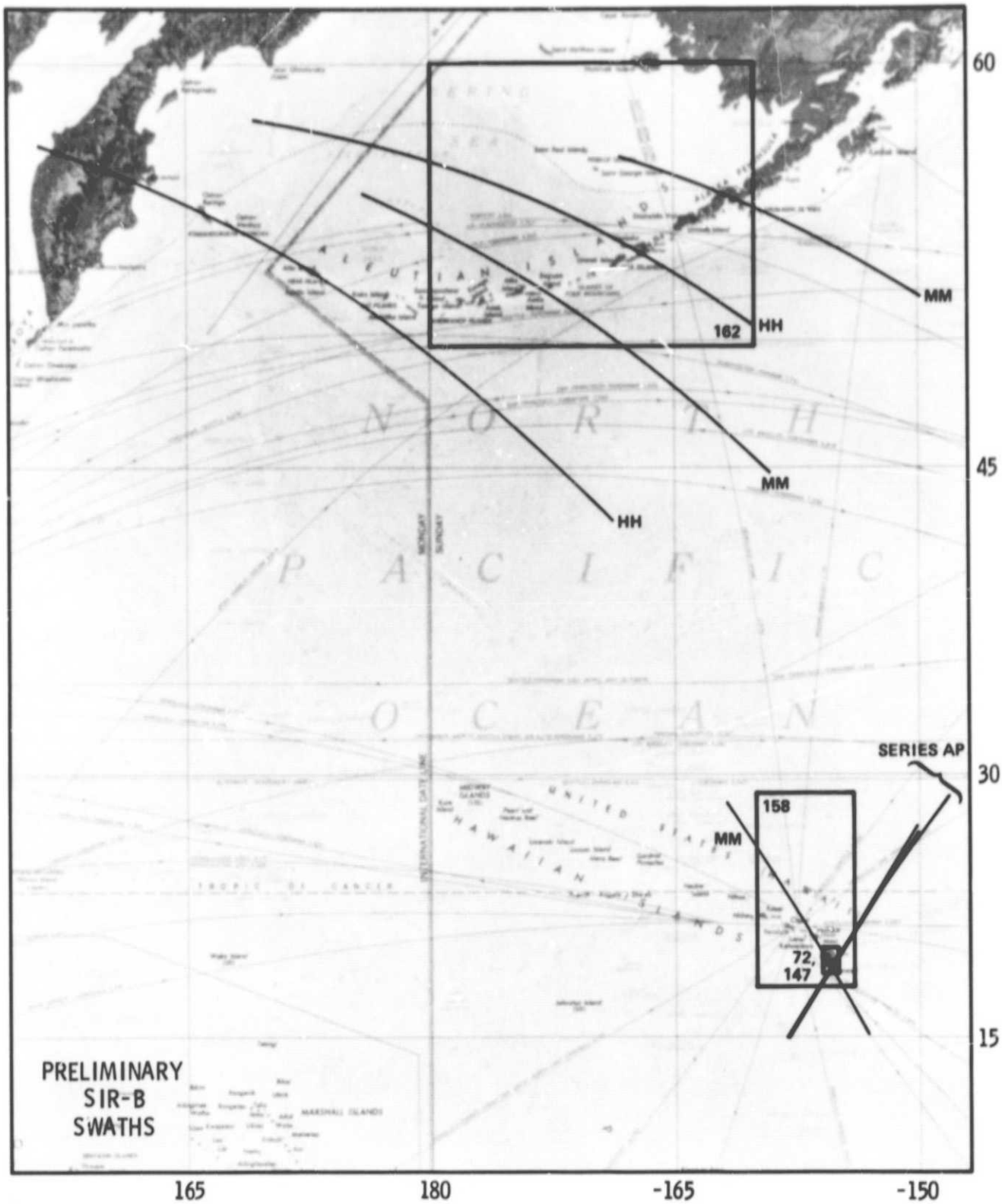

Fig. 3-3. Hawaii and the Aleutian Islands: preliminary SIR-B swaths

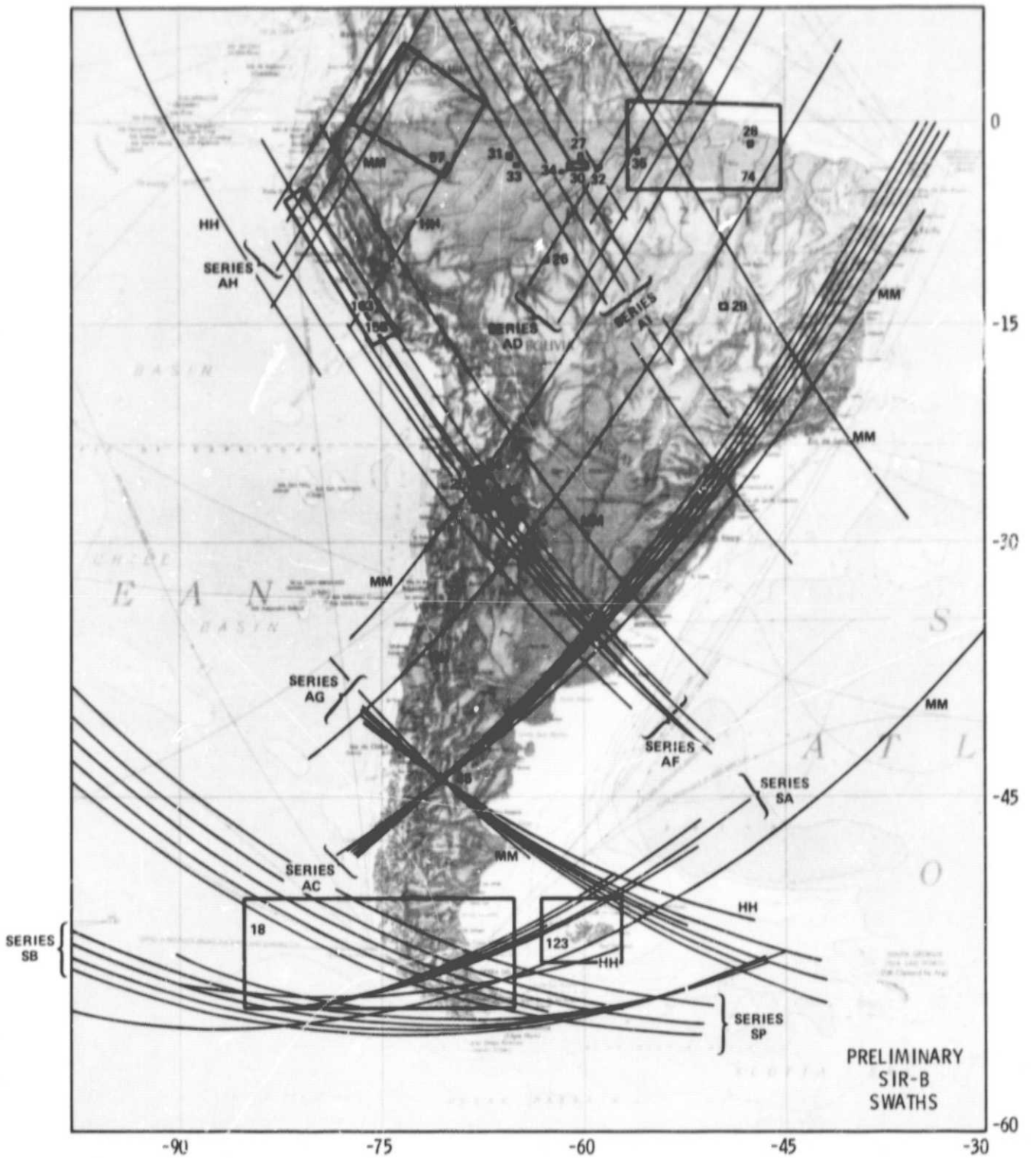

Fig. 3-4. South America: preliminary SIR-B swaths

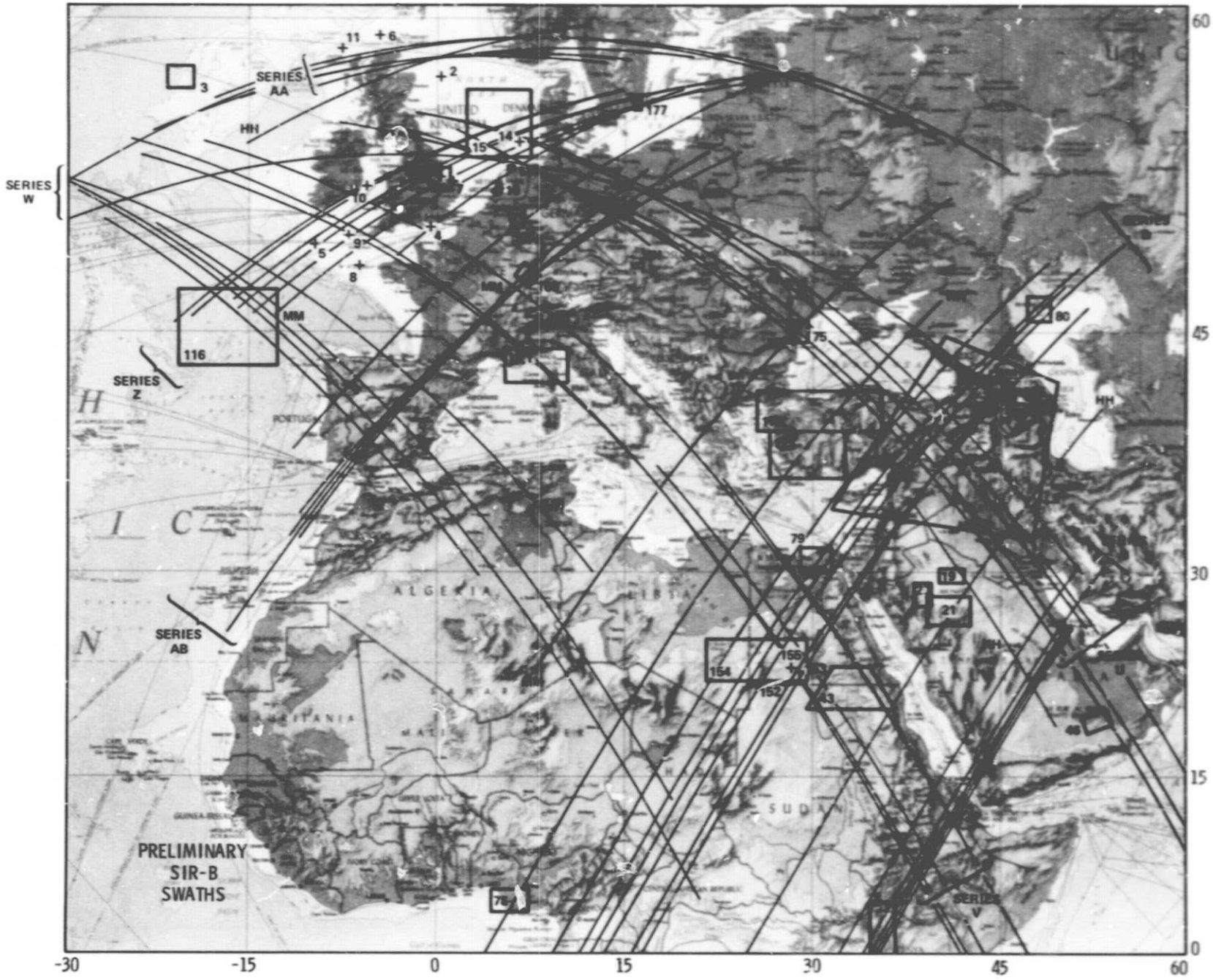

Fig. 3-5. Europe and North Africa: preliminary SIR-B swaths

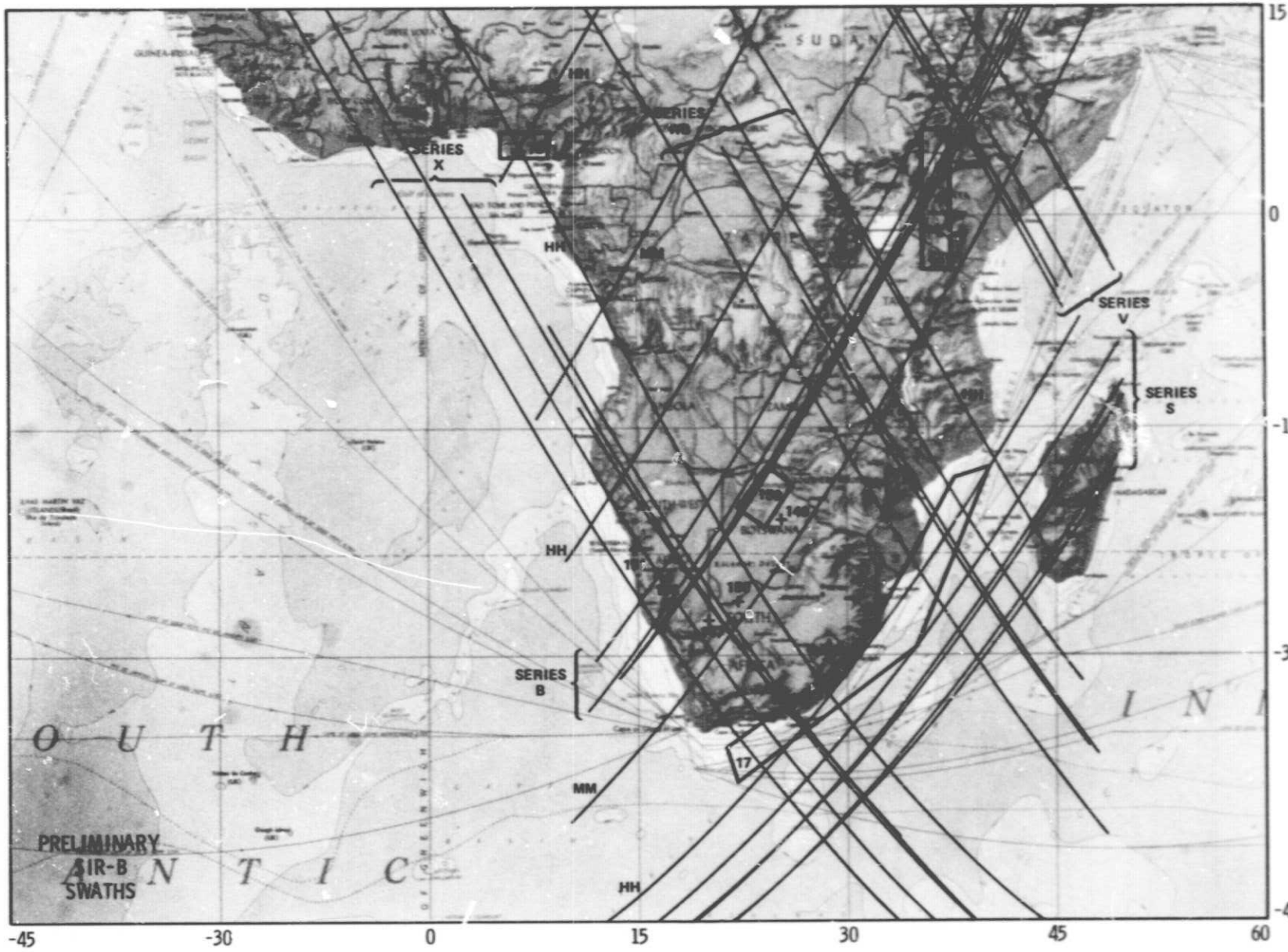

Fig. 3-6. South Africa: preliminary SIR-B swaths

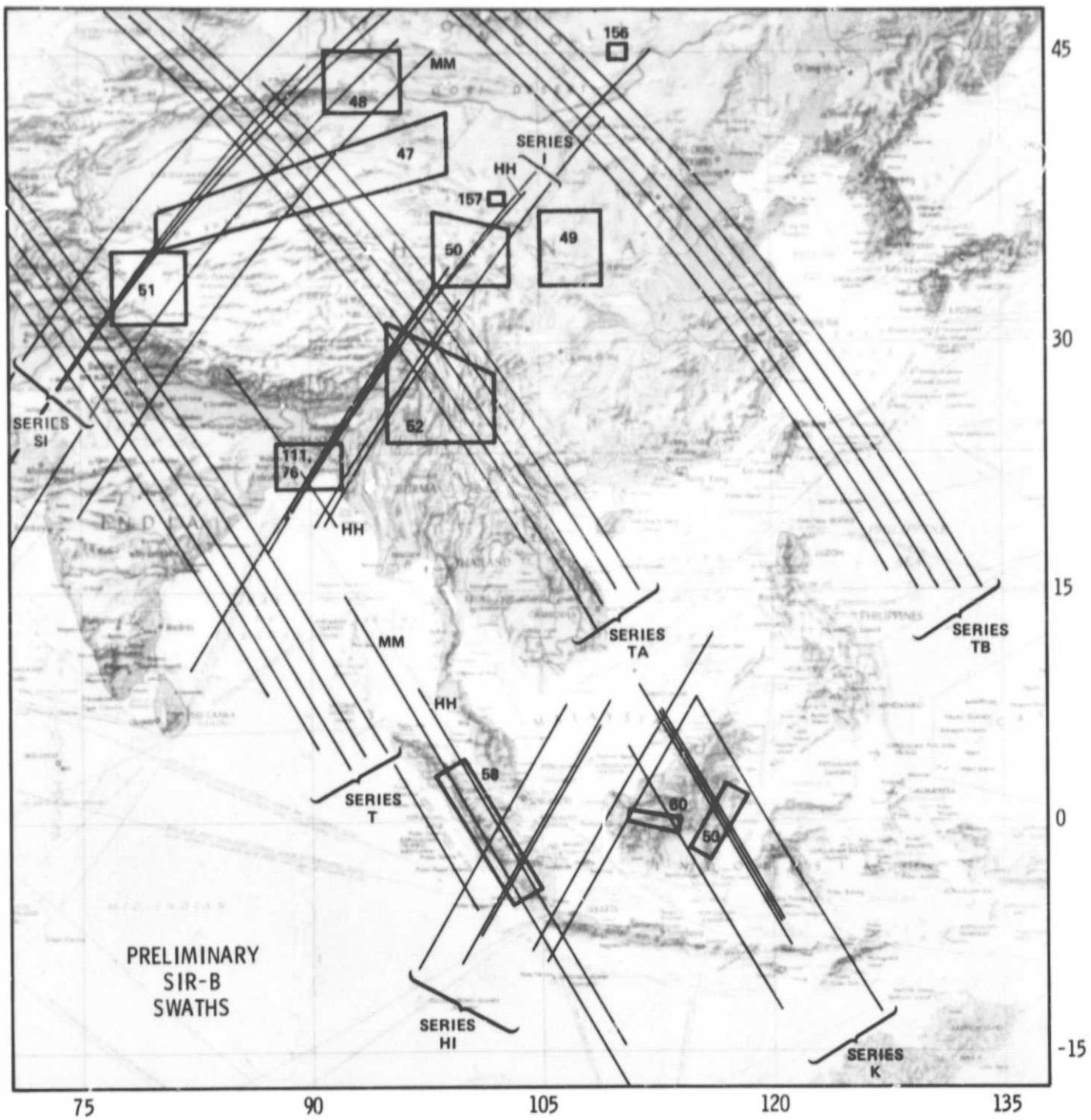

Fig. 3-7. Southeast Asia and Indonesia: preliminary SIR-B swaths

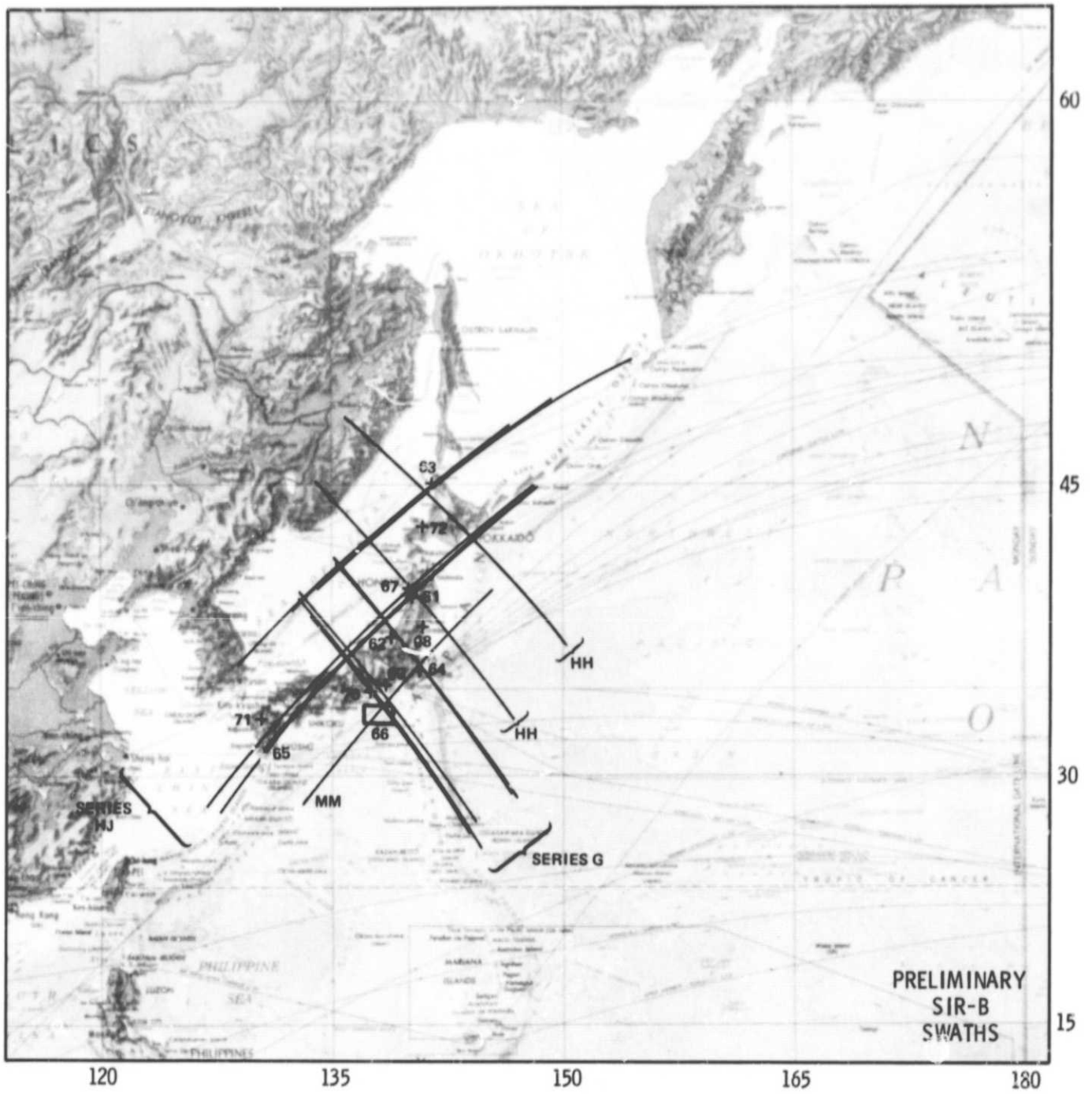

Fig. 3-8. Japan: preliminary SIR-B swaths

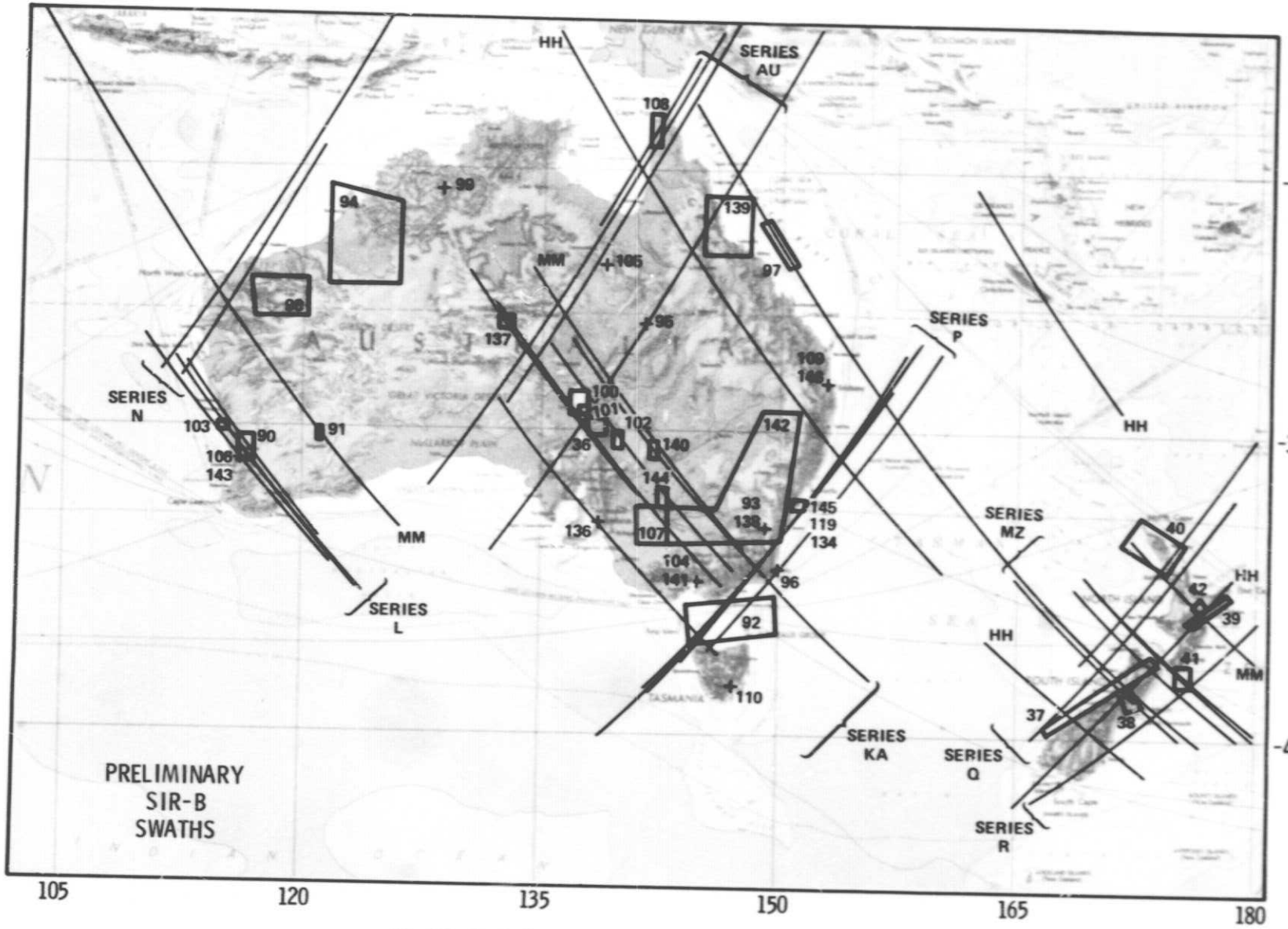

Fig. 3-9. Australia and New Zealand: preliminary SIR-B swaths

Section IV
The SIR-B Science Investigations

N85-17212

The Interpretation of SIR-B Imagery of Surface Waves and Other Oceanographic Features Using In-Situ, Meteorological Satellite, and Infrared Satellite Data

Team Member:

T. Allan
Institute of Oceanographic Sciences
Surrey, United Kingdom

Collaborators:

T. Guymer
Institute of Oceanographic Science
Surrey, United Kingdom

P. Muller
Imperial College
London, United Kingdom

I. Description of the Investigation

A. Main Objective

The overall aim is to interpret SIR-B imagery of selected ocean areas near the United Kingdom using available data from ships and buoys, with particular emphasis on understanding the mechanisms involved in the backscattering of microwaves from the sea surface and their relationship to surface gravity waves.

B. Secondary Objective

To use a multispectral approach to study sea-surface expressions such as slicks, internal waves, and eddies. Infrared imagery from the operational NOAA satellites will be received contemporaneously with the SIR-B mission at the National Environmental Research Council (NERC) receiving station at Dundee. The preferred area of operation is the Western Mediterranean because:

(1) It is more cloud free than the sea areas around the United Kingdom.

(2) It is known to produce many fronts, eddies, and slicks.

(3) It is the southern limit of NOAA coverage from Dundee.

II. Description of the Experiment

Emphasis will be placed on three areas around the United Kingdom where we know wave observations will be made. These, together with the surface data that may be available, are shown on the attached map (Fig. 1).

We should also like to carry out a multispectral analysis of surface expressions in the Western Mediterranean (Fig. 2).

Additionally, since our original proposal was submitted, we have been made aware of a large-scale Norwegian experiment to measure surface waves around the Ekofisk field in the North Sea; this experiment should be initiated in September 1984. The position of the Ekofisk platform is shown on Fig. 1.

III. Approach for Data Acquisition, Handling, and Analysis

Essentially, the Institute of Oceanographic Sciences has been involved in assessing the potential value of satellite microwave remote sensing of the ocean surface since before the launch of Seasat. Undoubtedly, synthetic-aperture radar imagery has revealed a wealth of surface detail that could have been observed in no other way. These surface expressions must be related to deep-ocean and coastal processes that take place within the water column and could therefore act as a valuable aid in interpreting physical interactions.

The striking wave imagery revealed by Seasat – especially around the Joint Air-Sea Interaction Experiment (JASIN) area, which we studied in detail – could prove to be of considerable value to commercial applications as well as to scientific investigations of wave generation and propagation. But there are severe doubts about the fidelity of the surface-wave directional spectrum revealed by an orbiting synthetic-aperture radar. The content of the SAR spectrum is almost certainly a function of the look direction relative to the dominant direction of wave propagation. It is this effect that we shall investigate by acquiring surface buoy measurements of wave height, direction, and period wherever they are reliably measured around the United Kingdom and by comparing these with two-dimensional Fourier transforms of the digital SAR scenes of surface waves.

The approach to a multispectral analysis of eddies and fronts will be different. We have noticed in the Western Mediterranean that Seasat SAR imagery revealed surface details that were completely absent from the corresponding infrared image taken from NOAA-5. Likewise, small temperature changes revealed in the IR record were not always evident in the SAR record. We wish to carry out further investigations on how best to integrate microwave and infrared imagery of the sea surface over an area that is relatively cloud free. The Western Mediterranean infrared data will be received by the NERC receiving station at Dundee.

IV. Expected Results

This is basically a high-risk experiment. The chances of surface waves around the United Kingdom being consistently large enough to be imaged over a series of consecutive days in September are not high. If we are lucky, waves might be imaged in one of the areas where we have reliable surface observations. Thus, although we would have preferred repeated passes over one location, DB 2, to increase the probability of imaging waves, we can now accept the alternative strategy of imaging over several areas around the United Kingdom and alerting all in-situ wave-measuring operations in these areas.

If all goes well, we expect to be able to extend the limited analysis already carried out on the Seasat SAR imagery.

Bibliography

Allan, T. D., "The Present Use of Satellites for Sea State Observations and Predictions," *J. Navigation*, Vol. 35, No. 3m, pp. 421-431, 1983.

Allan, T. D. "A Review of Seasat," in *Satellite Microwave Remote Sensing*, T. D. Allan, editor. Ellis Horwood, Chichester/Wiley, New York, 1983.

Allan, T. D., and Baker, J., "Digital Analysis of Seasat SAR Imagery Over the JASIN Area," in *Methods of Display of Ocean Survey Data*, R. Linton, editor. NERC publication, 1983.

Allan, T. D., "Oceanography from Space – Past Achievements, Future Programmes," in *Remote Sensing Applications in Marine Science and Technology*, A. P. Cracknell, editor. Reidel, Dordrecht, Netherlands, 1983.

Allan, T. D., and Guymer, T. D., "Seasat Measurements of Winds and Waves on Selected Passes Over JASIN," *Int. J. Rem. Sens.*, 1983 (in press).

Guymer, T. H., with Brown, R. A., Cardone, V. J., Hawkins, J., Overland, J. E., Pierson, W. J., Peteherych, S., Wilkerson, J. C., Woiceshyn, P. M., and Wurtele, M., "Surface Wind Analysis for Seasat." *J. Geophys. Res.*, Vol. 87, No. C5, pp. 3355-3364, 1982.

Guymer, T. H., "Validation and Application of SASS Over JASIN," in *Satellite Microwave Remote Sensing*, T. D. Allan, editor. Ellis Horwood, Chichester/Wiley, New York, 1983.

Guymer, T. D., "A Review of Seasat Scatterometer Data," *Phil. Trans. Roy. Soc.*, Vol. A309, pp. 399-414, 1983.

Guymer, T. H., and Taylor, P. K., "The Contribution of Seasat Microwave Data to the Joint Air-Sea Interaction Experiment," in *Large-Scale Oceanographic Experiments in the WCRP*, Vol. II, WCRP Publication Series, (1), 1983.

Kenyon, N. H., "Tidal Current Bedforms Investigated by Seasat," in *Satellite Microwave Remote Sensing*, T. D. Allan, editor. Ellis Horwood, Chichester/Wiley, New York, 1983.

Lonquet-Higgins, M. S., "Can Optical Measurements Help in the Interpretation of Radar Backscatter?" in *Satellite Microwave Remote Sensing*, T. D. Allan, editor. Ellis Horwood, Chichester/Wiley, New York, 1983.

Satellite Microwave Remote Sensing, T. D. Allan, editor. Ellis Horwood, Chichester/Wiley, New York, 1983, 526 pp.

Tucker, M. J., "Remote Sensing of the Marine Environment: the Potential for Engineering Application," *J. Soc. Underwater Tech.*, Vol. 9, pp. 8-13, 1983.

Tucker, M. J., "The Effect of a Moving Sea Surface on SAR Imagery," in *Satellite Microwave Remote Sensing*, T. D. Allan, editor. Ellis Horwood, Chichester/Wiley, New York, 1983.

Tucker, M. J., "Observation of Ocean Waves," *Phil. Trans. Roy. Soc.*, Vol. A309, pp. 371-379.

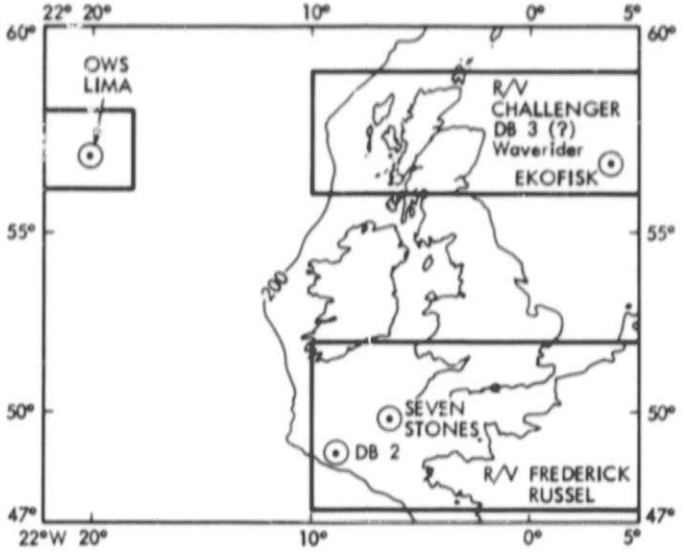

Fig. 1. Sites for wave observations around the United Kingdom

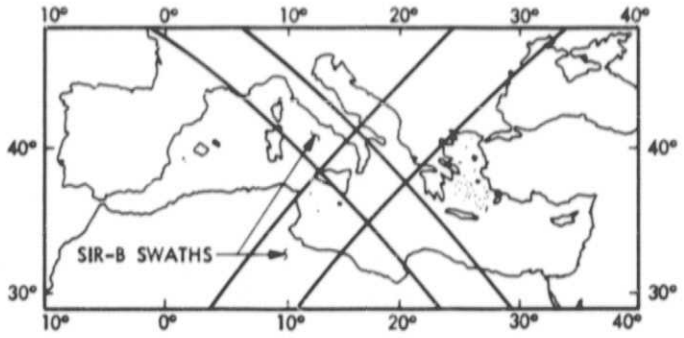

Fig. 2. Sites for multispectral analysis of surface expressions in the western Mediterranean

SAR Imaging Mechanisms of Ocean Surface Waves

Team Member:

W. Alpers
Max-Planck-Institut and Universität Hamburg
Hamburg, Federal Republic of Germany

Collaborators:

K. Richter
Deutsches Hydrographisches Institut
Hamburg, Federal Republic of Germany

H. Hühnerfuss
Institut für Organische Chemie und Biochemie
Hamburg, Federal Republic of Germany

I. Objectives

A. Ocean Surface Waves

The first objective of this investigation is to study the imaging mechanism of ocean surface waves by SAR. We will perform directional ocean wave spectrum measurements simultaneously with SIR-B overflights in the North Sea, and then compare these spectra with the SAR image spectra. Extensive theoretical studies on the imaging mechanism of surface waves by SAR have been performed by our group (e.g., Refs. 1 through 6); these studies need experimental testing. The main problem encountered in the imaging process is the proper description of the SAR response to the motion of the ocean surface. This response is highly nonlinear for a wide range of sea-state and radar parameters. We want to test with the SIR-B data whether the SAR response to wave motions is properly described by our theory. Since the sea state is very rapidly changing in the North Sea, we consider that the sea state is the principal variable parameter in this experiment for studying the imaging process. (That is, we have no specific requirements on the incidence angles.)

We have now a computer program (Monte-Carlo simulation) that allows computation of two-dimensional SAR image spectra from given two-dimensional ocean wave spectra. In our imaging model, the ocean wave L-band radar modulation transfer function (MTF) enters. Together with W. C. Keller of the Naval Research Laboratory in Washington, D. C., we will initiate a program in January 1984 to measure this MTF from the German North Sea Research Platform as a function of wind speed, incidence angle, and several ocean wave parameters. Inserting these MTFs, we anticipate that the calculated SAR image spectra will agree with the measured SAR image spectra.

B. Surface Films

The second objective of this investigation is to study the L-band SAR response to surface films of different chemical structure. A main goal of this part of the experiment is to find out whether mineral- (crude-) oil films can be discriminated against monomolecular surface films on L-band SAR images. Monomolecular films often occur on the ocean surface and are produced by plankton or fish. We plan to lay three

different artificial monomolecular films and a mineral-oil film on the ocean surface.

The three monomolecular surface-film materials are:

(1) Oleyl-alcohol.

(2) Oleic-acid-metyl ester.

(3) Poly-oxy-ethylene alcohol.

The film material of the monomolecular slicks is disseminated from a helicopter in small frozen chunks, such that large connected sea slicks covering an area of 1 to 3 km^2 are produced. The mineral oil is spilled from a ship. The amount of crude oil spilled into the North Sea will probably be 1000 kg, but it is subject to government permission.

The three monomolecular surface films of different chemical structure attenuate the short ripple (Bragg) waves differently. Therefore, we also expect different SAR responses. In addition, we will overfly these oil spills with a surveillance airplane that is especially equipped with sensors for detecting oil spills. These sensors are X-band SLAR, IR/UV scanners, and cameras.

II. Technical Plan

We have arranged that the German research vessel *Gauss* of the Deutsches Hydrographisches Institut (DNI, German Hydrographic Office) will be cruising from August 31 to September 14, 1984, in the German part of the North Sea shelf, which is shown on Fig. 1. A pitch-and-roll buoy for directional wave measurements will be operated from the ship. The position of the ship can be moved in this sea area such that it is in the SAR path during the Shuttle overflights. Wave directional measurements can be performed day and night.

The crude oil will be spilled from the *Gauss* during one suitable overflight. Adjacent to this mineral-oil film, the three monomolecular oil films will be laid from a helicopter. The helicopter will operate from the German North Sea Research Platform (54 degrees, 42.0 minutes N; 7 degrees, 10.0 minutes E).

We will arrange for the oil pollution surveillance plane owned by Riijkswaterstraat, North Sea Directorate, The Netherlands – but which is also at the disposal of the Deutsches Hydrographisches Institut – to survey the German Bight area and make several flights over the oil spills. The equipment used in this study is described below:

(1) Oil surveillance plane: Cessna-Titan 404. (The sensor package was developed by the Swedish Space Corporation.)

(2) SLAR: frequency, 9.4 GHz; ground resolution, 75m × 75m; display range, 20 to 80 km on both sides; peak power, 10 kW.

(3) IR/UV scanner: channels, 0 to 14 microns (IR) and 0.3 to 0.4 microns (UV); resolution, 2 meters at 1000 feet flying altitude; field of view, 80 degrees; sensitivity of the IR channel less than 0.5 K.

(4) Hand-held and vertical cameras.

References

1. Alpers, W. R., and Rufenach, C. L., "The Effect of Orbital Motions on Synthetic Aperture Radar Imagery of Ocean Waves," *IEEE Trans. Antennas Propagation*, Vol. AP-27(5), pp. 685-690, 1979.

2. Rufenach, C. L., and Alpers, W., "Imaging Ocean Waves by Synthetic Aperture Radars With Long Integration Times," *IEEE Trans. Antennas and Propagation*, Vol. AP-29, pp. 422-428, 1981.

3. Alpers, W., Ross, D. B., and Rufenach, C. L., "On the Detectability of Ocean Surface Waves by Real and Synthetic Aperture Radar," *J. Geophys. Res.*, Vol. 86, pp. 6481-6498, 1981.

4. Alpers, W., and Hasselmann, K., "Spectral Signal-to-Noise and Clutter Ratio for Ocean Wave Imaging Synthetic Aperture Radars," *Int. J. Remote Sensing*, Vol. 3, pp. 423-446, 1982.

5. Alpers, W., "Monte Carlo Simulations for Studying the Relationship Between Ocean Wave Spectra and Synthetic Aperture Radar Image Spectra," *J. Geophys. Res.*, Vol. 88, pp. 1745-1759, 1983.

6. Alpers, W., "Imaging of Ocean Surface Waves by Synthetic Aperture Radar – a Review," in *Satellite Microwave Remote Sensing*, edited by T. D. Allan. Ellis Horwood Ltd., England, Chapter 6, 1983.

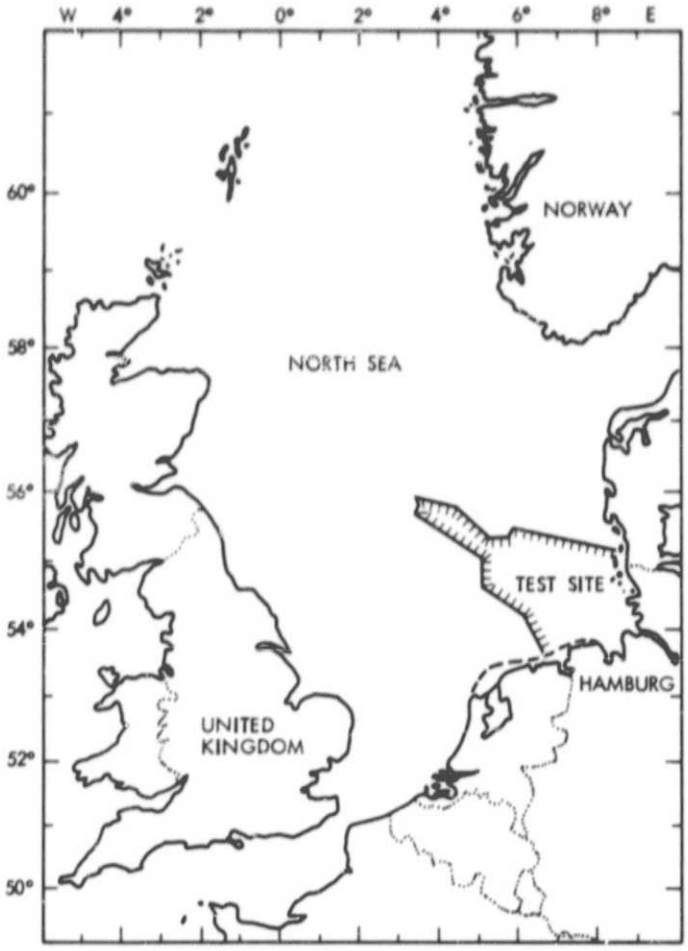

Fig. 1. Ocean surface wave experiment test site

ROVE Calibration and Inverse Scattering Experiment

Team Member:

E. P. W. Attema
Delft University of Technology
Delft, Netherlands

Collaborators:

P. Binnenkade
National Aerospace Laboratory
Amsterdam, Netherlands

Th. A. de Boer
Centre of Agrobiological Research
Wageningen, Netherlands

J. J. Gerbrands
Delft University of Technology
Delft, Netherlands

A. R. P. Janse and **L. Stroosnijder**
Agricultural University Wageningen
Wageningen, Netherlands

G. P. de Loor
Physics Laboratory TNO
Den Haag, Netherlands

J. Stolp
Stiboka Wageningen
Wageningen, Netherlands

I. Description of the Investigation

In contrast to remote sensing systems working in other portions of the electromagnetic spectrum, microwave remote sensing systems offer the important potential of measuring the parameters of the Earth's surface quantitatively without the need of supporting surface observations. Measurements can be made day and night under adverse weather conditions because of the transparency of the atmosphere at microwave frequencies. Important applications of this capability are in the areas of wind determination at sea and, for agriculture and forestry, the estimation of soil moisture, soil roughness, and vegetation cover.

To fully realize this potential with spaceborne SAR, the instruments involved must be calibrated and a reliable relation

must be available between the radar backscattering coefficient and the surface parameters of interest.

The objectives of the present experiment are, therefore, verification of SIR-B calibration using airborne scatterometer underflights and validation of surface parameter estimation using in-situ data collection in a unique well-controlled reclaimed land area (polder) in the Netherlands.

II. Description of the Experiment

An ideal method for validating the attempts made to radiometrically calibrate SIR-B would be to image a uniform extended target of known radar cross section. A very good approximation of such targets can be found in the Netherlands' polder area, where the agriculture is on large fields under strict governmental control (Fig. 1). The homogeneity of these fields in terms of flatness, soil type, and agricultural practice is unique. To determine the actual radar cross section of the fields under investigation, underflights with DUTSCAT, a specially designed multifrequency dual-polarization airborne scatterometer under construction at the Delft University of Technology, will be used (Fig. 2).

In the second part of the experiment, SIR-B imagery taken at different incidence angles will be used to produce estimates of soil moisture and microroughness by applying inverse scattering algorithms based on a currently available multilayer scattering model for vegetation-covered soil (Ref. 1). This model, based on past experience acquired in a radar signature research effort of over ten years (Ref. 2), indicates that the radar cross section of these types of targets depends on a limited number of predominant surface parameters, such as soil moisture, soil (micro-) roughness, and biomass. The relative importance of these depends on radar parameters (incidence angle, wavelength, polarization) and on crop type. For a one-dimensional SAR (single frequency, single polarization, single incidence angle) any of the above surface parameters can be remotely sensed successfully only if there exist sensor parameter combinations for which the sensitivity for one parameter dominates the others. However, when multiangle imagery is available, the inverse scattering problem may be solved using a suitable signature model. In the present experiment, radar-derived estimates will be compared with data acquired simultaneously in situ.

III. Approach for Data Acquisition, Handling, and Analysis

The acquired SIR-B imagery at different incidence angles will first be subjected to manual interactive or automated field boundary detection, in the latter case using a split-and-merge algorithm that has been successfully applied to radar data taken over the same area. The next step will be within field averaging of intensity to yield a table of field-averaged, radar cross sections as a function of incidence angle for a certain number of fields. These numbers will be compared to the airborne scatterometer results.

The same data will also be used to fit the soil scattering model described in Ref. 1 to yield best-fit soil moisture and roughness values for the fields under investigation, assuming, as a first-order approximation, the vegetation to be sufficiently transparent to L-band. The best-fit estimates are then compared with in-situ estimates.

As a second step, the model parameters will be adjusted to allow for an increasing effect of vegetation cover both in volume scattering and in attenuation. With the adjusted model, the soil moisture, roughness, and biomass will then be estimated again using the above fitting procedure.

The final estimates will be finally compared with the in-situ estimates.

IV. Expected Results

It is expected that the experiment will produce a table of SIR-B-to-DUTSCAT biases over a number of different uniform fields of sufficient size. To evaluate the significance of these biases, an error budget for DUTSCAT at L-band will be given.

Furthermore, the experiment will demonstrate the capabilities of quantitatively estimating both soil moisture and roughness with multiangular L-band imagery. The experiment will also shed some light on the effect of vegetation cover and the ability to estimate biomass for a certain number of important agricultural crops. If this part of the experiment meets with success, it would be the first time a spaceborne SAR proves to be an accurately radiometrically calibrated tool from which actual surface parameters can be derived quantitatively.

References

1. Hoekman, D., et al. (1982), "A Multilayer Model for Radar Backscattering From Vegetation Canopies," 1982 International Geoscience and Remote Sensing Symposium (IGARSS'82), *Symposium Digest,* June 1-4, 1982, München, West Germany, 1982, pp. 4.1-4.7.

2. de Loor, G. P., et al. (1982), "The Dutch ROVE Program," *IEEE Trans. on Geoscience and Remote Sensing,* January 1982, Vol. GE-20, No. 1, pp. 3-11.

Fig. 1. Seasat imagery of the Netherlands polder area; frame center: N 52° 30′, E 5° 30′ (image processed by DFVLR/WT-DA-BV for ESA/EARTHNET)

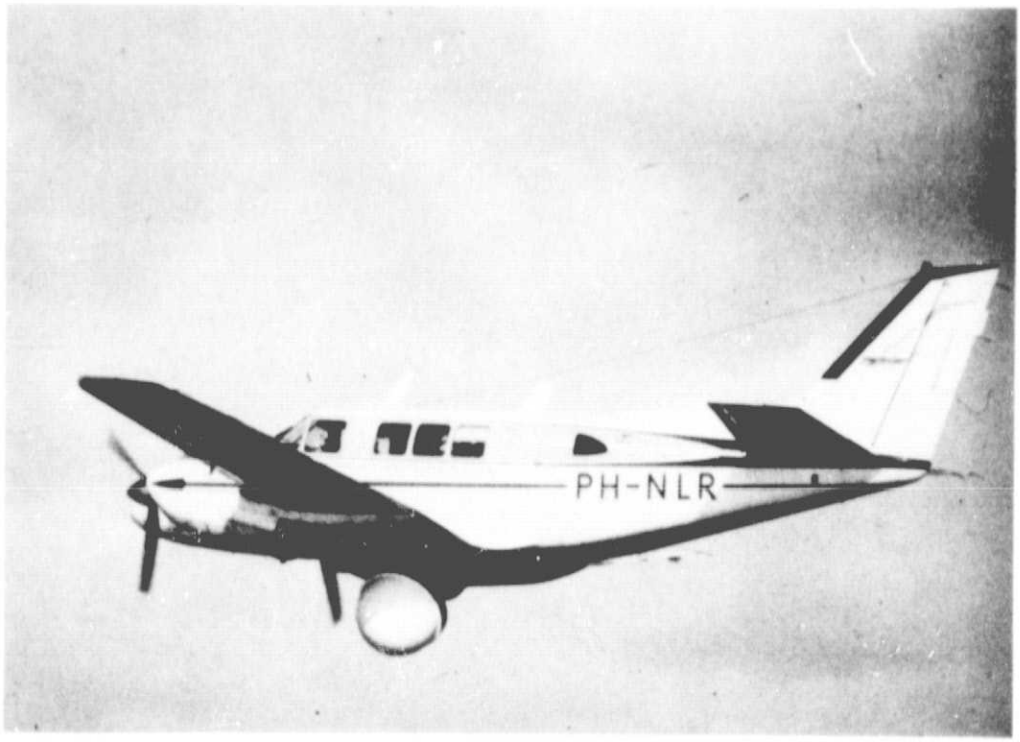

Fig. 2. DUTSCAT in flight

The Spatial Evolution of the Directional Wave Spectrum in the Southern Ocean: Its Relation to Extreme Waves in the Agulhas Current

Team Member:

R. C. Beal
The Johns Hopkins Applied Physics Laboratory
Laurel, Maryland

Collaborators:

A. Goldfinger, D. Irvine, F. Monaldo, and **D. Tilley**
The Johns Hopkins Applied Physics Laboratory
Laurel, Maryland

R. Shuchman, D. Lyzenga, and **J. Lyden**
Environmental Research Institute of Michigan
Ann Arbor, Michigan

P. DeLeonibus and **C. Rufenach**
National Oceanic and Atmospheric Administration
Washington, D.C.

F. Shillington
University of Cape Town
South Africa

E. Walsh and F. Jackson
Goddard Space Flight Center
Greenbelt, Maryland

I. Description of the Investigation

The primary geographic focus of this experiment is the southeastern coast of South Africa, a region long notorious for its hazards to ships attempting to take advantage of the strong Agulhas Current. The hazards, which sometimes take the form of extreme (>20-m height) waves, can sink or seriously damage ocean vessels (Ref. 1). Little data exists on the occurrence of these extreme waves, and little is known of their causes. They are known to originate from the interaction of swell (propagating northward from the extreme Southern Ocean) with the strong, generally opposing Agulhas Current, but they may be triggered by a particularly favorable set of local wave conditions.

With the recent advent of spaceborne SAR, it may be possible to monitor certain properties of the ocean wave directional spectrum, and to track the long swell systems as they

propagate northward to encounter the Agulhas. Recent Seasat SAR analysis on well-calibrated digital spectra has confirmed that spaceborne SAR, under at least some environmental conditions and instrument geometries, can accurately track multiple wave systems over several hundred kilometers (Refs. 2 and 3). Similarly, recent investigations have also suggested the possibility of measuring surface winds and ocean currents using SAR data (Ref. 4).

The secondary geographic focus is an area centered just off the southwest tip of southern Chile, at the northern limits of the Drake Passage. SIR-B verification and calibration experiments will be conducted by collecting simultaneous and coincident measurements of the directional energy spectrum from the NASA/Wallops P-3 aircraft, using a surface-contour (raster-scanning) radar and a surface-wave (conically-scanning) spectrometer.

II. Description of the Experiment

This experiment is specifically designed around the unique capability of SIR-B to overcome key limitations of the Seasat SAR data set, and to extend the existing Seasat results into new areas. Specifically, we intend to exploit SIR-B characteristics in the following ways:

(1) Track ocean wave systems having high significant wave heights over many thousands of kilometers and under a variety of environmental conditions.

(2) Utilize the variable-incidence-angle capability to examine wave imaging quality and to attempt Doppler current measurements.

(3) Verify that the lower range-to-velocity ratio of SIR-B will lead to improved response of azimuth-traveling wave systems.

As shown in Fig. 1, the primary scientific collection sites are in the vicinity of ascending orbits where the swell originates, and northeastward through and past the Agulhas core. Secondary verification sites are shown in Fig. 2. All ascending and descending passes in these two areas are of interest for data acquisition.

Our initial aims will be

(1) To obtain a single set of orthogonally-collected (20° incidence) ocean-wave spectra and to correct for the total system transfer function.

(2) To obtain two Doppler profiles (i.e., signal tapes) of the Agulhas Current at 45° incidence. This data set will be useful in studying current detection.

(3) To obtain at least one pass with variable squint, and to investigate the azimuth dependence of backscatter.

(4) To obtain at least two sets of SAR wave spectra for comparisons with the aircraft underflights off the coast of Chile, and to verify the SAR capability for measuring true directional energy spectra.

With these initial objectives accomplished, we will then move into the applications aspect of the experiment, i.e., global wave tracking and wave/current interactions both around the Agulhas region and the Drake Passage, and a more comprehensive time/space description of the two-dimensional wave-energy fields present during the experiement. This aspect of the experiment will involve blending together data from South African wave-rider stations (cf, Ref. 5), simultaneous current profiles of the Agulhas, and the various wave measurements obtained from the NASA P-3 aircraft in the Drake Passage.

References

1. Schumann, E. H., 1980, "Giant Wave: The Anomalous Seas of the Agulhas Current," *Oceans,* Vol. 13, pp. 27-31.

2. Beal, R. C., Tilley, D. G., and Monaldo, F. M., 1983a, "Large and Small Scale Spatial Evolution of Digitally Processed Ocean Wave Spectra from the Seasat SAR," *J. Geophys. Res.,* Vol. 88, No. C3, pp. 1761-1778, February 28.

3. Beal, R. C. et al., 1983b, *The Spatial Evolution of the Directional Wave Spectrum in the Southern Ocean: Its Relation to Extreme Waves in the Agulhas Current,* Proposal to the NASA Shuttle Imaging Radar-B Announcement of Opportunity, March 18.

4. Shuchman, R. A., Rufenach, C. L., Gonzalez, F. I., and Klooster, A., 1979, "The Feasibility of Measurement of Ocean Surface Currents Using Synthetic Aperture Radar," *Proc. 13th International Symposium on Remote Sensing of Environment,* Ann Arbor, Michigan, pp. 93-102.

5. Shillington, F. A., 1981, "Low Frequency 0.045 Hz Swell from the Southern Ocean," *Nature*, Vol. 290, pp. 123-125.

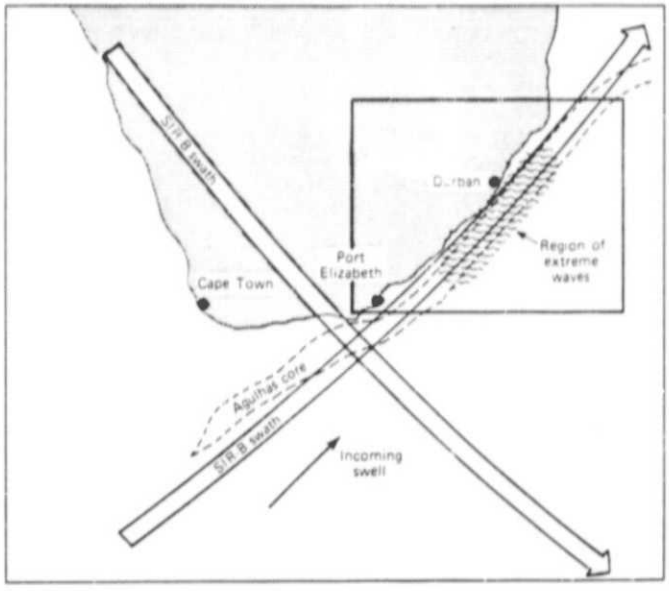

Fig. 1. SIR-B data processing priorities for the Agulhas/Rogue waves experiment (locations are approximate only)

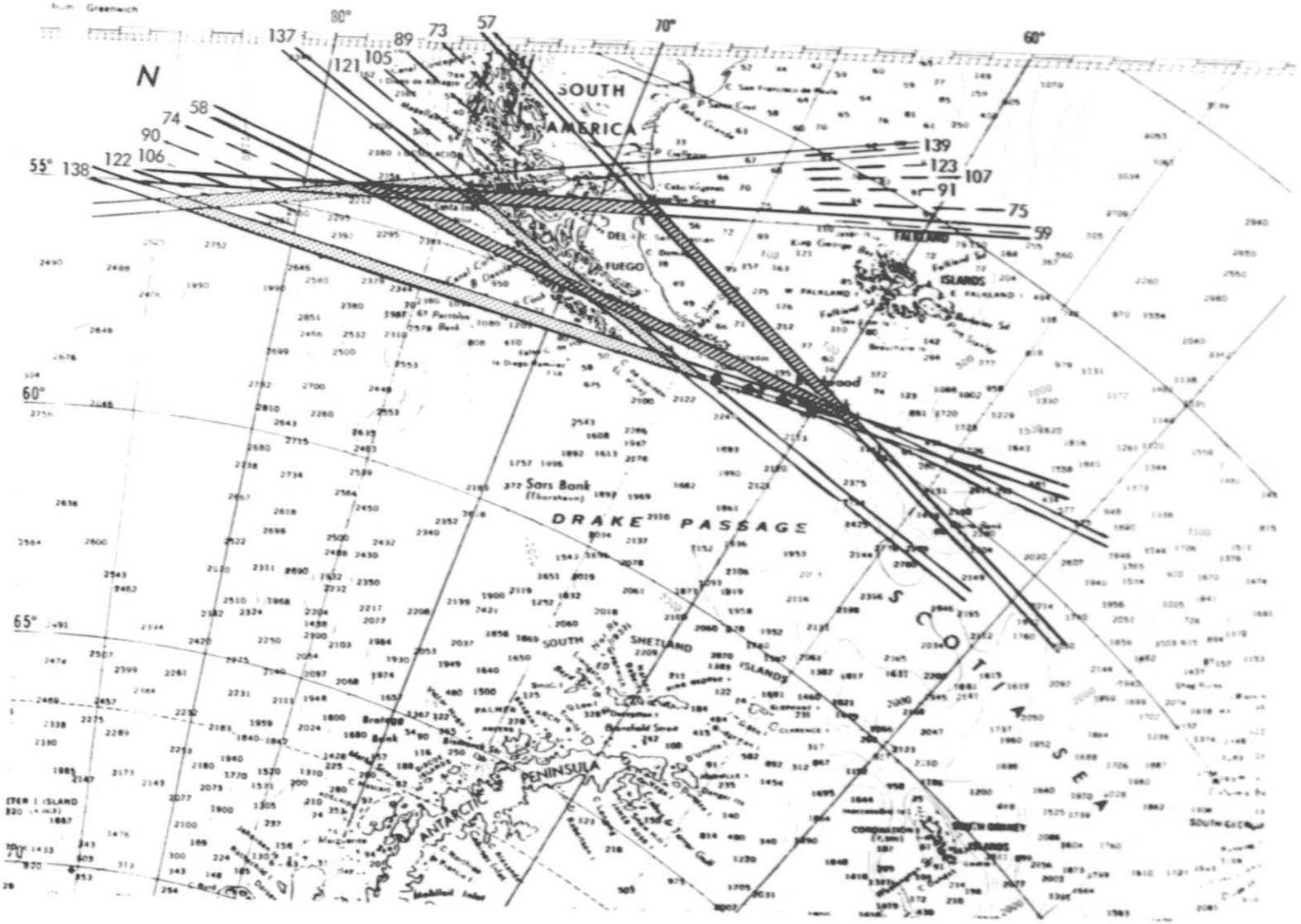

Fig. 2. Predicted SIR-B swaths for NASA P-3 aircraft underflights

Application of SIR-B Data for Groundwater Exploration in the Arabian Shield and Sand-Drift Monitoring in the An Nafud and Al Jafurah Fringe Areas, Kingdom of Saudi Arabia

Team Member:

G. L. Berlin
U.S. Geological Survey
Flagstaff, Arizona

Collaborators:

M. A. Tarabzouni and **Z. M. N. Munshi**
Saudi Arabian National Center for Science and Technology
Riyadh, Saudi Arabia

P. S. Chavez, Jr.
U.S. Geological Survey
Flagstaff, Arizona

I. Description of the Investigation

The primary objectives of the investigation are to determine fully the utility of SIR-B images for: (1) providing valuable surface indicators for ground-water prospecting in the Arabian Shield (Task 1), and (2) identifying and assessing defining characteristics of sand sheets, sand streaks, and sand dunes in the fringe areas of An Nafud and Al Jafurah (Task 2) (Fig. 1). Specific objectives include the following:

(1) Determine the incremental contribution of incidence angle to the total information that can be extracted from SIR-B standard and digitally-enhanced images in the Al Jafurah fringe area.

(2) Determine the incremental contribution of digitally-registered multisensor images (SIR-B, Landsat MSS, and Landsat TM if available in all test sites).

(3) Develop a groundwater exploration plan for the Ha'il test area in the Arabian Shield.

(4) Implement a multitemporal analysis (SIR-A and SIR-B images) to determine if sand movement occurred in the fringe area of An Nafud (Al Jawf test site) between 1981 and 1984.

(5) Determine if the SIR-B radar pulses penetrated drift sand in the Al Jawf and Al Jafurah test sites as was first discovered for the hyperarid region of the eastern Sahara with SIR-A data.

(6) Determine the best system parameters for future use of NASA spaceborne imaging radars for desert groundwater prospecting and eolian monitoring studies.

II. Description of the Experiment

This SIR-B investigation addresses two important problems in the Kingdom of Saudi Arabia – the discovery of new

groundwater reserves in the Arabian Shield (Task 1) and the monitoring of drifting sand deposits (Task 2). The Ha'il region serves as the test site for Task 1, and the Al Jawf and Al Jafurah areas serve as test sites for Task 2 (Fig. 1).

Task 1 is concerned with developing and testing a conceptual geohydrologic model applicable to groundwater exploration in the Arabian Shield. The three-dimensional model relates pertinent geologic, geomorphic, hydrologic, and biologic features and their interrelationships with subsurface hydrologic conditions. Our approach is to evaluate the utility of SIR-B standard and digitally-enhanced images and Landsat MSS and TM (if available) digitally enhanced images for identifying and assessing the environmental interrelationships. The incremental value of each data set will be determined, and integrated interpretive results will then be used to develop an exploration plan that predicts groundwater recharge, occurrence, and movement. We will visit those areas targeted as favorable groundwater sites to determine which warrant geophysical testing and/or the drilling of exploration wells.

Task 2 is concerned with determining the contribution of (1) multilook SIR-B images, (2) SIR-B digitally registered images, and (3) multisensor integrated images (SIR-B, Landsat MSS, and TM, if the latter is available) for identifying and assessing the defining characteristics of mobile sand sheets, sand streaks (stringers), and sand dunes. The test sites selected for this task lie in the fringe areas of two sand seas – An Nafud and Al Jafurah.

For the Al Jawf test site (An Nafud), which was imaged by SIR-A, the eolian deposits generally assume a streak of stringer form. Because the region is largely uninhabited, no stabilization programs have been implemented by the government. The second test site, Al Jafarah, represents an area where mobile sand has impacted upon transportation systems, urban centers, and agricultural areas. Unless stabilized, the eolian deposits are highly mobile and have been known to advance 12 meters in a single year. For this reason, government countermeasures have included the planting of millions of eucalyptus and tamarisk trees, the placement of sand fences, and the spraying of the windward side of dunes with asphalt or oil emulsions.

During the OSTA-3 mission, team members will collect ancillary ground-truth information in the Task 2 test sites. Helicopter and associated field vehicle and field camp support will enable us to reach numerous measurement stations (locations determined by advance field reconnaissance). Measurements will determine sand depth (hand digging, augering, and possibly electromagnetic sounding), moisture content, grain-size distributions, reflectance properties (hand-held radiometers), and vegetation cover when present (line-intersect method). Aerial-oblique and ground photographs (35-mm color and color infrared) will be taken at all sampling stations. In addition, supportive weather data for the period will be obtained from the appropriate meteorological stations.

Once the image interpretation phase has been completed, ground surveys will be carried out to provide necessary baseline information to evaluate the potential usefulness of SIR-B and other remotely sensed data for eolian applications in the Kingdom of Saudi Arabia. Results will be directly applicable to the goals of the Saudi Arabian National Desertification Committee, chaired by Dr. Zaki Munshi, who is a collaborator on the SIR-B Project.

III. Data Acquisition and Handling

A. Landsat MSS Independent Processing

Once the survey-optical SIR-B images are received from JPL, the appropriate digital Landsat MSS frames will be selected from the three test sites (Fig. 1). An attempt will be made to select MSS frames that have (1) no clouds, (2) high band-quality ratings, and (3) favorable Sun angles and azimuths. Digital subscenes that duplicate SIR-B ground coverage will be subjected to two types of digital processing – image restoration and image enhancement.

Image-restoration ("clean-up") algorithms, eliminate most of the undesired artifacts and distortions; the output data bases incorporate corrections for atmospheric scattering, Sun-elevation variations, noise striping, line drops, and geometric errors.

Theme-dependent enhancement algorithms will then be implemented on the three test-site data bases. Enhanced image products, incorporating contrast stretches, will include the following:

(1) Simulated natural color with edge enhancement.

(2) Color infrared with edge enhancement.

(3) High-pass filtered color images.

(4) First-difference horizontal, vertical, and diagonal images.

(5) Triple-ratio color images.

(6) Normalized-ratio color images.

Similar image restoration and enhancement algorithms will be applied to Landsat TM data if they are available.

B. SIR-B Independent Processing

If the standard digital SIR-B images are found to have speckle noise and/or shading problems, a correction technique

will be implemented to suppress these negative effects. Low-pass spatial filtering (smoothing function) may also be used to suppress noise.

Image enhancement in the form of various linear and non-linear stretches will be applied to those digital images lacking scene contrast to improve feature or pattern detectability. Certain of the multilook SIR-B images will also be filtered with high-pass spatial algorithms to enhance wadi networks, lineaments, and linear features (e.g., dikes) (Test Site 1), plus geologic and geomorphic contacts or boundaries (all test sites).

C. Data Merging

The first task will center on coregistering the Landsat MSS images and the SIR-B multilook images. To accomplish this, the following operations will be executed sequentially: (1) both the Landsat MSS (also TM data if available) and SIR-B image data will be preprocessed to remove undesirable artifacts and geometric distortions; (2) the MSS data will be scaled during the geometric correction stage to the same grid and pixel size as the higher resolution SIR-B data; and (3) corresponding tie-points will be identified on both the MSS and SIR-B data sets and used to digitally register the images.

Once the data sets have been coregistered, several avenues of enhancement will be explored in our study. For instance, one radar image in the digital domain can be added to, subtracted from, or divided into each of the MSS bands, producing new bands 4, 5, and 7 for color combining. Correlation matrices and arithmetic mean and standard deviation values for the SIR-B and MSS images will also be used to determine which data sets should be merged.

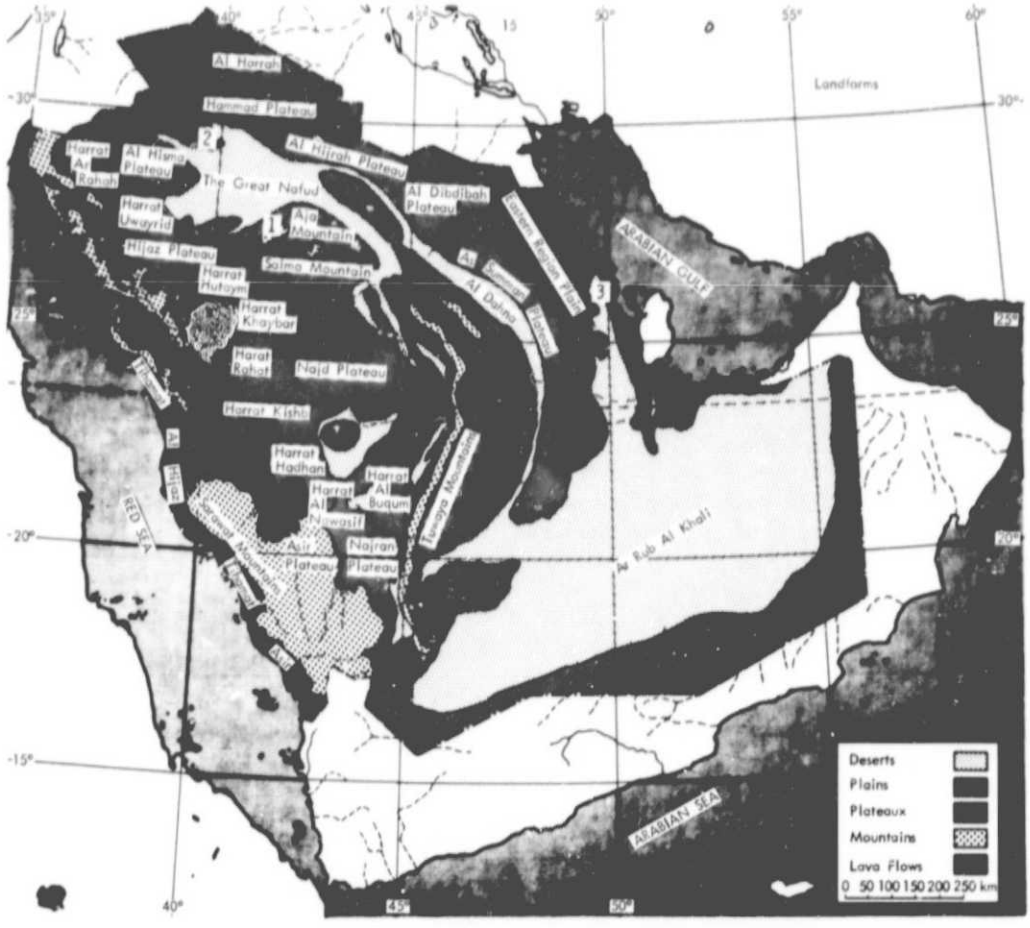

Fig. 1. SIR-B test sites, Kingdom of Saudi Arabia: (1) Ha'il, Task 1; (2) Al Jawf, Task 2; and (3) Al Jafurah, Task 2

Tectonic, Volcanic, and Climatic Geomorphology Study of the Sierras Pampeanas Andes, Northwestern Argentina

Team Member:

A. L. Bloom
Cornell University
Ithaca, New York

Collaborators:

M. R. Strecker and **E. J. Fielding**
Cornell University
Ithaca, New York

I. Introduction

The proposed analysis of SIR-B data extends our current research in the Sierras Pampeanas and the Puna of northwestern Argentina to three major topics:

(1) Determination – by digital analysis of mountain-front sinuousity – of the relative age and amount of fault movement along mountain fronts of the late-Cenozoic Sierras Pampeanas basement blocks.

(2) The age and history of the boundary across the Andes at about 27°S latitude between continuing volcanism to the north and inactive volcanism to the south.

(3) The age and extent of Pleistocene glaciation in the high sierras, and the comparative importance of climatic change and tectonic movements in shaping the landscape.

The integration of these studies into other ongoing Cornell geology projects (Ref. 1) will contribute to the understanding of landform development in this active tectonic environment and help distinguish between climatic and tectonic effects on landforms. On a larger scale, it will provide us with more knowledge about interplate dynamics and the deformation of two contrasting parts of the upper plate during ocean-continent subduction. The Sierras Pampeanas (between 27° and 33°S Lat) lie in a region of shallow and destructive seismicity over a segment of low-angle ("flat-slab") subduction of the Nazca lithospheric plate. No active volcanoes occur in this region in contrast to the Puna (north of 27°S), which has modern volcanism and lies over a steeply subducting Nazca Plate segment.

II. Style and Timing of Late-Cenozoic Fault Movements

Areas of active faulting can be evaluated with the mountain-front sinuosity index: the ratio of the measured length of a segment of mountain front to the straight-line distance between the end points along a fault-bounded mountain (Ref. 2). A low sinuosity index characterizes straight, and therefore presumably tectonically active, high-angle mountain-bounding faults. Exceptions occur however, such as the straight segment of Sierra Quilmes, which is only the contact of the dip slope with basin alluvium (Fig. 1). An embayed, eroded mountain front

with a higher sinuosity index is indicative of an inactive boundary. The western slope of Sierra Aconquija is bounded by a high-angle, east-dipping reverse fault with metamorphic rocks thrust westward over upper Tertiary sedimentary rocks (Fig. 1). The measured index of 1.7 (scale of 1 to 10) suggests considerably high tectonic activity. Tephra collected from undisturbed alluvial terraces along the western side of Sierra Aconquija will permit closer restraints on the minimum age of fault movements through radiometric dating. Mountain-front sinuosity indices that are calibrated with radiometric ages in this area will eventually be extrapolated to evaluate fault chronology of other mountain fronts within the Sierras Pampeanas.

III. Spatial Distribution and Timing of Volcanic Events

The Puna (north of 27°S) stands above 4 km elevation, and includes many young volcanic features. In its southern part is Cerro Galan, one of the world's largest resurgent calderas (Refs. 3, 4, and 5). We hope to characterize the age of the volcanic landscape in the southern Puna by measuring surface texture and roughness parameters. We want to test the hypothesis that the southern boundary of active volcanism coincides with the boundary between steep-slab and flat-slab subduction and determine the timing of volcanic shut-off over the flat-slab zone.

IV. Climatic Change vs Tectonics in Landform Development

Valleys and piedmont regions of northwestern Argentina are characterized by multiple valley and piedmont terraces that have traditionally been explained by alternating climatic changes in the Pleistocene Epoch. Terrace building has been correlated with glacial or pluvial intervals, and degradation or dissection correlated with interglacial or interpluvial intervals. However, Pleistocene glaciation was very restricted on the high but relatively dry mountain peaks. SIR-B images will permit detailed analyses of surface roughness, texture, and pattern to determine piedmont and valley terrace distribution adjacent to glaciated mountains. If extreme topographic distortion can be overcome, we will also look for surface roughness and textures characteristic of possible glacial features in high mountain valleys. The spatial and stratigraphic relations between the glacial features and terraces will help to discriminate between climatic and tectonic controls on terrace development. We will test SIR-B image analyses by continuing field studies such as terrace mapping and correlation, surface lithology and cobble-size measurements, and radiometric dating of terraces.

For mountain-front sinuosity indices, we will need SIR-B images at multiple azimuths to compensate for the directional dependence of the radar data. For surface-roughness analysis, we will need multiple look angles of the same areas. For both types of analyses, pixel-to-pixel registration will be required, where topographic distortion is not too severe. Coregistered images can then be analyzed in ways comparable to multispectral images, providing information about features that trend in various directions, and allowing parameters that are dependent on incidence angle, such as surface roughness, to be measured. If thematic mapper (TM) data are available, they will also be coregistered with SIR-B data and used to identify glacial and volcanic features. The response of surface materials to the different radar and multispectral wavelengths will be used to discriminate bedrock from its weathering and erosional products and, with pattern and texture analyses, will be used to discern the relative ages of volcanic and glacial landforms and sediments. In as many places as is possible, features will be studied on the ground to identify the surface materials and geomorphology that produce the radar and multispectral responses.

References

1. Jordan, T. E., Isacks, B. L., Allmendinger, R. W., Brewer, J. A., Ramos, V. A., and Ando, C. J., 1983, "Andean Tectonics Related to Geometry of Subducted Nazca Plate," *Geological Society of America Bulletin,* Vol. 94, pp. 341-361.

2. Bull, W. B., and McFadden, L. D., 1977, "Tectonic Geomorphology North and South of the Garlock Fault, California," in *Geomorphology in Arid Regions,* edited by D. E. Deohring. SUNY-Binghamton Publications in Geomorphology, pp. 115-138.

3. Friedman, J. D., and Heikan, G., 1977, in *Skylab Explores the Earth.* NASA Special Publication 380, National Aeronautics and Space Administration, Washington, D.C.

4. Francis, P. W., Hammill, M., Kretzschmar, G., and Thorpe, R. S., 1978, "The Cerro Galan Caldera, North-West Argentina and Its Tectonic Setting," *Nature,* Vol. 274, pp. 749-751.

5. Francis, P. W., O'Callaghan, L., Kretzschmar, G. A., Thorpe, R. S., Sparks, R. S. J., Page, R. N., de Barrio, R. E., Gillou, G., and Gonzalez, O. E., 1983, "The Cerro Galan Ignimbrite," *Nature,* Vol. 301, pp. 51-53.

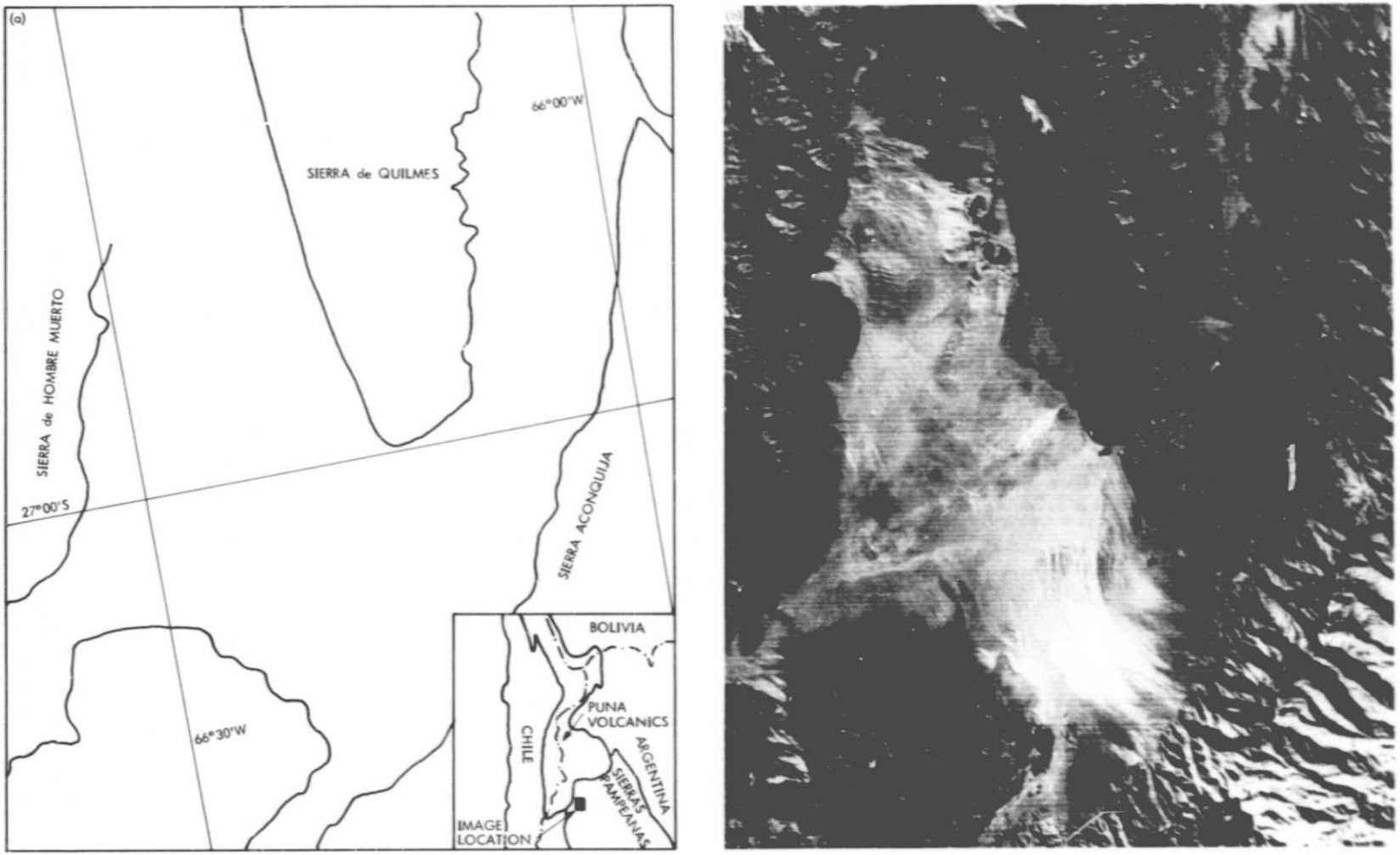

Fig. 1. Southern end of Sierra Quilmes, Sierra Aconquija and adjacent areas, northwestern Argentina: (a) map with inset showing location of image; (b) image enlarged from LANDSAT MSS-band 7 image E-2147-13381 of 18 June 1975, center latitude 27.2°S and longitude 66.3°W, Sun elevation 24° and azimuth 42°

N85-17216

Deforestation, Floodplain Dynamics, and Carbon Biogeochemistry in the Amazon Basin

Team Member:

M. L. Bryan
Jet Propulsion Laboratory
Pasadena, California

Collaborators:

T. Dunne and **J. Richey**
University of Washington
Seattle, Washington

J. Melack and **D. Simonett**
University of California
Santa Barbara, California

G. Woodwell
Marine Biological Laboratory
Woods Hole, Massachusetts

I. Description of the Investigation

Three aspects of the physical geographic environment of the Amazon Basin are considered: (1) deforestation and reforestation, (2) floodplain dynamics, and (3) fluvial geomorphology. Three independent projects are coupled in this SIR-B experiment to improve the in-place research and to ensure that the SIR-B experiment stands on a secure base of ongoing work. For each case, major benefits to be obtained from the SIR-B images center on: (1) areal and locational information, (2) data from various depression angles, and (3) digital radar signatures. Although the work conducted in these research projects extends over several years, specific ground truth for well defined areas will be obtained during SIR-B operations (1984). Detailed analysis will be conducted for selected sites to define how well SIR-B data can be used for: (1) definition of extent and location of deforestation in a tropical moist forest, (2) definition and quantification of the nature of the vegetation and edaphic conditions on the varzea (floodplain) of a central reach of the Amazon River, and (3) quantification of the accuracy with which the geometry and channel shifting of the Amazon River may be mapped using SIR-B imagery in conjunction with other remote sensing data.

II. Objectives

The objectives are to conduct investigations of a tropical rain forest. Three aspects of the physical environment to be studied in detail are:

(1) Deforestation and reforestation.

(2) Floodplain dynamics.

(3) Fluvial geomorphology of a large tropical river.

With respect to the first portion of the investigation, the objective is to determine the accuracy with which location, areal extent, and rate of deforestation (Ref. 1) can be measured using SIR-B data. This objective focuses on the development of quantitative and qualitative interpretation keys for orbital L-Band radar data. Such keys will be for recent clearcuts, row crops, and tree plantations in a moist tropical environment. Techniques for the extrapolation of these keys to other moist tropical forests of the world will be developed.

The second area of study concerns the dynamics of floodplains in wet tropical ecosystems. The range of radar detectability of different edaphic conditions is to be determined. The primary objectives are to (1) quantify the degree to which the presence or absence of water beneath the canopy may be detected under closed canopies and at three different look angles (20, 35, 50 degrees), (2) quantify the degree to which the presence or absence of water in the presence of low-floating vegetation and grasses may be detected at these different look angles, and (3) quantify the degree to which radar texture at L-Band may vary in response to different swamp conditions at the different look angles.

The third objective is to ascertain the utility of orbital radars for detecting river-channel changes and to determine the degree of connection between the river and the various kinds of lakes on its floodplain. Because of the annual flooding of large portions of the Amazon river, the application of a general biogeochemical river model is complicated and exchanges of water and nutrients between the channel and floodplain must be quantified (Ref. 2). It is proposed that SIR-B data be utilized to identify sectors that can be integrated into a larger model of the river being developed for study of the biogeochemistry of carbon in large river basins. All study sites are identified in Fig. 1 and Table 1.

III. Approach

A. Fiscal Year 1984

This period will be spent primarily in the acquisition of collateral information and the interpretation of SIR-A data collected in November 1981. Using these data, we plan to identify the spectral signatures of SIR-A data for row crops, river banks, tree plantations, pasture, rubber plantations, undisturbed forest canopy, and different varzea habitats in the test areas. Clearcuts adjacent to or upstream from current or potential dam sites will be identified and mapped. These quantitative and/or qualitative results on vegetation will be compared with the work presently being conducted at JPL and the published results of others. With respect to deforestation, this work will concentrate on the state of Rondonia and Mato Grosso, with additional sites being defined by the availability of satellite and collateral data. Studies of the floodplain dynamics will focus on (1) determination of the signature of the major varzea habitats, (2) determination of the rates of channel shifting, (3) determination of drainage patterns and areal extent of terra firma and of inundated and noninundated floodplains, and (4) documentation of lake morphometry and the degree of interconnection between the lakes and river. With respect to the fluvial geomorphology studies, three reaches of the Amazon/Solimoes River have been identified for study (Ref. 3), viz: (1) 400 to 1200 km downstream from Tabatinga, the only reach where the river is freely meandering; (2) 1500 to 2200 km downstream from Tabatinga (Manacapuru to Obidos), an area of a broad, active floodplain of low sinuosity; and, as a target of opportunity, (3) 1200 to 1500 km downstream from Tabatinga (R. Japura to Manacapuru), a confined reach with low sinuosity and narrow floodplain. Field work will be conducted during the flight of SIR-B.

B. Fiscal Year 1985

The work during this period will concentrate on the examination and analysis of the SIR-B data to (1) ascertain if the data expectations were met, (2) evaluate the veracity of the interpretation schemes developed during the previous year as applied to SIR-B data, and (3) study change detection through the comparison of Radar Mapping of the Amazon (RADAM), SIR-A, and SIR-B data. The determination of the areal extent of deforestation for particular regions through the comparison of the several data sets will be included in these activities.

C. Fiscal Year 1986

This year will be employed primarily in the final write-up of experimental results, together with statements and discussion of the problems encountered, and including recommendations for future work.

IV. Anticipated Results

Interpretation keys for SIR-A and SIR-B imagery with respect to deforestation, reforestation, land use, and floodplain habitats will be developed. Although they will be developed primarily for optically correlated data, statistical data from selected digitally correlated data will be included. It is anticipated that, through the incorporation of the several radar data sets, rates and trends of deforestation in the study areas will be defined. These results will provide valuable quantitative inputs to global CO_2 models. The quantification

of the degree to which the presence (or absence) of standing water under low vegetation and under closed rain forest canopy may be detected at different radar depression angles is a major anticipated result from the study of the floodplain. The assessment of how the effects of different radar depression angles (for L-HH data) appears to relate to the overall structure of the plant community is also a major anticipated result. Finally, it is anticipated that there will be an assessment of the utility of using orbital radars such as SIR-B for mapping river channels and vegetative boundaries in moist tropical forests, together with the identification of temporal changes in these features.

References

1. Woodwell, G. M., Hobbie, J. E., Houghton, R. A., Meillo, J. M., Peterson, B. J., Shaver, G. R., Stone, T. A., and Park, A. B., 1983, "Changes in the Area of Forest in Rondonia Amazon Basin, Measured by Satellite Imagery," presented at the 6th Oak Ridge National Laboratory Life Science Symposium Global Carbon Cycle, Knoxville, Tennessee, October 30 – November 2, 1983.

2. Richey, J. E., 1983, "Pathways of Organic Matter and Nutrients in the Amazon River," EOS, *American Geophysical Union Trans.* (abstr.), Vol. 64, p. 17.

3. Mertes, L. A. K., and Dunne, T., 1983, "Channel Changes on the Amazon River," EOS, *American Geophysical Union Trans.* (abstr.), Vol. 64, p. 23.

Table 1. Deforestation, floodplain dynamics and carbon biogeochemistry in the Amazon Basin

Task	Site description
Deforestation (sites in order of priority)	1. Center of Rondonia 2. SIR-A/Belem-Brasilia Highway 3. North of Manaus 4. 500 km NW of Brasilia
Floodplain dynamics	Area around Manaus includes L. Janauaca, L. Calada, L. Miriti
Carbon (fluvial geomorphology) (sites in order of priority)	1. Large meander in Rio Japura 2. Mouth of Rio Ica 3. Mouth of Rio Madeira 4. Mouth of Rio Japura 5. Mouth of Rio Purus 6. West of Obidos

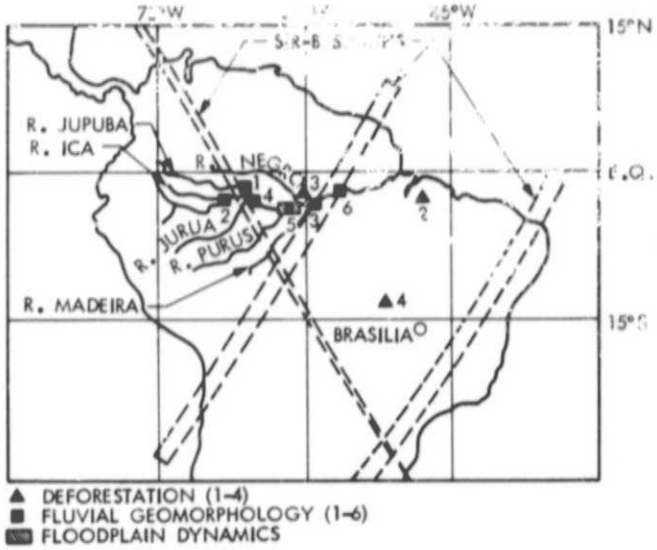

Fig. 1. Approximate SIR-B coverage

Investigations Involving Corner-Reflector Arrays, Signal Processing, and Oceanographic Studies

Team Member:

N. L. Bryans
Defence Research Centre Salisbury (DRCS)
Adelaide, Australia

Collaborator:

S. J. Anderson
Defence Research Centre Salisbury (DRCS)
Adelaide, Australia

I. Objectives

(1) To contribute to the effectiveness of the SIR-B program by deployment of arrays of passive corner reflectors on suitable surveyed sites to provide:

   (a) A surveyed ground marker for SIR-B orbital-correction calculations.

   (b) Reflectors for calibration.

   (c) Controlled distribution of reflectors for resolution and dynamic range investigations.

(2) To carry out signal processing investigations using a computing system based on three array processors.

(3) In conjunction with an existing DRCS program of oceanographic remote sensing using a large HF skywave radar, to investigate the synergistic benefits of simultaneous sensing of the ocean by two wide-area remote sensing systems (viz, SIR-B and the HF radar).

II. Description and Approach

A. Corner Reflector Experiment

The corner-reflector experiment will comprise two arrays situated at different locations and illuminated by different series of SIR-B passes.

It is planned that the main array will comprise eleven corner reflectors located so as to be illuminated by at least two passes at differing incidence angles. This array will be located at a suitable flat surveyed site on a dry lake bed in South Australia.

While dry conditions normally prevail in the far north of South Australia, the August/September period during which the SIR-B mission will occur is the end of winter and the beginning of spring, and thus the possibility of rain has to be considered. SIR-A imagery of Lake Torrens and some adjacent lakes (obtained at the end of summer) showed low reflectivity. The neaby Lake Eyre and Lake Frome was not covered by the SIR-A swath. A site survey early in 1984, including surface and subsurface soil sampling of Lake Eyre, Lake Frome, and

adjacent lakes covered by the SIR-A swath, will be carried out; from this, a site will be chosen. A secondary array comprising three reflectors will be placed at Fowlers Gap, New South Wales (latitude 31°10′S, longitude 141°40′E).

A conservative analysis was carried out of the reflector radar cross section (RCS) required to meet the objectives of the corner-reflector related experiments. Allowance was made for the same azimuth and incidence-angle losses used by Curlander (Ref. 1). The results obtained are the RCS sizes of triangular corner reflectors with a 9-dB RCS-to-clutter ratio allowance. 'Slightly' rough moist soil conditions were assumed.

On the basis of the foregoing, a corner-reflector array was determined with a range of radar cross-section reflectors to suit the objectives of the experiments.

For the dynamic-range experiment, it is planned to deploy corner reflectors with a range of radar cross sections. The largest will be a corner reflector with a gain in excess of 40 dB with respect to 1 square meter, and the lowest will be below 10 dB m^2. Intermediate values of RCS will be met by corner reflectors required for the other experiments described below.

For the radiometric calibration investigation, 1.7-m triangular corner reflectors are to be used (RCS = 28.0 dB m^2) to minimize errors due to angular orientation errors. These corner reflectors will be oriented as far as possible to the optimum azimuth and elevation angles for each SIR-B pass. The large size will reduce gain variation due to edge RCS-induced ripple. The use of an active radar calibrator (L-band transponder) would give greater accuracy, and the acquisition of such a unit is being investigated.

The resolution experiments will use five corner reflectors of approximately 20 dB m^2 RCS. These will supplement the corner reflectors already deployed by providing additional cases of more closely spaced reflectors.

For orbital-correction calculations, the corner reflectors deployed for the dynamic range and calibration experiments will provide a large-RCS, well defined array.

The extent to which geometric calibration will be addressed is dependent on the siting of the main array and the location in the image field of objects at surveyed locations. Additional markers for geometric correction may be deployed depending on assessed needs.

The spacing of corner reflectors will be chosen to allow investigation of image resolution using various signal processing techniques. The orientation of the array itself will be chosen to minimize the possibilities of side lobes from corner reflectors overlapping other corner-reflector images.

B. Signal Processing Experiment

1. Description of the Computing System. Signal processing will be carried out on an existing computing system that is presently optimized for the FFT-based Doppler processing of signals for another radar project.

The data processing/display system is under the control of a pair of PDP 11/34A computers. Attached to one computer via a UNIBUS are three array processors (ARO) and a 2-Mword multiport memory (MPM). Each of the AROs, for example, can perform a 2048-point complex FFT in 4.3 ms. A 40-bit complex word is used consisting of a common 8-bit exponent, a 16-bit real mantissa and 16-bit imaginary matissa. The MPM has up to 10 ports that can be simultaneously accessed at a 10-Mword/s rate. The MPM is linked to the second PDP 11/34A, which is used to control the displays. The primary display will consist of a Lexidata 3400 Graphics Processor.

The data input/output from the system will be via two STC 1951 tape drives. These two 9-track drives operate at 6250/1600 bits/in. The drives can dump data directly into MPM and then use an ARO to unpack the data.

2. Software Efficiency. Due to the size of the MPM, transform sizes should be limited to 2 Mwords for the sake of efficiency.

The time taken to process a 1024- × 1024-pixel SAR array based on the CRC digital processing (as an example) is estimated at 15 s. This figure is based on the assumption that techniques can be found to reduce the data-dependent operations to an insignificant fraction of the total number of operations involved in the processing and is achieved because of the large MPM.

For a typical SIR-B image array size, the efficiency drops dramatically, but is still very satisfactory by current standards. Allowing for disk shuffling required for nonconcurrent reading and writing of large amounts of data, the approximate time for a 4096 × 1024 CRC type of processing would be 300 s.

3. Proposed Experiments. In addition to the experiments described earlier, viz calibration (geometric and radiometric), resolution, and dynamic range, the following additional investigations are proposed.

(1) *Multilook Processing.* The Doppler bandwidth required for azimuth resolution varies from 310 Hz for 25 m to 1300 Hz for 6 m, assuming SIR-B has an orbital velocity of 7770 ms^{-1}. This means only one look can be utilized if an azimuth resolution of 6 m is to be achieved. Single- and multilook processing of various scenes will be investigated.

(2) *Speckle Noise Reduction.* Speckle noise reduction using spatial filtering instead of the multilook processing will be addressed. The speckle noise reduction inherent in the spatial filtering technique is greater than that achieved by multilook processing due to its two-dimensional nature.

(3) *Filtering.* Appropriate data will be selectively filtered to emphasize features of the data – for example, high-pass filtering to emphasize directionality. This is applicable to the investigation of periodic features in the landscape and to ocean imaging. Initially, the principal applications will be to ocean imaging, but at a later stage other land features may be investigated.

III. Oceanography

The JINDALEE Stage B radar is a large HF skywave radar located in Central Australia and looking to the northwest. Although it is being developed primarily for national defense, the remote sensing of the sea surface and subsequent inference of oceanic wind fields is an important mission for the radar. To support this part of the JINDALEE program, extensive observations and special experiments with off-shore beacons are planned. Particular emphasis will be placed on severe storms and tropical cyclones.

The viability of skywave radar sensing of the ocean surface at ranges up to 4000 km has been firmly established by U.S. researchers, particularly at NOAA, NRL, and SRI (e.g., Refs. 2 and 3). Australian scientists familiar with the U.S. work have already demonstrated similar capabilities with the JINDALEE radar and are presently attempting to extend them (e.g., Refs. 4 and 5). Observables include rms waveheight and swell period and direction. Not all of these are routinely available because of ionospheric distortion of the radar signal, but some (e.g., prevailing wind direction) are always accessible. Accuracies are typically comparable with values cited in the literature for Seasat.

HF radar shares with satellites the characteristic that its measurements are not point observations but averages over extended areas typically kilometers in extent. Thus, while they tend to be more meaningful than point observations as far as geophysical significance is concerned, it is difficult to obtain relevant sea-truth data for validation and refinement of the scattering models and the associated inversion algorithms. In this regard, any arrangement whereby satellite and HF radar measurements over a designated area could be compared would be of great mutual benefit.

The SIR-B mission provides an opportunity to acquire comparison data sets for a great expanse of ocean off northwest Australia.

The primary area of interest is between 10°S and 20°S latitude and 120°E and 130°E longitude, though some adjacent areas can be interrogated using the JINDALEE radar.

References

1. Curlander, J., Jet Propulsion Laboratory Interoffice Memo 3354-83-034, 17 October 1983 (JPL internal document).

2. Barrick, D. E., "Remote Sensing of Sea State by Radar," in *Remote Sensing of the Troposphere,* V. E. Derr, editor, Chapter 12. U.S. Government Printing Office, Washington, D.C., 1972.

3. Georges, T. M., "Progress Towards a Successful Skywave Sea-State Radar," *IEEE Tr.* Vol. AP-28, pp. 751-761, 1980.

4. Anderson, S. J., "The Remote Sensing of Tropical Meteorological and Oceanographic Phenomena by Over-the-Horizon Radar," invited paper presented to the International Conference on Tropical Cyclones, Perth, December 1979.

5. Anderson, S. J., "The Extraction of Wind and Sea State Parameters from HF Skywave Radar Echoes," paper presented at IREECON 83 International, Sydney, September 1983.

Southern Ocean Sea-Ice Morphology and Kinematics

Team Member:

F. Carsey
Jet Propulsion Laboratory
Pasadena, California

Collaborators:

B. Holt
Jet Propulsion Laboratory
Pasadena, California

S. Martin and **D. A. Rothrock**
University of Washington
Seattle, Washington

W. F. Weeks
U. S. Army Cold Region Research and Engineering Laboratory
Hanover, New Hampshire

V. Squire
Scott Polar Research Institute
Cambridge, England

I. Introduction

A number of scientific issues exist concerning the ice cover of the Southern Ocean. Up to the present, the only data of sufficiently fine resolution to resolve major ice features and thus permit description of ice conditions such as floe size and fracture patterns has been a few NOAA and Landsat scenes severely limitated by weather and light. Landsat scenes have not provided the repeated coverage required for fine-scale ice-velocity determination. The key scientific questions concern the transfer of momentum from the atmosphere to the sea, the consequent mixing of the upper ocean, and the budgets of heat and ice. To fully evaluate these processes, a detailed multiinvestigator, multidisciplinary study is needed involving scientists stationed on the ice, drifting data buoys, and satellite support. Prior to such a study, a pilot satellite experiment is called for to determine the applicability of imaging radar such as synthetic-aperture radar (SAR) for the description of ice type and movement. SIR-B is useful as the pilot instrument.

II. Objectives

The objectives of the proposed study are:

(1) For the Weddell Sea ice, to investigate the ranges of radar backscatter and the features identifiable as a function of illumination geometry.

(2) To conduct a scientific study, necessarily of a trial-study form, of the sea ice in the transition from compact pack to ice edge, including pack morphology, ice-drift speed, ice deformation, oceanic features, and ice and heat budgets.

(3) To examine the synergism of colocated radar and visible/IR images capitalizing on the differences in reflectance, backscatter, and surface temperature among the ice types expected in the region.

(4) To conduct correlation and image processing experiments on the SAR images to further an existing program in ice classification and feature tracking.

In the NASA Earth observations program, the SIR-B Southern Ocean ice study supports instrument and technique development for application of SAR and other observational data to scientific and operational problems. The large-scale, inhospitable conditions, and remoteness of the ice-covered seas calls for satellite observations, and the vigorous role of sea ice in climate, ocean dynamics, and operations motivates work in this area.

III. Description of the Experiment

These experiments will utilize spacecraft data exclusively; no in-situ measurements will be acquired. The attack on the four listed objectives involves the use of established methods of SAR image analysis in collaboration with recognized experts in the sea ice of the two polar regions and with the in-house expertise in remote sensing fundamentals. To investigate feature identification in the various images, the Shuttle photography, the Thematic Mapper (TM), and the SIR at various incidence angles, tables of features for each image "snapshot" will be constructed by a number of the individual collaborators. These tables will be compared and merged to find the relationship of discernability to instrument parameters. Once these tables are constructed for each image, the interinstrument synergism will be the natural outgrowth of differences in the tables. The principal kinds of differences will be of two sorts: features missed by one sensor and resolved by the other, and features of apparently opposite trends of strength or resolution in the images. Both such differences are valuable.

The approach to using SIR-B and TM in image-classification research is simply to utilize these images in an ongoing search for an optimum computerized classification scheme. At present, the source for images for this research is exclusively Seasat SAR, and it thus suffers from a severe regional, seasonal, and instrumental limitation. Even so, reasonable progress has been enjoyed in two methods of classification. One is based on attributes such as brightness itself, local mean, local variance, regional variance, and the like; the other is based on a mathematically strict method in which each pixel is described by a matrix of correlations with neighboring pixels.

The final and most difficult objective is the scientific study. This work will utilize the results of the other three tasks. The ice-velocity and deformation determination will be done using subsequent image feature tracking methods previously worked out for Seasat and now being used for Seasat data in a joint JPL-University of Washington deformation study, which will simply be extended for the SIR-B data. Data on deformation and drifts of Southern Ocean ice may be the most exciting results of the joint study. The determination of ice-pack morphology, the description of sizes, shapes, and frequency of occurrences of features, will be done by comparing the radar, photography, and TM data, and by referring to previous work on the Bering Sea by S. Martin and others. The estimation of SIR-B/TM data applicability in heat-flux and ice-budget calculations is somewhat risky and relies on the quality of result of the classification routine and on getting adequate TM coverage. It is not known if a significant fraction of the open-water features of importance to heat-flux calculation will be resolvable, as their size distribution in that area is simply not known. However, merging the results of the ice-velocity data and the ice-classification results will provide a trial ice budget and will guide future experiments seeking to refine the measurements. The role of Thematic Mapper is to improve ice classification in the scientific study.

IV. Expected Results

The experiments proposed should yield:

(1) Quantitative knowledge of gain and loss of resolvability of various features as a function of instrument parameters and hence an "ideal" instrument configuration.

(2) Values of ice-drift speed, deformation rates, floe sizes and shapes, ridging densities, ice loss and formation, and ice-edge characteristics.

(3) A determination of whether Thematic Mapper data can materially aid ice-condition description, expecially through improved information on surface albedo and temperature.

(4) An improved ice-classification scheme for use with SAR images in geophysics applications.

These results will constitute an important contribution to the understanding of the role of sea ice in air-sea interaction in the polar region.

N85-17218

New Zealand SIR-B Science Investigations

Team Member:

M. A. Collins
Department of Scientific and Industrial Research
Lower Hutt, New Zealand

Collaborators:

P. J. Oliver
Department of Scientific and Industrial Research
Lower Hutt, New Zealand

G. R. Cochrane
Auckland University
Auckland, New Zealand

J. Cole
Victoria University
Wellington, New Zealand

D. S. Coombs
University of Otago
Dunedin, New Zealand

E. J. Barnes
Department of Scientific and Industrial Research
Wellington, New Zealand

N. P. Ching
New Zealand Forest Service
Wellington, New Zealand

R. L. Bennets
Ministry of Agriculture and Fisheries
Darfield, New Zealand

P. J. Stephens
Ministry of Works and Development
Palmerston North, New Zealand

A. K. Laing
New Zealand Meteorological Services
Wellington, New Zealand

I. Introduction

We have prepared a coordinated national proposal for utilizing SIR-B data for scientific investigation in New Zealand (Ref. 1). New Zealand is an outstanding site for radar investigations for the following reasons. It lies on a tectonic plate boundary and is heavily faulted, volcanically active, and geologically diverse. It features one of the world's longest and clearest fault lines. Much of the country is covered in dense native forest, and large regions such as Fiordland and Northland are very rarely cloud free. Our proposals emphasize these special features of New Zealand.

At present, no synthetic-aperture radar imagery of New Zealand is available. Our overall objective is to use SIR-B data to study unusual features of New Zealand so as to increase our understanding of these features and the SIR-B data itself, and to develop SIR expertise in New Zealand.

II. Geological Investigations

The aim of the New Zealand geological investigation is:

(1) To delineate fault systems throughout New Zealand. This includes active faults and older faults associated with the several orogenic episodes throughout New Zealand's geological history. The location of New Zealand across the junction of two major tectonic plates, the Pacific and Indian-Australian Plates, makes New Zealand an ideal place for such tectonic studies. The active Alpine Fault is along the plate boundary and will be studied in detail.

(2) To map structural features in remote mountainous and heavily vegetated areas.

(3) To compare SIR-B imagery with LANDSAT multispectral imagery.

Ground-truth will come from surveys of active fault traces and from geological mapping. Existing surveys along the active faults will be compared to SIR-B imagery and extrapolations and interpolations made, where possible, from the new data. A comparison with existing geological maps will also be made and any newly discovered features will be investigated by field parties. The relationships between lineaments and structures with mineral occurrences will also be investigated.

Several university geology departments together with the New Zealand Geological Survey will be investigating the geological aspects of SIR-B imagery. The main areas of interest are shown in Fig. 1.

III. Oceanographic Investigation

The aim of this study is to correlate SIR-B and Advanced Very High Resolution Radiometer (AVHRR) imagery of an ocean eddy to increase our understanding of the interaction of the Southland Current with the East Cape Current in this region (Ref. 2).

The eddy is bathymetrically locked southeast of Wellington, and its behaviour is being regularly monitored using AVHRR data. SIR-B imagery of the study area (see Fig. 1) will be registered and correlated with rectified AVHRR data and with ground-truth data from other sources. These will include surface-ship measurements of temperature and tidal data.

The eddy may have enough change in reflectance at L band across its section to show its structure, especially under calm conditions.

IV. Forestry Investigation

The aim of this study by the New Zealand Forest Service is to assess timber volume by determining the age and size of pine forests from SIR-B data.

Ground-truth information on size, volume, and age of forest stands in the test area is available from the department's records. This information will be obtained, and, in addition, aerial photographs and further ground truth, such as forest moisture content, will be gathered during the Shuttle overpasses. Transponders may also be used to determine the amount of penetration of the radar through the forest canopy.

The test area is to be located in the Kaingaroa State Forest in the central North Island. The SIR-B data will be analyzed together with rectified Landsat imagery and digitized ground truth.

V. Agricultural Investigations

The aims of this project, to be carried out by the Ministry of Agriculture and Fisheries in Canterbury, are:

(1) To detect soil moisture by comparing SIR-B data with simultaneous gravimetric data, particularly in the low-lying area in Ellesmere County and adjacent to Lake Ellesmere, and to identify the "wet lands" in the mountain catchment of the Rakaia River.

(2) To use SIR-B data to discriminate land cover in a region that has previously been the subject of an intensive investigation using Landsat and aircraft scanner data.

The simultaneous ground data to be obtained will consist of soil-moisture analysis, and pasture, crop, and ground cover in terms of variety, stage of growth, disease, and weed infestation. The interactive image processing system at the Physics and Engineering Laboratory (PEL) will be used to analyze the available SIR-B, ground-truth, and Landsat data.

VI. Data Acquisition, Handling, and Analysis

PEL will fulfill a coordinating role. Digital and photographic data products will be received at PEL from NASA. Digital products will be processed at PEL as required, and, in addition, investigators from other institutions will be able to make use of the facilities at PEL for their data analysis. Photographic products will be duplicated at PEL and disseminated to other investigators.

References

1. McDonnell, M. J., *New Zealand Proposal for Participating in the NASA Shuttle Imaging Radar – B Science Programme Scheduled for August 1984,* PEL DSIR Report No. 818, February 1983.

2. Heath, R. A., *Oceanic Circulation Off the East Coast of New Zealand,* New Zealand Oceanographic Institute, Memoir No. 55, 1975.

Bibliography

Brooks, R. R., McDonnell, M. J., "Delineation of New Zealand Ultrabasic Rocks by Computer Processing of Digital Data from Satellite Imagery," *NZ J. Sci.,* March 1983.

Laing, A. K., *A Numerical Ocean Wave Forecasting Model for the Southwest Pacific* New Zealand Meteorological Service Technical Note No. 247, 1982.

Laing, A. K., *Wave Model Assessment: (1) Comparison with Ship Reports.* New Zealand Meteorological Service Technical Note No. 250, 1982.

Landsat II Over New Zealand, P. J. Ellis, I. L. Thomas, and M. J. McDonnell, editors. DSIR Bulletin 221, 1978; Landsat II Investigation Program No. 28230, Final Report.

McDonnell, M. J., Pairman, D., *Physics and Engineering Laboratory Image Processing System Documentation Manual,* PEL DSIR Manual No. 264, 1982.

McDonnell, M. J., Fowler, A. D. W., Pairman, D., *North Island Landsat Computer Mosaic,* PEL DSIR Report No. 767, 1982.

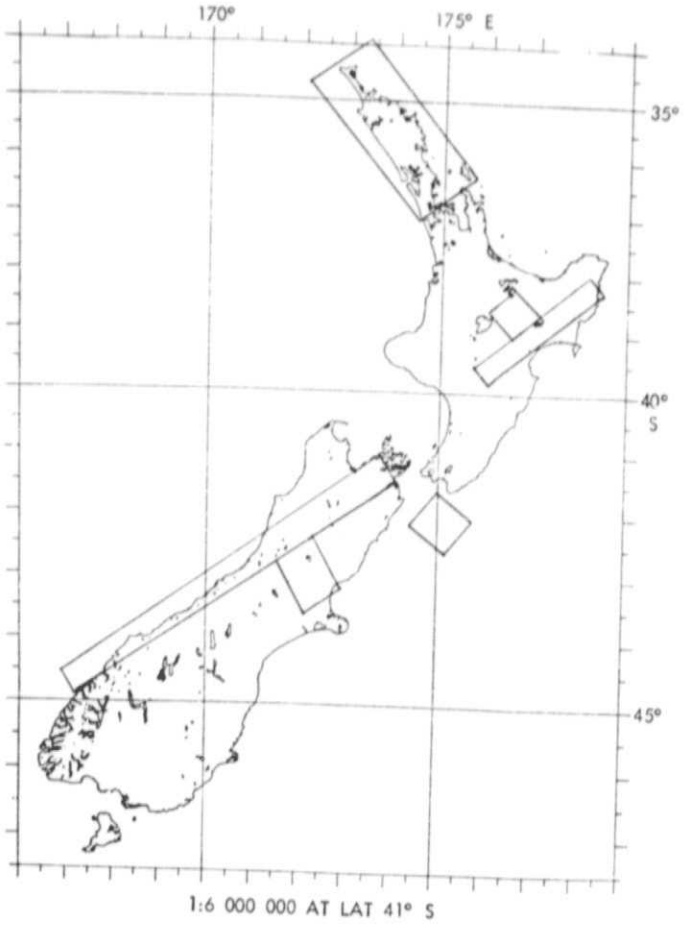

Fig. 1. Areas of SIR-B coverage in New Zealand

SIR-B Analysis of the Precambrian Shield of Sudan and Egypt: Penetration Studies and Subsurface Mapping

Team Member:

T. H. Dixon
Jet Propulsion Laboratory
Pasadena, California

Collaborators:

L. Roth
Jet Propulsion Laboratory
Pasadena, California

R. J. Stern
University of Texas at Dallas
Richardson, Texas

D. C. Almond
University of Khartoum
Sudan

A. Kroner
Johannes Gutenberg University
Mainz, West Germany

E. M. El Shazly
Atomic Energy Establishment
Cairo, Egypt

We propose a SIR-B study of the Precambrian Shield in southeast Egypt and northeast Sudan in an area east of the Nile.

The research would have two goals. First, we hope to confirm and quantify the phenomenon of radar penetration of thin (<5 m), dry eolian/alluvial cover, which can result in subsurface basement imaging. Second, we will use the penetration phenomenon to map presently covered or poorly known structural and lithologic features. Analysis of SIR-A imagery in the shield indicates that fault-related lineaments and folds are easily discerned with L-band radar imagery, but are not visible in Landsat MSS or RBV imagery. Buried granitic plutons and dyke swarms are also visible in the radar imagery. Detection of such features must be due either to radar penetration or subtle surface effects that are currently unmodeled and cannot be imaged with the high-Sun-angle Landsat system. The structural

data from our study should be a major new constraint on the late Precambrian tectonic history of northeast Africa. The identification of hitherto undetected granitic plutons and dyke swarms may have important economic implications. Economic metal deposits (e.g., Au, U) in the Sudanese/Egyptian Shield are often associated with late-state granitic magmas, but surface-visible deposits, especially gold, are largely depleted due to a long (~5000-year) mining history.

The proposed study area is optimum for studies of radar penetration and subsurface imaging since a strong contrast in dielectric constant exists between crystalline basement and covering layer. Surface outcrops are also abundant, enabling precise location and identification of features.

After image analysis, subsequent field work would measure "depth to basement" in a number of areas where penetration was observed. The effect of variable incidence angle (preferably between 20° and 50°) and the influence of signal quantization level (dynamic range) on detection of subsurface features will also be determined during post-mission image analysis. This requires at least one repeat pass and careful attention to signal calibration.

During image acquisition, variables related to the penetration phenomenon that might exhibit temporal variation will be measured or sampled in the field. Chief among these is soil moisture, which probably exhibits diurnal and seasonal variation. This will be measured directly by taking regolith samples in sealed containers. In addition, its effect on the dielectric constant will be measured in two ways. First, samples will be taken for postmission measurement of dielectric constant. Second, the attenuation of the SIR-B signal as a function of depth in the regolith will be measured at several test sites by deploying a multiantenna calibrated receiver. The antennae will be deployed on the surface and at several depths. This requires that SIR-B orbit predicts accurate to about 1 km be known at least 1 day in advance.

Quantitative Use of Multiincidence-Angle SAR for Geologic Mapping

Team Member:

T. G. Farr
Jet Propulsion Laboratory
Pasadena, California

Collaborators:

A. L. Albee, D. L. Evans, and **J. E. Solomon**
Jet Propulsion Laboratory
Pasadena, California

M. I. Daily
Mobil Field Research Laboratory
Dallas, Texas

T. C. Labotka
University of Tennessee
Knoxville, Tennessee

M. O. Smith
University of Washington
Seattle, Washington

I. Objectives

We propose to develop and use techniques for quantitative interpretation of SIR-B data for lithologic identification and mapping. Our specific objectives are to investigate the use of backscatter vs incidence-angle signatures derived from SIR-B images and SIR-B images in conjunction with images from other sensors for geologic mapping. This proposal addresses objectives stated in the SIR-B Science Plan (Ref. 1) under the heading of "lithologic mapping experiments."

A. Use of Backscatter vs Incidence-Angle Signatures

SIR-B images can be used to quantitatively determine the roughness, and in some cases the dielectric constant, of geologic surfaces. This may be accomplished through the use of scattering theories such as the Bragg-Rice theory (Ref. 2), which gives the backscatter cross section in terms of wavelength, incidence angle, dielectric constant, and size of scatterers. Surface roughness can be used to infer lithology and geomorphic processes, since physical weathering processes often lead to diagnostic surface configurations for different rock types in specific climates (Refs. 3 and 4). Dielectric constant is related to composition, packing, and moisture content of geologic units. These parameters are important for the mapping of alluvial and playa deposits.

The objectives of this part of the proposal are to develop the theoretical models necessary for the determination of surface roughness and dielectric constant from backscatter vs incidence-angle data (Fig. 1), and to define the surface

roughness and dielectric constant characteristics of rock types in various climates that may allow their identification in SIR-B image sets.

B. Use of SIR-B With Other Sensors for Geologic Mapping

One of the main goals of geologic remote sensing is to produce maps showing the distribution of rock types in an area. Visible-near-infrared and midinfrared sensors, such as the Landsat Multispectral Scanner (MSS) and Thematic Mapper (TM), and the airborne Thermal Infrared Multispectral Scanner (TIMS), are sensitive to surface chemical composition, and vegetation type and density; broad-band thermal infrared sensors, such as the TM and that used in the HCMM, are sensitive to bulk thermal properties of near-surface materials. Radar can provide information complementary to visible-near-infrared and infrared images about vegetation density, slope angles, and the physical geometry of rock outcrops. Taken together, radar, visible, near-infrared, midinfrared, and thermal infrared images provide a multisensor data set that can be used in a synergistic manner to resolve ambiguities that may be present in images from single sensors. Studies in Capitol Reef National Park, Utah, (Ref. 5) have demonstrated this potential and have shown the increased utility of multisensor image sets for the identification of specific rock types.

To map rock types from space using multisensor data sets, the multisensor "signature" of the rock types must be known. This has been accomplished for visible, near-infrared, and midinfrared wavelengths through the use of field and laboratory measurements (Refs. 6, 7, and 8). Theoretical and laboratory studies have also been used to calculate thermal properties for many rock types (Ref. 9). Field measurements can also be made of the surface roughness or backscatter response of geologic surfaces. Both airborne and truck-mounted scatterometers are available that give a calibrated measurement of backscatter from selected areas, while close-range stereo photogrammetry furnishes a way to measure surface roughness. Many radar signatures can be empirically derived from analysis of SIR-B images of areas of known rock types. The radar signatures described above furnish a potential input to assist in the identification of rock types.

Our objective is to integrate multiincidence-angle radar images from SIR-B with visible-near-infrared and thermal-infrared images in order to develop multisensor signatures for rock-type identification.

II. Approach

The assessment of techniques for the quantitative geologic analysis of SIR-B data will involve tests of their validity in geologically diverse terrains. In this section, we describe the techniques to be developed and ways for testing them, and give a list of potential test sites of diverse geologic setting.

A. Use of Backscatter vs Incidence-Angle Signatures

The availability of SIR-B images obtained at different incidence angles will allow us to use theoretical models to determine roughness of geologic surfaces from their backscatter vs incidence-angle response. Theories exist that predict radar backscatter from deterministic and statistical descriptions of surfaces (e.g., Ref. 2). Preliminary results using calibrated Seasat images and scatterometer data of Pisgah Crater show that these theories are accurate only for slightly rough surfaces (Ref. 10). A further drawback to the use of a single incidence angle for calculation of surface roughness is that like-polarized radar returns from a single incidence angle are most sensitive to only one scale of surface roughness. Since multiincidence angle SAR images are sensitive to a wider range of surface roughness, we will be able to more accurately predict surface roughness for a variety of geologic surfaces.

Supplementary data will be used to verify backscatter-surface-roughness calculations. To calculate backscatter vs incidence-angle response, an accurate representation of a surface must be obtained. We will use pole-mounted and balloon-borne cameras to obtain high-resolution stereo models of ground surfaces from which power spectral density and then backscatter can be calculated. The inverse problem of calculation of surface roughness from backscatter will be tested by the collection of calibrated scatterometer data at several incidence angles from both the JPL aircraft and truck-mounted systems, from which surface roughness will be calculated for the same test sites. Extensive field mapping and sampling will be required to assess the effects of soil moisture, dielectric constant, and vegetation density on the calculated returns.

Potential test sites for these studies will center on arid to semiarid climates, where vegetation does not completely mask the underlying surface. Table 1 lists potential sites, which include the Death Valley area, Pisgah Crater, Owens Valley, Capitol Reef, Snake River Plain, Patrick Draw and Hawaii. These areas contain a diversity of surface roughness related to mapped age and lithologic units, and exhibit a variety of vegetation cover. The response of different rock types to physical weathering in a range of climates can be assessed with these sites. This will also contribute a variety of backscatter vs incidence-angle signatures for rock types in different conditions.

B. Use of SIR-B With Other Sensors

Strategies must be developed to integrate the geologic information provided by the above techniques with data

obtained in other wavelengths. One of the most efficient ways to identify and map lithologic units with remote sensing is to compile a library of known signatures (backscatter function, spectral, thermal) for the rock types to be mapped. SIR-B signatures for various rock types must be obtained and stored in this library. Backscatter vs incidence angle, or surface roughness and dielectric constant signatures, can be gathered for rock types in arid to semiarid climates where vegetation is a minor factor.

The uniqueness of SIR-B-derived signatures for different rock types must also be evaluated. This will be done through statistical techniques such as principal component and linear discriminant analysis. The synergistic effects of the addition of SIR-B signatures to those from other wavelengths will also be evaluated by these techniques. Once we have confidence in our ability to identify rock types through these signatures, we can attempt extensions to geologic mapping in relatively unknown areas.

Test sites for this part of the study will include a variety of well-mapped areas of different climate and vegetation cover, that have been, or will be, covered by the TM, MSS, HCMM, or TIMS. Sites from Table 1 include the Death Valley-Panamint Mountains area, Owens Valley, Hawaii, Capitol Reef, and Patrick Draw.

III. Anticipated Results

We expect to demonstrate the value of multiincidence-angle SAR images alone, and in concert with images from other sensors, for use in geologic mapping by the application of quantitative interpretation techniques. Radar signatures for various rock types in different geologic settings will be derived from field measurements and tests, and the technique of searching SIR-B and multisensor image sets for known signatures will be used to map lithologies in test areas.

A. Use of Backscatter vs Incidence-Angle Signatures

We expect to be able to match theoretical and SIR-B-derived backscatter signatures for rough surfaces of specific lithologies. The compilation of a library of backscatter vs incidence-angle response of rock types in different climates will then allow rock-type identification within bounds determined by the uniqueness of the signature. This will improve our ability to map lithology from radar images alone and provide an input to multisensor signatures.

B. Use of SIR-B With Other Sensors

Combination of the above signatures with those obtained for other wavelengths should optimize our ability to map rock types from space. We expect to define some of the limits on lithologic identification from space through the analysis of multisensor image sets from test sites of diverse geologic and climatic character. The relative merits of different sensors for geologic mapping in different settings will be determined. We expect SIR-B to contribute to rock-type identification through its sensitivity to the physical character of rock outcrops and local slope angles. Visible, near-infrared, and midinfrared sensors furnish data on composition, while thermal-infrared images can be used to interpret bulk thermal properties.

Depending on the geologic problems to be solved, it may not be necessary to obtain data from all possible sensors. Through statistical analyses, we expect to be able to define the most useful data sets for the identification of specific suites of rock types in specific climates. This may allow future optimization of data collection before analysis.

C-2

References

1. Carver, K. R., chairman, Imaging Radar Science Working Group, 1982, *The SIR-B Science Plan*, JPL Publication 82-78, 67 pp. Jet Propulsion Laboratory, Pasadena, California.

2. Valenzuela, G. R., 1968, "Scattering of Electromagnetic Waves From a Tilted Slightly Rough Surface," *Radio Science*, Vol. 3, pp. 1056-1060.

3. Stone, R. O., and J. Dugundji, 1965, "A Study of Microrelief – Its Mapping, Classification, and Quantification by Means of a Fourier Analysis," *Eng. Geol.*, Vol. 1, pp. 89-187.

4. Hobson, R. D., 1972, "Surface Roughness in Topography: Quantitative Approach," in *Spatial Analysis in Geomorphology*, R. J. Chorley, editor. Harper and Row, New York, 393 pp.

5. Rebillard, P., and D. L. Evans, 1983, "Analysis of Coregistered Landsat, Seasat, and SIR-A Images of Varied Terrain Types," *Geophys. Res. Let.*, in press.

6. Abrams, M. J., R. P. Ashley, L. C. Rowan, A. F. H. Goetz, and A. B. Kahle, 1977, "Mapping of Hydrothermal Alteration in the Cuprite Mining District, Nevada, Using Aircraft Scanner Images for the Spectral Region 0.46 to 2.36 μm," *Geology*, Vol. 5, pp. 713-718.

7. Conel, J. E., M. J. Abrams, and K. W. Baird, 1980, "Uranium: Spectral Discrimination of Alteration Phenomena in Sediments," *Modern Geology*, Vol. 7, pp. 115-135.

8. Kahle, A. B., and L. C. Rowan, 1980, "Evaluation of Multispectral Middle Infrared Aircraft Images for Lithologic Mapping in the East Tintic Mountains, Utah," *Geology*, Vol. 8, pp. 234-239.

9. Kahle, A. B., J. P. Schieldge, M. J. Abrams, R. E. Alley, and C. J. Levine, 1981, *Geologic Application of Thermal Inertia Imaging Using HCMM Data*, Publication 81-55, 199 pp. Jet Propulsion Laboratory, Pasadena, California.

10. Farr, T. G., N. Engheta, and A. S. Sheehan, 1983, "Comparison of Surface Roughness to Radar Image and Scatterometer Data of the Pisgah Crater Area," Abstract, International Geosci. and Rem. Sens. Sym., San Francisco.

Table 1. Potential test sites for SIR-B data analysis

Site	Climate	Vegetation	Relief	Geologic Features
Death Valley–Panamint Mts.	Arid	O-scrub	O-high	Variety of well-mapped rock types, alluvial fans, playas, evaporites, pediments; surface roughness and scatterometer data available
Hawaii	Semiarid–tropical	O-jungle	Moderate	Well-mapped lava flows of different types and ages; vegetation variations
Snake River Plain	Semiarid	O-scrub	Low	Well-mapped lava flows of different types and ages; surface roughness and scatterometer data available
Owens Valley	Semiarid	Scrub	Low	Fans and glacial deposits of known ages; multisensor test site
Pisgah Crater	Arid	O-scrub	Low	Lava types, fans, playa; surface roughness, scatterometer, and calibrated Seasat and aircraft SAR data available
Galapagos Islands	Tropical	O-jungle	Moderate	Lava flows of different types and ages; SIR-A coverage
Patrick Draw	Semiarid	Scrub	Low	Subtle radar anomalies; Geosat test site (oil and gas)
Capitol Reef	Semiarid	Scrub	Moderate	Variety of well-mapped rock types, surface cover, and vegetation; multisensor test site (SIR-A, Seasat, Landsat, HCMM)

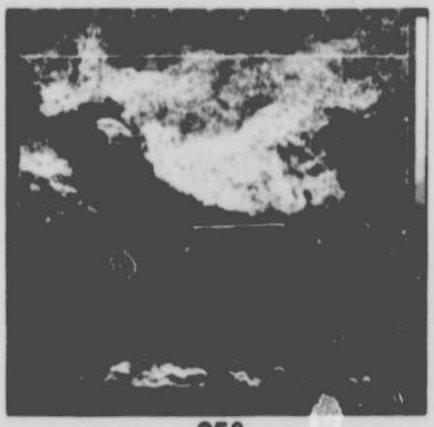

25°

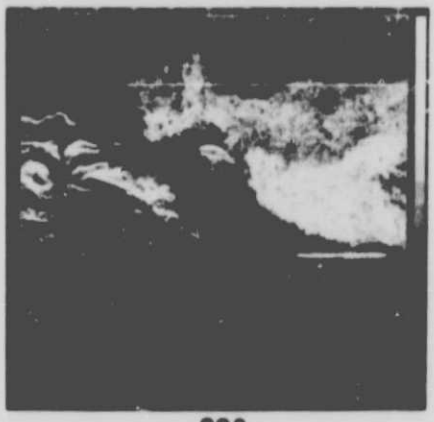

30°

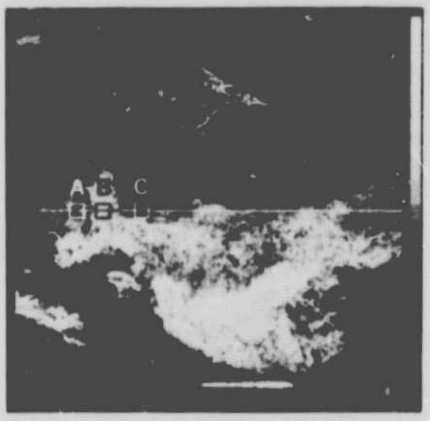

40°

AIRCRAFT SAR IMAGES OBTAINED AT THREE INCIDENCE ANGLES WITH SCATTEROMETER TRACK OVERLAID

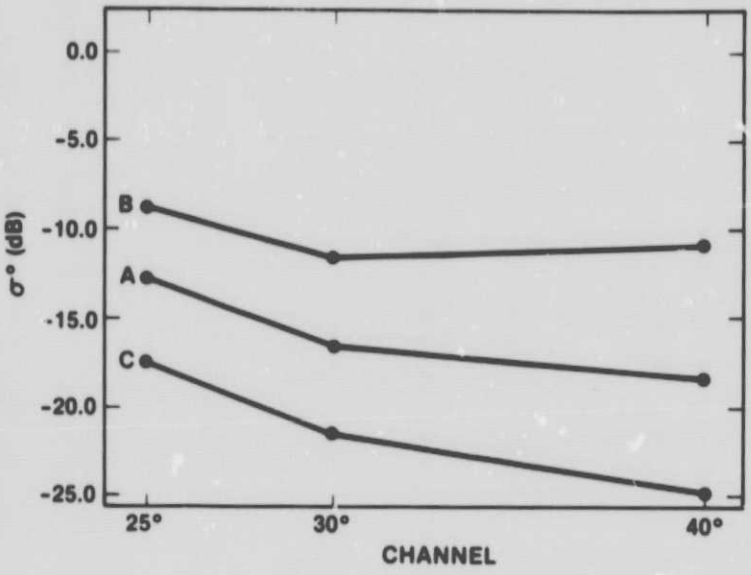

BACK SCATTER RESPONSE OF THREE AREAS SHOWN AT LEFT

A: SMOOTH LAVA

B: ROUGH LAVA

C: ALLUVIAL GRAVEL

Fig. 1. Simulation of multiincidence-angle SAR by the JPL aircraft SAR, and backscatter response from three geologic surfaces at Pisgah Lava Field, California

Geologic Mapping of Indonesian Rain Forest With Analysis of Multiple SIR-B Incidence Angles

Team Member:

J. P. Ford
Jet Propulsion Laboratory
Pasadena, California

Collaborators:

F. F. Sabins, Jr.
Chevron Oil Field Research Co.
La Habra, California

P. Asmoro, Jr.
National Coordinating Agency for Survey and Mapping
Cibinong-Bogor, Indonesia

I. Description of the Investigation

The principal objectives of this investigation are to evaluate SIR-B image coverage of equatorial rain forest in Indonesia (particularly Sumatra and Kalimantan) for the purposes of geological mapping through a diversity of incidence angles, and quantifying SIR-B signatures from the canopy as a function of incidence angle. A supporting objective is to compare the SIR-B backscatter from rain forest at L-band with backscatter acquired by the Seasat scatterometer system at Ku-band over corresponding areas.

The investigation is directed at achieving better quantitative understanding of the effects of radar illumination diversity for geologic mapping and interpretation in continuously vegetated tropical terrain. It forms part of the NASA research program to further our understanding of spaceborne imaging radar for purposes of evaluating and monitoring Earth resources.

II. Description of the Experiment

We will make a comprehensive evaluation of the discrimination and mapping capabilities on SIR-B images of geologic features in Indonesia that are covered by equatorial rain-forest canopy. Both mapping-mode and multiple-incidence-mode coverages are required. Map units based on image tone, texture, and pattern will be related to geologic features based on ground truth and supported by field checking. We will select equatorial rain-forest terrains that have varied and diverse geology for SIR-B mapping-mode coverage.

From the SIR-B coverage of equatorial rain-forest canopy, we expect to obtain radar signatures that express the topographic character of the underlying surface to some extent. We will quantify the radar signatures by relating backscatter (σ_0), as a function of incidence angle (θ), through the range of incidence angles available in the SIR-B data set. We anticipate obtaining an average value of σ_0 from dense level canopy and

observing a gradual variation of σ_0 with θ. This will serve as a standard of reference for comparison and for observing other variations that are due to slope effects, or radar penetration below the canopy, or local physical changes in the cover.

The SIR-B data will be compared to Landat multispectral scanner (MSS) and thematic mapper (TM) images wherever possible, and to available aerial photography. Corresponding SIR-A and airborne X-band SAR coverage will be contrasted.

III. The Approach for Data Acquisition, Handling, and Analysis

A. Geologic Mapping

Contiguous SIR-B swaths acquired in the mapping mode will be geometrically rectified and mosaicked prior to analysis. Visual contrasts of image tone, texture, and pattern in the mosaics and in the repetitive coverages at different incidence angles will form the basis for mapping geologic features and groups of features. Previous analyses of SIR-A scenes in the equatorial rain forest of Indonesia by the investigators of this proposal (Refs. 1 and 2) show that many geomorphic and structural features covered by rain-forest canopy are readily discriminated on the images. Some examples include humid equatorial karst terrain; dip and scarp slopes of layered rocks; volcanic cones and flows; crystalline, metamorphic, and melange terrain complexes; drainage alignments and offsets; and fold and fault patterns.

Contrasts in perception of the above types of geologic features and terrains on SIR-B images will be qualitatively related to incidence angle in areas of multiple-incidence coverage and same-side illumination. Wherever possible, the SIR-B mapping will be compared to existing geologic maps and to ground truth. Mapping will be done on a scale in the order of 1:250,000. From this portion of the study, we expect to determine the most favorable range of incidence angle for geologic mapping from spaceborne SAR in the equatorial rain-forest environment. Extensive mapping-mode coverage in Sumatra and Kalimantan will be interpreted in a regional tectonic framework.

B. Multiple-Incidence Coverage

Areas of level and apparently uniform canopy will be selected to obtain a reference standard for σ_0 as a function of θ. The approach will be to digitally correlate, geometrically rectify, and coregister each of the corresponding coverages at the different angles of incidence. This will produce a standard data set for each test site. Each data set should be provided with a nominal calibration of the digital number (DN) relative to σ_0 for each incidence angle. This is necessary as a basis for making meaningful quantitative comparisons between data sets.

The average value of σ_0 as a function of θ for a level, uniform, canopy surface will be determined by visual display of the SIR-B data and interactive image processing analysis. The relations observed from level surfaces will be compared to relations from canopy over sloping and dissected areas. Surface-slope measurements will be obtained from field checking. Contrasts in backscatter and slope angle will form the basis for quantitatively discriminating slope effects. Field work will be undertaken at specific locations to verify the results and to understand any anomalous conditions.

A supporting task to compare SIR-B multiple-incidence backscatter with measurements of a corresponding area acquired by the Seasat scatterometer system requires a test site with an extensive, relatively level, homogenous canopy. The only suitable site in Indonesia is in south-central Kalimantan. In the event that this site is insufficiently covered by SIR-B, an appropriate alternative site will be selected in Amazonia, South America. Scatterometer measurements will be extracted from the Seasat data set of the site that is selected and will be processed to obtain plots of σ_0 as a function of θ at Ku-band. The plots will be compared to corresponding SIR-B data acquired at L-band.

Usable Landsat MSS coverage in Sumatra and Kalimantan is limited in extent. This is due to the perennial cloud cover that exists in the equatorial latitudes of those islands. Figure 1 shows that Landsat images with less than 30% cloud cover do not exist for large areas of the islands. Partial coverage of the islands with aerial photography exists at a scale of 1:100,000 though there are many areas for which no imagery of any kind exists.

IV. Expected Results

We anticipate that this study will yield a significant advance in our understanding and interpretation of spaceborne radar signatures under varying conditions of radar illumination, specifically for geologic mapping in the equatorial rain-forest environment. We will determine the optimal range of radar incidence angle for mapping in this environment. We expect to obtain new improved geologic understanding of regional tectonic and basinal relations in Sumatra and Kalimantan within the constraints imposed by the available SIR-B coverage.

We shall quantify backscatter relative to incidence angle to obtain a characteristic value or range of values that are unique to equatorial rain forests. We expect to discriminate the slope effect quantitatively, and to evaluate any anomalous responses

by field checking and by comparison with remote sensing data sets acquired at other wavelengths. Our results will be based on SIR-B multiple-incidence angle data. Comparison with other data at optical and infrared wavelengths (Landsat MSS, TM, and aerial photos), and at different radar wavelengths (airborne X-band SAR, Seasat scatterometer system) will provide a limited basis for predicting the radar response that can be expected from equatorial rain-forest canopy with the SIR-C multiple-frequency, multiple-polarization radar. The results of this investigation will present a major advance in geologic mapping of little-known inaccessible terrains in Indonesia from spaceborne SAR, and in knowledge of the interaction of 23-cm (L-band) microwaves with equatorial rain-forest canopy.

References

1. Sabins, F. F., Jr., "Geologic Interpretation of Space Shuttle Radar Images of Indonesia," *Amer. Assoc. Petroleum Geologists Bull.*, Vol. 67, pp. 2076-2099, 1983.

2. Ford, J. P., et al., *Space Shuttle Columbia Views the World With Imaging Radar: The SIR-A Experiment.* JPL Publication 82-95, Jet Propulsion Laboratory, Pasadena, California, January 1, 1983, 179 pp.

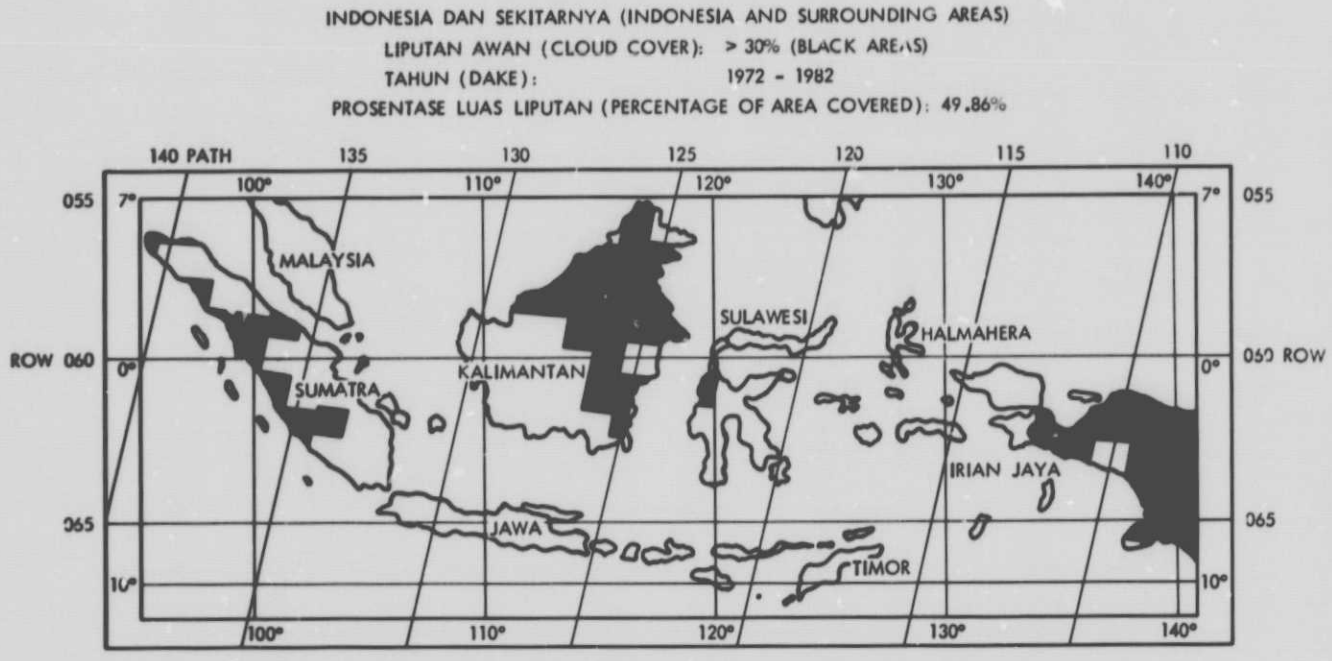

Fig. 1. Key to Landsat MSS coverage of Indonesia and surrounding areas with 30% or less cloud cover, acquired during 1972 to 1982. Less than 50% of the total area is covered (courtesy P. Asmoro, Chairman, BAKOSURTANAL)

Remote Sensing of Rice Fields and Sea Pollution by SIR-B

Team Member:

N. Fugono
Radio Research Laboratories
Tokyo, Japan

Collaborators:

Y. Furuhama, T. Takasugi, K. Okamoto, M. Fujita, S. Yoshikado, H. Masuko, T. Shinozuka, H. Inomata, I. Shiro, M. Ichinose, and H. Ohyama
Radio Research Laboratories
Tokyo, Japan

I. Description of the Investigation

This investigation plan consists of three experiments:

(1) Sensor Calibration.

(2) Rice.

(3) Sea Pollution.

The test sites of the three experiments, which were selected according to careful investigations and discussion, are shown in Fig. 1.

The description of each experiment follows.

II. Sensor-Calibration Experiment

A. Objective

The experiment has the following three objectives:

(1) To establish the relationship between backscatter cross section and image intensity.

(2) To evaluate the resolution characteristics of the SIR-B.

(3) To investigate the side-lobe characteristics of the SIR-B.

B. Description

For objective (1), a number of corner reflectors with square trihedral design will be used because of the large radar cross section. The side dimensions will be 2.0, 1.5, 1.1, 0.85, 0.60, and 0.46 meters, chosen so that the radar cross section decreases in approximately 5-dB steps. By evaluating an image of the corner reflectors with different sizes, it is expected that the relationship between backscatter cross section and image intensity will be established more clearly. The corner reflectors will be placed on the runway of the closed airport in Akita (39°42′N, 140°05′E), a wild-flower bed in Hokkaido (45°07′N, 141°42′E), and reclaimed land in Kagoshima (31°29′N, 130°31′E). At the airport, the old runway is still well maintained. In the other test sites, the surface is slightly rough and covered with short grasses. Since the background condition is different at those test sites, the influence of it on

the calibration characteristics will be obtained, as well as the effects of multilook angle on calibration characteristics.

For objective (2), several corner reflectors of the same dimension will be arranged in an "L" shape, separated by 25 meters or its multiple from adjacent reflectors. The images will be evaluated on a pixel-by-pixel basis, to measure the resolution by determining whether or not two adjacent targets can be distinguished. Dependence of the resolution characteristics on the background condition and on the look angle will be obtained by using the whole set of data taken at three test sites.

For objective (3), the large-diameter antennae at the Kashima Space Communication Center (35°57'N, 140°40'E) of the Radio Research Laboratories will be used as the imaging targets. Since the antennae have very large radar cross sections, the side-lobe structure of the SIR-B may appear clearly on the image, as was seen on the Seasat image of the Goldstone large antenna. At the Kashima Space Communication Center, there are a 26-meter-diameter antenna for 2 and 8 GHz; an 18-meter-diameter antenna for 136 and 400 MHz, and L- and S-band; two 13-meter-diameter antennae for 12/14 GHz and 20/30 GHz; and two 10-meter-diameter antennae for 4/6 GHz and 32/35 GHz. Detailed structure of the side lobe will be determined by evaluating the image intensity on a pixel-by-pixel basis.

In the calibration experiment, a large dynamic range is basically necessary to prevent image saturation and to assure its reliability. However, to assess the influence of the number of bits per sample on the final image, 3 bits-per-sample data will be taken for one of three orbits with similar look angles.

III. Rice Experiment

A. Objectives

The objectives of the rice experiment are as follow:

(1) To investigate the microwave-scattering characteristics of rice fields through observations by SIR-B.

(2) To examine the possibility of classifying crops including rice from the SIR-B data.

B. Test Sites

To obtain data on various crop conditions during the one-week experiment, several test sites have been chosen along the island of Japan. They are:

(1) Ohgata-mura	40°00'N,	140°00'E.
(2) The Ishikari Plains	43°05'N,	141°40'E.
(3) The Echigo Plains	37°40'N,	138°50'E.
(4) Suigo area	35°55'N,	140°30'E.
(5) The Toyohashi Plains	34°40'N,	137°20'E.
(6) The Tsukushi Plains	33°15'N,	130°25'E.

The most important site is Ohgata-mura, a village on the largest reclaimed land in Japan. The flat area is 18 km south to north and 11 km east to west; its agricultural area is about 8,790 ha including rice fields of 4,760 ha. Special importance is placed on the experimental farm operated by the Akita Prefectural College of Agriculture in the village. Detailed ground-truth data will be acquired in cooperation with the college. The total area of the farm is about 190 ha, and the products are rice, wheat, grass, fruits, corns, soybeans, vegetables, potatoes, rape, and others. The size of a unit section of the rice field in the farm is 130 m by 90 m.

C. Acquisition and Analyses of Ground-Truth Data

The following items of ground-truth data will be acquired from each unit section in Ohgata-mura.

(1) Species of rice or other crops.

(2) Planting density.

(3) Average height.

(4) Number of ears.

(5) Number of grains per ear.

(6) Crop weight per unit area.

(7) Expanse of plants seen from the incidence direction.

(8) Angle between the row and the incidence direction.

(9) Wind direction and speed.

(10) Disease, if any.

(11) Background soil moisture.

In addition, Landsat images and aerial photographs will be utilized as reference data for the crop classification. As for the other test sites, the data of items (1) to (6) are collected by the Ministry of Agriculture and Fishery every year. The relation between crop conditions and the SIR-B data for them will be clarified through various statistical methods.

IV. Sea-Pollution Experiment

A. Objectives

The objectives of the sea-pollution experiment are:

(1) To determine the characteristics of the radar image of oil-like surface films under several sea-surface condi-

tions such as wind speed and direction, wave, and current, and under the observation condition of incidence angle; to estimate the possibility of surveillance of oil pollutions using the satellite-borne imaging radar.

(2) To estimate the absolute measurement capability of the sea-surface scattering cross section using the satellite-borne imaging radar.

(3) To investigate the capability of surveilling various ships, vessels, and tankers using the satellite-borne imaging radar for the purpose of maritime safety.

B. Test Areas of Sea-Pollution Experiment

The test areas are, firstly, about 100 kilometers off the Kii-hanto cape in the Pacific where the mapping mode with a 30° look angle will be used, and secondly, about 100 kilometers off Hamamatsu City in the Pacific where the multiple-incidence-angle mode will be used.

C. Plans for Field Work Before, During, and After Flight

(1) Oil pollution experiment. Oil-like polluted areas will be artificially produced by expanding oleyl alcohol (9-octadecan-1-ol, cis isomer) to a thin layer over the sea surface by means of the aerial dispensing of frozen oleyl-alcohol cubes (freezing point, about 6°C; specific gravity, 0.85). These oleyl-alcohol cubes are melted under the condition of sea-surface temperature (about 25°C in August) and produce a monomolecular oil-like film. About 20 liters of oleyl alcohol are required for a one-square-kilometer monomolecular layer. Three different sizes of polluted area (0.3, 1, and 3 kilometers) will be produced to estimate the influences of surrounding natural sea-surface conditions on the SAR images of different sizes.

The oil-like polluted areas are simultaneously observed using the airborne dual-frequency (10.00 GHz and 34.43 GHz) scatterometer/radiometer system of the Radio Research Laboratories.

Various sea-truth data are collected during the SIR-B flights around the swath paths. The expected items of the sea-truth data are as follow:

(a) Sea-surface wind speed and direction; by ships.

(b) Significant wave height; by buoys.

(c) Significant wave length and its direction; by buoys.

(d) Current speed and direction; by ships.

(e) Atmospheric and water temperatures; by ships.

(f) Atmospheric pressure and humidity; by ships.

(g) Aerial photographs; by airplane.

In addition, the weather maps at and around the time will be furnished by the Japan Meteorological Agency.

(2) Calibration experiment on the sea surface. To make quantitative measurements possible, the standard reflectors such as corner reflectors and Luneberg lenses are placed on the sea surface in the SIR-B swath.

(3) Maritime surveillance experiment. For the purpose of the maritime surveillance experiments, as many as possible of the various ships, vessels, and tankers in the swath at the observation time of SIR-B will be listed after the Shuttle flight. Information about the position, speed, course, shape, length, width, height above sea surface, and tonnage of each ship, and the wind direction and speed and wave condition around each ship, will be collected by cooperating with the related organizations.

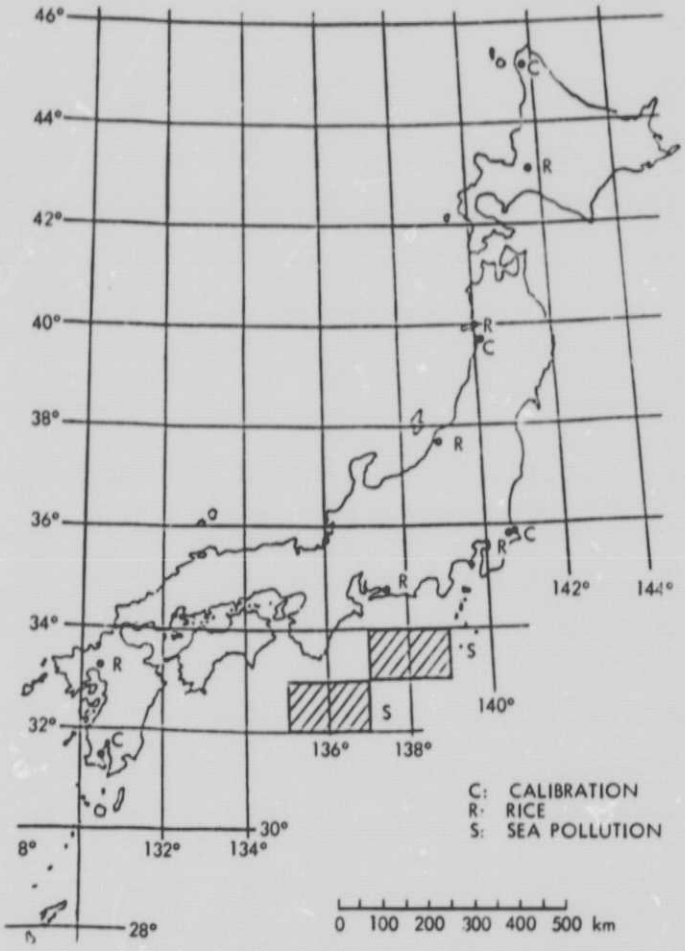

Fig. 1. Sites for calibration and remote sensing of rice fields and sea pollution by SIR-B

N85-17223

Evaluation of SIR-B Data for Identifying Rainfall Event Occurrence and Intensity

Team Member:

D. Garofalo
Earth Satellite Corporation
Chevy Chase, Maryland

Collaborators:

J. N. Cooper, J. R. Everett, L. J. Warnick, L. H. Wynn, C. Sheffield, M. Ruth, R. Perrine, and K. Estep
Earth Satellite Corporation
Chevy Chase, Maryland

I. Description of the Investigation

The objectives of this project are to evaluate the utility of SIR-B data for the detection and measurement of rainfall events, and to develop applications of SIR-B data to the improvement of existing rainfall models. This will be accomplished in two project phases discussed below in Section III. The objectives are as follow:

(1) To determine whether optical or digital SIR-B data allow consistent detection of rainfall events that are known to have occurred at the time and location of SIR-B data takes.

(2) To classify the independent variables of the surface environments (e.g., land use, land cover, climate, and terrain) where rainfall is detected and to correlate signal returns with these variables.

(3) To conduct a statistical analysis of signal returns where rainfall has been detected and to determine the extent to which rainfall intensity can be measured and contoured.

(4) To develop digital methods of SIR-B data enhancement for the purpose of rainfall detection, which may be used to increase resolution and accuracy of existing rainfall models.

II. Description of the Experiment

An important part of our SIR-B investigation is the estimation of rainfall. EarthSat's CROPCAST™ agricultural modeling capability includes a proprietary rainfall estimation system. The rainfall estimation system will be used to diagnose precipitation associated with rain events in the radar image. The events selected for study will be determined through the use of meteorological information normally received by CROPCAST.

The CROPCAST rainfall estimation technique integrates images from polar-orbiting or geostationary meteorological satellites with any available surface data to diagnose precipitation amounts in a grid cell. The cell size is variable, and depends primarily on the resolution of the satellite data.

By applying EarthSat's rainfall estimation system, rainfall events occurring at the same time as SIR-B radar data acquisition will be studied. Radar data for each rainfall event site

shall be evaluated to relate rainfall occurrence and intensity to radar signal returns under varying terrain (soil, vegetation, topographic, and land use) conditions. Digital SIR-B data shall be computer processed using EarthSat's image processing algorithms to maximize scene information content and enhance radar rainfall signal returns.

III. Approach for Data Acquisition, Handling, and Analysis

A two-phased approach is proposed. In the first phase, EarthSat scientists will undertake a visual, qualitative analysis of SIR-B data takes that are known to have imaged rainfall events to determine quickly whether rainfall signatures can reliably be delineated. EarthSat shall also ascertain whether there are any conventional methods of image processing that can be applied to digital SIR-B data to improve the sensitivity of the imagery to rainfall signatures. A variety of terrain, climatological, and sensor variables will be examined to evaluate whether, as expected, SIR-B data will allow discrimination of rainfall events preferentially in certain environments.

Upon completion of Phase I, reports and maps detailing the findings of the qualitative analysis of the SIR-B data will be produced and directions proposed for quantitative studies in Phase II. It is expected that positive findings from Phase I will allow specific definition of the tasks for Phase II. Phase II will consist primarily of specialized digital processing of the SIR-B data to enhance the rainfall signatures analyzed in Phase I. Digital procedures to interrelate thermally derived models with SIR-B data will be employed to determine whether the detectability of rainfall signatures can be increased and used interactively with thermal models to improve their resolution and the accuracy of their findings.

IV. Expected Results

It is expected that digital SIR-B data will provide the required resolution to allow delineation of rainfall event ground signatures, and possibly to identify rainfall event intensities. Positive results should lead to improvement in the resolution and accuracty of current rainfall monitoring and modeling systems, which in turn should enhance current crop-yield forecasting methods. In addition, positive results may lead to the development of a methodology for assessing rainfall event interactions under varying terrain and climatic conditions, and thus improve our knowledge of groundwater recharge, surface runoff, and evaporation within these areas.

SIR-B Interferometric Topography

Team Member:

R. M. Goldstein
Jet Propulsion Laboratory
Pasadena, California

Collaborator:

F. K. Li
Jet Propulsion Laboratory
Pasadena, California

I. Objective

The objectives of this experiment are to develop and test an interferometric method of using the SIR-B synthetic-aperture radar data for high-resolution elevation measurements.

Inteferometry can have several advantages over the more conventional stereoscopic methods. Foremost is the non-necessity of recognizing each surface feature to be measured in both images of the stereo pair. The speckle phenomenon, inherent in synthetic-aperture radar, makes such recognition difficult. With interferometry, however, the surface relief of featureless plains or the gentle slopes of alluvial fans can be observed easily.

II. Description of the Experiment

The essence of synthetic-aperture radar is the capability of storing echoes from successive pulses. The signals are then combined, after the fact, to produce high-resolution images. We propose to combine signals from separate SIR-B *passes* to provide the equivalent of an interferometer.

The accuracy of this technique increases with antenna separation (interferometer baseline) up to the limit where the signals from the two orbits become uncorrelated.

The SIR-B mission plan provides an ideal test vehicle for this approach to topography. Corresponding orbits on consecutive days will cross each other with a very shallow angle. This permits us to test the interferometry technique, with baseline as a parameter, and determine how to obtain the greatest accuracy.

III. Data Acquisition and Handling

Families of orbits are planned for SIR-B that reach their highest latitude (57°) within 80 km of each other. The crossover points of these orbits provide the opportunity to develop and test interferometric topography. We propose to take data on three to four passes each, over two of the crossover areas in Canada. One area has gentle topography; the other is more rugged.

Each pass need be only a few minutes long. However, it will be necessary to increment the SIR-B yaw angle about 1° for

successive passes. It is also necessary that orbit pairs have the same look angle.

The raw radar signals (not the images) will be analyzed because: (1) the images are needed in complex form before the looks are combined, which is not the standard format, and (2) a compensation is required to account for the changing antenna separation during the synthetic-aperture time. The raw signal tapes will be processed at JPL on a VAX 11-780 computer with an attached array processor. Programs to produce the images from raw Seasat and SIR-A data already exist and have been used in production.

The interferometer system measures the location of each pixel in terms of p, the slant range, t, the time along the orbital tracks, and the look angle, θ. If the orbital parameters are known, then the transformation to (x, y, and z) coordinates is straightforward. Because of the unknown multiple of 2π in the phase estimates, the elevation of at least one pixel in the scene (perhaps a shore line) must be known.

IV. Expected Results

We propose to provide and test the algorithms for interferometric altimetry. The test will be over the range of antenna separation afforded by the data.

Images of the best areas will be presented as elevation contours over a radar brightness image, corrected for foreshortening.

Using local topographic maps, an assessment of the accuracy of the technique will be made.

Use of SIR-B Multiincidence-Angle Imagery to Study Iceberg Detectability and Offshore Ocean Feature Extraction

Team Member:

A. L. Gray
Canada Centre for Remote Sensing
Ottawa, Canada

Collaborators:

J. Princz, C. E. Livingstone, R. K. Hawkins, and **M. Wong**
Canada Centre for Remote Sensing
Ottawa, Canada

D. Pearson
Petro-Canada Exploration, Inc.
Calgary, Canada

J. Gower
Institute of Ocean Sciences
Sydney, Canada

T. F. Mullane and **R. O. Ramseier**
Atmospheric Environment Service
Ottawa, Canada

I. Description of the Investigation

This SIR-B experiment forms part of ongoing cooperative work aimed at obtaining a better understanding of SAR performance in the context of iceberg detectability and reconnaissance of Canadian east-coast ice, ocean conditions, and hazards. Currently, there is extensive offshore fossil-fuel resource exploration in the area, principally on the Grand Banks and the Scotian Shelf, but also along the Labrador coast. Icebergs pose significant hazards to offshore structures on both the Labrador coast and the Grand Banks. As these icebergs can weigh several million tons and are carried by winds and currents at speeds of a knot or more, either the off-shore structures have to be exceedingly strong to withstand impact or, as at present, iceberg towing and quick disconnect techniques must exist for safe operations.

Figure 1 shows a 460×10^6 kg iceberg (0.4×10^6 tons) approximately 10 km from the drill ship *Pacnorse 1*, on location off the northern Labrador coast. This photograph of the 100-m-long iceberg was taken from a drilling support vessel that was towing the iceberg to a location that would not threaten the drill ship. Clearly, the threat from such ice hazards is compounded under severe weather conditions so that all-weather detection and monitoring systems are essen-

tial. In addition, because many of the wells are being drilled in relatively shallow water and pipelines along the sea bed are being considered for production systems, the possibility of bottom structure damage due to iceberg scouring makes iceberg management an important part of offshore development strategy.

Marine radars are used now on drill rigs and supply vessels as the primary, close-range iceberg detection system, often supported by visual aircraft reconnaissance over a much larger area. All-weather aircraft and satellite radar detection and tracking is attractive for larger area coverage, but the limits of applicability, particularly using satellite radars, can only be estimated. Performance of iceberg drift models is still recognized to be poor, largely because of insufficient and undersampled ocean current and wind data. There are definite implications for improved safety and efficiency of offshore activities in these areas if airborne or spaceborne radar techniques for monitoring icebergs and ocean conditions (wind speed, waves, current information) could be demonstrated.

The specific objectives of this SIR-B investigation are:

(1) To study the L-band satellite SAR detectability of iceberg targets as a function of incidence angle and observed conditions. By using meteorological data and any available backscatter models, attempt to estimate detectability under different conditions.

(2) To compare L-, X- and, hopefully, C-band aircraft imagery, and to use this data as a basis for an approximate simulation of satellite imagery and to compare the SIR-B images with such simulated L-band images derived from the aircraft data.

(3) To see if it is possible to carry out a comparison of any available surface, or near-surface, currents in the area with estimates of the range component of surface current derived from the SIR-B data (IOS experiment).

II. Description of the Experiment

The experiment involves the collection of airborne radar images, scatterometer data, photography, and, possibly, laser profiling data together with the acquisition of surface photographic, meteorological, and ocean data. Provisionally, the SIR-B site has been selected to be in the region of the Corte Real well (56°05′N, 58°12′W), but Petro-Canada cannot commit to this now, as decisions on 1984 drilling will not be made for some time. Summer iceberg fluxes in a 10- × 10-km area at this site are in the range 7 to 10 icebergs per day but may drop to an average of about 5 per day in August. Normally, the supply boat could be deployed up to about 50 km from their drill-rig, but this depends on conditions and iceberg positions at that time. The supply boats are equipped to make meteorological, ocean, and iceberg measurements, and will provide the primary source of in-situ data, supported by information from any drill ships in the area and relevant aircraft data.

Radar contrast measurements (iceberg-water and iceberg-sea ice), made in 1978 and 1979 and subsequent modeling work, show that the radar incidence angle is a very important parameter that can dictate detectability when the iceberg is surrounded by water (Refs. 1 and 2). SIR-A and Seasat imagery also shows clearly, but in a qualitative way, that targets in the ocean are much more readily visible at larger incidence angles. Because modeling is especially difficult for "many-pixel" targets, we have developed software that degrades aircraft high-resolution SAR data to produce simulated spaceborne SAR images.

Our basic objective for the SIR-B iceberg experiment is to investigate the target detectability as a function of radar incidence angle and environmental conditions. The key elements in the overall program are the use of existing and future X-, L- and C-band aircraft SAR data for modeling, satellite image simulation, and SIR-B underflights; the use of the airborne Ku- and C-band scatterometers to help with ocean measurements and modeling; and the acquisition, by the oil companies, of a range of relevant target, ocean, and meteorological parameters. It is also anticipated that the Atmospheric Environment Service (AES) will contribute to the experiment by flying iceberg reconnaissance flights (with SLAR) both before and during the SIR-B period.

III. Approach for Data Acquisition, Handling, and Analysis

Surface data acquisition will be the prime responsibility of Petro-Canada and will be carried out to the extent possible considering that the work boats are on station primarily for operational support of the drill ships. Data collected will include wind, wave, and iceberg measurements, as well as special efforts to measure currents in a region covered by at least one of the SIR-B swaths. Further iceberg and ocean information will be derived from aircraft data; this will include airborne photography, C- and Ku-band scatterometer data for wind speed modeling and, possibly, laser profiling. It is hoped and anticipated that an APS-94 D SLAR-equipped AES aircraft will do a prior iceberg survey mission along the Labrador coast, concentrating on the potential SIR-B swaths so that the best areas for detailed in-situ measurements can be chosen. The Convair-580 aircraft, belonging to the Canada Centre for Remote Sensing and containing the CCRS-ERIM X/L/C SAR, will be based in Frobisher Bay for part of the SIR-B period and will acquire scatterometer, radar, photographic, and pos-

sibly laser profile data. The detailed schedule for participation of this aircraft will be worked out when the SIR-B orbit and incidence-angle sequence is finalized, and will involve contributions to two other experiments during, and close to, the SIR-B period.

Initial analysis of survey optical SIR-B imagery will be carried out to help define scenes for digital processing and subsequent quantitative analysis. Some raw data will be requested for processing in Canada, and it is anticipated that this data would be used for special analysis, e.g., doppler centroid analysis. Quantitative analysis of digitally processed image data will allow evaluation of detection methods, extraction of contrast ratios, and comparison of clutter levels with C- and Ku-band backscatter measurements. The latter will help in evaluating relative ocean backscatter sensitivity to wind speed at the different wavelengths and, therefore, will help in modeling frequency sensitivity of iceberg detectability. All data, both aircraft and SIR-B, will be correlated with the in-situ meteorological and oceanographic data to the extent possible. It is hoped that some comparison of surface currents with data derived from SIR-B can be carried out by J. Gower of the Institute of Ocean Sciences.

IV. Expected Results

(1) The SIR-B experiment will add significantly to our overall program to evaluate the potential of aircraft and satellite radars for iceberg and ice hazard detection.

(2) Using the aircraft scatterometers, the in-situ wind data, and the SIR-B digitally processed data, it would be possible to evaluate relative backscatter sensitivity to wind speed at the three frequencies.

(3) The feasibility of using Doppler centroid estimation of the SIR-B data to estimate the surface-current range component will be evaluated by comparison with current measurements. (The possibility of even one component of the surface-current field would be very useful to the offshore exploration industry in terms of improving iceberg drift models.)

References

1. Gray, A. L., Hawkins, R. K., Livingstone, C. E., Lowry, R., Larson, R., and Rawson, R., "The Influence of Incidence Angle on Microwave Radar Returns of Targets in an Ocean Background," *13th International Symposium on Remote Sensing of Environment,* Ann Arbor, Michigan, pp. 1815-1837, 1979.

2. Pearson, D., Livingstone, C. E., Hawkins, R. K., Gray, A. L., Arsenault, L. D., Wilkinson, T. L., and Okamoto, K., "Radar Detection of Sea-Ice Ridges and Icebergs in Frozen Oceans at Incidence Angles from 0 to 90 Degrees," *Proceedings of the Sixth Canadian Symposium on Remote Sensing,* Halifax, Nova Scotia, pp. 231-241, 1980.

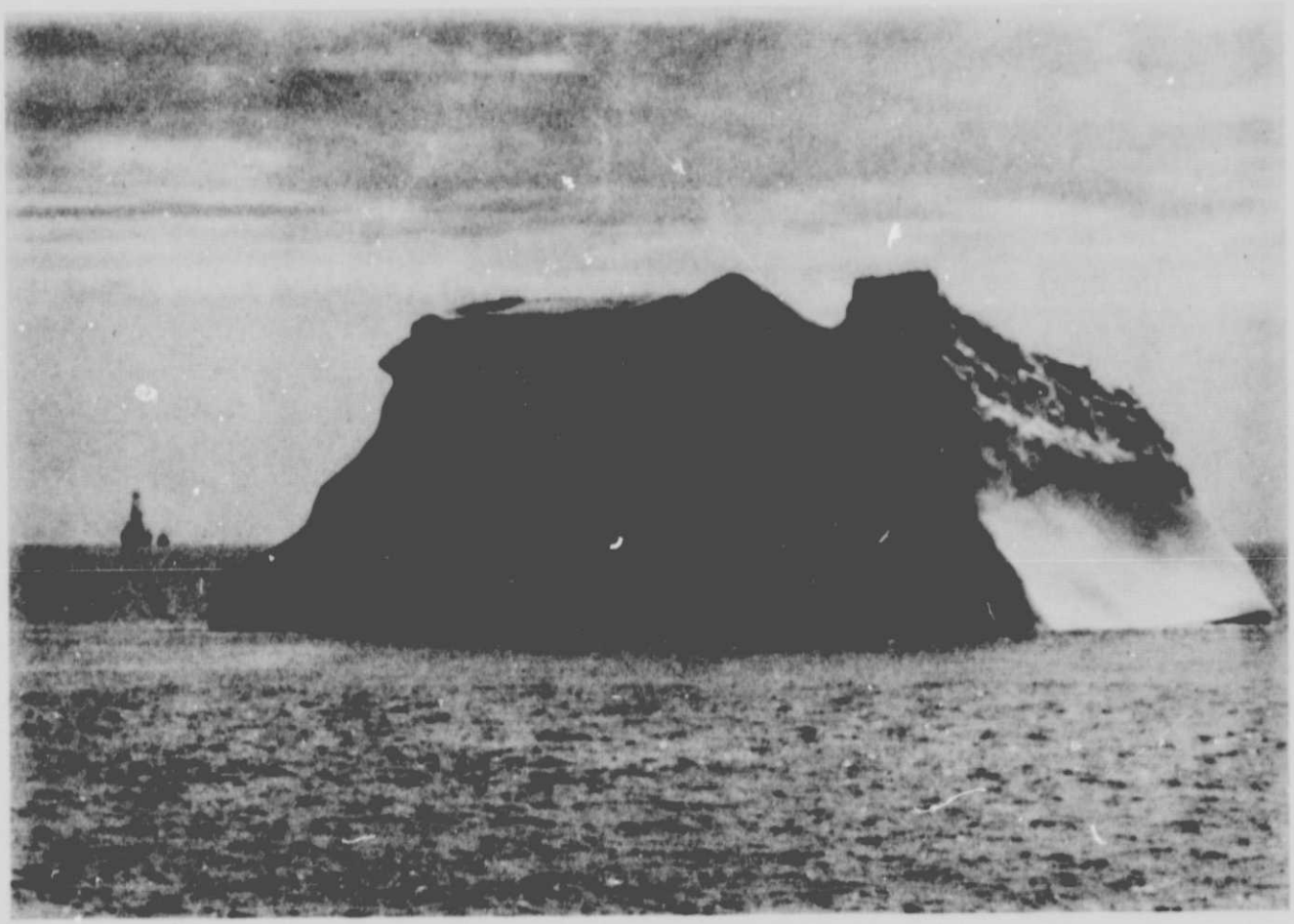

Fig. 1. Photograph of a 460 × 10^6 kg iceberg approximately 10 km from the drill ship *Pecnorse 1* off the Labrador coast. At the time of the photograph, the iceberg was being towed away from the drill ship. Previous water lines can be seen on the 100-m iceberg.

N85-17226

Geological, Structural, and Geomorphological Analyses From SIR-B

Team Member:

J. W. Head III
Brown University
Providence, Rhode Island

Collaborators:

P. J. Mouginis-Mark
University of Hawaii
Honolulu, Hawaii

S. H. Zisk
Haystack Observatory
Westford, Massachusetts

R. A. F. Grieve and **A. R. Peterfreund**
Brown University
Providence, Rhode Island

K. D. Sullivan
NASA Johnson Space Center
Houston, Texas

I. Introduction

The purpose of our study is to utilize the unique characteristics of the SIR-B mission to develop a better understanding of the application of radar in geologic studies. In deltaic environments, we examine delta morphology and the intertidal zone, the surface expression of shallow bathymetry, the characterization of vegetation cover, and the water balance of the delta. In impact crater environments, we seek to establish the radar characteristics of exposed impact craters and apply this knowledge to test for the detectability of very poorly exposed impact craters.

II. Deltaic Environments

The analysis of synthetic-aperture radar (SAR) images has been shown to be of value in the interpretation of structural and surficial geological features (Ref. 1). Preliminary studies of SIR-A data (Ref. 2) have shown that such data are also useful for the geomorphological analysis of coastal environments, particularly deltaic regions. We seek to extend such studies by exploiting the multiple-look-angle capability of the SIR-B experiment coupled with digital multispectral images from the Landsat Thematic Mapper and a thermal infrared mapping spectrometer experiment. These data will be used to

(1) map the water-land interface of deltas over an entire tidal cycle; (2) investigate the potential that surface wave forms can provide information on shallow-water bottom topography (Ref. 3), and (3) characterize the diverse range of salt- and fresh-water vegetation types that are located on the stable portion of deltas.

The Mississippi Birdsfoot Delta is the primary test site, because this is the classic example of a constructional (sediment-dominated) delta. The Birdsfoot also has numerous logistical advantages in comparison to deltas elsewhere in the world, in that pertinent information on the river sediment load and flow rate, the tidal regime, and the local bathymetry are all frequently monitored by the U.S. Army Corps of Engineers. Additional deltas from around the world are also SIR-B targets, both because they represent delta types in contrast to that of the Mississippi (i.e., their coastlines are wave or wind dominated; Ref. 4) and because they provide alternative targets should it be impossible for the Shuttle to image the primary site.

A. Delta Morphology and the Intertidal Zone

Detailed knowledge of the sedimentation rates at different parts of the Mississippi Delta are of critical importance for assessing navigation hazards, changing direction of river flow, and the stability of subaerial sand bars (Refs. 5 and 6). Major problems in the monitoring of this sediment movement lie with the need to rapidly measure both the changing distribution of exposed deposits and the distribution of slopes in the intertidal zone: working conditions in these areas are difficult because of very shallow water and soft sediments (Ref. 4). With our preliminary analysis of the SIR-A data of the Mississippi (Ref. 2), it was strikingly clear that at depression angles of about 50°, the boundary between the water and the exposed sediments was very clearly depicted. Quantification of the exposed land area is thus possible in this area, due to the strong contrast in radar returns from these two targets.

The SIR-A experiment provided a single image of the middelta; we will extend this study by using multiple SIR-B images acquired at varying times in the tidal cycle. An aspect of this repeat coverage will be that changes in the delta between the years 1981 and 1984 (SIR-A vs SIR-B data) could be investigated. More importantly, however, multiple SIR-B images will enable the area of land (and thus the local intertidal slopes, Fig. 3 of Ref. 5) to be measured at different times in the tidal cycle. The Gulf of Mexico has a tidal range of 1 to 1.5 m at this location, so that the shallow sediment slopes will permit large areas of the delta to be exposed at low tide. A quantification of this increase in land area as the tide retreats will therefore permit low energy (shallow slopes – large area variation) and high energy (steeper slopes – small area variation) environments to be distinguished. Acquired as a snapshot in time, these data on the delta will be of use in the more general characterization of the area should repeat coverage be obtained from subsequent Shuttle missions; the dynamic response of the delta to periods of river flooding (accentuated by greater sediment deposition due to greater up-river erosion) can be precisely monitored (Ref. 5).

B. Surface Expression of Shallow Bathymetry

A discovery from the Seasat mission was the ability of high-depression-angle radars (67°) to recognize wave forms in shallow water that appear to indicate local submarine topography (Ref. 3 Plates 31 and 32). Similar observations from Seasat show that the shallow waters (1 to 2 m) at the mouth of the Birdsfoot Delta indicate some aspect of the submarine slopes. We will use SIR-B data obtained at steep depression angles (65 to 75°) to further investigate the shallow sediment deposits around the Birdsfoot. In particular, a range of radar depression angles that will allow selection of the most useful viewing geometry for studying this phenomenon is requested. The relevance of this kind of analysis lies with the fact that submarine deposition is the initial stage of deltaic growth (Ref. 7), and changes in this submarine topography are primary indicators of the evolving sedimentation history of the delta (which in turn is critical for continued navigation of the channels). Such an investigation of submarine topography is also of value for comparison with the analyses to be carried out in experiment A above.

C. Characterization of Vegetation Cover

Comparison of SIR-A and U-2 high-altitude near-infrared images of the Mississippi Delta (Ref. 2) revealed that many of the similar radar returns were generated by different types of vegetation cover. Not only do different types of marsh exist (fresh to saline water marshes), but also the degree to which cypress swamp is flooded varies from free-standing water to relatively dry areas (Ref. 8). Distinguishing between these vegetation types proved to be very difficult from the single SIR-A image; however, it is evident that multiple-depression-angle SIR-B data, used in conjunction with a Thematic Mapper image, would greatly improve this characterization capability. Multiple-depression-angle radar data (acquired on the same orbits as the data for experiments A and B above, i.e., 45 to 70°) would permit the scattering properties of the vegetation types to be distinguished by using techniques similar to those employed in Refs. 9 and 10. It is believed that this approach would be particularly helpful for interpreting the effects of free-standing water beneath trees (Ref. 11).

We plan to conduct a basic experiment into the utility of using both SIR-B radar images and thermal infrared data (collected by NASA with one of their thermal IR mapping spectrometers). It is believed that the thermal signature of still-standing water will be different (warmer) than the frequently recharged bodies of water (colder). Once the distribution of inland standing water is measured by the SIR-B radar (at the same time as the data for experiment A is taken), the thermal properties of each water body will be investigated with the computer facilities at our respective institutions.

In summary, it is believed that the proposed experiments will be very beneficial in the rapid monitoring of coastal processes in depositional environments. The distribution of wetlands, an assessment of intertidal slopes, shallow submarine deposition, and vegetation characterization can all be achieved for the Mississippi and, depending on data coverage, the other targeted deltas. In view of the rapidly changing morphology of the Mississippi (variations occur on a timescale of months to a few years; Ref. 5), these data will form a base-line data set for subsequent investigations of temporal change in this economically critical area of the Gulf Coast.

III. Impact Craters

The number of recognized terrestrial impact structures with diameters larger than a kilometer stands at approximately 100 (Ref. 12). As a result of the dynamic nature of the terrestrial geologic environment, much of the characteristic crater topography has been removed at many structures and recognition has been from the presence of a circular geologic or structural anomaly, detected initially on high-level aerial photographs or, more recently, synoptic images obtained by [illegible] processes of erosion that hamper recognition [illegible] the substructure to various levels and [illegible] duction of the petrologic and structural [illegible] the structures. This provides a data set [illegible] ntary to studies of planetary craters, where init[illegible]phologies are well-preserved but the subsurface structural relationships are inaccessible (Ref. 13).

Although terrestrial crater studies have provided considerable insight into impact cratering as a geologic process on the planets, the place of impact cratering in the geologic evolution of the Earth has received little attention. Some recent studies, however, have centered on possible links between the development of the primary oceanic and continental crustal dichotomy in early Earth history and very large, basin-sized ($\sim 10^2$ to 10^3 km) impact structures (Refs. 14, 15, and 16). In addition, the discovery of relative enrichments in meteoritic signature elements at Cretaceous-Tertiary boundary sites throughout the world have pointed to a major impact event 65 Myr ago, which had global effects. The coincidental mass extinction of approximately half the faunal genera living at the time has led to considerable discussion of a cause-effect relationship between major impact events and the biological and climatological evolution of the Earth (Ref. 17). In terms of Earth resources, various large impact structures are known to be related to concentrations of minerals, hydrocarbons, and, in some cases, increased hydroelectric potential. These concentrations are due to a number of crater-related features, including the creation of a topographic depression, postcrater sedimentation in a restricted environment, primary localization of economic materials within the crater structure, and secondary mineral enrichments due to increased fracturing associated with the crater.

For the reasons of long-term geologic stability and vigorous crater-search programs, the majority of known terrestrial craters are located on the North American and European cratons. The potential coverage of SIR-B extends to approximately 60°N and includes most of these structures. For structures on the North American craton, those occurring on the Canadian Shield represent a sample with relatively constant target characteristics and for which the geology and geophysics are relatively well-known. Accordingly, a selected number of these structures will constitute the primary targets for study. Two principal experiments will be undertaken.

A. Establish Radar Characteristics of Exposed Impact Craters

We will use SIR-B data to establish the radar characteristics of a selected number of large terrestrial craters and thereby augment our knowledge of terrestrial craters. As a first step, the SAR data obtained by SIR-B will be compared with Landsat and geological data to establish correlations between radar characteristics and ground-truth information. The structures selected for study are: Manicouagan (D ~ 100 km), the twin Clearwater Lake structures (D ~ 32 km and 22 km), Mistastin (D ~ 28 km), Charlevoix (D ~ 54 km), and Sudbury (D ~ 140 km).

Target rock fracturing is a well recognized feature at eroded impact structures. Fracturing is a reflection of the structural disturbance of 100 to 1000 km^2 of the target in a large impact event. Its significance, however, is not well understood. Although some field studies of fracturing around large impact craters have been attempted (Ref. 18), they have had limited success because of the large areal extents involved. Landsat images of Manicouagan and Clearwater Lake have revealed a halo of increased fracturing in the basement rock,

which extends out beyond estimates of the original rim diameter (Refs. 19 and 20). In the case of Manicouagan, changes in fracture pattern with radial distance have been used to estimate original crater dimensions (Ref. 13). The SIR-B data will help refine these estimates and provide new information on the nature, distribution, and origin of the structure associated with impact craters. Mistastin has only a subtle fracture halo on Landsat images. The series Mistastin, Clearwater Lake, and Manicouagan represents increasing erosional level. The SIR-B data may help determine whether the indistinct halo at Mistastin is real or apparent and clarify the relationships of fracturing to crater size and depth of erosion. SIR-B data on these structures will be used initially in comparison with Landsat data to characterize the nature and extent of the fracture halo. Charlevoix was chosen for study as the region with the most seismically active area in eastern North America, with numerous earthquakes in a tight zone 30 by 90 km and parallel to the St. Lawrence River. The activity is probably related to failure in the Grenville basement along normal faults that predate the impact event (Ref. 21). Although not directly related to the impact event, the seismic activity appears spatially related to the crater and thus may be due to an increase in crustal weakness produced by the impact event. Considerable geophysical data are available for Charlevoix and the SIR-B data will provide a valuable supplement in determining the relationship of crater structure and seismic activity. An analysis of Sudbury presents an opportunity to refine structural relations of this geologically complex area and to define relationships between crater structure and ore concentrations. Nickel-sulphide ore deposits at Sudbury are concentrated in radial offsets of the Sudbury Irruptive, and Morrison (Ref. 22) has suggested that ore emplacement is controlled by crater structure. SIR-B images of the heavily eroded and relatively flat Sudbury area may provide previously unobtainable information on crater structure and lithologies. Quantitative techniques of unit definition and characterization outlined above will be applied to these several areas to establish the radar characteristics of exposed impact craters and to test the ability of SIR-B's unique illumination geometries to reveal structural information beyond that commonly revealed by solar illumination.

B. Test Detectability of Very Poorly Exposed Impact Craters Using Radar

It is unlikely that radar will detect impact craters that are completely buried. There are, however, a number of structures that are partially buried or extremely heavily eroded and have little known surface expression. To determine the utility of radar in defining structural elements of craters of these types, the Carswell and Lake St. Martin structures have been selected as potential test sites. Lake St. Martin ($D \sim 23$ km) is partially buried beneath postcrater red beds and evaporites of Jurassic age. The evaporite deposits are exploited commercially. The geology of the area is poorly exposed, as there is a covering of glacial clays. As a result, the structural elements and size of the structure are not well defined and are known only from a shallow drilling program. SIR-B data on Lake St. Martin will be analyzed to determine whether it provides additional structural information on partially buried craters. In the case of Carswell, the structure has been eroded to the extent that it has no topographic expression. As with Sudbury, it has considerable economic interest. Uranium mineralization, related to a basement regolith, is exposed in a few places by the structural uplift of the central portion of the crater (Ref. 23). The Carswell structure is virtually undetectable on Landsat images, although a circular pattern is visible on geologic maps as the discontinuous distribution of various lithological units. The area is relatively featureless and the geologic outcrop relatively poor. Radar images of the structure may help define better the radial dimensions of the structure and details of the uplifted central area, which is of economic interest.

In summary, it is believed that the experiments will be very useful in providing basic supplemental information in the characterization of terrestrial impact craters, particularly in reference to their structure, where the unique capabilities of SIR-B will be utilized. In addition, criteria for the identification of exposed and buried impact craters will be developed. These results could have significant economic potential and will provide a basis for input into the design of future radar experiments and instruments.

References

1. Elachi, C., (1980) "Spaceborne Imaging Radar: Geologic and Oceanographic Applications," *Science*, Vol. 209, pp. 1073-1082.

2. Mouginis-Mark and Zisk, in preparation.

3. Fu, L.-L., and Holt, B., (1982) *Seasat Views Oceans and Sea Ice with Synthetic-Aperture Radar*. JPL Publication 81-120, 200 pp. Jet Propulsion Laboratory, Pasadena, California, February 15, 1982.

4. Miall, A. D., (1979) "Deltas," in *Facies Models*, Walker, R. G., editor. Geol. Soc. Canada Publications, Toronto, Ontario, pp. 43-56.

5. Rouse, L. J., Roberts H. H., and Cunningham, R. H. W., (1978) "Satellite Observation of the Subaerial Growth of the Atchafalaya Delta, Louisiana," *Geology*, Vol. 6, pp. 405-408.

6. Roberts, H. H., Adams, R. D., and Cunningham, R. H. W., (1980) "Evolution of Sand-Dominant Subaerial Phase, Atchafalaya Delta, Louisiana," *Amer. Assoc. Pet. Geol. Bull.*, Vol. 64, pp. 264-279.

7. Coleman, J. M., (1966) *Recent Coastal Sedimentation: Central Louisiana Coast.* Louisiana State University Press, Baton Rouge, pp. 1-16.

8. Demarke, J. A. S., (1981) *Analysis of Seasat Radar Imagery for Geologic Mapping in Louisiana, Kansas and Oklahoma*. Unpublished M. Sc. Thesis, University of Arkansas, 118 pp.

9. Blom, R. G., and Daily, M., (1982) "Radar Image Processing for Rock-Type Discrimination," *IEEE Trans. Geosci. Rem. Sen.*, Vol. GE-20, pp. 343-351.

10. Sharmugan, K. S., Narayanan, V., Frost, V. S., Stiles, J. A., and Holtzman, J. C., (1981) "Textural Features for Radar Image Analysis," *IEEE Trans. Geosci. Rem. Sen.* Vol. GE-19, pp. 153-156.

11. Engheta, N., and Elachi, C., (1982) "Radar Scattering From a Diffuse Vegetation Layer Over a Smooth Surface," *IEEE Trans. Geosci. Rem. Sen.*, Vol. GE-20, pp. 212-216.

12. Grieve, R. A. F., (1982) "The Record of Impact on Earth: Implications for a Major Cretaceous/Tertiary Impact Event" *Geol. Soc. Amer. Sp. Paper 190*, pp. 25-38.

13. Grieve, R. A. F., and Head, J. W., (1983) "The Manicouagan Impact Structure: An Analysis of Its Original Dimensions and Form," *Jour. Geophys. Res.*, Vol. 88, Supplement, pp. A807-A818.

14. Frey, H., (1980) "Crustal Evolution of the Early Earth. The Role of Major Impacts," *Precamb. Res.*, Vol. 10, No. 3-4, pp. 195-216.

15. Grieve, R. A. F., (1980) "Impact Bombardment and Its Role in Proto-Continental Growth on the Early Earth," *Precam. Res.* Vol. 10, No. 3-4, pp. 217-247.

16. Klasner, J. S., and Schulz, K. J., (1982) "Concentrically Zoned Pattern in the Bouguer Gravity Anomaly Map of Northeastern North America," *Geology*, 10, Vol. 10, pp. 537-541.

17. *Geol. Soc. Amer. Sp. Paper*, Vol. 190, 1982.

18. Roy, D. W., (1969) *Etude de la Fracturation dans la Partie Ouest de la Structure Circulaire de Manicouagan*. M. Sc. Thesis, Univ. Montreal, Quebec.

19. Dence, M. R.. Grieve, R. A. F., and Robertson, P. B., (1977) "Terrestrial Impact Structures: Principal Characteristics and Energy Considerations," in *Basaltic Volcanism in the Terrestrial Planets*, (Roddy, D. J., Pepin, R. O. and Merrill, R. B., editors. Pergamon Press, N.Y., pp. 247-275.

20. Orphal, D. O., and Schultz, P. H., (1978) "An Alternative Model for the Manicouagan Structure, *Proc. Lunar Planet. Sci. Conf. 9th*, pp. 2695-2712.

21. Anglin, F., and Buchbinder, G., (1981) "Microseismicity in the Mid-St. Lawrence Valley Charlevoix Zone, Quebec," *Bull. Seism. Soc. Amer.*, Vol. 71, pp. 1553-1560.

22. Morrison, G. G., (1982) "Impact Crater Morphology and Its Relevance to the Emplacement of the Sudbury Basin Ore Deposits," *Geol. Assoc. Canada Ann. Mtg. Program with Abstract*, Vol. 7, p. 68.

23. Johns, R. W., (1980) "Athabasca Sandstone and Uranium Deposits, *Western Miner.*, Oct. 1980, pp. 42-52.

Amplitude Calibration Experiment for SIR-B

Team Member:

D. N. Held
Jet Propulsion Laboratory
Pasadena, California

Collaborator:

F. T. Ulaby
University of Kansas Center for Research, Inc.
Lawrence, Kansas

I. Summary

The quantitative use of synthetic-aperture radar (SAR) image data requires that the imagery be well calibrated. To obtain accurately calibrated imagery, it is necessary to account for a sizable list of variables; among them are the antenna pattern, spacecraft attitude, transmitter power, receiver gain, system linearity, and SAR correlator effects. Only some of these corrections are currently being implemented on the JPL SIR-B operational SAR processor, and, in particular, the digital imagery produced by that processor will not be labeled in units of sigma zero.

Our investigation will seek both to calibrate the SIR-B imagery and then to verify that calibration by conducting appropriate "ground-truth" measurements, utilizing in part the NASA CV-990 L-band SAR and the University of Kansas Mobile Radar Scatterometer.

II. Objectives

There are four major objectives in this experiment:

(1) To measure the repeatability (stability) of the SIR-B system,

(2) To relatively calibrate the SIR-B system,

(3) To absolutely calibrate the SIR-B system,

(4) To verify the accuracy of the calibration by comparing the results to measurements made by a ground spectrometer and an airborne SAR.

There are few authors with publications in the formally reviewed literature claiming to have calibrated a SAR absolutely. Recently, papers have begun to emerge presenting the results of calibration experiments that have actually been conducted (Refs. 1 through 4); results indicate that significantly more work must be done in the field. For instance, Held (Ref. 4) has recently reported on the calibration of the SEASAT SAR, which resulted in a repeatability accuracy of between 0.35 and 0.8 dB (Ref. 4) and an absolute accuracy of 2-3 dB (Ref. 5).

We propose to use the signal from the calibrator module being built for SIR-B (designed under the direction of D. Held) along with orbit attitude and various sensor performance parameters to calibrate portions of the SIR-B image data set. Target areas will be independently measured by a calibrated Mobile Radar Scatterometer, supplied by T. Ulaby, and by the NASA CV-990 SAR, which D. Held is attempting to calibrate

in an effort to verify the σ_0 estimates produced by the calibrated SIR-B imagery.

III. Approach

Any time-invariant linear system can be calibrated. However, the typical SAR is neither time-invariant nor linear. When measuring the small-signal gain of a system, one makes the implicit assumption that the system is linear and that all signals are treated the same and independently by the system. Thus, the principle of *superposition* is assumed to be valid.

Unfortunately, many (if not most) SAR systems violate this basic assumption, optically recorded SAR systems being the classic case in point, since the transfer function of the film is highly nonlinear. SAR systems employing digital data recording are more amenable to accurate calibration. However, it is all too easy but incorrect to assume that the digital recording and processing of SAR data will cure all the nonlinearity and dynamic range difficulties encountered when optically recording SAR data.

To preclude nonlinearities induced by an analog-to-digital converter (A/D), it is necessary to employ a sufficient number of bits in the digital representation of the analog signal, and to verify that the radar signal is neither overflowing nor underflowing the dynamic range of the A/D. Further, even if the entire digital recording and processing system can be shown to be linear, it is still possible to have nonlinearities in the radio frequency (RF) sensor electronics. Therefore, for SIR-B, the RF and A/D systems have been carefully designed such that the A/D subsystem saturates before the RF subsystem, and the saturation can be easily detected by monitoring a histogram of the digital data.

Thus the SIR-B calibration procedure involves:

(1) Data screening, to monitor A/D overflow or underflow.

(2) Normalization with respect to the onboard calibrator.

(3) Correlation of the raw data into images.

(4) Correction for thermal noise.

(5) Final corrections for slant range, transmitter power, incidence angle, antenna pattern, and Shuttle attitude.

Many of the steps listed above will not be performed by the operational SIR-B processor, which will provide only a limited calibration capability on an operational basis.

The tasks involved in this research are:

(1) Calibrating the CV-990 SAR (not currently funded by SIR-B).

(2) Building calibrated ground receivers at JPL.

(3) Mission and logistical planning,

(4) Development of preprocessing, postprocessing, and correlation software for SIR-B and the CV 990 SAR,

(5) Flying the CV 990 SAR over the test areas,

(6) Deploying ground receivers in the test area,

(7) Deploying the radar spectrometer in the test area,

(8) Data reduction from the three radars and the ground receivers,

(9) Overall assessment of calibration experiment results.

IV. Expected Results

It is anticipated that the results from the three radars employed in this experiment will be in agreement to within 3 dB. This will represent a major milestone in the field of active microwave remote sensing. If SIR-B and the CV 990 can be shown to be stable over time, it will be possible to cross-calibrate each with the ground spectrometer, substantially improving the absolute calibration of the airborne and spaceborne sensors.

It is anticipated that this experiment will prove that two generically different active microwave sensors are capable of making comparable estimates of common targets, a result that has generally been difficult to obtain in the past.

It is anticipated that as a result of this experiment, it may be possible to calibrate all SIR-B data taken in the calibration mode to a relative accuracy of 1.0 dB, and an absolute accuracy of between 1.5 and 2.0 dB.

References

1. Held, D. N., Bennet, J., and Shuchman, R., "The SEASAT SAR: Engineering Performance Evaluation," in *Digest of the 1982 International Geoscience and Remote Sensing Symposium*, Vol. I, Munich, June 1-4, 1982.

2. Held, D. N., Brown, W. E., Mehta, N. C., and Croft, C., "Amplitude Calibrating the SEASAT SAR Imagery," in *Digest of the 1892 International Geoscience and Remote Sensing Symposium*, Vol. II, Munich, June 1-4, 1982.

3. Larsen, R., at the EARSel Workshop on Radar Calibration, Alpach, Austria, December 6-10, 1982.

4. Held, D. N., "Amplitude Calibration of Spaceborne Synthetic Aperture Radars," presented at the EARSel Workshop on Radar Calibration, Alpach, Austria, December 6-10, 1982.

5. Held, D. N., Werner, W. A., "The Absolute Amplitude Calibrations of the SEASAT Synthetic Aperture Radar," in *Digest of the 1983 International Geoscience and Remote Sensing Symposium*, San Francisco, August 1983.

N85-17228

Microwave and Optical Remote Sensing of Forest Vegetation

Team Member:

R. M. Hoffer
Purdue University
West Lafayette, Indiana

Collaborators:

M. E. Bauer, L. L. Biehl, and **R. P. Mroczynski**
Purdue University
West Layfayette, Indiana

I. Introduction

Experience with the repetitive, synoptic view of Earth provided by satellite-borne sensors such as Landsat MSS and TM, and NOAA AVHRR have clearly indicated the value of such systems in obtaining much of the information needed on vegetation types, areas, and conditions. Some studies have found that results in classifying land use or cover type are improved if both optical and radar data are used, rather than utilizing the data from only one portion of the spectrum (Refs. 1 and 2). To date, these research results tend to indicate that neither data set is a replacement for the other; however, the combined data sets can be an improved means to better characterize the scene with remote sensing.

The research described here will focus on two aspects of the data to be obtained as part of the SIR-B program:

(1) Digitally registered TM and SIR-B data, which will allow assessment of the potentials and limitations of each type of data, as well as the *synergistic effects* of combining these types of data.

(2) *Multiple-look angles* of SIR-B data, which will enable quantitative assessments to be made of the effect of different look angles on the radar return from varied forest-cover type, height and density characteristics, planting direction and crown spacing, topographic and soil variations, and other variables specific to the test sites.

Recent work by Laboratory for Applications of Remote Sensing (LARS) researchers with X-band, dual-polarized SAR data obtained over a test site in South Carolina has clearly shown some of the potentials and limitations for differentiating various agricultural and forest-cover types. In this study, deciduous forest could be separated easily and reliably from coniferous forest on the HH polarized data, but not on the HV polarized data (both qualitative and quantitative methods of data analysis were used). Of great interest (and concern) was the fact that coniferous-forest- and pasture-cover types could not be separated on either polarization, even though they are so very different in morphology (Refs. 3 and 4). Similar results have also been found with L-band systems in some cases, such

as the confusion between forest canopies and corn reported by Batlivala and Ulaby (Ref. 5) and Paris (Ref. 6).

II. Objectives

The overall objective of this research is to define the strengths and limitations of microwave (SIR-B) and optical (TM) data, *singly* and in *combination*, for the purpose of identifying and characterizing forest-cover types and condition classes.

Specific objectives include the following:

(1) To determine the relative advantages and limitations of SIR-B SAR data and Thematic Mapper/MSS data, in combination and separately, in quantitatively identifying and measuring the areal extent of forests in northern Florida.

(2) To define the effectiveness of a contextual classification algorithm (SECHO), as compared to standard "per-point" classifiers (Gaussian Maximum Likelihood and Minimum Distance), in classifying the Landsat TM and SAR data in a manner that will utilize the *spatial* characteristics of such data for purposes of cover-type discrimination.

(3) To evaluate the relative utility of different look angles of SAR data in determining differences in stand density of commercial stands of coniferous and hardwood forests.

(4) To determine the effectiveness of the L-band HH polarized SIR-B data as compared to X-band dual polarized SAR obtained from aircraft, in differentiating various forest-stand densities.

III. Test Site Characteristics and Reference Data

The test site is located in northeastern Florida just west of Jacksonville, and consists of a large number of well-defined, operationally managed forest stands. These stands contain a wide variety of species, age, basal area, tree height, stand volume, tree spacing, site index, stand history, and soil type. Aerial photography of the study site also exists. Since the area is within the managed forest-land holdings of the St. Regis Paper Company, detailed records of the stand characteristics as well as past management practices have been maintained, and will be made available in support of the proposed research.

Ground observation/measurement data to be obtained at the time of the SIR-B data collection will include information on stand conditions, species, and species mixtures of forest stands outside of the St. Regis holdings; understory vegetation at the time of SAR data collection, and, for 10 stands, the foliage moisture content.

Ancillary data to be assembled in support of the investigation include soil-type maps and topographic maps, and definition of ground control points for registration of Landsat and SIR-B data.

IV. Data Analysis

To address the primary objective of evaluating the synergistic effects of combined optical and microwave data, Landsat TM and the multiple-look angles (3, above) of SIR-B will need to be digitally registered. The Landsat TM data will be obtained as nearly as possible to the date that the SIR-B is obtained.

Once the necessary data sets are registered, we will locate coordinates of stands that have been previously selected using the existing aerial photography, and for which ground observation data will have been obtained. Initially, a supervised analysis approach and a maximum likelihood classification algorithm will be utilized. The classification results will be evaluated using a statistically defined random sample of test areas.

The classification will then be repeated using the SECHO (Supervised Extraction and Classification of Homogeneous Objects) classifier to determine the effectiveness of the use of spatial context as compared to per-point classifications. Both the SECHO and the Gaussian Maximum Likelihood (GML) results will then be compared to results obtained from the Minimum Distance per-point classifier.

Next, a series of analyses will be conducted in which various "optimum" subsets of 3, 4, or more channels (either SIR-B or TM channels or transforms of SIR-B and TM channels) will be defined, based on transformed divergence values. The defined combinations of channels will be used, in conjunction with the "best" of the three classification algorithms evaluated, to classify the data. These results will enable an evaluation to be made of the information content or value of the various wavelength bands of TM data and the different incidence angles of the SIR-B data. The results of all these classifications will be based on test field-classification performances.

Another portion of this study will address the question of the accuracy and reliability of area estimates of forest and adjacent nonforest-cover types as a function of SIR-B incidence angles. This work will also provide an evaluation of

the accuracy of the geometric rectification procedure applied to the SIR-B data.

V. Anticipated Results

It is anticipated that this data set will provide an excellent opportunity to study the synergistic effects obtained by using combined L-band SAR and TM data for identifying and characterizing forest-stand characteristics. The effectiveness of quantitative computer classification using SAR data also will be compared with visual analysis and interpretation of the data. The use of both the per-point and contextual classification algorithms will provide definitive results concerning the value of utilizing both the spectral and the spatial information content in the data when classifying forest cover.

In addition to the above results, the channel-evaluation analysis will indicate the relative values of the different look angles and the individual TM wavelength bands. The area-evaluation study will also provide data concerning the fidelity of the geometric rectification of the SAR data and the effectiveness of area estimates based solely on single look-angle SAR data – a result that could be important in attempting to use SAR data for monitoring tropical deforestation on a worldwide basis.

Since extensive and detailed data on the vegetative-canopy characteristics (e.g., height, spacing, and stand volume) are already in existence for this test site, the results of this SIR-B incidence-angle study are expected to provide very valuable information regarding the forest-canopy parameters that may or may not be of particular significance in determining the strength of the radar return signal. Such information is critical in determining the effectiveness of SAR systems for obtaining much needed data on standing vegetation biomass.

References

1. Li, R., and Ulaby, F. T., (1980) "Crop Classification With a Landsat/Radar Sensor Combination," in *Proc. Symp. on Machine Processing of Remotely Sensed Data*, Purdue University, West Lafayette, Indiana, pp. 78-87.

2. Wu, S. T., (1982) "Multisensor Data Analysis and Its Application to Monitoring of Cropland, Forest, Strip Mines and Cultural Targets," in *Proc. Symp. on Machine Processing of Remotely Sensed Data*, Purdue University, West Lafayette, Indiana, pp. 313-320.

3. Hoffer, R. M., Dean, M. E., Knowlton, D. J., and Latty, R. S., (1982) *Evaluation of SLAR and Simulated Thermatic Mapper Data for Forest Cover Mapping Using Computer-Aided Analysis Techniques*. Final Report on NASA Contract NAS9-15889. LARS Technical Report 083182, Purdue University, West Lafayette, Indiana, 271 pp.

4. Knowlton, D. J., and Hoffer, R. M., (1981) "Radar Imagery for Forest Cover Mapping," in *Proc. Symp. on Machine Processing of Remotely Sensed Data*, Purdue University, West Lafayette, Indiana, pp. 626-632.

5. Batlivala, P. P., and Ulaby, F. T., (1975) *Crop Identification From Radar Imagery of the Huntington County, Indiana Test Site*. RSL Technical Report 177-58, University of Kansas Center for Research, Inc., Lawrence, Kansas.

6. Paris, J. F., (1982) "Crop Identification With Multifrequency, Multipolarization, and Multiangle Radars," in *Proc. Symp. on Machine Processing of Remotely Sensed Data*, Purdue University, West Lafayette, Indiana, pp. 273-280.

Evaluation of SIR-B Imagery for Geologic and Geomorphic Mapping, Hydrology, and Oceanography in Australia

Team Member:

F. R. Honey
Commonwealth Scientific and Industrial Research Organization
Wembley, Australia

Collaborators:

C. J. Simpson
Bureau of Mineral Resources
Canberra City, Australia

J. Huntington, R. Horwitz, G. Byrne, and **C. Nilsson**
Commonwealth Scientific and Industrial Research Organization
Wembley, Australia

I. Introduction

These investigations cover specific projects that will evaluate most of the applications for which radar imagery has significant potential, particularly when the radar data are analyzed in combination with ancillary information such as digital elevation data, Landsat MSS and TM, and airborne multispectral scanner data. Imagery from SIR-A acquisitions over Australia has been evaluated by several of the investigators. The major sections of the investigation are to:

(1) Develop techniques for registration of multiple acquisition, varied illumination, and incidence-angle SIR-B imagery, and a model for estimation of the relative contributions to the backscattered radiation of topography, surface roughness, and dielectric and conductivity components.

(2) Evaluate the application of SIR-B imagery for delineation of agricultural lands affected by secondary salinity in the southwest and southeast agricultural regions of Australia.

(3) Develop techniques for application of SIR-B imagery for geologic, geomorphologic and soils mapping and mineral exploration in a variety of terrain types in Australia, and investigate the backscatter properties of a range of vegetation-soil-rock outcrop targets.

(4) Evaluate the use of SIR-B imagery in determining ocean currents, current shear patterns, internal waves and bottom features for specific locations off the Australian coast.

For each of these major objectives there are several projects distributed over a large portion of the Australian continent, varying from tropical through arid and semiarid regions to temperate regions. Vegetation densities vary from a completely barren, unvegetated area in central Australia to almost closed-canopy forests in southeastern Australia. The individual

investigations will be conducted in five separate remote sensing laboratories, each of which is equipped with image analysis equipment. All investigators involved have extensive experience in analyses of Landsat MSS and RBV, NOAA-AVHRR, NIMBUS CZCS, and SIR-A imagery.

II. Geology and Geomorphology

The broad objectives of the geologic/geomorphologic projects in this investigation are to determine the ability to discriminate and map physiographic features and materials with SIR-B data, and to determine the effects of surface roughness, moisture, conductive lag, and vegetation patterns on the radar backscatter.

The specific projects are:

(1) The study of SIR-B responses over Lake Eyre, which is a very large (9000 km^2), nonvegetated, essentially flat dry playa lake with subtle microtopographic features less than 25 cm in height. The SIR-B data will be analyzed, discretely and in combination with Landsat data to determine:

   (a) The degree of detectability and identification of salts and clays, and to map their distribution.

   (b) The different incidence angles for the detection of subtle topographic features.

   The SIR-B data will be compared with surface microrelief roughness estimates and moisture characteristics from ground information.

(2) The determination of the contribution orbital radar imagery may have in assisting differentiation of various irons and clay minerals, and in reliably assessing their regional distribution. The SIR-B data will be merged with Landsat data for the study of terrain that has been chemically altered by deep weathering, and covered with extensive areas of ferruginous lag material and varying clay concentrations at the surface. This research has important implications for geochemical exploration and the mineral industry in general.

(3) The use of SIR-B imagery to verify and identify the precise location and nature of a lineament extending across the Australian continent. This lineament has recently been observed on shaded relief images derived from a digital terrain model of continental Australia.

(4) The evaluation of the capability of SIR-B imagery for delineation of paleoriver systems in the Canning and Officer Basins of Western Australia. A paleoriver system crossing the Great Sandy Desert in northwestern Australia was observed on NOAA-AVHRR imagery in 1982 (Ref. 1). The SIR-B data will be correlated with digital elevation data and with NOAA-AVHRR data to refine the mapping of this and other paleodrainage networks.

(5) The investigation of the ability to discriminate with multiincidence SIR-B data the microrelief and terrain texture associated with erosion of deeply weathered profiles in extremely flat terrain in the Archaean of Western Australia. From the analysis, the optimum SIR-B geometry for this discrimination will be determined. The SIR-B data will be supported by data from visible and infrared reflectance measurements, and aircraft scanner data.

(6) The investigation of the ability to discriminate with multiincidence-angle SIR-B data vegetation and hydrologic characteristics that have been demonstrated, from Landsat data, to correlate with the distribution and grade of very large area bauxite resources at Weipa in northern Queensland. It is proposed to test the established relationship further by studying the backscatter characteristics of the eucalyptus forest cover at various incidence angles to detect changes in forest canopy structure, height, density, and type that appear to be associated with the bauxite type and grade. The diurnal variation in the leaf alignment will need to be considered, as the eucalyptus leaves align themselves during the day to minimize leaf area exposed to the Sun.

(7) The evaluation of the capability of the mapping-mode SIR-B imagery to delineate and map the duricrust-covered Proterozoic Hamersley Surface in the Hamersley Basin, Western Australia. An understanding of the distribution and weathering of this surface, which has been subjected to considerable Tertiary erosion, is important for delineation of pisolitic iron deposits. The surface is characterized by its smooth, rounded surface, a property that should cause it to be highlighted on SIR-B imagery.

III. Hydrology and Soils

(1) Multiple-incidence- and illumination-angle SIR-B data will be analyzed to determine its capability for discrimination and mapping of agricultural lands affected by salinity. Salt affected soils in southwest and southeast Australia are often due to rising groundwater tables resulting either from clearing of native forests or from irrigation. In August, the saline areas are generally characterized by high soil moisture, high electrical conductivity, and either no vegetation or sparse, salt-tolerant vegetation. Multiincidence angle and look-

direction data acquired over the experimental sites will be merged with multispectral data from Landsat and from a 15-channel airborne multispectral scanner using a digital elevation model to correct for parallax error. These data will be correlated with spectral moisture and conductivity data collected at the sites.

(2) The suitability of SIR-B data for mapping stream networks in highly productive Australian hardwood-forest catchments will be investigated; also, estimates will be made of the aerodynamic roughness, an important parameter in calculating forest evapotranspiration, and the distribution of standing vegetation in the catchments.

IV. Oceanography

The broad objectives of the oceanographic investigations are to evaluate the capability of SIR-B imagery to delineate ocean currents, current shear patterns, internal waves, small-scale advection patterns, and bottom topography. The investigation is comprised of five separate projects. The principal location for the oceanographic research is in the Tasman Sea/Bass Strait region, with other projects located on the Great Barrier Reef, the Southeast Indian Ocean, and the Gulf of Saint Vincent. The projects in the Tasman Sea/Bass Strait area will be supported by an intensive oceanographic program involving vessels of the Royal Australian Navy (RAN) and CSIRO, airborne XBT data, current meters and directional swell arrays, and instruments on oil platforms in Bass Strait. Cloud cover permitting, NOAA-AVHRR data will be recorded for all projects. The specific oceanographic projects are:

(1) East Australian Current: The SIR-B imagery will be processed and evaluated to determine the capability to define the East Australian Current, upwelling associated with the front, and current shear patterns. Currents on the continental shelf will also be studied.

(2) Bass Strait area: Bragg wave spatial data will be determined from time-lapse photography from an oil rig and will be correlated with radar backscatter. The SIR-B data will be studied to determine the SIR-B's ability to delineate the eastern Bass Strait front and internal waves in Bass Strait. Using an array of current meters, the SIR-B data will be assessed to determine its use in estimating current flow in Western Bass Strait. This project will be part of a joint CSIRO/RAN Bass Strait Oceanography Study.

(3) Western Tasmania: SIR-B imagery will be studied to determine river outflow, stream patterns, and evidence of bottom bathymetric variations in the estuary and near-estuary areas of the Pieman River; this study will provide baseline data prior to the development of the Pieman River Dam.

(4) Northern Spencers Gulf, South Australia: SIR-B imagery will be evaluated, in comparison with vessel and current meter data, to determine its use in monitoring currents in a semienclosed gulf.

(5) Leeuwin Current: The patterns on SIR-B imagery will be studied for an area with an established, southward-flowing current, the Leeuwin Current, which interacts with prevailing southwesterly winds, to determine the effects of frictional energy loss on the wave and swell patterns.

(6) Great Barrier Reef: The SIR-A imagery will be evaluated for its capacity in determining refraction around reefs and detecting the existence of large internal waves. One objective is to determine the interreef nutrient pathways.

Reference

1. Honey, F. R. and Tapley, I. J., "Evaluation of Shuttle SIR-A Imagery for Geological and Geomorphologic Mapping in N.W. Western Australia," presented at the International Symposium on Remote Sensing of Environment, Second Thematic Conference, *Remote Sensing for Exploration Geology*, Fort Worth Texas, December 6 through 10, 1982.

The Use of Digital Spaceborne SAR Data for the Delineation of Surface Features Indicative of Malaria Vector Breeding Habitats

Team Member:

M. L. Imhoff
Goddard Space Flight Center
Greenbelt, Maryland

Collaborators:

C. H. Vermillion
Goddard Space Flight Center
Greenbelt, Maryland

F. A. Khan
Space Research and Remote Sensing Organization
Dacca, Bangaladesh

I. Introduction

Malaria and other vector-borne diseases presently affect the lives of over 500 million people worldwide. Hundreds of millions of dollars are spent on the control of these diseases annually. Vector control programs in the tropics are hindered by a deficiency of information concerning the existence and location of vector breeding habitats due to cloud cover, dense vegetation, and a lack of skilled manpower. The hypothesis presented by this proposal is that spaceborne radar image data can provide crucial information concerning land use, land cover, surface hydrology, and topography upon which present day vector control programs are based.

II. Objectives

Proof of the hypothesis will be supported by three major research objectives defined as tasks. These tasks involve an analysis of radar illumination geometry vs information content, the synergy of radar and multispectral data mergers, and automated information extraction techniques. The tasks are defined as follow:

(1) Identify illumination angles yielding the maximum delineation of vegetated and nonvegetated surface features of natural and anthropomorphic origin.

(2) Test and analyze textural and hybrid spatial-spectral classifiers on SAR and merged SAR/multispectral image data for improved information extraction.

(3) Determine the utility of SAR and hybrid SAR/multispectral products as input to an automated resource decision making process.

A. Site Selection and Preparation

The survey site will be located along a Shuttle orbit path in the country of Bangaladesh. The test site will consist of a

10 km × 10 km section at a to-be-determined point within the transect.

Site preparation will consist of a cooperative effort between NASA and the host government. An approximate 10 km × 10 km area will be selected along the transects defined above or along lines that most closely correspond to the SIR-B estimated flight paths. The survey site will contain examples of all the desired target objectives for intensive ground truthing. A field team comprised of botanists, soil scientists, hydrologists, and epidemiologists under the direction of a remote-sensing specialist will define in detail the types of units that should be delineated. The test area will be surveyed and mapped into terrain units most compatible with the remote sensor and the application objectives.

A control grid for all the data will be established by the construction of a series of reflector towers or transponders spaced throughout the survey area. The locations of these towers will be measured and mapped in relation to the ground-truth information to form a grid for the geometric registration and comparison of radar responses to ground truth.

For vegatation penetration analysis, a transponder setup will be established at a surveyed location along the center line of the projected flight path. Three transponders will be positioned at measured depths in the tree canopies. Tree canopy crown closure measurements will be made as well as leaf-area indices and species and type determinations for the transponder setup area.

B. Task 1

1. Part A. Identify the illumination angles that yield the maximum delineation of surface features of natural and anthropomorphic origin.

The larger incidence angle will be used to provide maximum resolution for the mapping of soil, land use, and vegetation types, while the lower incidence angles will be examined for vegetation penetration. The data for each incidence angle will be compared with the survey set of defined terrain units.

The data for all incidence angles will be processed to full spatial resolution. The data sets will be geometrically registered to a control base defined by the reflector towers and other surrounding land marks and subsequently registered to the digitized ground-truth information, thus facilitating comparison on a pixel-by-class level.

2. Part B. As an addition to this task, the investigators will use active radar calibrators in an attempt to obtain direct measurement of σ_0 at several measured depths in the vegetation canopy for the various incidence angles. The precision targeting of the SIR-B flight path is critical for this task.

C. Task 2

Test and analyze textural and hybrid spatial-spectral classifiers on spaceborne SAR and merged SAR/multispectral image data for improved information extraction. This task is comprised of two parts: (1) an evaluation of texture analysis as a means of improving radar data utility, and (2) an analysis of the synergistic effect of merged SAR/MSS data sets on information content and extraction. The analysis of part 2 is contingent upon the availability of MSS-type data over the test area near the time of the SAR acquisition.

1. Texture Analysis. The textural classification algorithms that will be applied to the radar data are:

(1) Angular Second Moment: a measure of homogeneity.

(2) Contrast Features: measure of numbers of boundaries in an image.

(3) Correlation Feature: measure of linear grey-tone dependencies (Ref. 1).

These algorithms will be run at four different angles, 0°, 45°, 90°, and 135°.

2. Radar-MSS Merger Analysis. The texture-analyzed radar data set with the highest classification accuracy will be merged as an additional band with multispectral data. A supervised classification will be performed on the merged data and an accuracy assessment taken. The resulting products will then be compared to their singular counterparts for information content analysis.

D. Task 3

Determine the utility of SAR and hybrid SAR/multispectral data products as input to an automated resource decision making process. This task is designed to utilize the properties of a geographic information system (GIS) to create 2nd- and 3rd-derivative information products. This task will accomplish two objectives: (1) test utility of radar data products in an automated decision making process, and (2) test geographic information systems as a means of further information extraction.

Input to the GIS will consist of the following data defined as layers in the system:

(1) Radar and hybrid SAR/multispectral classification products (from Tasks 1 and 2).

(2) Ground survey information.

The following spatial analysis and modeling experiments will be performed on the merged data sets to create new information products for analysis: (1) information convergence or overlay functions: 2nd-derivative products. The GIS compares and cross examines the class designations defined on each data layer to create a new map identifying important user specified occurrences of target objectives. The 2nd-derivative products can then be used as separate products or as new data layers in the GIS; (2) research and applications modeling: 3rd-derivative products will be generated using models specifically designed for ecological research and applications.

III. Anticipated Results

The significant results expected as an outcome of this experiment can be divided into three categories: information content, information extraction, and applications. They are defined as follows:

(1) Information Content: (a) an improved understanding of the effects of a vegetation canopy and surface geometry and composition on radar backscatter as a function of radar illumination geometry; (b) a better understanding of overall scene information content as a function of illumination geometry; (c) a better understanding of the relationships between radars of various illumination geometries and multispectral image data for information content.

(2) Information Extraction: (a) a better understanding of the value of using merged multi-illumination geometry radar data sets for information extraction; (b) a better understanding of digital texture analysis as method of information extraction for radar imagery; (c) a better understanding of the effectiveness of a GIS system for improving information extraction of radar imagery.

(3) Applications: (a) successful use of radar imagery for land-cover/land-use mapping in a tropical ecosystem; (b) better understanding of radar as a means of vegetation penetration for resource assessment; (c) the exploration of the potential use of radar imagery as an aid to malaria and other disease vector control programs.

Reference

1. Haralick, R.M., et al., 1973, *Preliminary Report on Land Use Classification Using Texture Information in ERTS-A MSS Imagery*, Kansas University Center for Research. Jan. 1973.

Interlobate Comparison of Glacial-Depositional Style as Evidenced by Small-Relief Glacial Landscape Features in Illinois, Indiana, and Ohio, Utilizing SIR-B

Team Member:

W. H. Johnson
University of Illinois
Urbana, Illinois

Collaborators:

N. K. Bleuer and **G. S. Fraser**
Indiana State Geological Survey
Bloomington, Indiana

S. M. Totten
Hanover College
Hanover, Indiana

I. Description of the Investigation

The objectives of the proposed research are:

(1) To evaluate the ability of SIR-B to delineate varying sizes, shapes, and relief of surface forms within the glaciated, cultivated, road-gridded areas of Wisconsinan glaciation in northeastern Illinois, northern Indiana, and western Ohio (Fig. 1).

(2) To compare and contrast SIR-B imagery with selected Seasat SAR imagery.

(3) To utilize SIR-B imagery synergistically with available Seasat SAR, Landsat RBV, and false-color imagery; Soil Conservation Service county-wide photomosaics; high-altitude infrared imagery; and conventional aerial photography to identify and map suites of glacial landforms.

(4) Eventually to interpret the suites in terms of ice dynamics and conditions of deglaciation, to relate them to the stratigraphic record, and to evaluate interactions of the major lobes and sublobes; to attempt to determine the degree of synchroneity of major ice events; and to evaluate the interaction of major ice events and meltwater drainage positions, drainage changes, and the location of major sand and gravel deposits. Many of these objectives are long-term goals that become possible if the detailed morphologic delineations can be carried out on a synoptic scale.

This experiment is part of a continuing evaluation of SIR as a tool in geomorphic mapping. It is an extreme test in that the landscape consists of relatively subtle landforms and low relief, and the area is characterized by agricultural crop and road patterns.

II. Description of the Experiment

Developing concepts of the complexity of glacier dynamics and the resulting, varied depositional styles require that regional comparisons be made of the depositional patterns of the Wisconsinan-aged glacial lobes of the lower Midwest. The future understanding of stratigraphic sequences of mappable till units and associated deposits, including those of economic and environmental importance, requires some measure of restructuring of the hypotheses by which these units are interpreted.

Synoptic views of this area now available from Landsat, in part tied back to conventional and high-altitude air photography, indicate the likelihood that diverse modes of flow and deposition characterize the area, particularly in Indiana (Refs. 1 and 2). The lobate "normal" glacial mode of Illinois and Western Ohio did not hold true in Indiana, which was the site of repeated slab-like flow, perhaps as ice streams as modeled and hypothesized by Mayewski, Denton, and Hughes (Ref. 3). This realization opens the possibility that portions of the Wisconsinan glaciation of northeastern Illinois or western Ohio might also be different, and indeed aspects of some till mapping in Illinois suggests that locally this might be the case.

A stratigraphic-morphological approach, such as that which has been successful in the northern Great Plains (Refs. 4 and 5), is planned for obtaining the data needed to better understand and interpret the conditions of past glaciations. Suites of morphologically distinct landforms must be delineated and mapped, investigated in the field for stratigraphic and sedimentologic data, and interpreted in terms of dynamics of glaciation and conditions of deglaciation. The ability to delineate and map morphologic suites of different origins will provide a powerful basic tool in understanding the process response of the Laurentide glacier near its southern margin, as well as the local stratigraphy.

Thus, SIR-B will be evaluated as a basic tool in the recognition and mapping of subtle small-scale to relatively large-scale glacial landforms. Landform relief varies from less than 3 m to over 30 m, and the features vary in size from minor moraines about 30 m wide with a spacing of 100 m or so to large troughs 100 m wide and over 10 km long. Known examples of critical landform types indicated by existing, more conventional sources will be compared to radar imagery to discern the type and magnitude of such features that are detectable by SIR-B.

III. Data Acquisition, Handling, and Analysis

Digitally processed images of SIR-B data will be obtained for selected study sites within the area. Data analysis will be an extrapolation of conventional methods that have been traditionally employed in aerial image analysis to space-acquired image data. Digital tape data will be utilized in an attempt to enhance pattern contrast and to delineate subtle landscape patterns in critical areas. The type, scale, and orientation of glacial and meltwater features will be determined on the SIR-B images.

To maximize the synergistic approach, further available materials including selected Seasat SAR imagery, Landsat (RBV, false color, and TM), and high-altitude infrared and conventional photography will be obtained. For the latter three types of materials, late-spring photography will be selected where possible so that most agricultural fields will not have been planted and soil tones and patterns will be visible.

From available data, landscape suites will be mapped to the extent possible. Field studies will be undertaken to determine the internal characteristics of critical landforms and to interpret their origin with respect to the conditions of glaciation and deglaciation. From these, further regional interpretations and interlobate comparisons will be made.

IV. Expected Results

The results of the proposed research are dependent on the ability of the SIR-B imagery to assist in the delineation of small- to large-scale glacial landforms in an area of relatively low relief, and of its ability to extend such delineations in a mapping mode over a broad region along the southern margin of the Laurentide Ice Sheet. If these objectives can be met, the opportunity exists for a number of fundamental problems and questions to be addressed in conjunction with ongoing stratigraphic and sedimentologic studies of the deposits. Among these are the fundamental questions raised in the last objective, as well as numerous local geomorphic and stratigraphic problems.

References

1. Bleuer, N. K., 1982, "Stratigraphy and Style of Trafalgar (Wisconsinan) Glaciations in Central Indiana," *Abstract with Programs*, Geol. Soc. America, Vol. 14, No. 5, pp. 225-256.

2. Bleuer, N. K., 1983, "Lobe and Slide Deformation of Wisconsinan Substrates in the Central Indiana Till Plain," *Abstracts with Programs*, Geol. Soc. America, Vol. 15, No. 4, p. 250.

3. Mayewski, P. A., Denton, G. H., Hughes, T. J., 1981, "Late Wisconsin Ice Sheets of North America," in *The Last Great Ice Sheets*, G. H. Denton and T. J. Hughes, editors. John Wiley and Sons, New York, pp. 67-178.

4. Clayton, L., and Moran, S. R., 1974, "A Glacial Process-Form Model," in *Glacial Geomorphology*, D. R. Coates, editor. Publications in Geomorphology, State University of New York, Binghamton, pp. 89-119.

5. Moran, S. R., Clayton, L., Hooke, R. LeB., Fenton, M. M., and Andriashek, L. D., 1980, "Glacier-Bed Landforms of the Prairie Region of North America," *Glaciology*, Vol. 25, pp. 457-476.

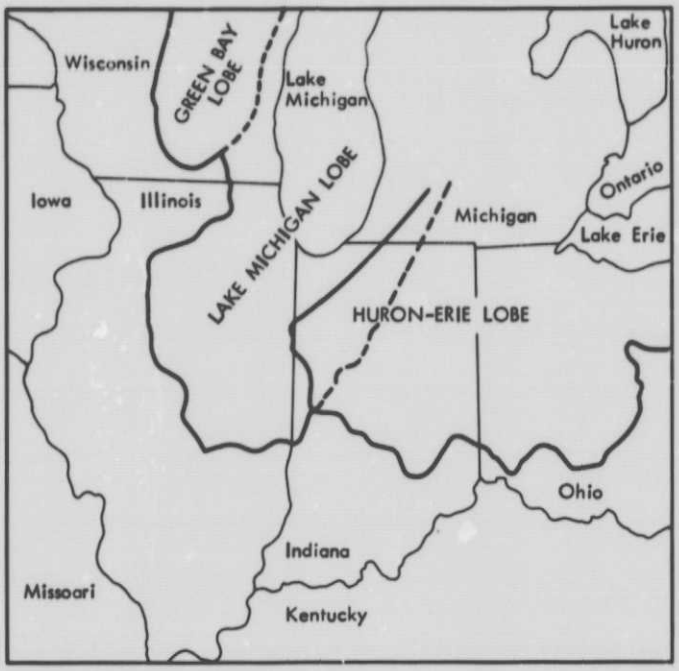

Fig. 1. Late-Wisconsinan glacial border for the Green Bay, Lake Michigan, and Huron-Erie Lobes. Dashed lines show interlobate position in Wisconsin and the buried Lake Michigan Lobe till margin in Indiana. Experiment will concentrate on portions of northeastern Illinois, northern Indiana, and western Ohio.

Evaluation of the L-Band Scattering Characteristics of Volcanic Terrain in Aid of Lithologic Identification, Assessment of SIR-B Calibration, and Development of Planetary Geomorphic Analogs

Team Member:

V. H. Kaupp
University of Arkansas
Fayetteville, Arkansas

Collaborators:

W. P. Waite and H. C. MacDonald
University of Arkansas
Fayetteville, Arkansas

P. J. Mouginis-Mark
University of Hawaii
Honolulu, Hawaii

S. H. Zisk
Haystack Observatory
Westford, Massachusetts

I. Objectives

The objectives of the SIR-B scattering study and calibration investigation of volcanic terrain are to delineate textural and structural features, to evaluate the L-band scattering characteristics, and to assess SIR-B calibration.

SIR-B is the first orbital imaging radar system to provide multiple images of the same target at different look angles. This unique capability offers the opportunity to obtain multiple-angle radar data from a space platform and will provide a chance to assess look-angle and illumination-direction relationships of volcanic terrains. In addition, scattering theory and radar-image simulation can be used with such SIR-B data for assessing the surface scattering characteristics of volcanic terrain. This offers an opportunity to aid lithologic identification of volcanic terrains and to develop planetary geomorphic analogs, and also to independently assess the calibration of the SIR-B.

Volcanic terrains generally differ from other landforms because the landscape and geomorphic features are usually constructional (built up). The erosion of volcanic terrain and the subsequent landforms produced are controlled to a large extent by the volcanic rock involved. The correlation between

rock type and landform is so great that it is impossible to interpret volcanic physiography without some knowledge of the rocks themselves. Thus the best approach to interpreting volcanic history is to combine detailed field work with laboratory studies. Such an approach is presently not possible except for Earth, and a few localities on the Moon from which samples have been returned. Thus the ideal sequence of planetary exploration begins with unmanned remote sensing reconnaissance missions, followed later by more comprehensive surveys.

Recent studies using radar for lithologic mapping involve the use of radar to obtain information concerning the surface roughness and/or dielectric properties of rock surfaces. Variation in radar backscatter related to these parameters can be used to detect areal variations in physical structure, mineralogy, and bulk chemistry of exposed volcanic rock. Radar studies of Iceland's volcanic terrain, for example, have provided a correlation between variations in surface roughness and some previously mapped geologic units. Volcanic terrains offer ideal potential test sites for evaluating radar roughness parameters as a lithologic discriminant and also a means for developing planetary geomorphic/lithologic analogs. The use of multiple-look-angle imagery from SIR-B provides an ideal data set for evaluating microwave techniques for lithologic mapping. Multiple SIR-B imagery of selected volcanic test sites can, in principle, be used to determine the L-band scattering characteristics of volcanic terrains.

II. Description of the Experiment

We propose to exploit the multiple-look-angle capability of the SIR-B together with our radar simulation facility to match theory, SIR-B data, and simulation imagery of volcanic terrains. The approach proposed will use scattering theory and simulation for scene matching of SIR-B data from volcanic test sites. This will require detailed knowledge of the roughness and dielectric characteristics of our test sites together with a capability for using these in creating simulated images.

The styles of volcanism and eruptive histories displayed on planetary surfaces can be determined to some degree through the interpretation of volcanic landforms. The SIR-B mission will provide unique data for comparative planetology. The similarity of Earth to Venus in size, composition, and proximity to the Sun implies that any differences between the Earth and Venus will be due to small but significant factors. These factors can be compared with models for geologic processes occurring on the Earth. The scientific results from SIR-B will be related directly not only to intepretation of volcanic landforms, but also to understanding and developing roughness measurements and scattering theory that have, at L-band wavelengths, scientific merit for certain volcanic terrains on Earth and possibly Venus. Three test sites that have contrasting styles of volcanism displayed in the rocks and landforms have been selected for our study. These include Kilauea Volcano, Hawaii; Cuillin Hills, Skye, United Kingdom and the volcanic region in the northwest United States (including Mount Shasta, Medicine Lake Caldera, Newberry Volcano, and Harvey Lake, Oregon).

These three sites have been selected for very specific reasons. The primary test site proposed is the Kilauea Volcano area of the big island of Hawaii. The pristine, unvegetated condition of many diverse volcanic terrains at this site make it an ideal location for the analysis of young basaltic volcanic landforms with space imaging radar.

The second test site, the Cuillin Hills of Skye off the west coast of Scotland, is a major Tertiary igneous complex with an extensive dyke swarm radiating from this part of the island for distances in excess of 100 km. In addition, because Skye is located at about 57°N, the island will be near the northward extent of the Shuttle orbital track, permitting the radar to illuminate the test area in a north-south configuration (as opposed to the usual east-west solar illumination).

The third test site consists of two volcanic areas in the northwest United States (Mt. Shasta-Medicine Lake Caldera and the High Lava Plains of Oregon). These two locations offer strikingly different examples of volcano-tectonic features that are thought to be the products of changing tectonic stress fields associated with the Cascade Range and the Basin and Range Provinces. As a transitional region for tectonic processes, this area is of great interest to field geologists.

Three main categories of experiments have been identified, each with several specific tasks:

(1) Delineation of textural and structural features.

  (a) Prepare geomorphological maps.

  (b) Investigate multilook radar.

  (c) Evaluate multisensor data combinations.

(2) Determine L-band scattering characteristics.

  (a) Model surface scattering.

  (b) Create simulation imagery.

  (c) Match scattering models, simulation imagery, and SIR-B imagery.

(3) Assess calibration.

(a) Evaluate stability by scene matching.

(b) Estimate errors.

Each of these tasks will be performed to empirically test existing theory and previous experimental work. The results should be an increased understanding of the electromagnetic surface scattering from volcanic terrain, an assessment of look angle and look orientation of volcanic landforms, and an assessment of the calibration of the SIR-B sensor. These results should be an important aid in lithologic identification of volcanic terrains, and should also be useful for developing Earth-based geomorphic analogs for extraterrestrial reconnaissance missions.

III. Expected Results

A summary of expected results include:

(1) Obtaining a catalog of multiangle and multilook direction imagery of volcanic terrains. The catalog should contain imagery of volcanic terrains representative of various textural and electrical conditions.

(2) Developing surface scattering relationships for lithologic identification. The relationships should be characteristic of various textural and electrical conditions.

(3) Evaluating multisensor data combinations for lithologic identification.

(4) Determining long-term stability of the SIR-B.

(5) Cataloging landforms as potential planetary analogs.

(6) Determining the L-band scattering characteristics by means of roughness measurements and scattering theory for certain volcanic terrains, not by empirical measurements (i.e., truck- or aircraft-mounted scatterometers).

(7) Using simulation to create scenes that match the SIR-B data by varying parameters in the scattering theory until matches occur.

(8) Attempting to separate scattering parameter effects from absolute calibration errors.

(9) Evaluating SIR-B data over volcanic test sites for feature vector parameters such as tone and texture; this will aid lithologic identification of these types of terrains both on Earth and extraterrestrial bodies.

(10) Identifying theoretical (or heuristic) scattering models that are capable of predicting the SIR-B response over volcanic terrains.

(11) Assessing the SIR-B calibration for specific points, and estimating the deviation from the true state of nature at these points for the passes from which the data were collected.

5

N85-17233

The Investigation of Selected Oceanographic Applications of Spaceborne Synthetic-Aperture Radar

Team Member:

G. E. Keyte
Royal Aircraft Establishment
Farnborough, United Kingdom

Collaborators:

B. C. Barber, M. B. Barnes, and **G. C. White**
Royal Aircraft Establishment
Farnborough, United Kingdom

M. Bagg
Admiralty Underwater Weapons Establishment
Portland, United Kingdom

B. d'Olier
City of London Polytechnic
London, United Kingdom

N. Lynn
Royal Navy College
Greenwich, United Kingdom

I. Objective

Synthetic-aperture radar images obtained from Seasat and SIR-A showed that a number of oceanographic features were imaged in considerable detail, for example, internal waves, large ocean waves, bathymetric features, eddies, and slicks. However, the imaging mechanisms are not generally well understood, and for both Seasat and SIR-A there were relatively few supporting sea-surface measurements to assist in the study of these imaging mechanisms.

The objective with SIR-B is to conduct three separate experiments that will all be aimed at providing a better understanding of the use of spaceborne SAR for imaging (1) internal waves, (2) ocean surface waves, and (3) shallow-water bathymetry. Examples of these features are shown in Figs. 1 and 2. These experiments have been chosen because they lead to possible applications for microwave remote sensing of the ocean surface and will also allow a better understanding to be developed of the microwave/sea-surface imaging mechanism.

II. Description of the Experiments

The internal wave and ocean surface wave experiments will both be located in the northeastern Atlantic in a deep-water region likely to contain both phenomena. The shallow-water experiment will be located along the east coast of the United

Kingdom in a region that contains numerous shoals and sandbanks (Fig. 3).

A. Investigation of Internal Wave Imaging

This investigation will study the relationship between surface expressions of oceanic internal waves and the underlying internal wavefield in deep water. Seasat-SAR imagery revealed that internal wave features are common (Ref. 1) throughout the northeast Atlantic, including the general area chosen for this study (Fig. 3). Here it is intended to have shipborne measurements of the internal wavefield in the upper layers of the deep ocean for comparison with the imagery.

A research ship will deploy equipment to continuously monitor the upper-ocean internal wavefield, the characteristics of which are derived from fluctuations of temperature and density. This has been proven in previous shipborne experiments. In addition, records of local surface conditions will be kept. The ship will be marked by a radar reflector.

Two methods of analysis are proposed. Digital imagery of the experiment area containing internal wave surface features will be compared with shipborne measurements taken at a time similar to that of the imaging pass. The relationship between the internal wavefield and its surface expression will be derived. The second technique will require the imagery of the northeast Atlantic in survey processed form. From this, an atlas of internal wave features will be compiled, including observations from ships of opportunity.

Optical and infrared satellite imagery will be sought to look for internal wave features (Ref. 2) and to monitor mesoscale ocean dynamics in the experiment area.

This study is aimed to yield knowledge on the imaging of internal waves in deep water by spaceborne SAR. Such systems have a large potential for aiding studies of upper-ocean dynamics. Its major advantage is offering a scale of coverage unattainable with shipborne measurement systems.

B. Ocean-Wave Imaging Experiment

In this experiment the aim is to measure the ocean waveheight spectrum at the time of imaging and to compare this with the SAR image spectra. The measurements will be made at a region located at the intersection of north- and south-going SAR swaths, thus allowing the sea surface to be imaged in different directions within a few hours.

The waveheight spectrum will be measured by means of a "Marex" data buoy towed from one swath intersection to another in the period between pairs of north- and south-going passes. The buoy will be instrumented to measure the two-dimensional waveheight spectrum, and the data will be received and recorded by equipment on a neighbouring research ship. This vessel will also carry out local meteorological observations.

In addition, it is intended that a number of wave-rider buoys will be deployed, each containing instrumentation to measure the one-dimensional waveheight spectrum. These buoys will also carry radar transponders that will enable the position of the buoy in the image to be identified to within one pixel. Knowing the position of the buoy to this accuracy should enable the phase between the imaged waves and in-situ ocean-wave field to be estimated. The value of this parameter is of importance in SAR ocean-wave imaging theory.

The SAR ocean-wave images will be processed to yield SAR image spectra; the relation between these spectra and those of the ocean surface will be studied with the objective of (a) understanding the imaging mechanism and (b) determining the transfer function relating the two spectra and its functional dependence.

C. Shallow-Water Bathymetry Experiment

Seasat images of shallow-water and coastal regions frequently contain features that can be associated with the change in topography of the sea bed (Ref. 3). The action of tidal currents flowing over these topographical variations will cause disturbance at the sea surface; this disturbance will interact with the wind field to produce a change in the local surface radar backscatter characteristics. These changes are hence related to sea-bottom topography although their appearance is clearly dependent on the prevailing tide and wind conditions at the time of imaging.

The aim in this experiment is to obtain a set of SAR images of a shallow-water region at different tide states. This region will be located on the east coast of the United Kingdom and will contain numerous sandbanks and shoals. Part of this area will be selected for detailed hydrographic surveys (using side-scan sonar and depth transducers) to provide an accurate measurement of bottom topography immediately before imaging.

In addition, a research ship will be deployed at the time of imaging to carry out a number of measurements, including sea state and temperature, current speed and direction (as a function of depth), and meteorological observations. It is also intended that data for this area will be obtained from existing meteorological and Earth resources satellites and also from aerial photography surveys.

The above data will be used to establish the empirical relation between the radar image and bottom topography for

different tide states and environmental conditions. The data will also be used to support continuing theoretical studies of radar imaging of the sea surface.

III. Data Processing

It is intended that the SIR-B data for these experiments will be processed on the RAE experimental SAR processor. The processing algorithms used in this processor are both well defined and variable; hence the effect of these algorithms can be studied as part of the overall imaging process.

To check processor performance and also evaluate the overall SIR-B image quality, it is intended that a number of corner reflectors and radar transponders will be set up at suitable locations in the United Kingdom.

References

1. Bagg, M. T. and Johnson, K. I., "Internal Wave Features in the Northeast Atlantic as Imaged by Seasat-SAR." Presented at Oceans' 1983 Conference, San Francisco, 30 August 1983.
2. Apel, J. R., Burne, H. M., Prapi, J. R., and Charwell, R. L., "Observations of Oceanic Internal Surface Waves From the Earth Resources Technology Satellite," *J. Geophys. Res.*, Vol. 80, pp. 865-881.
3. Lodge, D. W. S., "Expressions of Bathymetry on Seasat Synthetic Radar Images." in *Satellite Microwave Remote Sensing*, T. D. Alton, Ellis Horwood, 1982.

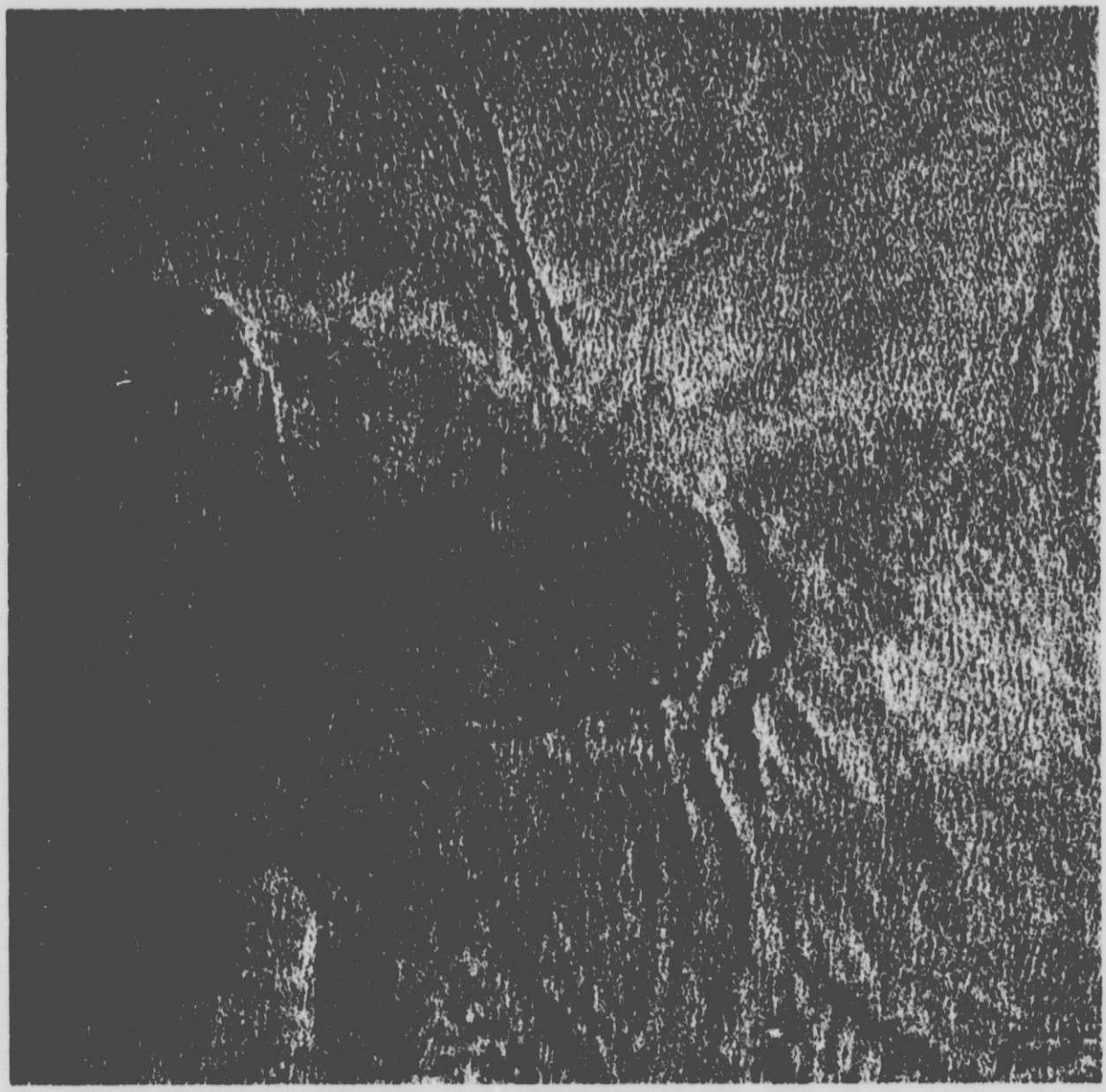

Fig. 1. Internal waves and swell waves in the Bay of Biscay. (Seasat SAR image, Rev. 785, 20 August 1978, latitude 46.86°N, longitude 5.17°W.) (ESA/EARTHNET Seasat SAR image made by the Space Department of RAE Farnborough.)

Fig. 2. Bathymetric features off Dunkerque. (Seasat SAR image, Rev. 762, 19 August 1978, latitude 51.06°N, longitude 2.43°E.) (ESA/EARTHNET Seasat SAR image made by the Space Department of RAE Farnborough.)

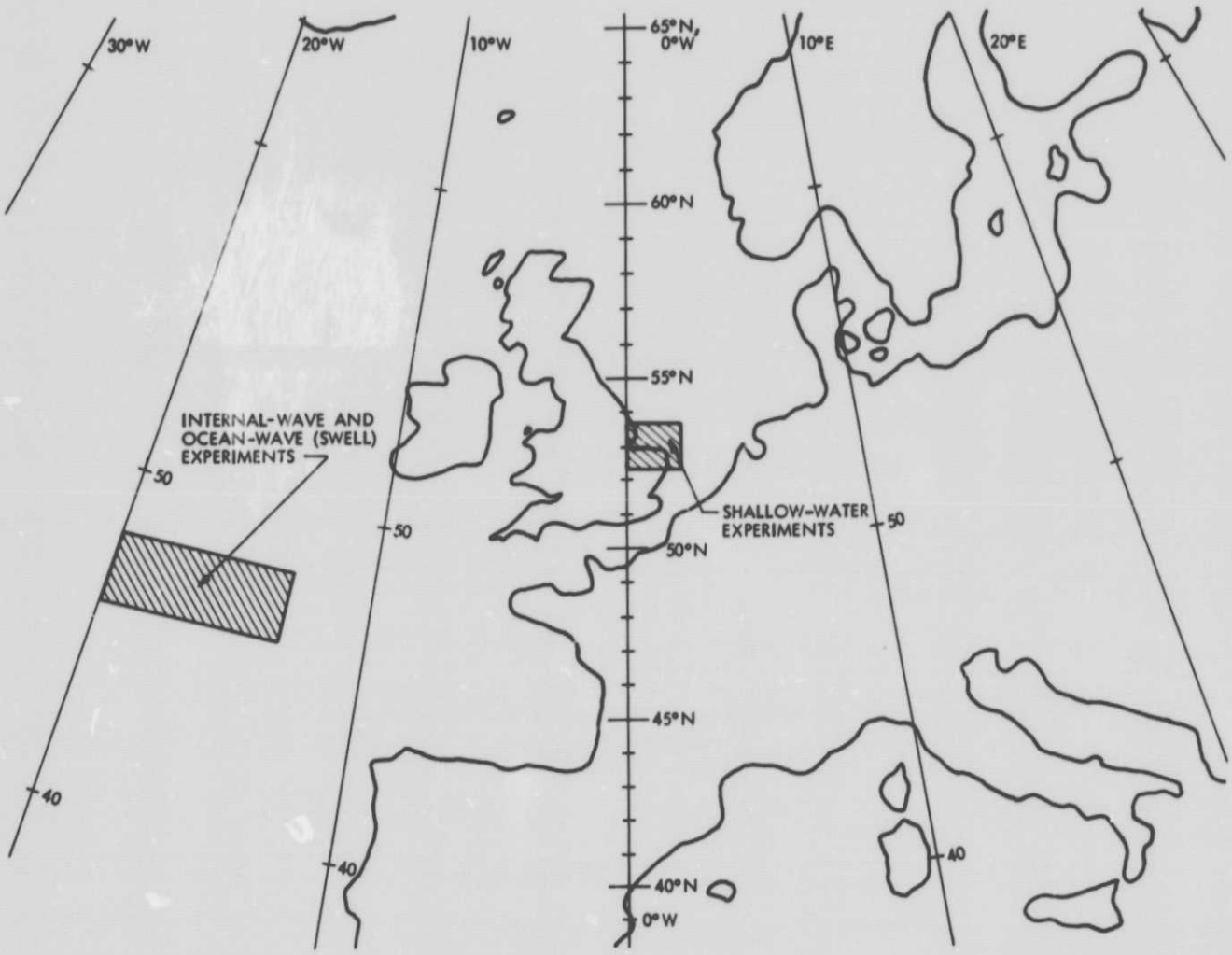

Fig. 3. Locations of RAE SIR-B experiments

SIR-B Cartography and Stereo Topographic Mapping

Team Member:

M. Kobrick
Jet Propulsion Laboratory
Pasadena, California

Collaborators:

F. Leberl, J. Raggam, and **G. Domik**
Institute for Image Processing and Computer Graphics
Graz, Austria

R. Welch
University of Georgia
Athens, Georgia

H. Carr and **J. Hammak**
U.S. Naval Observatory
Washington, D.C.

V. Kaupp, H. C. MacDonald, and **W. P. Waite**
University of Arkansas
Fayetteville, Arkansas

J. Curlander and **S. P. Synnott**
Jet Propulsion Laboratory
Pasadena, California

I. Experiment Objectives

The objective of the SIR-B mapping experiment is to evaluate the utiiity of SAR images taken singularly, in pairs, and in combination with other data sets for cartographic, topographic, and thematic mapping, and to determine the optimum configuration of a SAR system for future mapping missions.

SIR-B is the first orbital imaging radar mission to incorporate a serious attempt at maintaining geometric image fidelity along with careful calibration and documentation of internal timing and frequency parameters. This, along with its ability to obtain, for the first time, the multiple incidence angle images of the same target necessary f stereoscopy and topographic mapping, make it the ideal opportunity for cartographic experimentation. Mapping should therefore comprise a significant part of the overall experiment objectives.

II. Experiment Plan

A. Planimetric Mapping

The most fundamental element of mapping from remotely sensed data is the ability to locate an image resolution cell or

pixel with respect to a chosen map coordinate system. There are basically two ways to do this.

1. Unsupervised maps. The first requires detailed knowledge of the sensor and data processing (image correlation) parameters so that a map may be produced without any a priori knowledge of the target area. This method is required in mapping previously unexplored or poorly mapped terrain (such as many regions of South America and all of Venus) and is preferred in any case since it is automatic, i.e., it requires no manual feature identification or image manipulation. We will attempt to produce such unsupervised maps for a number of target areas that are well surveyed and mapped (see section on target selection and premission planning), and analyze quantitatively the planimetric accuracy we are able to attain. The process will be repeated for as many incidence angles as possible, although some of our target areas will not be accessible at the full range of angles.

2. Control points. The second method for producing planimetric maps involves the use of image control points, imaged features for which the Earth-centered coordinates are known with high accuracy. For radar imaging, these are best established with well-surveyed corner reflectors located in regions of low radar backscatter. Several such sites will be or already have been established (see below) and the accuracy of maps produced using varying numbers of these benchmarks will be quantitatively analyzed and compared with the unsupervised maps.

3. Extended target control points. In mapping areas where ground control is not available or where point targets are not identifiable in the radar images, it may be possible to improve mapping accuracy by using extended targets, i.e., natural features whose positions are known within some bounds. We will attempt to produce a map of at least one of the target areas using only extended targets as ground control and assess its accuracy.

4. Unsupervised mosaics. One of the important applications of SAR mapping is the production of mosaics from images obtained during different orbits. We anticipate that there will be several sets of SIR-B data available in the mapping mode, that is, taken at the same incidence angle with some amount of overlap. We will attempt to construct unsupervised mosaics of these images using the automatic pixel location algorithms and assess their accuracy. Hopefully, sufficient data will be available to repeat this at several different incidence angles and compare the results.

5. Ephemeris improvement. A very strong constraint is placed on the cartography experiment by the spacecraft ephemeris. Even in the best case (see below) the sensor position can be determined by standard methods only to about 300-meter one-sigma accuracy (D. Osburn, OSTA-3 Investigator's Working Group meeting, Jan., 1983). This is far poorer than the accuracy we feel we will be able to attain in mapping, i.e. tens of meters. We will therefore attempt to actually correct the ephemeris for at least one orbit using imaged features, either natural extended targets, natural or cultural point targets, or corner reflectors.

This will be done by measuring the range to the control points using data from an orbit arc where a minimum of Shuttle maneuvers occurred, and comparing to the theoretical values computed from the a priori Shuttle orbit. The orbit will then be differentially corrected using standard orbit determination software available at JPL until these residuals are zero mean, Gaussian, and of the order of the SAR resolution (assuming there are no systematic errors). The new orbit will then be checked by predicting the positions of other targets either within or outside the calculated arc and comparing to their surveyed positions.

B. Stereo and Topographic Mapping

There are four basic stereo arrangements possible with synthetic-aperture radar. Convergent, overlap, and opposite-side stereo have been demonstrated on previous missions (although on a less than systematic basis), and multiple look angle is the primary mode for SIR-B.

1. Stereo viewability. There are two main applications of radar (and photographic) stereo; visual interpretation of topography for geologic or terrain analysis, and production of topographic maps. Any investigation of the first of these is necessarily qualitative in nature, but there exists a body of work analyzing multiple-look-angle stereo in terms of the stereo exaggeration factor q through the use of image simulation. Several members of the mapping team have developed image simulators, and we propose to verify the results of these studies with the SIR-B data.

2. Topographic mapping. One of the most important results of the cartography experiment should be an empirical determination of the optimum incidence angle combination for stereo topographic mapping. This determination will require a number of images at different incidence angles of a scene for which independent topographic data is available, preferably in digital form. It is important that as many images as possible be obtained, since they are analyzed in pairs and the number of pairs available from n images goes as n squared. For example, if the number of images increases from three to four, the number of pairs doubles.

The stereo pairs will be analyzed and topographic maps produced using the Kern hybrid digital/analog stereoplotter

that generated the map of the Greek island Cephalonia from SIR-A data. These maps will be compared quantitatively to independently derived topographic maps. In addition, data reduction will also be performed by purely digital methods using interactive image-processing-type software. This software has been used to analyze simulated stereo pairs and will be modified to handle the slightly more complex SIR-B geometry (which will always contain a convergent component) during the first year of the effort.

3. **Radarclinometry**. A well known technique for deriving topographic information from photographs for which only single images are available is called photoclinometry. This involves knowledge of sensor and illumination geometry, and calculation of local slope (and, by integrating, elevation) from image brightness. In principle this will also work for radar images, which is in fact a simpler case since we are always dealing with backscatter. Presumably the same error sources will manifest themselves, namely intrinsic albedo differences will show up as slope changes. In addition, the method may be more successful at smaller incidence angles because of the increased sensitivity of radar backscatter to slope, but the effect may be canceled out by the increase in image distortion.

We plan to test these hypotheses by producing radarclinometric topographic maps of scenes for which multiple incidence angles are available. These will be evaluated by the same techniques used to analyze the stereo-derived topographic maps.

C. Image Manipulation

One of the key applications of topographic data in radar image analysis is the removal from the images of the distortions (foreshortening and layover) due to elevation changes within the scene. It is only when the images are so rectified that they can be registered to data from other sensors. SIR-B affords the first opportunity to perform a rectification experiment with digital images obtained at intermediate to high incidence angles.

1. **Rectification**. Using SIR-B images, we will attempt to produce rectified versions of images that have been oriented and located under the planimetric mapping task. This will be done by using digital elevation maps from the USGS and also elevation data resulting from the topographic mapping task. Our success in accomplishing this in an unsupervised (automatic) fashion will constitute a good test of the planimetric mapping and pixel location algorithms.

2. **Scatterometry and radiometric correction**. An important potential use of orbital SAR images combined with topographic data is the production of backscatter curves, i.e., plots of radar cross section per unit area versus incidence angle. Several SIR-B experiments will involve attempts to discriminate and identify surface geologic units or rock types by measuring the change in radar brightness between images obtained at different look angles. A drawback inherent in this approach is that the number of data points available to characterize the backscatter curve equals the number of images available. For SIR-B this is a maximum of six.

When a radar image is combined with a digital topographic map, however, whether a preexisting digital elevation map (DEM) or one derived from the radar data themselves, such a curve with a much larger sampling of incidence angles may be derived from a single image. This can be done when all the imaging parameters (sensor position and timing) are known by calculating the incidence angle at each pixel using the topographic map.

To the extent that the SIR-B instrument will be calibrated (a few dB absolute and less than one dB relative) such curves derived from these data will be real backscatter curves. We will produce such curves for several test sites using both DEM's and stereographically derived topography and, in cooperation with other team members who will be performing geologic discrimination experiments, compare them with the curves derived from the multiple image technique. We expect that scatterometer and ground-truth data will also be available from these sites from other experimenters for independent verification of the results.

3. **Map quality**. One of the unique elements of the SIR-B instrument is that it allows us to perform for the first time a truly quantitative, systematic radar mapping experiment. Evaluation of the planimetric and topographic maps we produce must also be quantitative and systematic, so we have identified as a separate task the establishment of a formal procedure for evaluating their accuracy in terms of National Mapping Accuracy Standards (NMAS). This may seem trivial but problems arise in that the NMAS and most other accepted standards for planimetric and topographic maps are generally defined in terms of contour intervals and position error on maps of certain scales. They are not particularly applicable to digital maps such as those SIR-B will provide.

To present our results in terms of generally accepted mapping standards, we will define the theoretical error limits (from knowledge of the radar parameters and spacecraft ephemeris) and actual errors (from comparing map products to ground truth) in terms of root mean square errors (RMSE) in X, Y, and Z, and convert these to the 90% confidence levels required by the standards. In this way we can accurately define the scales (1:250000, 1:10000, etc.) at which radar images can be used to produce planimetric and topographic maps of acceptable quality.

Monitoring of the Tidal Dynamics of the Dutch Waddensea by SIR-B

Team Member:

B. N. Koopmans
International Institute for Aerial Survey and Earth Sciences (ITC)
Enschede, Netherlands

Collaborators:

D. van der Zee, A. Th. Verstappen, T. Woldai and H. Hoschititzky
International Institute for Aerial Survey and Earth Sciences
Enschede, Netherlands

I. Introduction

The Waddensea is an area of 8000 km^2 along the coast of Northern Netherlands, Northwestern Germany, and Southwestern Denmark. It is one of the many coastal areas in the world that are constantly remodeled under the influence of the tidal regime. Erosion and sedimentation cause a constant change in bottom configuration. The monitoring of such dynamic coastal areas is of importance for coastal protection, maintenance of safe navigation channels, conservation of fishing grounds, and of the nursery function that such shallow tidal waters have for many commercial fish species.

ITC seeks to use the results and survey methodologies to be developed in comparable areas, especially in the Third World.

II. Objectives

Conventional survey methods of the tidal flats consist of terrestrial leveling and shipborne sounding. Weather conditions and sea state often interfere with surveying. The areas covered are usually of limited extent for technical and economic reasons. The effectiveness of a photogrammetric survey is often impeded by weather conditions in combination with the users requirements concerning the tidal situation.

The potential of Landsat data, covering the entire tidal flats at a certain, known, tidal situation, has been assessed by the investigators; they discovered that the data cannot be used for systematic survey because: (1) of the long interval between subsequent passes, (2) weather conditions often interfere with recording, and (3) of the lack of correlation between passes and the tidal situation.

The objective of the present project proposal is to overcome the problems met with existing survey methods as outlined above, making use of (1) the synoptic view obtained by SIR-B, which has the potential of surveying large areas of the flats simultaneously; (2) the all-weather capability of the microwave system; (3) the recording during consecutive days, which results in a straightforward correlation with the tidal cycle and the picturing of different tidal stages; and (4) the multiangle incidence of SIR-B for analyzing the bottom configuration of submerged parts of the flats. The use of a weather-independent monitoring device, such as radar, can

mean a major improvement of the technique of monitoring tidal coastal areas.

III. Description of the Experiment

To test the possibilities of SIR-B radar, the northeastern part of the Dutch Waddensea area (6°15′ to 6°40′E and 53°35′ to 53°25′N) has been selected as the study area. The same area has been used for an airphoto experiment. Figure 1 shows the configuration of channels, tidal flats, mainland, and islands of the area. The average tidal amplitude varies from 1.5 to 2.5 meters with a tidal period of 12 hours and 25 minutes (Fig. 2). For this study, five SIR-B passes are at present planned, corresponding with different stages of the tidal cycle (see Table 1). This will render it possible:

(1) To map the emerged and submerged parts of the flats at different tidal levels. The water lines so obtained are formlines rather than contour lines due to deformations of the water surface caused by tidal currents and lateral shifts in the tidal cycle. The water lines will be transformed into contour lines on the basis of spot-heights obtained by echo sounding and by information from RWS gauging stations situated in the area.

(2) To assess the radar response to bottom configuration at five different stages of submergence of the tidal flats. The response to depth relation thus can be studied in the tidal zone. The effect of incidence angle can also be analyzed by comparing the radar response during subsequent passes in areas of equally deep submergence.

(3) To study the radar response of the emerged parts of the tidal flats in its relation to the time elapsed since the emergency and thus to the degree of drying-out, as well as the influence of microrelief (ripples) and soil type: sand, mud, or shells.

An attempt will be made to assess the influence of t wave pattern over the tidal flats as compared with that in t gullies with respect to the radar backscatter under differe conditions of submergence during the tidal cycle.

IV. Approach

The approach to the project is basically geared to th extrapolation of conventional methods of aerial image analys of tidal flats to space-acquired microwave SIR-B data. To thi end the SIR-B data are complemented by airborne-acquire data and by ground-truth gathering including sounding an gauging. The digital SAR data will be enhanced and geo metrically corrected with respect to control points (corne reflectors for location), so that images of the different stage in the tidal cycle can be superimposed. Field parties wil collect terrain observation data at the time of each Shuttl pass, and measure the exact location of water/land boundary with respect to control points at a number of places.

V. Anticipated Results

It is expected that SIR-B data will give a complete synoptic view of the morphology of the tidal flats in the northern part of the Netherlands with water lines as a guiding element.

It is also expected that the methodology developed will be applicable to areas of similar nature in the other parts of the world. The radar response to bottom topography will, in all likelihood, also provide information about the emerged deeper parts of the tidal channels. Analysis of Seasat (Fig. 3) data has already yielded interesting results in this respect. It stands to reason that the optimal angle of incidence for obtaining such responses can also be determined. A better insight is expected to be gained on the influence of wave pattern and stream velocity along the gully edges on the radar return signal.

Bibliography

Schutt-Taverna, M. R., "The Westplaat (S.W. Netherlands). A Study of Coastal Dynamics From Sequential Aerial Photography," *ITC Journal*, 1975-2, pp. 173-185.

Verstappen, H. Th., *Interpretation of Some Aerial Thermographs of an Estuarine Environment.* ITC Publication Series B, Number 65, 1979.

Van der Zee, D., Waterlijnen 1980. "Rapport Over the Stand van Zaken met Betrekking tot het Waterlijnenkarteringsprojekt, Deelprojekt van Onderzoekprojekt nr. 452: Morphodynamiek van Estuering en Getyde Gebieden," *Afdeling Geografie en Geomorfologie*, ITC Enschede, Netherlands, January 1981.

Table 1. Planned passes over Waddensea — SIR-B

Orbit	GMT	EMT	HW	HWET	LT
17	10.47	11.47	13.31	-1.44	12.47
31	6.53	7.53	1.58	+5.55	8.53
64	9.30	10.30	3.10	+7.20	11.30
96	8.53	9.53	5.28	+4.39	10.53
112	8.34	9.34	6.54	+2.40	10.34

GMT Greenwich meantime; time based on launch at 10:50 GMT
EMT European meantime
HW High water
HWET High-water elapsed time
LT Local summer time

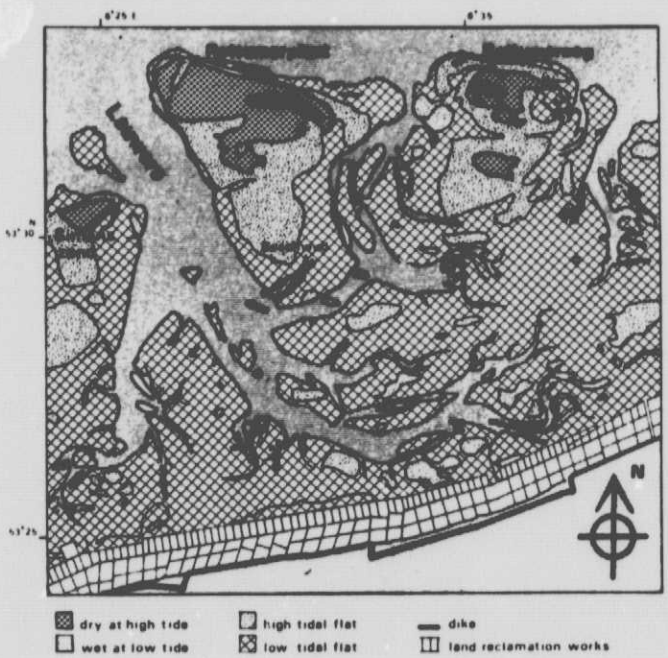

Fig. 1. Tidal flat area of the Dutch Waddensea test site

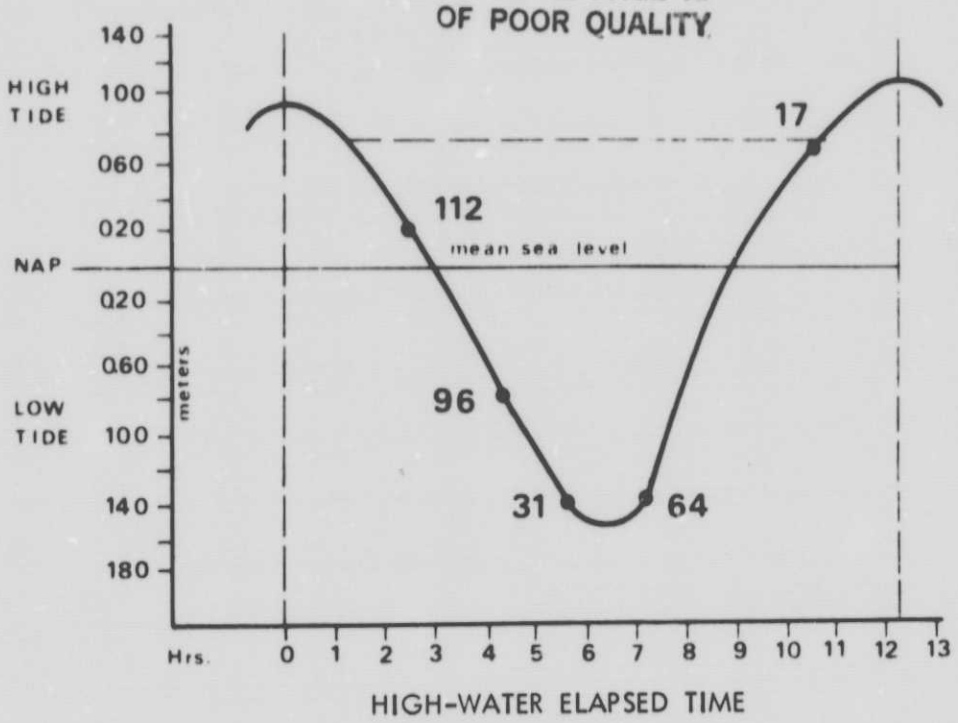

Fig. 2. Tidal cycle of Wadden sea test areas with planned SIR-B passes

ARCHNO S 1493 N 05318 E 00557 091078 1803 ORBIT 1493 OCT 9, 1978
4 LOOKS 25-m RESOLUTION SCALE 1:250000

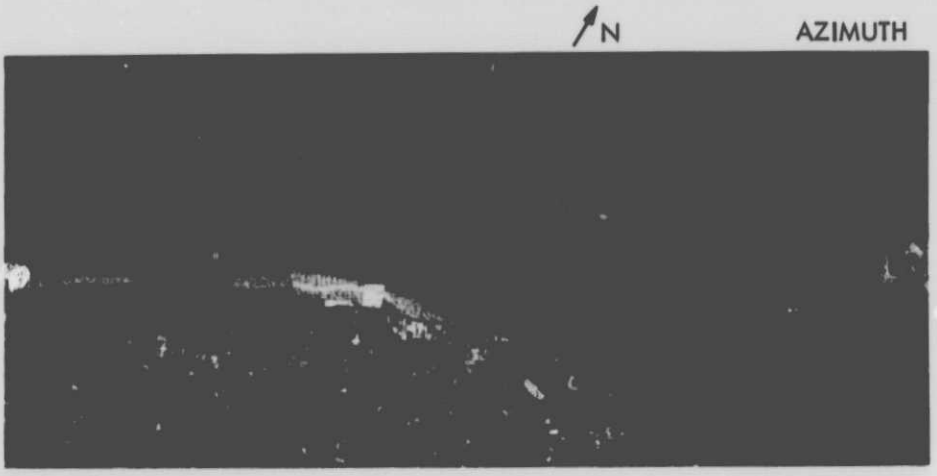

Fig. 3. Seasat image of western part of Dutch Waddensea (image processed by DFVLR/GSOC for ESA/EARTHNET)

Structural Investigation of the Canadian Shield by Orbital Radar and Landsat

Team Member:

P. D. Lowman, Jr.
Goddard Space Flight Center
Greenbelt, Maryland

Collaborators:

H. W. Blodget and **W. J. Webster, Jr.**
Goddard Space Flight Center
Greenbelt, Maryland

S. Pala and **V. H. Singhroy**
Ontario Centre for Remote Sensing
Toronto, Canada

V. R. Slaney
RADARSAT Project Office
Ottawa, Canada

I. Objectives

This experiment is a cooperative American-Canadian radar study of the Canadian Shield. Its objectives can be categorized as science-oriented and technique-oriented. The primary objective is scientific: to investigate and clarify the tectonic relationships of the Churchill, Superior, and Grenville Provinces (Figs. 1 and 2), concentrating on their geologic boundaries, the Nelson and Grenville Fronts. The nature and origin of these fronts, which have counterparts in most other Precambrian shield areas, are not understood. Theories range from in-situ regional metamorphism to tectonic sutures resulting from terrain accretion. The SIR-B investigation is intended to clarify this problem. Secondary objectives are oriented toward technique development, and include: (1) evaluation of the use of orbital radar in high-latitude Precambrian terrains, (2) evaluation of look-azimuth biasing in radar and Landsat imagery, and (3) investigation of the synergistic use of radar, Landsat, and geophysical data in Precambrian studies.

II. Description of the Experiment

The experiment is essentially a traverse across the Canadian Shield using SIR-B imagery acquired during several descending passes, with as much overlap as possible, at three incidence angles. Imagery on ascending passes that cross the line indicated (Fig. 1) will also be used as available. This experiment is closely coordinated with the experiment "Structural Investigation of the Grenville Province by Radar and Other Imaging and Nonimaging Sensors," described separately, which is concentrated on the Bancroft area in southern Ontario. Landsat

imagery of the Canadian Shield is already under study at GSFC in an investigation of regional fracture patterns; this investigation is being phased into the SIR-B experiment.

This experiment is primarily a structural study, focused on fractures, dykes, folds, and major intrusions in the vicinity of the Nelson and Grenville Fronts as well as other sections covered in the swath. Aspects of regional structure that will be investigated include the degree of structural continuity across the fronts, evidence for lateral displacement along them, the nature of regional fracture patterns, and the like.

III. Approach for Data Acquisition, Handling, and Analysis

The general approach for data handling will be to analyze SIR-B imagery of the exepriment both by itself and in combination with other data types, including Landsat and 70-mm hand-held photography acquired by the Shuttle crew during the mission. Since structure in this area is expressed primarily as topography, the data analysis will concentrate on this rather than lithology. Specific procedures to be used include the following: (1) texture analysis, (2) high-pass filtering, (3) contrast stretch, (4) median boxcar filtering, (5) coregistration of SIR-B, Seasat, and Landsat imagery, (6) fracture pattern analysis, and (7) photogeologic overlay techniques. These methods are, in general, adaptations of already available techniques, although some specialized software may be developed. In addition, statistical comparisons will be made of structural rendition of SIR-B imagery as a function of incidence angle and illumination azimuth, and of illumination-azimuth biasing in SIR-B and Landsat imagery by cross comparison. Field work will be conducted to the extent possible. However, because of the very large area to be covered, field work will be limited to spot-checking of critical localities rather than systematic areal mapping.

IV. Expected Results

The broadest result expected is a better understanding the nature of metamorphic fronts and, by implication, crustal provinces. This may come from *un*expected resul such as the discovery of previously unknown structures structural relationships. For example, should the SIR-B ima ery show that dykes of Archean age cross a front witho significant deflection or offset, this would put strong limits c the theory that fronts represent the suturing of accreted te rains. Another result that can be expected, judging from pr vious experience with orbital remote sensing, is the discover of unmapped or mismapped structures of lithologic units.

Specific products expected from the investigation will in clude: (1) linear radar mosaics of the region between Manitob and New York, (2) improved structural maps along the experi ment swath, (3) combined maps of the exepriment swath o portion thereof showing the relation of SIR-B imagery t structure, seismicity, and other geological or geophysical fea tures, (4) special-purpose images of selected regions produced by the data analysis techniques previously listed.

General results expected in the area of technique development include an evaluation of the effectiveness of orbital radar imagery in a high-latitude shield, both by itself and in comparison with Landsat and other types of remote sensing data. A specific result will be a quantitative estimate, from cross comparison of SIR-B and Landsat, and of SIR-B imagery with different look azimuths, of the degree of structural biasing caused by azimuthal variations. It should also be possible to produce an assessment of the best combination of incidence angles and illumination azimuths for structural mapping by orbital radar. Finally, we should gain considerable experience in combining orbital radar data by digital techniques with other types of remote sensing data.

Bibliography

Elachi, C., et al., "Shuttle Imaging Radar Experiment," *Science*, Vol. 218, pp. 996-1003, 1982.

Price, R. A., and Douglas, R. J. W., *Variations in Tectonic Styles in Canada*, Sp. Paper 11, Geological Association of Canada, 688 p., 1972.

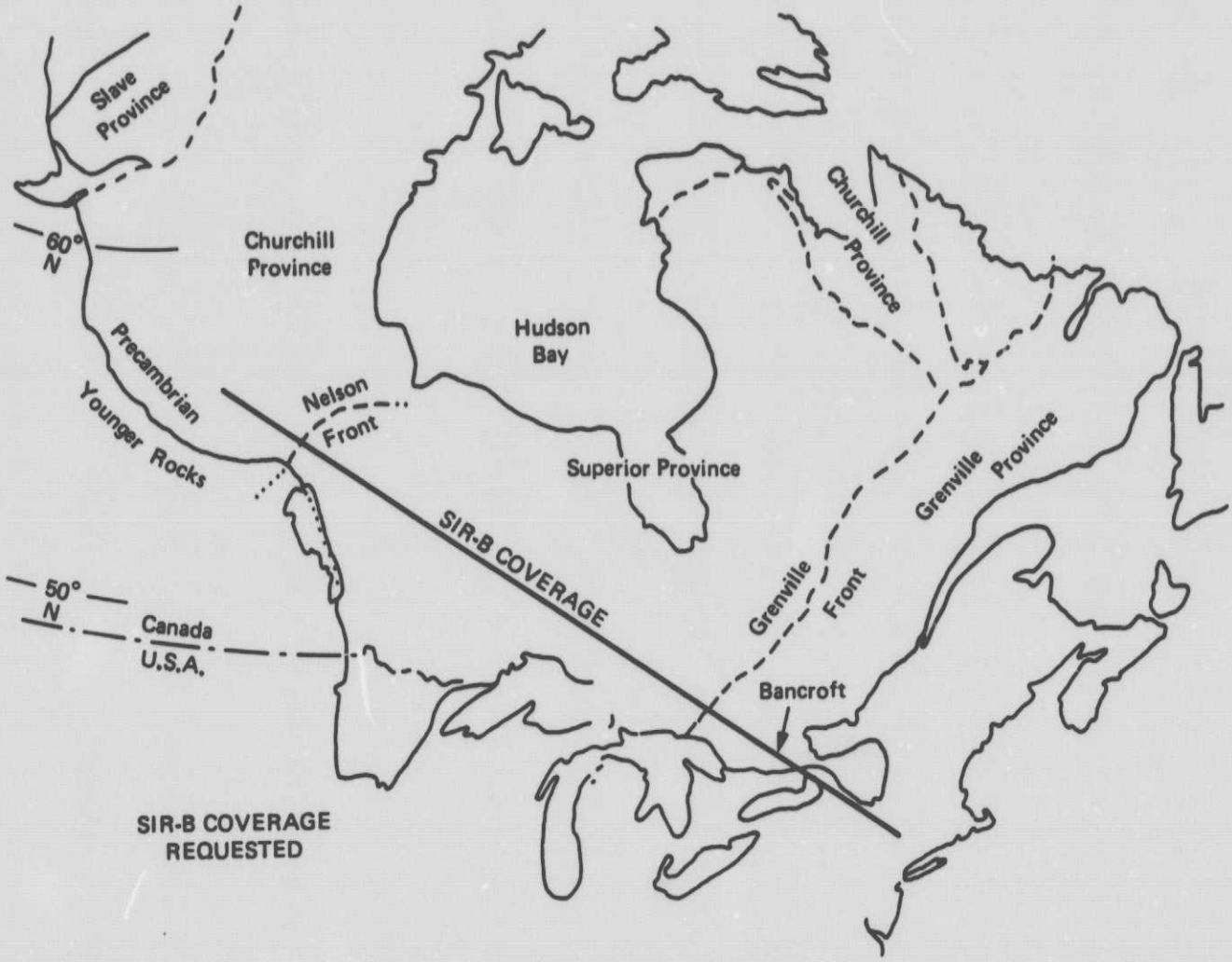

Fig. 1. Map of Canadian Shield, showing major geologic provinces and SIR-B coverage desired

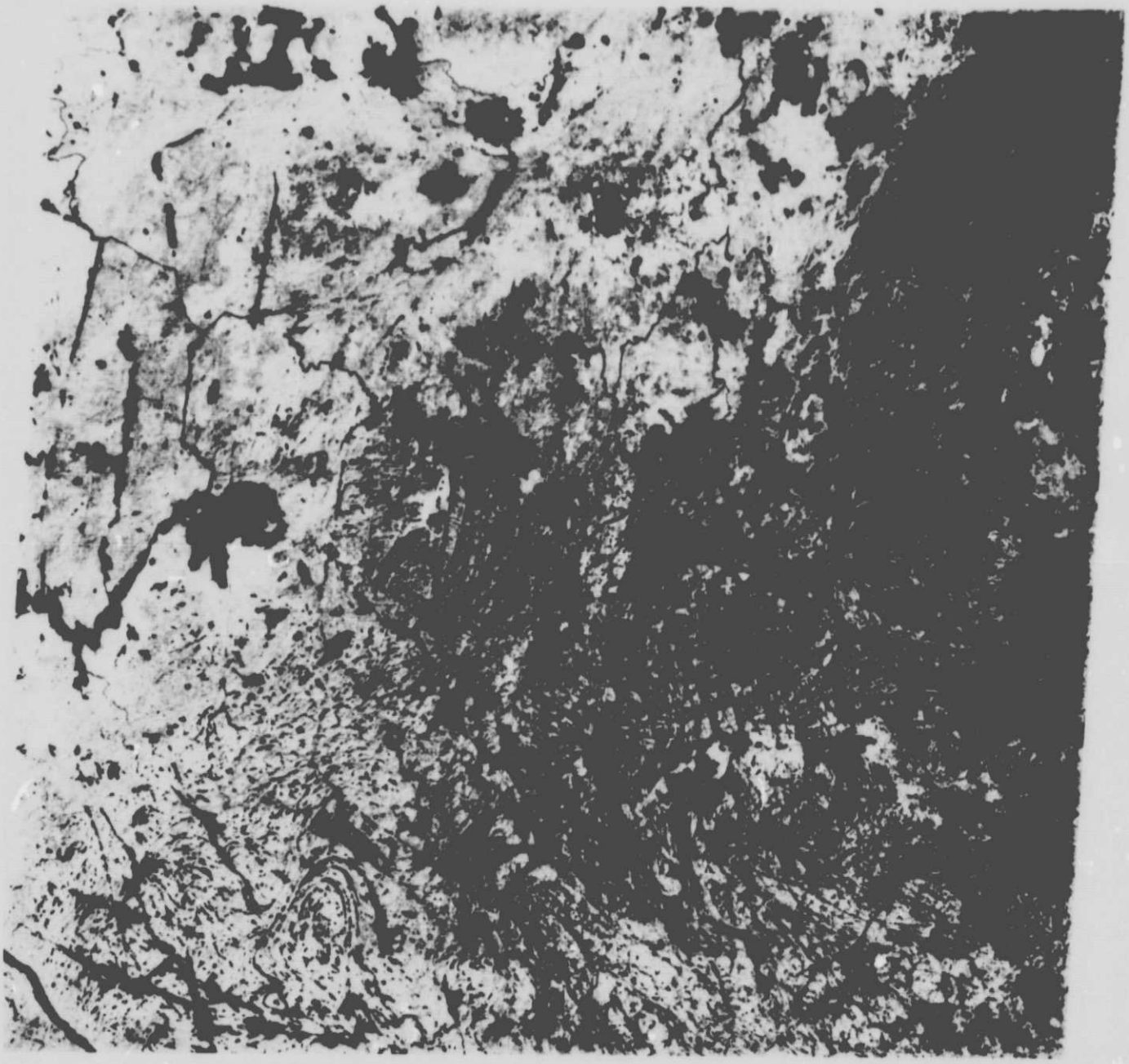

Fig. 2. Landsat MSS Band 7 (image No. 1443-15322) showing Grenville Front in southern Quebec. Superior Province at upper left, Grenville Province at lower right. Northwest-trending lineaments in Grenville are brittle fractures cutting irregular ductile structures in igneous and metamorphic rock

Structural Investigation of the Grenville Province by Radar and Other Imaging and Nonimaging Sensors

Team Member:

P. D. Lowman, Jr.
Goddard Space Flight Center
Greenbelt, Maryland

Collaborators:

H. W. Blodget and **W. J. Webster, Jr.**
Goddard Space Flight Center
Greenbelt, Maryland

S. Pala and **V. H. Singhroy**
Ontario Centre for Remote Sensing
Toronto, Canada

V. R. Slaney
RADARSAT Project Office
Ottawa, Canada

I. Objectives

This experiment, to be carried out by the staff of several Canadian federal and provincial organizations, is an integral part of the more broadly scoped experiment entitled, "Structural Investigation of the Canadian Shield by Orbital Radar and Landsat," described separately, and shares its general objectives to a large degree. However, this investigation is concentrated on the Bancroft area in southern Ontario (Fig. 1), a representative section of the southwest Grenville Province. The area includes parts of the central metasedimentary belt and the Ontario gneiss belt, and major structures are well-expressed topographically (Fig. 2).

The primary objective of this experiment is to apply SIR-B data to the mapping of this key part of the Grenville orogen, specifically ductile fold structures and associated features, and igneous, metamorphic, and sedimentary rock (including glacial and recent sediments).

Secondary objectives are intended to support the Canadian RADARSAT Project by helping evaluate the baseline parameters of a Canadian imaging radar satellite planned for late in the decade. These include optimum incidence and azimuth angles. In addition, the experiment is intended to develop techniques for the use of multiple data sets.

II. Description of the Experiment

A very wide range of geological and geophysical data is available for the Bancroft test site, including Seasat, Landsat

MSS, and Landsat TM imagery, aerial photography, gravity data, a digital terrain model, and airborne magnetic and gamma-ray surveys. Considerable field work has been done in the area by Geological Survey of Canada geologists, and more is planned for 1984. The SIR-B imagery will also be used by the staff of the Ontario Centre for Remote Sensing and by the Canadian Forestry Service. Both these organizations have extensive experience in studying the vegetation cover of Canada by remote sensing techniques.

III. Approach for Data Acquisition, Handling, and Analysis

Data handling can conveniently be described under the three following headings.

A. Viewing Geometry

To determine the best radar incidence angles for structural studies in the Canadian Shield, imagery from each of the three incidence angles requested will be combined to produce three alternative stereo configurations. These will then be used for geologic interpretation to determine which provides the most information.

B. Look Bias

After image processing techniques, such as shadow enhancement, have been applied to the data, visual and statistical studies will be made of biasing caused by look azimuth. Structural trends in the Grenville Province have a wide range of directions; this, and the expected variety of look azimuths available in Seasat, Landsat, and SIR-B should permit a good evaluation of the importance of look biasing.

C. Multiple Data Sets

The various data sets listed under "Description of tl Experiment" will be geometrically corrected and coregistere Each data set will be processed independently, preparatory t correlation with other sets. Processing techniques will incluc contrast enhancement, band ratioing, classification, an frequency filtering. Correlation with Landsat data will b stressed, based on previous studies.

IV. Expected Results

Scientifically, a major result expected from the experimen will be better mapping and hence better understanding of the nature and origin of the Grenville Province. There are presently two major hypotheses for the southwest Grenville orogen, one that it consists largely of diapiric granite intrusions, the other that it is large thrust slices separated by broad mylonite zones. Which, if either, is correct may be answered with the help of SIR-B and related data.

In technique development, the experiment should contribute to both the use of orbital radar in general and to the RADARSAT Project in particular. It will permit much more intelligent selection of incidence angles and wavelengths, and better allowance for look-azimuth bias.

Finally, results of this experiment may be applicable to the larger area of its companion experiment that will investigate the Canadian Shield. The Bancroft area can serve as a training site for interpretation of imagery in other parts of the Canadian Shield, with proper allowance for differences in vegetation and topography.

Bibliography

Culshaw, N. G., Davidson, A., and Nadeau, L., "Structural Subdivisions of the Grenville Province in the Parry Sound-Algonquin Region, Ontario," in *Current Research, Part B., Geological Survey of Canada*, Paper 83-1B, p. 243-252, 1983.

RADARSAT Project Office, *RADARSAT Mission Requirements*, Document 82-7, 1982.

Singhroy, V. R., Bruce, W.D., and Stevens, G.R., "Geological and Terrain Analysis of the Annapolis County Region of Nova Scotia: an Application of Digital Landsat, Radar, and Colour Infrared Data," 6th Canadian Symposium on Remote Sensing, Halifax, Nova Scotia, 1980,

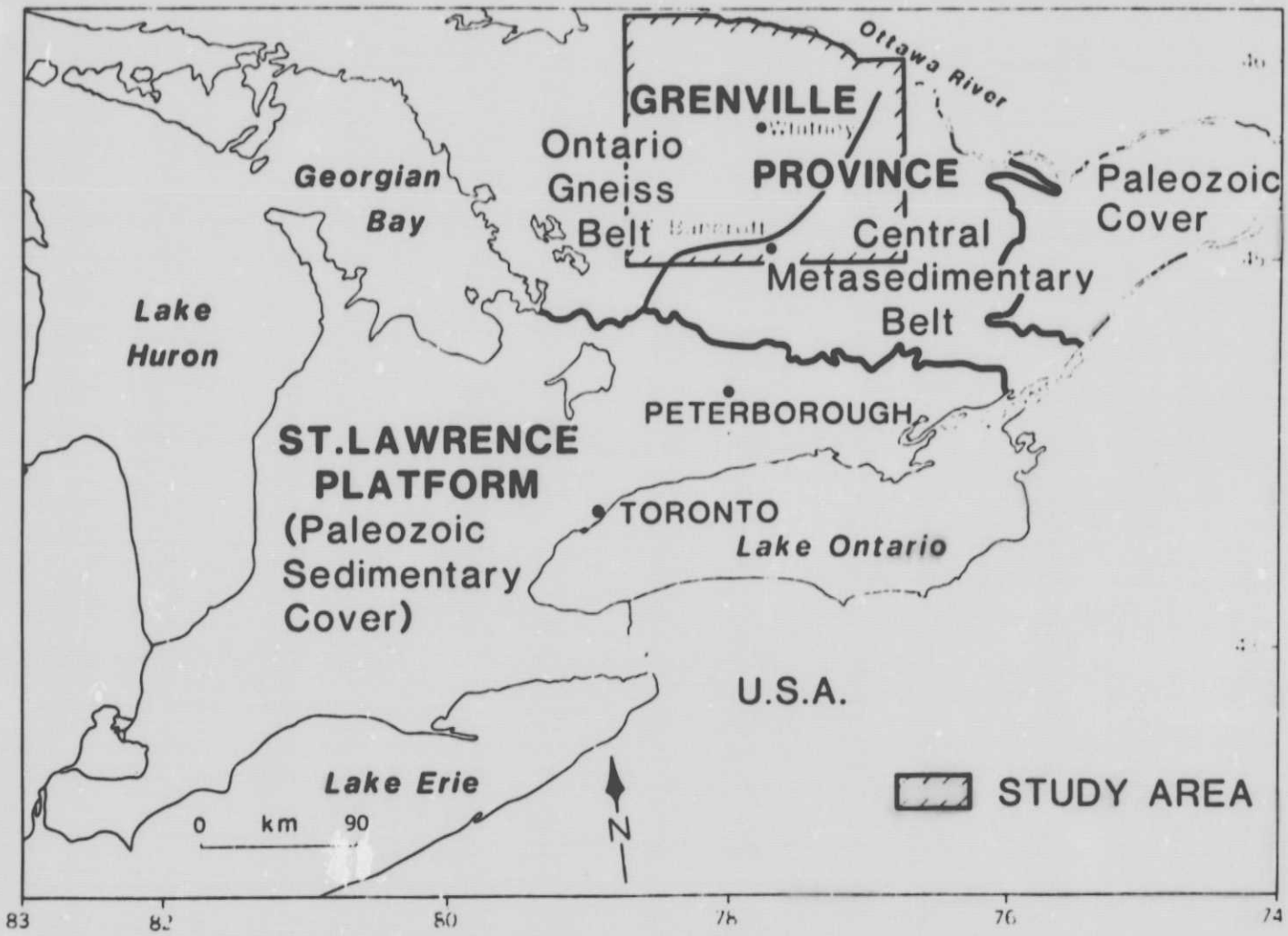

Fig. 1. Index map of southern Ontario showing Bancroft test site

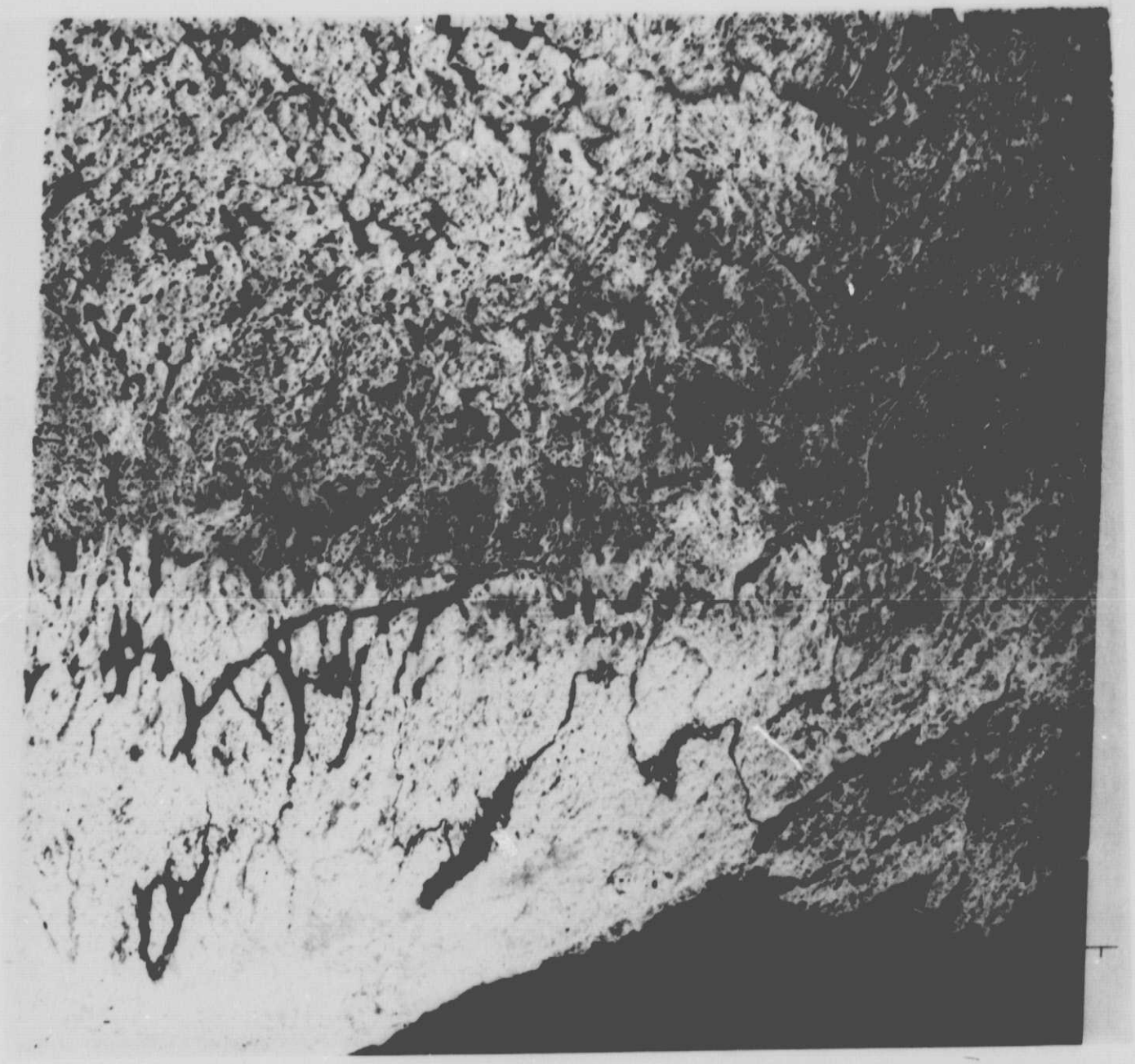

Fig. 2. Landsat MSS scene (Image No. 2816-15001) showing southern Ontario; Lake Ontario at bottom right, Bancroft near top center. Lighter-toned terrain in lower part of picture is Paleozoic and glacial cover; shield area to north is part of Grenville metasedimentary belt

Studies of Coastal Mesoscale Winds Using SIR-B

Team Member:

R. K. Moore
University of Kansas Center for Research, Inc.
Lawrence, Kansas

Collaborator:

W. J. Pierson
City University of New York
New York, New York

I. Summary

The variability of the mesoscale wind fields near coastlines can be caused both by mountains that shadow offshore winds and by valleys that enhance them. These wind patterns are of scientific interest in their own right, of practical interest in local marine activities and weather forecasting, and provide relatively fixed patterns that must be considered in the development of algorithms for future spaceborne scatterometer systems; mesoscale variability over the offshore regions is random and must be averaged out for forecasting, but nearshore fixed patterns must be treated differently.

Before the patterns of interest can be defined quantitatively, the scattering response of the ocean to winds at the L-band frequency and SIR-B angles of incidence must be developed from the SIR-B data. Once this is done, patterns can be analyzed on the images both in regions selected for high probability of the occurrence of suitable patterns, and in other regions where the patterns are observed. The patterns will be analyzed both in terms of the topographic effects and the distance to sea over which these effects cause variations in the oceanic wind patterns. The results will be interpreted both in terms of quantitative description of the processes involved and in terms of the need for modifications of future scatterometer algorithms.

II. Objectives

Most spaceborne measurements of wind vectors in the future will be made with derivatives of the Seasat scatterometer such as those proposed for NROS, the ESA ERS-1, and the NASDA MOS-2. For the synoptic-scale numerical weather predictions using data from these systems, mesoscale variations will be a nuisance (Ref. 1) and must be treated as part of the problem of turbulence and sampling variability. Hence they must be filtered out to obtain the best synoptic-scale winds.

While midocean mesoscale variability needs to be smoothed and eliminated, coastal-scale variability in the winds must be treated differently, for some of these coastal variations are not random. The final algorithms for use of the future systems near coastlines will have to be adjusted for the effects of per-

sistent local wind field patterns so that these variations will not be mistaken for parts of the synoptic patterns. Moreover, knowledge of local persistent wind patterns is of importance to navigation in the areas affected, as well as to forecasting local weather and sea conditions.

A major objective of this research is to develop the methodology for use of SAR in space to establish these wind patterns so that, with the aid of future SAR missions, they may be incorporated into the algorithmic development process for future scatterometers. A second related objective is to identify the patterns in as many places as feasible within the mission constraints. Since little is known about the size and nature of these effects, even though their existence is well-known, a third objective is to quantify the nature of these wind patterns. This means that the differences in the offshore patterns need to be established for different mountain and valley configurations. A very important objective is to quantify the downwind extent of such patterns, and the rates of falloff of their effects.

These coastal-scale wind variations are expected to be repeatable because they are caused by geographical effects, whereas the midocean mesoscale variations are random. Examples of regions where the surface winds over the water are expected to vary by large amounts over short distances for similar reasons include the Straits of Juan de Fuca, in and seaward of the Alexander Archipelago, around Kodiak Island, in the straits of and around the Aleutian chain, and around islands such as the Hawaiian chain, Puerto Rico, Haiti, Jamaica, the Bahamas, and the Antilles. Indeed, Sun-glitter variations caused by light winds have been observed in the lee of the Antilles in geostationary images, and apparent wind shadows appear in many places on Seasat and SIR-A images.

The islands and straits listed above vary in size from barely mappable in a major atlas to quite large, and in location they vary from regions where the climatological winds are relatively steady in both speed and direction to regions where stormy conditions with high winds sometimes occur. Comparison of SIR-B backscatter observations over the sea with images of the adjacent land areas should allow identification of coastal features such as mountains and valleys that will make possible definition of the offshore mesoscale variability caused by these features.

Averaging of the signal strengths observed with a synthetic-aperture radar to obtain scatterometer-like observations over small areas seems an ideal way to study this phenomenon, although the azimuth variation of the backscatter will, of course, be difficult to ascertain.

Further study will be needed to establish the L-band response to wind speed at the different angles of incidence for the SIR-B. This will require comparison of the SIR-B observations with surface-truth wind vectors at both designated observation points and points of opportunity such as ships with anemometers. The error structure of conventional measurements is better understood since the recent work of Pierson (Ref. 1). Hindcasting in certain areas can be used as with Skylab (Ref. 2) if too few opportunities for direct observation are found during the mission.

III. Approach

To study these coastal mesoscale variations will require two major tasks: improving on the estimate of the relation between scattering coefficient and wind vector given in Ref. 1 and using this improved estimate to calculate the wind speeds (and hopefully the wind vectors) in areas where the topographically induced wind variations are present in the SIR-B images.

The first major task will be accomplished by comparing averaged scattering coefficients measured by SIR-B with buoy- and ship-measured winds for the available points and, if necessary, with hindcast winds for other areas. For most situations, signals obtained prior to both range and azimuth compression can be used (after detection) for this purpose, since the footprint so obtained will be of suitable size after some range averaging. The results are expected to be biased toward the lower wind speeds if the summer flight schedule is maintained because winds in the northern hemisphere are usually moderate during the summer and surface-truth information for the southern hemisphere is too sparse to allow calibrations there.

The second major task will be accomplished by a combination of planned observations for selected locations where suitable conditions are expected to occur with high probability during the short mission. Observations in the Caribbean Sea are particularly important both because of the trade-wind stability and because of planned cooperation with Jamaican authorities. Meteorological conditions for the relevant areas will be obtained from nearby weather-station reports, and the expected patterns synthesized for comparison with the radar observations. If the pass is made during daylight hours, geostationary images of Sun glint obtained within a few hours of a SIR-B pass can be compared with the areal extent of the phenomenon observed in the SIR-B images.

Tasks that are more suited to the oceanographic/meteorological capabilities of CUNY will be performed there and tasks more suited to the radar capabilities of Kansas will be performed there. Specific tasks to be performed are:

(1) Establish the best format for obtaining the backscatter data and develop local algorithms for handling them (KU).

(2) Determine locations and characteristics of suitable surface-truth buoys, ships, and coastal weather stations. Make arrangements to obtain data from them for the mission period. Feed this information into the mission planning (CUNY).

(3) Identify the regions for most intensive study of the topographically induced mesoscale variations and feed these locations into the mission planning to assure that some of them will be covered (CUNY).

(4) Obtain radar backscatter data and correlated meteorological information for the areas selected in (2) and (3) (KU and CUNY). Develop a preliminary model of the variation of σ_0 for angles larger than the 20° of Seasat (KU). Determine whether hindcast data will be needed to improve these estimates (KU).

(5) If needed, prepare hindcast objective analyses of wind fields for areas where coverage is available in the North Atlantic and/or North Pacific (CUNY).

(6) Obtain additional radar data, process them, and combine with the results of (4) and (5) to obtain the final estimate of scattering coefficient model parameters (KU).

(7) Determine the level below which these phenomena are obscured by the effects of communication noise and sampling variability in scatterometers and show the value of such data for modifying the algorithms for wind-vector scatterometers in coastal areas (KU and CUNY).

(8) Quantify the nature of the effects studied and show their application to coastal meteorological and oceanographic problems (KU and CUNY).

IV. Anticipated Results

A more complete description of the relationship between scattering coefficient and wind vector will be obtained than was possible with Seasat because of the wider range of angles of incidence of SIR-B. The precision of the estimate, however, will probably be less because of the limited length of the SIR-B mission.

A quantitative description of some of the effects of different coastal configurations on downwind patterns over the sea will be obtained. This will include both the effects of valleys that funnel high winds over the sea because of venturi effects and of mountains that cast wind shadows. The downwind extent and gradient of these effects will be determined. Of course, these determinations, too, will be somewhat limited by the short mission duration.

A beginning will be made on the determination of the size, nature, and locations in coastal areas of persistent wind patterns that may have to be considered in algorithmic development for future wind-vector scatterometers.

References

1. Pierson, W. J., "Measurement of the Synoptic-Scale Wind Over the Ocean," *JGR*, Vol. 88, No. C3, February 1983, pp. 1683-1709.

2. Young, J. D., and Moore, R. K., "Active Microwave Measurement from Space of Sea-Surface Winds," *IEEE J. Oceanic Engr.*, Vol. OE-2, No. 4, 1977, pp. 309-317.

Information for Space-Radar Designers: Required Dynamic Range vs Resolution and Antenna Calibration Using the Amazon Rain Forest

Team Member:

R. K. Moore
University of Kansas Center for Research, Inc.
Lawrence, Kansas

Collaborator:

V. S. Frost
University of Kansas Center for Research, Inc.
Lawrence, Kansas

I. Summary

Calibration of the vertical pattern of the antennas for the Seasat scatterometer was accomplished using the nearly uniform radar return from the Amazon rain forest (Ref. 1 and 2). A similar calibration will be attempted for the SIR-B antenna. Such a calibration will be important in establishing the radiometric calibration across the swath of the SIR-B, and the methodology developed will provide an important tool for evaluation of future spaceborne imaging radars.

This calibration was possible for the very-wide-beam Seasat scatterometer antennas because at 14.65 GHz the scattering coefficient of the rain forest is almost independent of angle of incidence, as had been demonstrated by the Skylab measurements (Refs. 3 and 4). Although we do not know that this condition will prevail at L band, one can expect that the variation in scattering coefficient for the rain forest across the relatively narrow vertical beam of the SIR-B will be very small; even at L band the forest should be essentially impenetrable for radar signals, so the volume scatter from the treetops should predominate as at higher frequencies.

Ideally, aircraft measurements over the rain forest should be conducted at L band before the SIR-B mission, but this probably is not feasible. The basic elements of the research include: (1) examination of SIR-B images (and SIR-A images, if available) over the rain forest to establish the variability of the scattering coefficient at finer resolutions than that of the Seasat scatterometer; (2) analysis of the variability of SIR-B data detected prior to processing for either azimuth compression or, possibly, range compression so that averages over relatively large footprints can be used; (3) processing of data of the form of (2) using algorithms that can recover the vertical pattern of the antenna.

II. Objectives

The first, and most important, objective is to aid in determining the radiometric calibration of the SIR-B images for other parts of the world. The antenna pattern measured before launch is, of course, a first approximation to the pattern that exists in flight. Possible deviations from this pattern can occur because of distortions resulting from erection of the antenna

on the Shuttle. Thus, verification of the actual pattern of the flight instrument is important.

The second objective is to develop this technique for calibrating the antenna pattern for future spaceborne imaging radars. Such a technique can result in a full definition of the vertical pattern for any spaceborne radar.

III. Approach

A. Background

During the Skylab mission, numerous passes were made over the Amazon rain forest at the behest of Brazilian investigators. The Skylab RADSCAT (13.9 GHz) was operated in its cross-track contiguous scanning mode. Investigators at the University of Kansas noted that the scattering coefficients obtained for the large Skylab footprints (about 12- × 14-km ellipses) were very stable and almost independent of position within the rain forest, although a minor distinction could be made between the two major forest categories (less than 1 dB apart) (Ref. 4). This led to the consideration of this area as a potential test target for the Seasat scatterometer antenna.

In planning for the Seasat scatterometer, the need for a calibration target was established. Various potential "standard targets" were investigated, including deserts in Africa, Australia, and southwest Asia, as well as forested areas in several locations. The investigation showed that the *only* area meeting the requirements of homogeneity over a very large area was the rain forest in the Amazon basin. Deserts are less homogeneous than frequently supposed, and sand dunes shift with the winds, making sand targets unstable. Dense forests exist in many other places in the world, but each one examined had undesirable features not found in the Amazon basin: too many clearings, seasonal variations, hilly or mountainous terrain. Preliminary examination of the scatterometer outputs from several passes over the Amazon forest showed that the stability of the scattering that had been predicted was verified (Ref. 1). Preliminary calibrations of the different scatterometer beams were then made from a few passes over the Amazon forest (Ref. 2), and the algorithms were developed to permit a more complete calibration to be made using all available data (Ref. 2). These calibrations then formed the basis for final determination of the scatterometer performance and consequent correction of the processing algorithms.

B. Research Plan

The research to be done here involves the following steps:

(1) Develop criteria for determining from processed images, from maps, and from the Seasat data which areas of the rain forest are sufficiently stable to be used for this purpose. For example, in the Seasat work a digital map of the rain forest was prepared so that footprints containing rivers could be excluded from the analysis. This map might be used here, but a more definitive and less complex approach probably is to use the processed SIR-B images themselves. Optical processing is adequate for this purpose.

(2) Develop preliminary algorithms for determining the antenna pattern from the SIR-B measurements over the Amazon area. These will be different from those used for the scatterometer because the vertical beamwidth is much smaller for SIR-B, and they must also take into account possible larger variations in scattering coefficient with angle of incidence. The algorithms must consider measurements made at different elevation pointing angles as part of the verification procedure. However, because of the swath-width limitations imposed by telemetry considerations, reasonably complete patterns can be obtained only at the steeper angles. The algorithms must also include provisions for comparing vertical- and horizontal-polarization patterns.

(3) Perform analyses of SIR-B images to establish the areas to be used for the antenna calibration.

(4) Perform preliminary analyses of uncompressed data at different pointing angles to establish the pattern of variation of scattering with angle of incidence.

(5) Apply the algorithms of (2) to the selected data, after making suitable modifications to account for the results of (4).

(6) Report the results both to JPL for use in updating the estimates of the antenna patterns to aid in radiometric calibration of the instrument and to the community at large as an indication of the techniques to be used for future spaceborne imaging radar calibration.

IV. Anticipated Results

The result of the first objective should be an improved estimate of the radiometric calibration of all SIR-B images, with consequent benefits to all other investigators, provided of course, that the rain forest proves stable enough at L band for this calibration to be of the high quality found at Ku band.

The result of the second objective will be provision of a procedure to use in performing such calibrations on all future spaceborne SAR missions.

References

1. Bracalente, E. M., et al., "The SASS Scattering Coefficient Algorithm," *IEEE J. Oceanic Engr.*, Vol. OE-5, 1980, pp. 145-154.

2. Birrer, I. J., et al., "Signature of the Amazon Rain Forest Obtained from the Seasat Scatterometer," *IEEE Trans.*, Vol. GE-20, No. 1, January 1982, pp. 11-17.

3. Sobti, A., *Terrain Response to an Orbiting Radiometer/Scatterometer*, Ph.D. dissertation, University of Kansas, Lawrence, Kansas, 1975.

4. Sobti, A., and Davison, E. C., *Microwave Scattering Measurements Over Brazil at 13.9 GHz*, Remote Sensing Laboratory Technical Report 234-11, University of Kansas Center for Research, Inc., Lawrence, Kansas, September 1975.

N85-17240

Development and Evaluation of Techniques for Using Combined Microwave and Optical image Data for Vegetation Studies

Team Member:

J. F. Paris
Jet Propulsion Laboratory
Pasadena, California

Collaborators:

B. N. Rock
Jet Propulsion Laboratory
Pasadena, California

S. Y. Hsu
Susquehanna Resources and Environment, Inc.
Johnson City, New York

I. Description of the Investigation

Our broad objective is to develop and to evaluate techniques for using combined image data from the Shuttle Imaging Radar (SIR-B) and the Landsat Thematic Mapper (TM) or Multispectral Scanner (MSS) for studies of irrigated crops, and boreal and deciduous forests. In particular, we will strive

(1) To increase the understanding of the physical bases for combined radar and optical remote sensing of vegetation.

(2) To investigate the effects of the structure and composition of crop canopies and soil surfaces on multiangle L-band HH (horizontal polarization for transmission and reception) backscattering and on optical reflectance (in TM or MSS bands viewed at the nadir).

(3) To increase the understanding of the roles of microwave (L-band HH) scattering by canopies and surfaces and transmission by canopies at different angles of incidence.

(4) To evaluate the absolute and relative accuracy of digital, calibrated SIR-B image data and Landsat TM or MSS image data.

(5) To develop and to evaluate textural information extraction-techniques for radar and optical image analysis.

Concerning our role in the NASA Earth Resources Program, our investigation is relevant to both remote-sensing science and to Earth botanical sciences (crop and forest studies, biomass and leaf area index surveying, and soil surveying).

II. Description of the Experiment

A. Study Areas and Sites

We will use sites (approximately 10 by 10 km each) in two areas: (one is the irrigated cropland in the San Joaquin Valley

or the Sacramento Valley, California, and the other is the boreal and deciduous forests in New England and New York. We chose these large areas to ensure that the sites would contain a wide variety of crops or forests even with the change in the position of SIR-B coverage that is likely to occur after launch.

B. Cropland Conditions and Ground Truth

In the irrigated cropland sites, crops of different types will have different biophysical properties, surface roughnesses, row directions, and surface moisture conditions. We will acquire ground truth in a number of these to characterize their identities and biophysical conditions. As a basis for the analysis of the optical and radar images, we will use aerial photography to aid in the mapping of ground-truth information.

C. Crop Canopy Transmittance

Since variations in soil moisture and surface roughness often produce significant differences in surface radar backscatter, we can observe the reduction of these differences due to canopy attenuation and deduce the transmittance of many different types of canopies.

D. Calibration Accuracy Measurement

With well calibrated L-band airborne radar scatterometer measurements across the image area, we will be able to check the relative accuracy of the backscatter coefficients measured by SIR-B. We will use the Barnes Multimodular Radiometer (MMR), which has a set of spectral responses similar to those of the TM and MSS, to measure the reflectance factors of a sampling of fields. We can use these to quantify the reflectances of fields as viewed by the Landsat sensors (under the assumption that the atmosphere is horizontally homogeneous across the site).

E. Cropland Image Data Analysis

We expect registration and rectification of SIR-B and Landsat sensor data to be relatively straightforward in irrigated cropland test sites. We will use standard data extraction and classification procedures to process image data to produce thematic maps of appropriate cropland features. In addition, we will use the Hsu texture-feature extraction algorithms to study the texture information content in Landsat sensor image data and SIR-B image data for crop-type identification.

F. Forests Conditions and Ground Truth

In the forest test sites, a variety of mixtures of tree types with some pure stands of conifers and deciduous trees will exist. Here, ground truth will be less extensive than that o irrigated fields; however, changes in biophysical conditions ar slower. This will provide more time to assess these. We wil rely heavily on aerial photography to map forest communities

G. Forests Image Data Analysis

In the forest, we will be primarily interested in the congruence of spectrally similar areas in the Landsat TM or MSS image data with those of the SIR-B data. We will identify similar and disparate areas with aerial photography and with field checks. We will use the Hsu texture-feature algorithms to investigate the possibility of identification of forest types by texture and backscatter.

H. Use of Combined Optical and Microwave Data

In both areas and for both sets of vegetation types, we will use the hypothesis that optical and radar sensors respond to different biophysical conditions. The Landsat sensors should provide information on *leaf* properties (e.g., green leaf area and perhaps leaf water content) and canopy percent cover (for crops where bare soil is visible due to cultivation). The long wavelength (L-band) of the SIR-B will tend to penetrate the leaves and will be more responsive to stems, stalks, and trunks. Also, due to the HH polarization of the SIR-B, planophile plants may differ from erectophile plants in that the former will display less backscatter and the latter greater penetration. The SIR-B may be sensitive to those plant-part sizes near the sensor wavelength (23 cm or 9 inches), whereas Landsat sensors tend to be insensitive to such considerations. Expected changes in the appearance of vegetation canopy elements for different angles of viewing may lead to better classification results with multiangle SIR-B data than with any given single angle.

III. Approach for Data Acquisition, Handling, and Analysis

A. SIR-B Data

We will use multiangle data over the test sites at a minimum of two sensor view angles that span the range from 20 to 50 degrees. We will use the larger-angle data first in digitally processed format for the irrigated crops test site.

B. Landsat MSS and TM Data

We will use either TM or MSS data for the areas that the SIR-B has viewed during a time period near (within two weeks) the times of acquisition. Airborne TM simulator data may be used in lieu of actual TM or MSS data.

Airborne Data

Low-altitude (500 m from the ground) radar scatterometer ta (L-band HH) for several flight lines across the SIR-B age (crosstrack) will be acquired within one day of the bject SIR-B image data acquisition. (The C-130 radar scatter-neters acquire data at angles from 5 to 50 degrees from the dir). We will use radar scatterometer data at L-band HV and C-band (HH and HV) for comparison to the L-band HH data extend the results to other microwave bands and polariza-ons. Also, we will use images acquired with the JPL airborne -band synthetic-aperture radar (SAR) over the cropland sites om opposing directions with an azimuthal direction that is ie same as that of SIR-B. These data will allow us to extend ie analysis to VV and VH (or HV), that is, the complete set f standard linear polarization combinations with the HH olarization combination of SIR-B.

D. Ground-Truth Data

We will visit a sampling of fields in the cropland test sites to ather closeup photographs, to identify plants, to estimate reen-leaf area index, to collect biomass samples (for estima-ion of wet and dry biomass and of plant water content by arts), to estimate growth stages, to measure plant height, to uantify plant structure, to estimate small-scale surface rough-ess, to measure row spacing, row direction, row depth, and ow shape, and to estimate surface-soil moisture condition. We vill acquire these data during the time period of the experi-nent. We will visit a sampling of areas in the forest test sites to nake qualitative estimates of community mix and condition. Ve will acquire these data shortly after the time period of the Shuttle mission.

E. Data Handling

We will use standard optical and digital products from the spacecraft and airborne sensors. We will register the multiangle SIR-B, Landsat sensor, DTM, and ground-truth raster-scan image data sets by using the capabilities of the Image Processing Laboratory (IPL) at JPL. We will use supervised and unsupervised classification algorithms, contrast enhancement algorithms, color combinations, data extraction, and other facilities of the IPL. We will use Hsu's feature-extraction algorithms at his facility in New York. After data extraction, we will perform calculations of canopy attenuation and will analyze the correlation of raw and transfomed remotely sensed data averages (field and subarea).

IV. Expected Results

We expect to increase our understanding of the capabilities of L-band, single-polarization combination (HH), single-date (one-week), multiangle, optically and digitally processed radar image data with and without concurrent Landsat MSS or TM image data for vegetation discrimination, canopy penetration and condition assessment, and substrata condition assessment. We expect to increase our understanding of the role of surface roughness, row structure and direction, and sensor look angle in microwave remote sensing of vegetation. We expect to increase our understanding of the use of combined optical and radar data (including bands, polarizations, and angles different from those of SIR-B). We expect to be able to quantify the calibration accuracy of SIR-B processed image data. We expect to evaluate procedures to reduce radar image speckle (by areal averaging and use of texture-extraction algorithms) and to extract radar image texture for identification of vegetation.

Investigation of SIR-B Images for Lithologic Mapping

Team Member:

J. T. Parr
The Analytic Sciences Corporation
Reading, Massachusetts

Collaborator:

R. V. Sailor
The Analytic Sciences Corporation
Reading, Massachusetts

I. Description of the Investigation

Remote sensing has been recognized for some time for its potential in exploration geology, resource assessment, mapping, and land-use studies. Most applications of remotely sensed data have focused on multispectral imagery. This situation arose in large measure due to data availability. Synthetic-aperture radar (SAR) imagery was generally not accessible to most investigators; also significant were the difficulties many image analysts had in interpreting radar data.

It is immediately apparent from the examination of almost any SAR data that the radar return is primarily a function of the topographic relief. Yet radar reflectance is dependent on both surface roughness and the dielectric constant of the surface material. These two parameters can in many cases be related to lithologic units. Thus, if the first-order terrain effects due to topographic relief could (in essence) be removed from the radar image, the SAR data might well be used for lithologic discrimination. The objective of this investigation (Ref. 1) is to evaluate such an approach. The results will be compared with lithologic classification based upon multispectral (visible and infrared) data.

II. Overview of Investigation

Field geologists recognize that many lithologic units have characteristic differences in their basic texture and their response to erosional mechanisms. These differences are direct consequences of such factors as chemical and mineralogical composition, alteration or cementation, age, and stress history. The assumption behind this investigation is that such textural differences contribute to characteristic roughness properties at L-band wavelengths. Through compensation for local radar incidence angle, discrimination of lithologic units, according to variations in roughness, may be possible.

The SIR-B experiment with its multiple-incidence-angle capability makes investigation of the roughness properties possible. By using high-resolution digital terrain data, the local incidence angle for each radar pixel can be calculated. Areas of range ambiguity can be masked to avoid contamination of the data set. By geometrically registering the imagery from multiple SIR-B passes over the test site, multiple values of radar reflectance (each at a different incidence angle) will be obtained.

Landsat Thematic Mapper data along with ground truth will be used to define training cells that characterize the various

lithologic units in the area. By aggregating the radar data for these cells, curves of radar reflectance versus local incidence may be estimated. These curves, one for each lithologic material, will then be used to classify the test area. Classification will be performed using first the radar data only. The results will be compared with a similar classification based upon the Thematic Mapper data. Field investigation will be performed to evaluate the results of these classifications.

The test site for this investigation will be an area of approximately 400 km^2, probably in western Nevada. Actual site selection will be based upon considerations of radar geometry, geologic diversity, topography, and the availability of necessary support data.

III. Approach for Data Acquisition, Handling, and Analysis

Several data sets are required for this study. The SIR-B imagery will be supplied by JPL on computer-compatible tapes (CCTs). Seasat data for the test site will also be provided as available. In addition, JPL will supply Landsat Thematic Mapper and/or airborne multispectral scanner imagery (on CCTs) for the test site.

Most important to the effort is digital topographic data. Level 2 DLMS (Digital Land Mass System) data, having a spatial resolution of approximately 30 m, will be required. NASA will be coordinating the effort to ensure the availability of this information for all test sites. The Analytic Sciences Corporation (TASC) will be responsible for compiling ground truth from the published literature and other nonrestricted surveys.

The digital data will be processed using TASC's VAX-based Image Processing Laboratory (IPL). Available in the IPL is an extensive set of TASC software for interactive image processing, including a SAR simulation package (SARSIM™)* and utilities for image registration, radiometric correction, and image classification. All SIR-B data processing and associated analysis will be done on this system.

IV. Anticipated Results

It is expected that the investigation will demonstrate the extent to which multiple-incidence-angle SIR-B data can be used to discriminate lithologic units. Estimates of radar backscatter versus angle of incidence will be provided for the significant units in the evaluation area. The SIR-B data will be used to classify the lithologic units in the test site, and a comparison of these results with a similar classification using optical sensor data will be presented. Field activities will be oriented toward understanding both the success and failure modes for lithologic discrimination using SIR-B data.

*SARSIM is a trademark of The Analytic Sciences Corporation.

Reference

1. Parr, J. T., *Investigation of SIR-B Radar Images for Lithologic Mapping*, TP-4813 (as amended by TP-4813-1, 9 April 1984). The Analytic Sciences Corporation, Reading, Mass., March 1983.

N85-17242

Automatic Terrain Elevation Mapping and Registration

Team Member:

H. K. Ramapriyan
Goddard Space Flight Center
Greenbelt, Maryland

Collaborators:

C. W. Murray, J. P. Strong, and **H. W. Blodget**
Goddard Space Flight Center
Greenbelt, Maryland

I. Introduction

This research will deal with two primary objectives. They are:

(1) To determine optimum radar illumination geometries for stereoscopic analysis of surface topography.

(2) To construct correlation and image processing experiments on SAR data for improved information extraction.

Specifically, we propose to:

(1) Develop models of the geometry of the multiple SIR-B views of the Earth and establish the sensitivity of the derived terrain altitude data to the various system parameters.

(2) Derive the limits of accuracy of terrain data achievable with SIR-B.

(3) Develop algorithms for matching multiple SIR-B images to generate digital terrain maps.

(4) Demonstrate the use of such terrain maps in geometric correction and registration of SIR-B and Landsat Thematic Mapper data.

A survey by the United Nations (Ref. 1) indicates that the coverage of the world by existing topographic maps is not adequate to meet the demands. Further, it is not expected that conventional techniques of ground and aerial surveys will be able to keep up with the requirements. It has been shown that the Landsat Multispectral Scanner (MSS) images meet mapping accuracy standards at 1:250,000 scale (Ref. 2). Visual inspection of Landsat Thematic Mapper (TM) images indicates that they are at least comparable to 1:62,500 scale maps in terms of detail, which would make them very useful for quick satisfaction of the cartographic requirements of large portions of the world. At this scale, however, map accuracy standards equate to errors less than 0.5 pixel at 90% of the locations. A simple calculation indicates that if terrain altitude variations are not accounted for in the rectification of TM images, an altitude change of 1000 meters will result in an apparent displacement of about 5 pixels in the worst case (that is, at the

st and west edges of the image). Hence, it is evident that to ap regions with significant terrain variations accurately, it is sential to take altitude changes into account. With even gher resolution sensors being considered and requirements r better mapping accuracy, it becomes essential to account r altitude in the geometric correction of remotely sensed ata.

In addition, altitude data are essential for geological mapng and extrapolation of surface data provided by Landsat to the subsurface (Ref. 3). Also, the effect of altitude on the pes of vegetation that can grow at a given latitude are well nown and the inclusion of altitude as an additional data plane multispectral classification will result in more accurate estiates of land cover. The need for altitude and slope informaion in hydrological runoff modeling and sediment yield estination is quite obvious.

II. Description of the Experiment

The experiment involves the derivation of three major algorithms. In the first, equations for mapping two corresponding points in two stereo slant-range images into a single point in the x, y, z geodetic elevation map coordinates will be derived. The accuracy with which the coordinates can be obtained depends ultimately on the slant-range resolution accuracy of the radar sensor. Figure 1 illustrates the region of uncertainty in the ground range and the height due to the slant-range resolution accuracy of the sensor. (Graham's (Ref. 4) and Leberl's (Ref. 5) accuracy calculations are based on the model illustrated). One can see that for the large look angles illustrated (best suited for stereo analysis), the uncertainty in height is larger than the uncertainty in the ground range. Even this accuracy can be achieved only if all other parameters in the model are known precisely. As part of the experiment, ground-truth points in each image will be matched to estimate the parameters to as great an accuracy as can be statistically obtained. Curlander's work (Ref. 6) shows that, assuming a smooth Earth, points in a single SAR image can be located on the surface to an accuracy at least commensurate with the slant-range resolution using only the model parameters supplied from the spacecraft ephemeris and ground tracking data. We expect to perform the same experiment deriving elevation data based on a stereo geometric model.

The second algorithm will match corresponding points in two overlapping SIR-B images. The Massively Parallel Processor is capable of computing match functions for all points in the reference image simultaneously. Thus it is possible to use this machine to obtain height information for all points in the reference image rather than just on a coarse grid. For this purpose, we propose to employ the method used by Marr and Poggio (Ref. 7). With this method, we apply a coarse (narrow "pass-band") filter to the two stereo images. Then correlation is performed within a search area and over a window whose size corresponds to the filter function (such that it is unlikely for more than one match point to be within the search area). The relative locations of the resulting matched points are then used to locate the edges of hills and valleys in the SAR images such that corresponding areas where there is relative distortion between the two images can be located. Image data in these areas can then be "rubber-sheet stretched" (or compressed) prior to the next correlation step. The hierarchical approach used in the Marr-Poggio algorithm to obtain matches at higher and higher resolution will be evaluated.

The third algorithm deals with the errors and "no-match" points. It is expected that, due to inherent differences between the images, no algorithm will be able to perform the matching correctly at all points. For instance, it is obvious that, in SAR images, points in the areas that are shadowed in either of the two stereo images cannot be matched. However, one would like to detect points that are incorrectly matched and perhaps correct the match. One way to do this is to examine neighborhoods of points in the reference image and look for the matching distances calculated for those points which are out of line in some manner. The technique would be appropriate to elevation data since there should be no points that "float" much above or below all of their neighbors.

III. Expected Results

The overall results of this work will be the increased ability to combine or merge image data inputs from several separate sensors and to extend the present standard rectified spectral image data base down into the microwave spectral bands. A secondary result will be new algorithms for automatically establishing height information from stereo pair images. Specific results will be:

(1) An analysis of error accumulations in the location of points on the ground due to spacecraft, sensor, and orbit uncertainties. The resulting analysis will produce system models that will be useful in designing, in the future, more accurate SAR sensor systems that will be complementary to other multisensor imaging systems.

(2) Automatic techniques for matching corresponding points in stereo pair images.

(3) Automatic inclusion of height distortion effects in geometric correction of Landsat TM and future imaging sensors.

(4) Automatic means for merging height, radiance, and shadow information from SAR imagery with Landsat imagery, and the ability to incorporate this data into classification algorithms.

References

1. United Nations, "The Status of World Topographic Mapping," *World Cartography*, Vol. 14, 1976, pp. 3-70.

2. Welch, R., "Map Accuracy Requirements: The Cartographic Potential of Satellite Image Data," *Proceedings of the NASA Workshop on Registration and Rectification*, JPL Publication 82-23, Jet Propulsion Laboratory, Pasadena, Calif., June 1, 1982, pp. 215-223.

3. Goetz, A. F. H., "Stereosat: A Global Digital Stereo Imaging Mission," *International Archives of Photogrammetry*, 14th ISP Congress, Hamburg, W. Germany, July 13-25, 1980, pp. 563-570.

4. Graham, L., "Stereo Radar for Mapping and Interpretation," *JPL Radar Geology: An Assessment of the Radar Geology Workshop*, Snowmass, Colorado, July 16-20, 1979, pp. 336-350.

5. Leberl, F., "Accuracy Analysis of Stereo Side-Looking Radar," *Photogrammetric Engineering and Remote Sensing*, Vol. 45, No. 8, August 1979, pp. 1083-1096.

6. Curlander, J. C., "Geometric and Radiometric Distortion in SAR Imagery," *Proceedings of the NASA Workshop on Registration and Rectification*, JPL Publication 82-23, Jet Propulsion Laboratory, Pasadena, Calif., June 1, 1982, pp. 163-197.

7. Marr, D. And Poggio, T. "A Computational Theory of Human Stereo Vision," *Proceedings*, Royal Society of London, 1979, pp. 301-328.

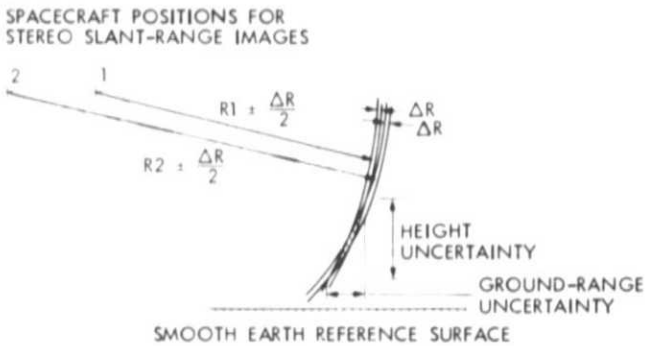

Fig. 1. Uncertainty in ground range and height due to limit in slant-range resolution

Australian Multiexperimental Assessment of SIR-B (AMAS)

Team Member:

J. A. Richards
University of New South Wales
Kensington, Australia

Collaborators:

B. C. Forster, A. K. Milne, G. R. Taylor, and **J. C. Trinder**
University of New South Wales
Kensington, Australia

I. Description

This investigation consists of five experiments that treat different aspects of the interpretation and application of synthetic-aperture radar data. It is to be conducted under the administration of the Centre for Remote Sensing at the University of New South Wales and will involve staff and facilities of the Centre and other Schools of the University. The experiments are described in the following.

A. Arid Zone Studies

This experiment will investigate the utility of SIR-B data for analysis of surface properties and subsurface morphology in three arid regions of Australia. The regions define three subprograms:

1. **Fowler's Gap**. This study area is located in western New South Wales (31°00'S, 142°00'E). It contains extensive aeolian and alluvially derived depositional plains and is the site of the University's Arid Zone Research Station; it is well-mapped and surveyed. The specific objectives of the experiment are

(1) To evaluate and map radar backscatter against known terrain conditions.

(2) To determine relative components of surface and subsurface return with a view to identifying structural properties of surface and subsurface morphology.

(3) To assess the capability of microwave remote sensing in locating likely groundwater sources in the Bancannia Basin, near Fowler's Gap.

2. **Pooncarie**. The region around Pooncarie (33°30'S, 142°40'E) contains a delicate ecosystem known as Mallee. It has been the site of environmental, ecological, and anthropological investigations (Refs. 1 and 2) with current programs of study directed to monitoring the rate and extent of clearing and associated soil erosion (Ref. 3). The experiment to be carried out in this region will examine the relationship between the structure and distribution of Mallee vegetation, surface roughness, and radar backscatter. This will demonstrate the potential of radar-derived information for mapping and monitoring land-cover changes in Australian arid environments.

3. **Amadeus Basin**. The Amadeus Basin is a petroleum exploration region to the west of Alice Springs in central

Australia (24°00'S, 132°30'E). In this subprogram the potential of radar data for mapping surface lithology and subsurface structure in the basin is to be evaluated. Of particular interest in this low-rainfall region will be whether significant penetration is possible as an aid in the identification of structural and stratigraphic traps of significance to petroleum exploration.

The study is likely to have value also in exploration for mineral commodities other than oil and gas.

B. Surface and Subsurface Microwave Properties

This experiment has two components related to empirical and modeled radar-scattering coefficients. One is concerned with arid-zone soils and soil/rock layered structures; the other is related to agriculture.

Because of likely L-band penetration in arid zones, it is anticipated that vertical moisture profiles will be determinants of radar backscatter. This will be addressed by measurement of soil moisture and complex permittivity profiles at Fowler's Gap, followed by a theoretical analysis of radar scattering from permittivity profiles. A similar study will be performed with layered structures in the Amadeus Basin.

The effect of tillage practices and crop canopies in so far as they induce periodic or quasi-periodic permittivity variations within a radar resolution cell are also to be examined in agricultural regions.

C. Topographic Mapping

This experiment will investigate the geometric accuracy of features derived from SIR-B data, and the detectability of features required for particular cartographic and thematic map scales in Australia. This will include a study of whether stereoscopic (multiple-angle) images can give improved plainimetric accuracy compared with single-incidence-angle data. Heighting and contour accuracy from multiple-incidence-angle imagery will also be assessed. (Refs. 4 and 5).

An essential aspect of the experiment will be rectification of SIR-B image data and registration of multiple-incidence-angle coverage. This will involve use of correction formulas and ground control points (Ref. 6). These will be used also to coregister radar and Landsat data, as required for experiments described in Sections D and E.

The sites for the study will be the city of Sydney (33°50'S, 151°00'E), for which accurate control is available, and the Fowler's Gap site in A.1 above. Fowler's Gap is well surveyed and has an adequate logistics infrastructure to support the placement of corner reflectors for accurate control. A third site near Mt. Kosciusko in New South Wales may also be used since near-orthogonal Shuttle paths are anticipated in that region. Together, these sites provide a range of terrain types to allow the mapping capabilities of SIR-B to be assessed.

D. Urban Monitoring

The urban environment consists of multifaceted and -oriented features of differing spatial frequencies. This experiment will investigate their effect on radar backscatter as a function of incidence angle, with a view to determining an optimum derived radar signal for merging with visible and infrared data in urban information extraction. It is expected that separation of urban land use classes (industrial, commercial, and residential) not currently possible with existing satellite spectral data will be improved by the analysis of merged data sets.

Sydney (33°50'S, 151°00'E) has been chosen as the site for the study since previous investigations have established a large number of residential training areas (Refs. 7 and 8) and control points (Ref. 9). Morphological and orientation data will be determined from air photographs and ground visits, and will include variables that measure street and building orientation, roof facet area and inclination, building size and density, surface material, and vegetation proximity. Multiple linear regression will be used to determine relationships between varying incidence-angle and look-angle responses and the various interpreted variables.

E. Information Extraction

This experiment will address three issues in agricultural classification from radar data. The first is concerned with crop discrimination in multiple-incidence-angle imagery. Fenner et al. (Ref. 10) and Ulaby et al. (Ref. 11) have noted that tillage practices lead to dependence of radar backscatter on incidence angle. It is expected that this dependence may contribute to crop discrimination. This will be tested for SIR-B data using clustering procedures and separability measures on wheat crops in the state of New South Wales.

The second aspect is concerned with the use of spatial context in the accurate classification of radar data. Common image classification techniques label pixels in isolation from their neighbours using spectral data alone. Context classification allows near neighbouring pixels to influence the labeling process by incorporating a spatial model of the region examined. This can reduce errors due to unknown factors such as topography and soil moisture. In the case of microwave data, confusion will also result from cultivation practices, canopy density, and speckle. It is anticipated, therefore, that acceptable classification accuracies in practice will demand context-sensitive algorithms such as label relaxation techniques used with Landsat image data (Ref. 12).

Label relaxation methods can also be used, in a modified form, to permit improved classification accuracy from combined data sources (Ref. 13). In the third part of this experiment, these techniques will be available for integrated radar and Landsat data.

A related aspect of this project is to interpret radar imagery of sugar cane fields in the State of Queensland. This will be carried out in association with the Bureau of Sugar Experiment Stations.

II. Data Acquisition, Handling, and Analysis

Field data will be gathered for each site to support the experiments described. In the case of Sydney, much exists already, and for Pooncarie, supporting SIR-A ground truth has been evaluated and is available. An L-band apparatus is being designed for on-site soil complex permittivity measurements capable of transmission or resonator operations. The New South Wales Department of Agriculture is a participant in the information extraction experiment and will undertake associated field checking of interpreted imagery.

SIR-B image data will be analyzed using a Dipix Aries II image-analysis system. Raw signal data is required for some aspects of the topographic mapping experiment and for the experiment dealing with scattering from complex permittivity profiles. This data will be correlated using commercially available SAR software installed on a VAX/array processor facility.

References

1. Mulvaney, D. J., and Golsen, J. (1971), *Aboriginal Man and Environment in Australia.* Australian National University Press, Canberra.

2. Graetz, R. D., Gentle, M. R. and O'Callaghan, J. F. (1981), "The Application of Landsat Image Data to Land Resource Assessment in the Arid Lands of Australia," *Bulletin of the Remote Sensing Association of Australia,* Vol. 4, pp. 5-26.

3. Chartres, C. J., Mabbutt, J. A., Johnson, D., Stanley, R. J., and Walker, P. J. (1982), *Land System Mapping as a Basis for Desertification Assessment and Mapping in N.S.W. Australia.* Report to FAO Rome, 3rd Expert Consultation on Desertification Assessment

4. Konecny, C., Schuhr, W., and Wu, J. (1982), "Investigation of the Interpretability of Images of Different Sensors and Platforms for Small Scale Mapping," *Proc. ISPRS Comm. I Symp., Canberra,* pp. 11-22.

5. Leberl, F. (1976), "Imaging Radar Applications to Mapping and Charting," *Photogrammetria* Vol. 32, pp. 75-100.

6. Trinder, J. C., and Smith, C. J. H. (1979), "Rectification of Landsat Digital Data," *Aust. J. Geod., Photog. & Surv.*, Vol. 30, pp. 15-30.

7. Forster, B. C. (1980a), "Urban Residential Ground Cover Using Landsat Digital Data," *Photog. Eng. & Rem. Sens.*, Vol. 46, pp. 547-558.

8. Forster, B. C. (1981), *Some Measures of Urban Residential Quality From Landsat Multispectral Data.* UNISURV S-18, University of New South Wales, Australia.

9. Forster, B. C. (1980b), "Urban Control for Landsat Data," *Photog. Eng. & Rem. Sens.* Vol. 46, pp. 530-545.

10. Fenner, R. G., Pels, G. F., and Reid, S. C. (1981), "A Parametric Study of Tillage Effects on Radar Backscatter," *Proc. IEEE IGARSS '81,* pp. 1294-1308.

11. Ulaby, F. T., Kouyate, F., and Fung, A. K. (1981), "A Backscatter Model for a Randomly Perturbed Periodic Surface," *Proc. IEEE IGARSS '81,* pp. 638-647.

12. Richards, J. A., Landgrebe, D. A., and Swain, P. H. (1981), "On the Accuracy of Pixel Relaxation Labelling," *IEEE Trans. Systems Man & Cyber. SMC-11,* pp. 303-309.

13. Richards, J. A., Landgrebe, D. A., and Swain, P. H. (1982), "A Means for Utilizing Ancillary Information in Multispectral Classification," *Rem. Sens. Envirn.*, Vol. 12, pp. 463-477.

Application and Calibration of the Subsurface Mapping Capability of SIR-B in Desert Regions

Team Member:

G. G. Schaber
U.S. Geological Survey
Flagstaff, Arizona

Collaborators:

J. F. McCauley, C. S. Breed, and **M. J. Grolier**
U.S. Geological Survey
Flagstaff, Arizona

B. Issawi
Egyptian Geological Survey and Mining Authority
Cairo, Egypt

C. V. Haynes
University of Arizona
Tucson, Arizona

W. McHugh
GAI Consultants
Monroeville, Pennsylvania

A. S. Walker
U.S. Geological Survey
Reston, Virginia

R. Blom
Jet Propulsion Laboratory
Pasadena, California

I. Introduction

The overall objective of this investigation is to fully exploit, principally by means of expanded coverage, the penetration capability of the SIR-B sensor in desert regions and to devise refined models to explain this penetration capability in terms of radar physics and regional geologic conditions. Specific objectives will be to: (1) image a far larger area of the Western Desert than the single swath obtained by SIR-A in order to better define the sand-buried "radar-rivers" discovered and first described by this Investigator Team following SIR-A, and to determine their sizes, extent, sources, ages, and rela-

tions to present drainage systems of the Sahara; (2) extrapolate results and procedures developed during our SIR-A investigations and in (1) above to test the application of SIR sensor capability for geologic research in other desert regions where major sand-buried drainages are suspected to exist, and where these investigators have relevant ground and literature expertise; (3) determine, as precisely as possible, the boundary conditions and evaluate the various parameters of the SIR signal penetration phenomena; this will include the development of empirical signal-penetration algorithms for sand-mantled hyperarid-to-semiarid terrains.

As reported in Ref. 1, SIR-A images of the Western Desert in Egypt and Sudan show buried fluvial topography, faults, and intrusive bodies that are otherwise largely concealed beneath unconsolidated sand sheets, dunes, and alluvial deposits. The various tones on the radar images result from absorption or penetration of the radar signals in dry, relatively fine-grained surficial sediments, and specular reflection or backscatter from surface or subsurface interfaces. Relict river valleys containing deep alluvium appear as dark, dendritic networks bounded by bright zones that are interpreted as low (sand-mantled) bedrock divides (Fig. 1). Field investigations of sites where the sand-mantled bedrock appears bright on the radar images confirm signal penetration through at least 1.0 m of fine sandy alluvium and through as much as 3 m of dry, loose sand sheets and dunes. Theoretical estimates of signal penetration, based on laboratory measurements of electrical properties of the sediments, are as much as 5 m.

Conditions in regions of the Eastern Sahara are ideal for pictorial representation of the now obscured shallow subsurface. The sand plains are typically flat, smooth, and unvegetated. Rainfall is practically unknown in the Western Desert, which lies in the core of the largest hyperarid region on Earth. Thus soil moisture, which largely controls the electrical properties and thus the "effective penetration" depth of SIR radar signals, is essentially absent, resulting in very low loss of signal in the surficial sediments. The signal is actually enhanced as it is refracted through this nearly transparent surface medium, reaching the reflecting substrate at a higher angle of incidence (Ref. 2).

The proposed work is directly applicable to the objectives of NASA's Non-Renewable Resources Program: to use space methods for the exploration, assessment, development, and management of mineral and energy resources, and to use space methods to assess the hydrologic environment through analysis of drainage basins, recharge areas, aquifers, and groundwater flow. Although all of the work proposed is outside the United States, it has a direct bearing on U.S. interests abroad, particularly the ongoing USAID Mineral, Petroleum and Groundwater Assessment Program (MPGAP Project 263-0105) in Egypt and the cooperative work already done between the USGS, JPL, and the Egyptian Geological Survey and Mining Authority (EGSMA). By using the Western Desert as the end member in the global aridity sequence, we hope to develop a new reference framework for studies of the American Southwest.

II. Description of the Experiment

This SIR-B investigation will consist of three closely related tasks. *Task 1*: Use SIR-B mapping mode image data to visually depict and map the old master streams and other geologic features in the Western Desert and surrounding areas of the Eastern Sahara. The SIR-based maps will show the sources and directions of former stream flow, the extent of tributary networks, stream-capture patterns, and the locations of regional divides between the drainage basins. Interpret the subjacent geologic information shown on these maps, in concert with existing geologic and geophysical data, to assess possible groundwater and placer mining resources associated with subjacent stream valley alluvial fills. A secondary objective within Task 1 will be to investigate possible ancient fluvial interconnections between the major depressions or "mega-oases" in the Western Desert, including Kharga, Farafra, Bahariya, Qattara, and Siwa. *Task 2*: Use SIR-B mapping-mode and multiple-incidence-angle-mode image data to test and model subsurface mapping capabilities in other foreign desert regions where sand-buried drainage systems are known to exist and where the USGS Desert Studies Group has extensive ground and/or literature experience coordinated with Landsat studies. Through this task we hope to provide a spectrum of documented penetration locales for areas that differ from the Western Desert in degree of dryness – annually, seasonally, and diurnally. Specific areas of limited extent in Peru, the Northern Sahara, India, southern Africa, China, and Australia are included in Task 2. *Task 3*: Use SIR-B multiple-incidence-angle-mode data to continue the development of empirical radar-backscatter and -signal penetration algorithms for hyperarid-to-arid terrains initiated following SIR-A (Ref. 2).

III. Approach for Data Acquisition, Handling, and Analysis

Only one tantalizing pass of SIR-A image data was obtained across the hyperarid Western Desert in Egypt and Sudan, thus leaving us with a glimpse of major subsurface river valleys and a variety of buried geologic structures, but with no way to extrapolate these to the Eastern Sahara as a whole. Inspection of SIR-A images of other deserts suggests that signal penetration occurred in at least two other arid regions, e.g., parts of the An Nafud, Saudi Arabia, and part of the Alashan Plain,

northwest China (Ref. 3), but proof of the penetration capability of the SIR sensor, on a global scale, will require more data from SIR-B.

Our basic approach will be to use SIR-B images (in concert with field observations, electrical properties measurements, Landsat MSS, and new data requested from the Landsat Thematic Mapper and the Large Format Camera (LFC)) as a new reconnaissance tool to interpret the subjacent geology of arid regions where the bedrock and topographic framework are hidden by a veneer of dry, windblown sand, and where resource exploration otherwise requires the use of expensive geophysical tools and exploratory drilling.

A. Task 1: Investigation of the Paleodrainage, Subsurface Structure, Geoarcheology, and Mineral Potential of the Eastern Sahara, North Africa

Prior to SIR-B, the team will participate in a U.S. Agency for International Development (USAID)-funded joint USGS and EGSMA expedition to the Egypt-Sudan border and Safsaf Oasis regions in March 1984. The purpose will be to explore a number of key "radar-river" localities by means of deep trenches cut by a backhoe. Traverses will be made across and along the banks and channels of the buried rivers. The trench sections will be mapped in detail and studied for their fossil, archeological, and heavy mineral content. Samples will be collected for laboratory analysis of the electromagnetic properties at varying depths. Navigation to and positioning of the trenches will be accomplished by use of newly prepared Landsat and radar images coregistered to the 1:500,000 scale AMS Series 1501 maps. In addition, we will use a Magnavox MX4102 Satellite Navigator (first used during the March 1983 expedition) to determine the latitude and longitude, to within 100 meters, of each trench. The expedition in March 1983 represented the beginning of systematic work on the radar rivers by EGSMA, in cooperation with the USGS. From data collected on the 1984 expedition we will locate seismic profile lines and positions for an array of deep-core holes to be drilled in the thalwegs of the channels to determine their depth, groundwater, and mineral potential. The above work will essentially complete the field exploration phase of the USGS work on the limited area imaged by SIR-B.

Extensive image coverage of the Eastern Sahara has been requested with the LFC during the STS-14 flight, and photographs obtained by the Metric Camera experiment on STS-9 (Spacelab) in 1983 have been requested.

Well log data from some 1412 wells drilled by the Government of Egypt (GOE) and foreign groups are now being compiled by the Egyptian General Petroleum Company (Ref. 4, pp. 44–50) and will be acquired, along with airborne geophysical data, including the existing aeromagnetic and seismic surveys and the new surveys currently underway in the Western Desert. Existing water wells will be sampled for C_{14} dating to determine if groundwater is ancient or currently being replenished. The above data sets will be standardized for coregistration on maps of the paleodrainage, which will be based on the SIR-A and SIR-B data extrapolated to adjacent areas on Landsat images.

B. Task 2: Global Test of SIR Subsurface Mapping Capability in Sample Hyperarid-to-Semiarid Desert Areas

Analysis of selected desert areas for the SIR-A Team Report (Breed and others in Ref. 5) indicates some degree of penetration by the SIR sensor in desert regions less arid than southwest Egypt and northwest Sudan. For Task 2, a global sample of deserts has been selected specifically to test the ability of the SIR sensor to detect and map subsurface features through sand sheets and minor dunes in other foreign regions; each has different conditions of aridity but, like the Western Desert, a shallow sand cover that obscures the subjacent geology. SIR-B mapping mode coverage has been requested for each test area, and multiple-incidence-mode coverage for a few selected sites. Apparent imaging of subjacent features will be assessed by comparison of geologic features revealed on the SIR-B images with the visibility of these features on specially processed Landsat images, and on ground and aerial photographs. Apparent penetration will be compared with the theoretical penetration depths at given localities, as calculated from laboratory tests of the surficial materials already collected from most of these areas in the course of related field studies, and from climatological data. In preparation for SIR-B, samples from several test sites are being analyzed for grain size and composition, and the appropriate Landsat and photographic data are being assembled.

C. Task 3: Development of Radar Backscatter and Penetration Algorithms for Hyperarid-to-Arid Sand-Covered Terrains

Given the SIR-B availability of digitally processed images at selectable incidence angles, "it will now be possible to enter an entirely new era of radar image analysis in which quantitative methods and mathematical models of backscatter will provide a powerful enhancement to the traditional photointerpretative methods" (Ref. 6). Task 3 directly addresses this objective by determining, as precisely as possible, the boundary conditions for spaceborne radar subsurface imaging in hyperarid areas as a function of moisture content, grain size, sand depth, and incidence angle. The Western Desert is selected as the major test area for this task because in this region as many variables as possible (such as vegetation) can be eliminated.

Work prior to the SIR-B mission involves grain-size, moisture, and electrical properties measurements on samples in hand, continued field and theoretical SIR signal penetration studies of the Western Desert materials based on SIR-A results, field sampling of test sites that will undergo multiple-incidence-angle imaging during SIR-B, and the integration into Task 3 of Landsat and Large Format Camera image data as they become available. During expeditions into the Western Desert in September 1982 and March 1983, samples of the sand sheet, drift sand, dunes, and sandy alluvium beneath the sand sheet were collected in moisture-tight plastic bottles for laboratory measurement of electrical properties, including the real (e_r) and imaginary (e_j) component of the dielectric constant. From these measurements, calculations of the loss tangent (e_j/e_r), effective penetration depth, or "skin depth," and attenuation (dB/m) can be calculated. As part of Task 3, we will pursue the use of a portable radar instrument for direct measurement of near-surface electrical properties simultaneously with direct recording of the depth to a shallow subsurface interface.

Following the discovery of significant penetration by the SIR-A signals in the Western Desert, Elachi, Roth, and Schaber (Ref. 2) showed theoretically that, under hyperarid conditions, a low-signal-loss sand layer can actually enhance the capability to image the subsurface due to refraction of the signal at the air-sand interface. The refraction, they found, results in a smaller effective incidence angle and a stronger backscatter, which can compensate for losses due to absorption of the signal in the dry sand layer and its reflection at the air-sand interface. This initial theoretical study into SIR signal penetration in hyperarid sand-covered terrains also showed that the enhancement effect, described above, is most pronounced with the H-H polarization (that of SIR-A and SIR-B) and at large incidence angles. Task 3 will further investigate this enhancement effect and attempt to verify it empirically for application to the design of future SIR experiments.

IV. Expected Results

Results of field expeditions into the Western Desert during September 1982, March 1983, and March 1984, supported by NASA (Non-Renewable Resources Branch) and USAID-Cairo, will be submitted for publication in the open literature prior to launch of SIR-B and should provide a useful baseline for the interpretation of these new data. Major contractual products will include interim and final contributions to the SIR-B Team reports in addition to formal publications of final results in the open literature.

References

1. McCauley, J. F., Schaber, G. G., Breed, C. S., Grolier, M. J., Haynes, C. V., Issawi, B., Elachi, C., and Blom, R., 1982, "Subsurface Valleys and Geoarchaeology of the Eastern Sahara Revealed by Shuttle Radar," *Science*, Vol. 218, No. 4576, pp. 1004-1020.

2. Elachi, C., Roth, L., and Schaber, G. G., 1984, "Radar Subsurface Imaging in Hyperarid Regions," *IEEE Antennas and Propagation*.

3. Breed, C. S., McCauley, J. F., Schaber, G. G., Walker, A. S., and Berlin, G. L., 1982, "Dunes on SIR-A Images," in *Shuttle Imaging Radar-A (SIR-A) Experiment*, JPL Publication 82-77, Jet Propulsion Laboratory, Pasadena, Calif., J. B. Cimino and C. Elachi, editors.

4. McCauley, J. F., and Stancioff, A., 1982, *Review of Current Status of Egypt: Project 263-0105, Mineral Petroleum and Groundwater Assessment*, U.S. Agency for International Development, Washington, D.C. 90 pp.

5. Cimino, J. B., and Elachi, C., 1982, *Shuttle Imaging Radar-A (SIR-A) Experiment*. JPL Publication 82-77, Jet Propulsion Laboratory, Pasadena, Calif.

6. Imaging Radar Science Working Group, 1982, *The SIR-B Science Plan*. JPL Publication 82-78, Jet Propulsion Laboratory, Pasadena, Calif.

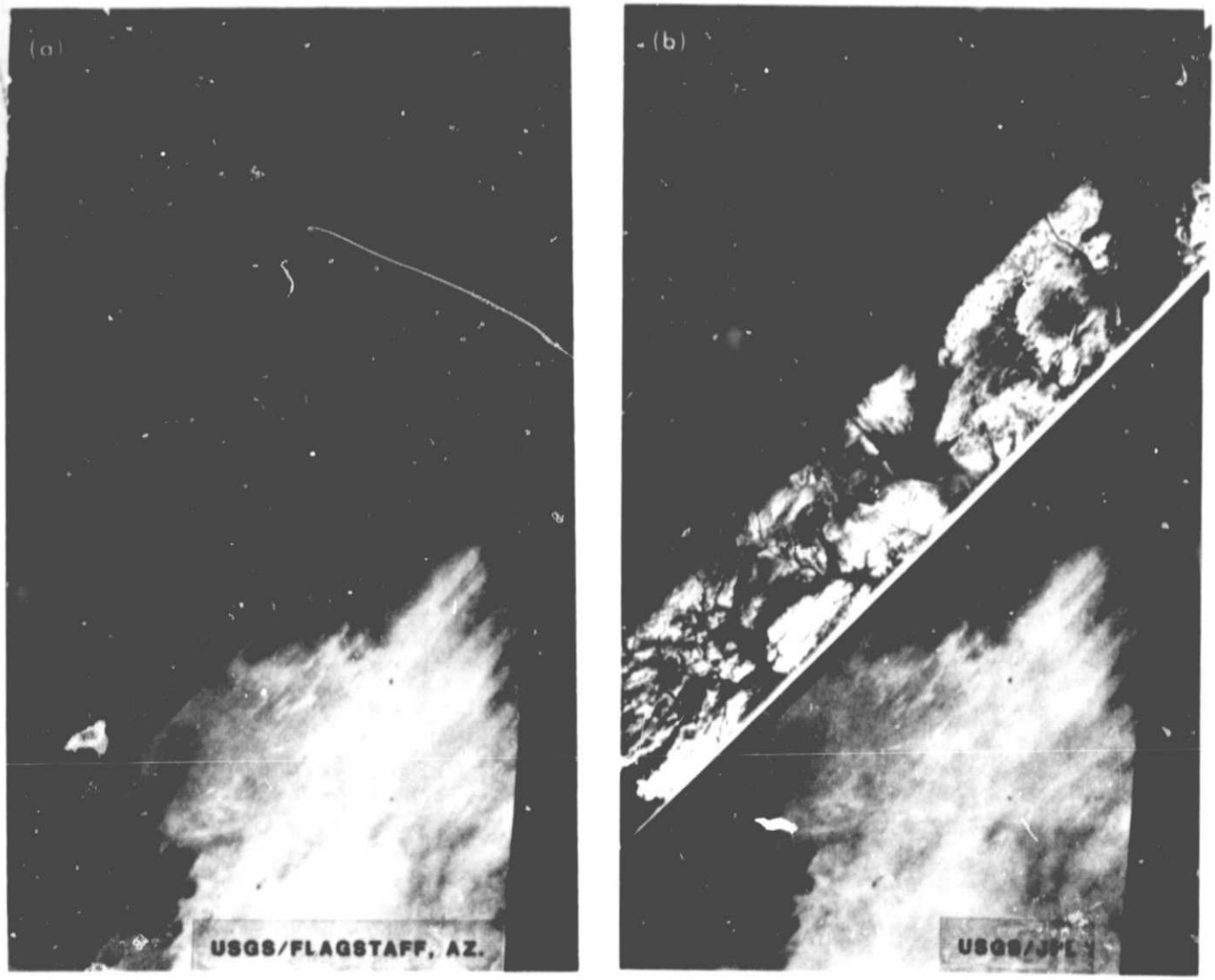

Fig. 1. Images of hyperarid regions of the Libyan Desert. (a) Two-frame Landsat mosaic of region in northwest Sudan and southeast Libya between latitudes 18 degrees 30 minutes to 21 degrees N, and longitudes 24 degrees to 26 degrees 30 minutes E. Black lines outline the swath (50 km wide) of SIR-A data take 28, Rev. 27 shown on Fig. 1b. Most of the region is mantled by the sand sheets (centimeters to meters thick) and isolated dune trains, with local outcroppings of sedimentary rocks visible on the upper Landsat frame. (b) Same two-frame Landsat Mosaic as in Fig. 1a with SIR-A image superposed. Lighter areas on the SIR-A image represent mostly subsurface electrical interfaces (primarily roughness and caliche-cementation of sediment beneath the loose sand cover). Buried stream valleys, obscured on Landsat but revealed by dark patterns on the SIR-A image, are filled with many meters of sand and alluvium that contain no significant subsurface radar interfaces to backscatter the signal. The larger valleys are thought to be Middle Tertiary in age and the smaller dendritic channels to be of Pleistocene Age. The buried (22-km-wide) "radar-river" valley on the northeast edge of the SIR-A strip is as wide as the Nile Valley but was not recognized prior to the SIR-A mission.

N85-17245

German Radar Observation Shuttle Experiment (ROSE)

Team Member:

A. J. Sieber
Deutsche Forschungs- und Versuchsanstalt fur Luft- und Raumfahrt
Federal Republic of Germany

Collaborators:

Ph. Hartl
University of Stuttgart
Federal Republic of Germany

R. Haydn
University of Munich
Federal Republic of Germany

G. Hildebrandt
University of Freiburg
Federal Republic of Germany

G. Konecny
University of Hannover
Federal Republic of Germany

R. Mühlfeld
Federal Institute for Geoscience and Natural Resources
Federal Republic of Germany

This proposal includes several different application areas and Earth sciences. The success of radar sensors in these areas of interest depends on the knowledge of the backscatter of radar waves from the targets of interest, the variance of these interaction mechanisms with respect to changing measurement parameters, and the determination of the influence of the measuring systems on the results. Supplementing the use-oriented parts of this proposal, the following methodological experiments are anticipated:

(1) The derivation of the incidence-angle dependency of the radar cross section of different natural targets.

(2) The analysis of problems involved by the combination of data gained with different sensors, e.g., MSS-, TM-, SPOT- and SAR-images; this analysis will be done with reference to differences in spatial resolution and observation geometry (nadir-looking via side-looking).

(3) The determination of the correlation of radar cross-section values gained with ground-based radar spectrometers and spaceborne radar imaging, and non-imaging scatterometers and spaceborne radar images from the same areal target; this work package also includes the analysis of the speckle texture gained with

the different sensors for the potential derivation of target signatures.

(4) The development of new approaches of SAR-image processing algorithms.

(5) The calibration of the SIR-B data.

(6) The analysis of the penetration of L-band radar waves into vegetated and nonvegetated surfaces.

The experiments will be undertaken at three different test sites: Freiburg and Cologne in the Federal Republic of Germany, and Botswana.

The Freiburg test site is the prime area for the calibration and land-use inventory.

As regards calibration, the following activities are foreseen:

(1) Application of "active radar calibrators." The objective is to calibrate the SIR-B Radar for point targets with an accuracy of 1 dB.

(2) Measurement of significant extended targets (fields) in the area of Freiburg by means of L- and X-band scatterometers to study the sigma-naught development as a function of the season for various crop types.

(3) Study of the interrelation between extended-target and point-target response of SIR-B by comparison between the SIR-B signal values received from the ARCs and from the fields studied with the scatterometers.

(4) Use of corner reflectors for geometric corrections and as markers to identify the test site dimensions.

(5) Antenna pattern measurement by use of a set of calibrated receivers.

(6) Penetration measurements of SIR-B signals in bare soil, forests, and corn fields by use of the calibrated receivers.

As regards agriculture and land use, the following activities are foreseen:

(1) Comparative study between the CV-580 aircraft SAR results for the Freiburg test site and the SIR-B data.

(2) Extension of the Freiburg digital terrain data base to 100×100 km^2.

(3) Realization of radar simulation for the Freiburg test site and improving the data base catalog and the simulation model by comparison between the simulated and the actual radar data.

Freiburg has been used for many remote sensing experiments for many years. Therefore, it is a well-known reference for the SIR-B experiment. Cologne has been selected as the test site mainly for:

(1) The production of topographic maps in the scale of 1:200,000.

(2) Multisensor comparison (this site is the only area that has been imaged by Seasat).

(3) Geometrical rectification and correlation with data from other sensors.

The experiment at Botswana is intended to evaluate the information content of L-band SAR data for hydrogeological problems. It is intended to study the groundwater balance in the foreland of the intracontinental Okawango delta in northern Botswana.

The determination of the quantity of groundwater flow, which is of economic interest for this country, could be approached in two different ways:

(1) By the detection and delineation of higher permeable zones in the Kalahari beds; these zones are expected at the only surface outflow, the Chobe river, which flows toward the Sambesi.

(2) By the discrimination and delineation of clay and salt in the depression (base levels) whereby the evaporation area could be determined directly and the quantity of evaporated water indirectly. In Landsat imagery, clay flats and salt flats could not be separated. Concerning the application of L-band SAR, it is expected to differ between the following Quaternary deposits because of surface roughness and different vegetation: clay, salt, sand, and calcrete. Furthermore, it is hoped to discriminate and to delineate soil of higher moisture content with characteristic vegetation, which may indicate shallow fresh groundwater. The differentation between salty and salt-free soils in the depressions will lead to the delineation of fresh and mineralized groundwater. Finally, the discovery of old river courses and valley fills of coarse material below uniform layers of fine sand are expected. The anticipated results are:

   (a) Improvement of methods in remote sensing for discrimination and delineation of unconsolidated Quaternary deposits under semiarid conditions.

   (b) The possibility of detecting material of higher permeability (coarse-grained sediments) below a relatively thin and uniform sand cover.

   (c) The improvement of the overall water budget of the Okawango delta, which is of vital importance for the economy, the natural environment, and the preservation of wildlife of Botswana.

The Extension of an Invertible Coniferous Forest Canopy Reflectance Model Using SIR-B and Landsat Data

Team Member:

D. S. Simonett

University of California
Santa Barbara, California

Collaborator:

A. H. Strahler

City University of New York
New York, New York

I. Investigation and Technical Plan

In this proposal we wish to extend an invertible coniferous canopy reflectance model, developed by Strahler and Li (Ref. 1). The extension will involve the joint use of SIR-B multilook angle data, the multispectral scanner (MSS), and the thematic mapper (TM) on Landsat. In the event that near-contemporaneous Landsat data is not available to go with the SIR-B data, the most recent existing Landsat data will be used, because of the very slowly changing nature of the forest canopy in mature coniferous forests.

Work on visible and near-infrared forest canopy modeling is continuing by both Strahler and Li. The team member's role in this proposed project represents a continuation and extension of his interest in mapping natural vegetation using radar imagery, including coniferous forests in the United States (Refs. 2 through 11). In addition, the team member has worked extensively with radar imagery in project RADAM in Brazil, in Nigeria, in northern Australia and New Guinea, and Venezuela, mostly in broad vegetation-community mapping and geomorphological mapping.

The extension and modification of the model into the L-band radar region will, at least initially, treat the coniferous tree trunks as dielectric cylinders, surrounded by cones of thinly dispersed water droplets, the latter in part following the treatment by Fung and Ulaby (Ref. 12) of water in crop canopies in the radar region as a dispersed system of water droplets equal in depth to the crop height. It is anticipated that there will be some difficulties with these models with respect to invertibility. In particular in open canopies it may be necessary to try several sizes of aggregation of pixel elements, because the long wavelength and Rayleigh distribution of the radar signal will give rise to high radar-signal variance, which may confound the inversion process or at least degrade the potential accuracy of the inversion. The necessary theoretical calculations will be carried out with respect to reasonable assumptions of differential scattering and penetration as a function of radar wavelength, covering the radar region from 1 cm to 23 cm, in order to place the L-band radar in the appropriate context in this range. Detailed fieldwork at the time of passage of SIR-B, and detailed photo interpretation, will be carried out and tests will be made with subsamples of the field data to calibrate the model and verify accuracy.

Same-side stereoscopy achievable with multiangle radar images in addition to aiding geologic, geomorphic, and drainage-network analyses, is of considerable aid in vegetation mapping. Any subtle textures in forest communities that are indistinguishable when viewed monoscopically become detectable with stereoscopy. Those with experience in mapping vegetation with radar recognize that textural variations are of more than equal rank with tone as a discriminant. However, in heavily treed areas, dissimilar plant communities (associations) frequently appear similar on radar, primarily because they are similar structurally. It appears that some previously indistinguishable communities may be separable with stereoscopy, and that variations in stand density may also be observed better with stereoscopy.

Overall there are issues of look angle, resolution cell size, and possibly wavelength that need to be explored in attempting to develop an invertible model using a 23-cm radar system. These considerations will be included in the experimental design.

II. Approach

As noted above, the model developed by Strahler and Li (Ref. 1) will need to be modified substantially with respect to its assumptions in order to accommodate the long wavelength radar, to make use of radar multiple look angles, and to incorporate both TM and radar. The necessary theoretical work for this development will occupy much of the first year of the study, with appropriate computer simulation using modifications of the existing software.

To test the model on real data, we have chosen the Dock Well area in the Goose Nest Ranger District of Klamath National Forest in northern California, used already by Strahler and Li. Color aerial photographs at 1:16840 scale are already available. We have selected three stands ranging from very sparse to moderately stocked ponderosa pine, in the gently sloping portions of the forest, in order to avoid problems associated with terrain irregularities in both the radar and, to a lesser extent, the optical sensors. In previous work in this area we have relied on photo interpretation for calibration, estimating heights and densities of the stands from the air photos, and using the measurements both to calibrate the model and, in lieu of field data, to serve as controls for evaluating the operation of the model. For this proposal, we will field sample to provide an accurate base of ground measurements of tree height and spacing to compare model results with reality. Determinations of tree height and spacing from air photographs are subject to error and bias. Ground and air photo measurements are needed at sufficiently high precision to facilitate accurate calibration.

Ground photographs will be taken along with enough observations on tree height, spacing, ground slope angle and aspect, so that any errors and biases from the photo interpretation will be established. Corrections for both bias and variance in the data will be employed thereafter with the air-photo interpretation data.

For the relatively small area involved in this study, we will take care with aerial photographs to bring all three sensors (MSS, Thematic Mapper, SIR-B) into high spatial congruence. River junctions, river bends, and ridge tops where shadows begin in the radar are likely sites for mutual registration.

The multiday variable look-angle radar images will be used to prepare a grid of spatial resolution elements to place over the stereoscopic aerial photographs. The variance in spatial densities within the three primary conifer stocking densities will be assessed so that the consequences of spatial misregistration, or mislocation of resolution element sites, can be determined. Since the radar signal is sampled from a Rayleigh distribution, it will naturally have high variance within a single broad class. This variance will be superimposed on the variance attributable to differential stocking density of conifers and to misregistration, and will degrade, to some unknown degree, the ability to invert the model and achieve high accuracies of stand-density estimation. Amongst other procedures to investigate, we will look at multilook angle and signal averaging over larger resolution cells – for single images – to see whether this intrinsic high variance in the radar signal can be reduced enough so that the intrinsic scene variance rather than the noisy radar-signal variance is the dominant element in the return.

We will resample the radar, Thematic Mapper, and MSS data so that we develop two sets of spatially registered data initially at 30-m and 80-m resolution. Further stepped degradations in resolution will be assessed by weighted pixel averaging. These variable-resolution, registered image sets will be coregistered with areal counts of coniferous trees, unshadowed and partially shaded by adjacent conifers, for each radar look angle and direction, and for the actual solar-illumination direction and angles at the time of Landsat passage. This will constitute the basic data set for analysis of look angle, image texture, and inversion processes.

The implementation of this approach in a fiscal-year context is given below:

(1) FY 1984: this period will cover field work at the time of passage of SIR-B.

(2) FY 1985: this period will be devoted to:

   (a) Theoretical development of radar modeling.

(b) Preparation of corrections to air-photo interpretation using such parameters as ground observations of tree height and spacing.

(c) Modification of existing forest-canopy modeling software to accommodate TM bands and radar multilook images.

(d) Simulation runs using Monte Carlo simulations to test the sensitivity of the revised model to the new kinds of errors with radar inputs.

(e) Development of spatially registered data sets resampled to 30 m and 80 m; these sets will be capable of weighted aggregation in integral steps of 30 m and of random number selection of 100-pixel samples within each of the three selected density classes of the ponderosa pine forest:

(i) MSS.

(ii) TM.

(iii) SIR-B, multilook angle.

(iv) Topographic data.

(3) FY 1986: this period will be devoted to:

(a) Calibration of model with further sensitivity analysis.

(b) Testing of model against Dock Well area data and ground observations.

(c) Overall assessment of project results with respect to sensitivity of L-band radar to differential height and spacing of conifers, to look-angle effects, to misregistration, to its incremental value in a multispectral system, and to the invertibility of L-band radar-based, or L-band radar-augmented, models.

(d) Preparation of final report and papers for publication.

References

1. Strahler, A. H., and Li, X. W., 1981. "An Invertible Coniferous Forest Canopy Reflectance Model," in *Fifteenth International Symposium on Remote Sensing of the Environment*, Ann Arbor, Michigan, May, pp. 1-8.

2. Morain, S. A., and Simonett, D. S., 1966. "Vegetation Analysis with Radar Imagery," in *Proceedings of the 4th Symposium on Remote Sensing of Environment*, University of Michigan, Ann Arbor, pp. 605-622.

3. Morain, S. A., and Simonett, D. S., 1967. "K-Band Radar in Vegetation Mapping," *Photogrammetric Engineering*, 33:730-740.

4. Simonett, D. S., 1966. "Applications of Color-Combined Multiple Polarization Radar Images to Geoscience Problems," in *Computer Applications in the Earth Sciences: A Colloquium on Classificational Procedures*, (D. F. Meriam, ed.) Computer Contribution #7, State Geological Survey of Kansas, pp. 19-23.

5. Simonett, D. S., 1968. "Potential of Radar Remote Sensors as Tools in Reconnaissance Geomorphic, Vegetation and Soil Mapping," *Transactions*, 9th International Congress of Soil Science, IV:271-280.

6. Simonett, D. S., 1976a (Ed.), *Applications Review for a Space Program Imaging Radar*, Santa Barbara Remote Sensing Unit, SBRSU Technical Report 1, University of California, Santa Barbara, pp. 1-231.

7. Simonett, D. S., (Ed.), 1978. *Active Microwave Applications Research and Development Plan*. Santa Barbara Remote Sensing Unit, SBRSU Technical Report 2, University of California, Santa Barbara, January, 1978.

8. Moore, R. K., and Simonett, D. S., 1967. "Radar Remote Sensing in Biology," *BioScience*, 16:384-390.

9. Simonett, D. S., and Morain, S. A., 1967. "Remote Sensing from Spacecraft as a Tool for Investigating Arctic Environments," in *Arctic and Alpine Environments*, (J. E. Wright, Jr., and W. H. Osburn, eds.), pp. 295-306, Indiana University Press.

10. Peterson, R. M., Cochrane, G. R., Morain, S. A., and Simonett, D. S., 1969. "A Multi-Sensor Study of Plant Community Densities and Boundaries at Horsefly Mountain, Oregon," in *Remote Sensing in Biology* (Ed. P. L. Johnson), University of Georgia Press, pp. 63-94.

11. Simonett, D. S., and Davis., R. Interpretation of Microwave Remote Sensing Imagery. Chapter 25, *Manual of Remote Sensing*, Second Edition. To be published 1983.

12. Fung, A. K., and Ulaby, F. T., 1978. "A Scatter Model for Leafy Vegetation," in *Proceedings of AGARD Conference Aspects of Effective Scattering in Radio Communications*, Cambridge, MA. Oct. 1977.

N85-17247

An Investigation of Ionospheric Irregularity Effects on SIR-B Image Processing and Information Extraction

Team Member:

E. P. Szuszczewicz
Naval Research Laboratory
Washington, D.C

Collaborators:

M. A. Abdu and **J. H. A. Sobral**
Instituto de Pesquisas Espaciais
São Paulo, Brazil

J. Jost
Johnson Space Center
Houston, Texas

B. M. Reddy
National Physical Laboratory
New Delhi, India

C. Rino
Stanford Research institute
Menlo Park, California

T. Robinson
University of Leicester
Leicester, United Kingdom

P. Rodriguez
Naval Research Laboratory
Washington, D.C

M. Singh
Sachs/Freeman Associates, Inc
Bowie, Maryland

R. Woodman
Instituto Geofisico del Peru
Lima, Peru

I. Objective

The object of this investigation is to conduct extensive correlative studies into ionospheric irregularities and associated effects on space-time SAR image processing and information extraction, including sensor calibration, target statistics determination, resolution, distortion, and overall image integrity.

II. Experiment Concept, Plans, and Products

The processing of SAR images assumes that the phase and amplitude of the radar is known or can be modeled throughout the end-to-end system so that the required coherency of the SAR radiation can be preserved in the image-processing procedure. It is known that certain ionospheric domains can introduce substantial phase fluctuations in the SAR satellite-

to-target channel with frequency components comparable to and higher than $1/T$, where T is the integration time for the synthetic aperture. It is also known that uncompensated phase errors will cause the synthetic pattern to exhibit a fluctuating main lobe with a broader beam, less peak gain, and an axis that points in a different direction from that of the unperturbed synthetic beam. The side-lobe structure will also be observed to fluctuate. It is possible that the fluctuations in phase across a synthetic-aperture length can be so severe that the main lobe is destroyed.

The ionospheric domains most likely to degrade spaceborne SAR images (see Fig. 1) include the nighttime equatorial region (approximately within a band $\pm 20^\circ$ of the magnetic equator, during the period 2200 ±300 h local time) and the high-latitude regions ($|\mathrm{MLAT}| > 55^\circ$ (night), $> 65^\circ$ (day)) nearly always. Ionospheric structure at the equator most likely to degrade the SAR system has a least lower bound near 225 km while the same parameter at high latitudes can extend down to 150 km. SIR-B provides a mission of opportunity to study these effects with swath coverage over or near planned ionospheric stations in Peru, Brazil, India, Greenland, and the U.K.-Norway-Sweden-Finland sector (see Table 1 for station coordinates and planned instrumentation). Additionally, a mobile ionospheric ground station can provide coverage in the Indonesian quadrant with correlative tests conducted by a collaborating science team in Japan. Ionospheric measurement techniques planned for the SIR-B investigation include ionospheric backscatter radars, polarimeters, scintillation receivers, and all-sky and scanning photometers. With our ground-based ionospheric diagnostics array, we will assess the ionospheric condition, the height and density of the F-layer peak, its state of irregularity, its variations in total electron content, and the spatial and temporal distributions of the irregularities themselves. With the ionospheric data, and coordinated SIR-B operational periods, we will conduct correlation and image processing experiments on the SAR data to determine and quantify ionospheric effects on information extraction from the SIR-B image. As an "Ionospheric Effects Science Team," we will be available to all SIR-B experimenters as consultants on the various unstable and irregular states known to exist in the ionosphere. We will be available for the definition, planning, and implementation of microwave technique tests such as sensor calibration, target statistics determination, and radar imaging in spotlight or squint mode. As ground-based experimenters and SIR-B science team participants, our activities, inputs, and analyses will provide the first extensive correlative tests of ionospheric irregularities and associated effects on spaceborne SAR imaging integrity. These results will have global implications with multiple ground sites in the equatorial and high-latitude domains.

SIR-B is unique in that it is a mission of opportunity heavily leveraged with multinational agency support; it will provide a subset of information supporting the development of a global map of SAR operational characteristics and related ionospheric effects as a function of latitude, day/night operations, and phase path distortions.

Table 1. Ground-based SIR-B ionospheric network

Country	Station		Facilities									
			Iono-sonde	Radar		Polarimeter,	Optical	Scintillation				Other
	Site	Coordinates		Coherent	Incoherent	136 MHz	6300 A	137 MHz	254/327 MHz	1.54 GHz	3.9 GHz	
Brazil	C. Paulista	22°, 41'S, 45°00'W, -26° dip	X			X	Scan	A				
	S.J. d. Campos	23° 12'S, 45°51'W, -26° dip				X				A		Corner reflector
	Fortaleza	3°52'S, 38°25'W, -3.5° dip	X									Corner reflector
	Brazilia	15°52'S, 48°01'W, -10° dip	X									
	Belem	1°25'S,48°25'W ,.2° dip	X									
	Blumenau	28°S,49°W,-29° dip	X									
	Natal	5°51'S, 35°14'W, -10° dip							A			Corner reflector
India	Kodaikanal	GM LAT 10.2N, 77.5 E, 0.6	X									
	Tiruchi	10.8N, 78.7 E, 1.0	X									
	Ooty	11.9N, 76.7 E, 1.9							A			
	Waltair	17.7N, 83.2 E, 6.4				X						
	Bombay	19.0N, 72.8 E, 9.8	X			X						
	Calcutta	23.0N, 88.6 E, 12.3				X						
	Delhi	28.6N, 77.1 E, 18.9	X								A	
Peru	Jicamarca	GM LAT ~75°W, 12°S, ~1°S	X	55 MHz	55 MHz							
	Ancon	~75°W, 12°S, ~1°S					X	A		A		
	Huancayo	~74°W, 13°S, ~1°S	X				X	A		A		
	Arequipa	~73°W, 16°S, ~3°S				X	X					Corner reflector
	Piura	~80°W, 5°S, ~7°N	TBD	TBD								Corner reflector
Greenland	Sondrestrom	67°N, 48°W, 75° INV (40° dip @ station) Can map 10°-15° south of station			4 MW 1290 MHz							
	Labrador											Corner reflector
Northern Europe	Wick (U.K.)	58.5°N, 3°W	TBD	144 MHz (SABRE)								Corner reflector
	Troniso (Norway-Sweden-Finland)	69°N, 19°E, 78°		948 MHz (EISCAT)								Corner reflector (57° Lat)
Indonesia	Jakarte	GM LAT 105°E, 6°S ~	50 MHz			6300 A all-sky						
	Sumatra	~104°E, 2°S,~16°S										Corner reflector

Table 1. Ground-based SIR-B ionospheric network (cont.)

Country	Station		Facilities								
			Iono-sonde	Radar		Polarimeter,	Optical	Scintillation			Other
	Site	Coordinates		Coherent	Incoherent	136 MHz	6300 Å	137 MHz	254/327 MHz	1.54 GHz	3.9 GHz	
Puerto Rico	Arecibo	18.35°N, 66.75°W, 45 dip	X		430 MHz							HF heater
	Puerto Rico Island	~18°N, 67°W										Corner reflector

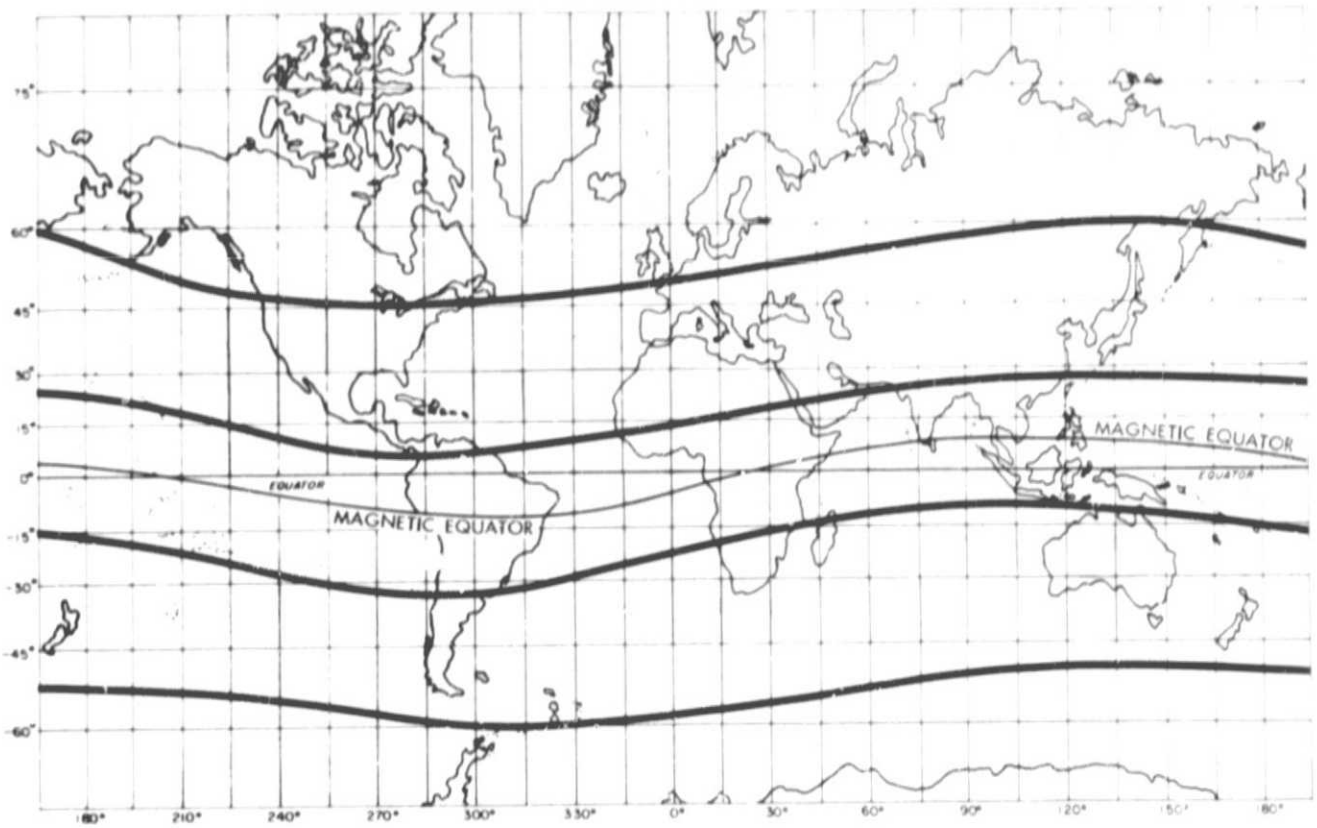

Fig. 1. Geomagnetic contains of ionospheric F-region irregularities. The equatorial F-region irregularities are a nighttime phenomena while the structures and irregularities at high latitudes occur on a nearly 24-hour basis. The high-latitude boundary is shown at 55°N (magnetic latitude) and reflects a nominal least-lower-latitudinal bound.

Analysis of SIR-B Radar Illumination Geometry for Depth of Penetration and Surface Feature and Vegetation Detection, Nevada and California

Team Member:

J. V. Taranik
University of Nevada
Reno, Nevada

Collaborators:

D. B. Slemmons, E. J. Bell, M. Borengasser, T. P. Lugaski, H. Vreeland, P. Vreeland, E. Kleiner, F. F. Peterson, and **H. Kleiforth**
University of Nevada
Reno, Nevada

I. Background

The gradual increase in the price of precious metals is accelerating exploration in Nevada. Indications are that exploration and mining in the Great Basin will be conducted on an unprecedented scale during this decade. Currently, explorationists are prospecting for ancient, high-energy channels in intermontane alluvium using a variety of techniques including ground- and helicopter-based P-band radar surveys. Because the Shuttle Imaging Radar flown on STS-2 demonstrated potential for detection and mapping of ancient channels below alluvium, explorationists in Nevada have wondered if such radar could be used to detect and map similar features in Nevada.

A second major problem facing geoscientists in Nevada is the analysis of seismic hazards in the state. Recent fault scarps are difficult to detect in alluvium because they are subtle features with low relief. Low Sun-angle photography must be used for detection and mapping of scarps with low relief, and such photography is limited by the azimuth of solar illumination.

Specific questions related to the use of spaceborne imaging radar are:

(1) To what depth could L-band radar be expected to penetrate alluvial fans, bahada slopes, and playa lakes in Nevada?

(2) What are the effects of variations in soil moisture and soil salinity on depth of penetration?

(3) What are the effects of variations in vegetation on detection of subsurface features?

(4) Do vegetation types associate with buried alluvial channels and can these vegetation differences be detected by L-band radar?

(5) Is stereoscopic radar imagery useful in the evaluation of surface and subsurface alluvial channels?

(6) What is the optimal radar illumination geometry for mapping structural features in basinal areas and in mountainous areas?

(7) Will stereoscopic radar imagery allow detection and mapping of more structural features than monoscopic radar imagery?

(8) What is the effect of vegetation on detection of structural features?

II. Research Objectives and Methodology

The following program of fundamental research was formulated to answer the previous questions using the measurement capability provided by Shuttle Imaging Radar (SIR-B). The general objectives of this program are:

(1) To determine the relationships between radar illumination geometry and depth of penetration in different climatic and physiographic environments in Nevada.

(2) To determine the relationships between radar illumination geometry and detection and analysis of structural features in different climatic and physiographic environments in Nevada.

We plan an integrated program of field and laboratory research and computer and photointerpretive analyses. SIR-B L-band imagery will serve as a data base to determine the relationships between radar illumination geometry and depth of penetration in different climatic and physiographic environments in Nevada and California. SIR-B data will also be used to determine the relationships between radar illumination geometry and detection and analysis of structural features and vegetative types in different climatic and physiographic environments in Nevada and California. SIR-B imagery will be used for the determination of the optimum depression angles for stereographic analysis of various topographic terrains. Available SIR-A, Seasat, Landsat, and X-band data will be used to augment the SIR-B data analysis.

Prior to the SIR-B mission, we will analyze each study area to determine the thickness of unconsolidated materials over consolidated bedrock and produce an isopach map. We will also determine the depth to the water table in unconsolidated materials, and will collect alluvium samples to determine grain-size distribution, roundness, porosity, and permeability. Also, we will collect soil samples and determine the type of soil, the type and volume of vegetative material, and the porosity.

During the SIR-B mission, our field parties will be at the proposed study areas. Within hours of the SIR-B overflight, they will measure the moisture content of the unconsolidated materials. The Geobotany Team will collect data concerning the distribution and density of vegetation by type, and will collect additional soil and plant samples for biogeochemical analysis.

An interactive image processing system will be used to determine quantitatively the relationships between radar illumination geometry, depth of penetration, and backscattered signal on a resolution element scale in different climatic and physiographic environments in Nevada and California. Landsat data will be used interactively in conjunction with SIR-B data to map vegetation communities that affect backscatter. We will also employ standard photointerpretation techniques of analyzing image tone, texture, and pattern.

A. Coverage and Field Study Areas

Our planned swaths cover parts of Nevada and California (Fig. 1). Imagery will be acquired in a multiple-incidence-angle mode. Several swaths also cross SIR-A Data Take 24A and Data Take 24B, which we plan to use in our analysis.

Of the nine study areas shown on Fig. 1, three specific study areas have been delineated for intensive field study. To determine the relationship between radar-illumination geometry and detection and analysis of structural features in different climatic and physiographic environments, we have selected the northern Walker Lane test site. To determine the relationships between radar-illumination geometry and detection and identification of vegetation and depth of penetration, we have selected the Fish Lake Valley test site and the Mount Grant test site. The six other test sites were chosen for experiments involving structural and seismic studies, synergistic analysis, and comparison with other types of remote sensing data.

B. Field Investigations

Prior to the SIR-B mission, we will visit the three intensive field study areas. These areas are favorable for L-band radar penetration evaluation because they all have areas of exposed bedrock, and along one edge of this exposed bedrock is a line of zero-thickness unconsolidated Quaternary alluvium. Departing from the zero-thickness line, the alluvium thickens and is generally wedge shaped in cross section. We will conduct a seismic refraction survey in at least two directions across the Quaternary alluvium. With the data from this survey, we will construct a sand thickness (isopach) map and a contour map on the top of the water table (if present). Also, we will take samples of the alluvial material to determine grain-size distribution and roundness.

Within hours of the SIR-B overflight, field parties will measure the moisture status of the alluvium and soil profiles by volumetric sampling. The Geobotany Team will spend a week at each of the intensive field study areas for the purpose of vegetation analysis and mapping, obtaining additional soil samples, and ground truthing the radar data.

C. Laboratory Investigations

With digital SIR-B imagery data, we will use enhancement algorithms to improve display of the radar penetration study areas. The purpose of enhancing the penetration study area imagery is to maximize any differences in radar return across the transverse direction of the alluvial or soil wedge. Once a suitable enhancement has been produced for all depression angles, each image resolution cell will be density sliced. These quantized resolution cells will then be contoured and displayed on a cathode ray tube (CRT) by the Mackay School of Mines' interactive image analysis computer system. Similarly, the depth-to-water-table, alluvium, and soil-thickness maps will be digitized and overlayed with the imagery on the CRT. Using statistical methods, we will test for a relationship between radar-signal return and alluvium thickness and water-table depth. Also, we will visually examine the overlays and make qualitative determinations of any correspondence between the density slice contours and the isopach and water-table maps.

D. Stereo Radar

In the past, interpretation of radar imagery has been done mainly with monoscopic techniques. With the capability of SIR-B to image a test site with varying depression angles, stereo radar could be a very effective data base for geologic reconnaissance and mapping.

The stereo-radar imagery produced from the planned swaths (Fig. 1) will not be subject to the problems that arise from radar images acquired with opposite look directions. In addition to evaluating different depression angles for stereo radar, we plan to study the applicability of stereo-radar imagery for delineating structural features. If penetration of unconsolidated materials with L-band radar in Nevada is established, we will evaluate stereoscopic viewing to determine if subsurface features can be better delineated using stereoscopic-radar imagery.

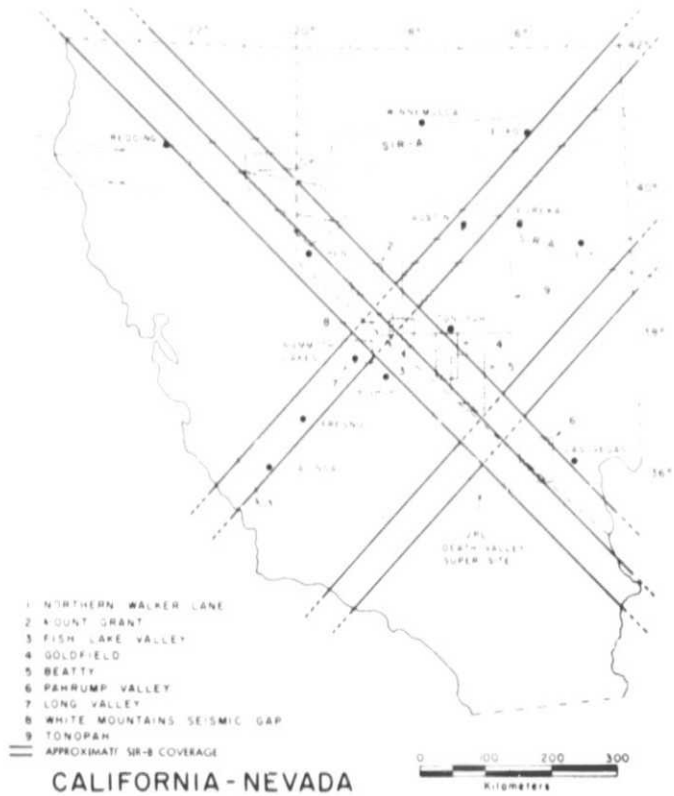

Fig. 1. Proposed SIR-B swaths and test sites for Nevada and California

N85-17249

Delineation of Major Geologic Structures in Turkey Using SIR-B Data

Team Member:

M. N. Toksoz

Massachusetts Institute of Technology
Cambridge, Massachusetts

Collaborators:

G. H. Pettengill, P. Ford, and **L. Gulen**

Massachusetts Institute of Technology
Cambridge, Massachusetts

Plate tectonics can satisfactorily explain the seismic activity and deformation that is confined to narrow zones within oceanic crust, allowing the precise identification of plate boundaries and their kinematics. However, continents display much more complex internal deformational styles that incorporate spatially and temporally coexisting compressional, extensional, and transform regimes, evidenced by the heterogenous, diffuse seismicity within broad zones, making the strict application of large-rigid-plate concepts almost impossible in continental areas.

Under the influence of the overall convergence of African-Arabian and Eurasian continents, Turkey displays all major features of continental tectonics (Refs. 1 through 4). It is a part of the Alpine-Himalayan orogenic belt. Although some major tectonic elements such as the North Anatolian Fault (NAF), the East Anatolian Fault (EAF), the Bitlis Thrust Zone (BTZ), and the West Anatolian Graben System (WAGS) have been recognized so far (see Fig. 1), their detailed characterizations are incomplete and the kinematics of their interactions are poorly understood. This stems partly from the unidentified, potentially important fault zones and partly from the lack of detailed knowledge on tectonic structures of key areas such as Karliova Junction, the intersection of NAF and EAF; Karasu Junction, the intersection of EAF and the Levant Transform; and the Mudurnu region, where NAF changes character, starting at about 30°E westward, from right lateral strike-slip to predominantly normal faulting.

The main objectives of this study are the delineations of fault zones — the detailed study of regions where major faults intersect.

The study of SIR-B images of well-mapped segments of major faults, such as NAF and EAF, will be carried out first to identify the prominent signatures that characterize the fault zones for those specific regions. The gathered information will be utilized to delineate the unmapped fault zones in areas with similar geological and geomorphological properties. The data obtained from SIR-B images will be compared and correlated with:

(1) Landsat TM.

(2) Seismicity alignments based on well-constrained earthquake epicenters.

The SIR-B data will be acquired using mapping-mode imaging with varying incidence angles to maximize the swath

widths without leaving gaps between adjacent swaths. The currently existing software and hardware at M.I.T., augmented with some additions, will be employed to catalog and display the data for interactive analysis and to apply digital techniques to enhance linear fault features.

The importance of radar images for identifying fault zones was demonstrated by a recent (October 30, 1983) earthquake in northeastern Turkey (Ref. 5). This earthquake (M = 7.1) was located on an unknown fault zone. A tract that is about 30 km north of the epicenter had been imaged during the SIR-A experiment. The shear zone is clearly visible in the SIR-A images. The sense of displacement (left-handed) and the strike of the zone (N40°E) are consistent with the mechanism of the earthquake.

In light of the encouraging results obtained from the SIR-A experiment, this proposed study attempts to characterize the complex fault systems, which, in turn will contribute to a better understanding of the continental tectonics.

References

1. McKenzie, D. P. 1972. "Active Tectonics of the Mediterranean Region." *Geophys. J. R. Astr. Soc.*, Vol. 30, pp. 109-185.

2. Sengor, A.M.C., 1979. "The North Anatolian Transform Fault: Its Age, Offset and Tectonic Significance." *J. Geol. Soc. Lond.*, Vol. 136, pp. 269-282.

3. Kasapoglu, K. E. and Toksoz, M. N., 1984, "Tectonic Consequences of Collision of Arabian and Eurasian Plates: Finite Element Models." *Tectonophysics* (in press).

4. Gulen, L., 1984, "Deformational Domain Continental Tectonics in the Lake Van Region, Eastern Turkey: Implications on the Origination of an Extensional Regime Associated With Compression" (in preparation).

5. Toksoz, M. N., Guenette, M., Gulen, L., Keough, G., and Pulli, J.J., 1984, "Source Mechanism of 30 October 1983 Earthquake in Northeastern Turkey" (to be submitted to *J. Geophys. Res.*).

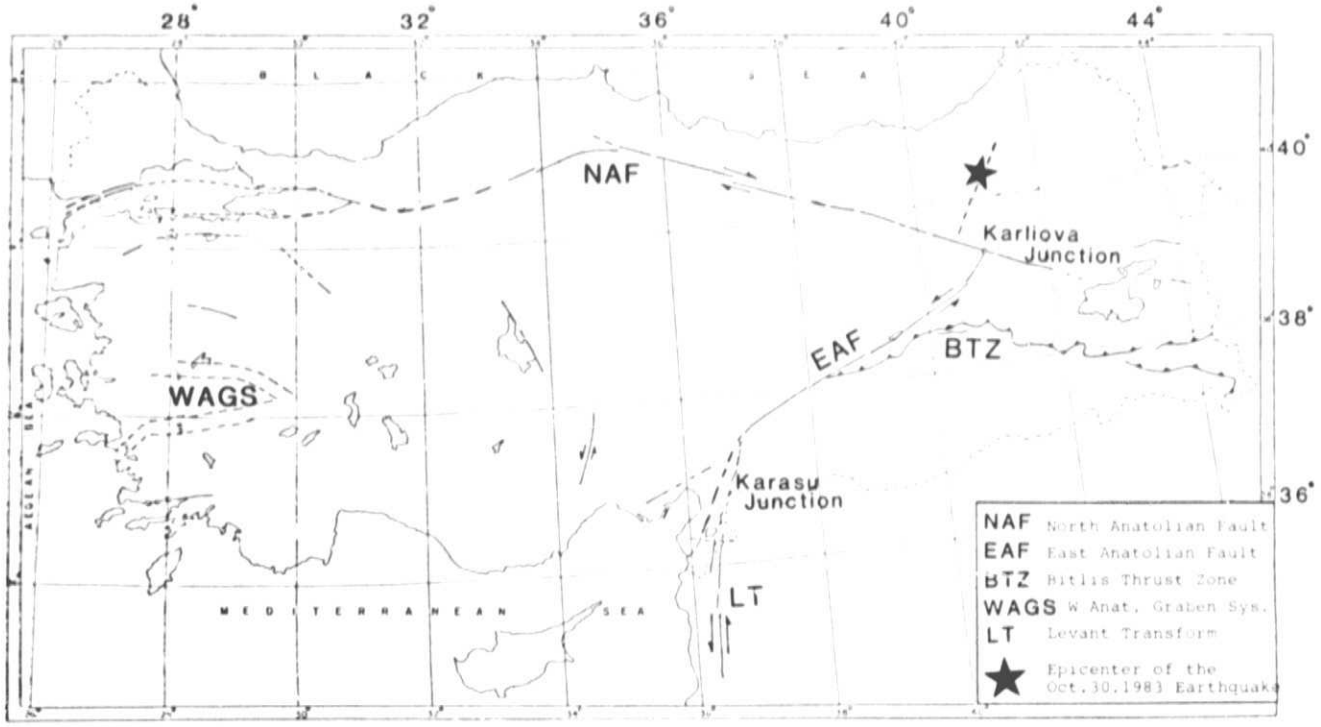

Fig. 1. Major active tectonic elements of Turkey

N85-17250

Evaluation of the Radar Response to Land Surfaces and Volumes: Examination of Theoretical Models, Target Statistics, and Applications

Team Member:

F. T. Ulaby
University of Kansas Center for Research, Inc.
Lawrence, Kansas

Collaborators:

A. K. Fung and **M. C. Dobson**
University of Kansas Center for Research, Inc.
Lawrence, Kansas

J. Cihlar
Canada Centre for Remote Sensing
Ottawa, Canada

I. Summary

This study is intended to improve our understanding of L-band radar remote sensing of terrain. It is divided into four interrelated investigations that examine: (1) the behavior of the radar backscatter coefficient σ_0 of distributed surfaces and volumes as a function of the targets' dielectric and geometric parameters and as a function of their physical parameters (such as soil moisture and plant-leaf-area index), (2) the correspondence of the angular behavior of the relative backscatter coefficient as extracted from SIR-B digital imagery to σ_0 (θ) as measured by a truck-mounted L-band scatterometer system for about 100 agricultural fields, (3) the statistical behavior of SIR-B image density for targets that appear "homogeneous" on Thematic Mapper (TM) optical imagery and/or color-IR photography (within-field variability, between-field variability for the same target class, and between-class variability), and (4) the applicability of SIR-B imagery both alone and in conjunction with TM imagery for the classification and monitoring of land cover and renewable resources (i.e., crop-type classification and monitoring the spatial and temporal variations in soil moisture in the United States and in Canada).

This study will be conducted as a joint effort involving the Remote Sensing Laboratory (RSL) of the University of Kansas and the Canada Centre for Remote Sensing (CCRS), and will use test sites in both the U.S. and Canada. The study will be supported by five types of data: (1) SIR-B imagery for two U.S. sites and two Canadian sites, (2) TM imagery of the above four sites, (3) aerial low-altitude color-IR photography, (4) radar backscatter coefficient measurements of about 100 fields to be made by RSL's truck-mounted MRS (Mobile Radar Scatterometer) system, and (5) ground-truth data for the above 100 fields. In addition, CCRS hopes to obtain airborne

SAR imagery of the Canadian sites, and efforts will be made to image the U.S. sites with the JPL airborne L-band imager.

II. Backscatter Behavior of Surfaces and Volumes

The relatively calibrated data extracted from the SIR-B imagery and the airborne imagery will be used together with the fully calibrated data obtained by the MRS system from 100 fields to examine the correspondence between theoretical models and experimental observations. Two classes of models will be considered: relatively simple semiempirical models and mathematically more sophisticated theoretical models. The empirical models seek to relate σ_0 to physical parameters such as soil-moisture content, plant height, and canopy water content (which is highly related to leaf-area index). The theoretical models seek to relate σ_0 as measured for each target class to that calculated for an inhomogeneous multilayered medium in which backscatter is dominated by three mechanisms: (1) volume scattering from an inhomogeneous layer (vegetation), (2) surface scattering from the ground as attenuated by the inhomogeneous layer, and (3) combined surface-volume scattering from the layered media. For given target classes, the model's sensitivities to various physical parameters will be used to define optimum radar illumination geometries with respect to angle of incidence and azimuth viewing angle.

III. Comparison of SIR-B Data With MRS Measurements

For one of the U.S. sites, the fully calibrated σ_0 measured for about 100 fields by the MRS system will be compared with the relative σ_0 measured by SIR-B to evaluate the presence of any systematic differences related to platform height and system operating or processing characteristics. In addition, airborne imagery will be included in this analysis for both the U.S. and Canadian sites, if available.

IV. Determination of Target Statistics

A typical SAR image of a "homogeneous" target contains a distribution of σ_0 values related to random fading variations for a given number of independent looks-per-image pixel and to true spatial variability within the scene. For a given target, these two sources of variance in backscatter can be separated statistically. In addition to establishing target separability characteristics, knowledge about the ways in which within-class variance differs among target classes can provide valuable information pertaining to trade-offs between resolution and number of independent looks and pertaining to the design of optimal automatic classifiers.

V. Land-Cover and Crop-Type Classification

This investigation will address the applicability of SIR-B imagery both alone and in conjunction with Landsat TM data as a means of mapping and monitoring land cover and crop type. Aerial color-IR photography and ground-truth data will be used to generate inventories of cover type for approximately 300 fields in each site. A Level-I land-use classification and a Level-IV cropland classification will be tested for each site and the results analyzed as a function of SIR-B incidence angle and azimuth view angle. These results will be compared with those obtained from similar classifications using TM data only and combined TM and SIR-B data.

VI. Soil-Moisutre Detection

The SIR-B data will be analyzed for each site with respect to their potential to map instantaneous soil-moisture distributions within a scene and to detect multidate change in near-surface soil moisture. Analysis of single-date SIR-B imagery will parametrically test the extension of truck-mounted and airborne scatterometer results to the orbital imagery for various combinations of sensor parameters (angle of incidence and azimuth view angle) and target parameters (crop canopy cover, row tillage patterns, random surface roughness, slope, and soil type). In addition, analysis of multidate SIR-B observations at an incidence angle near 20° with the same azimuth view angle will provide a test of the change-detection methodology for monitoring hydrologic state. At least one Canadian and one U.S. site will be used for this purpose.

VII. Data Acquisition

As shown in Figs. 1 and 2, the SIR-B data for each site will be supplemented by closest-clear-day Landsat TM data, airborne color-IR photography, and ground-truth data. In addition, concurrent airborne SAR data may be available for sites in both the U.S. and Canada. At one U.S. site, the MRS system will also measure the radar backscatter from approximately 100 fields at each angle of incidence used by SIR-B.

All SIR-B data are to be digitally processed and coregistered. Each of the four sites will be observed by SIR-B at five incidence angles between 15° and 50°. In addition, one U.S. and one Canadian site will be observed on both the ascending and descending orbital passes in order to examine the effects of azimuth view angle and also will be observed twice at a fixed incidence angle in order to examine temporal change in the scene.

Ground-truth data will consist of canopy-cover type, canopy condition, soil moisture, and soil-surface roughness. Dynamic parameters such as 0- to 5-cm soil moisture will be measured on each day with a SIR-B overpass.

Fig. 1. Sketch of the two Kansas sites

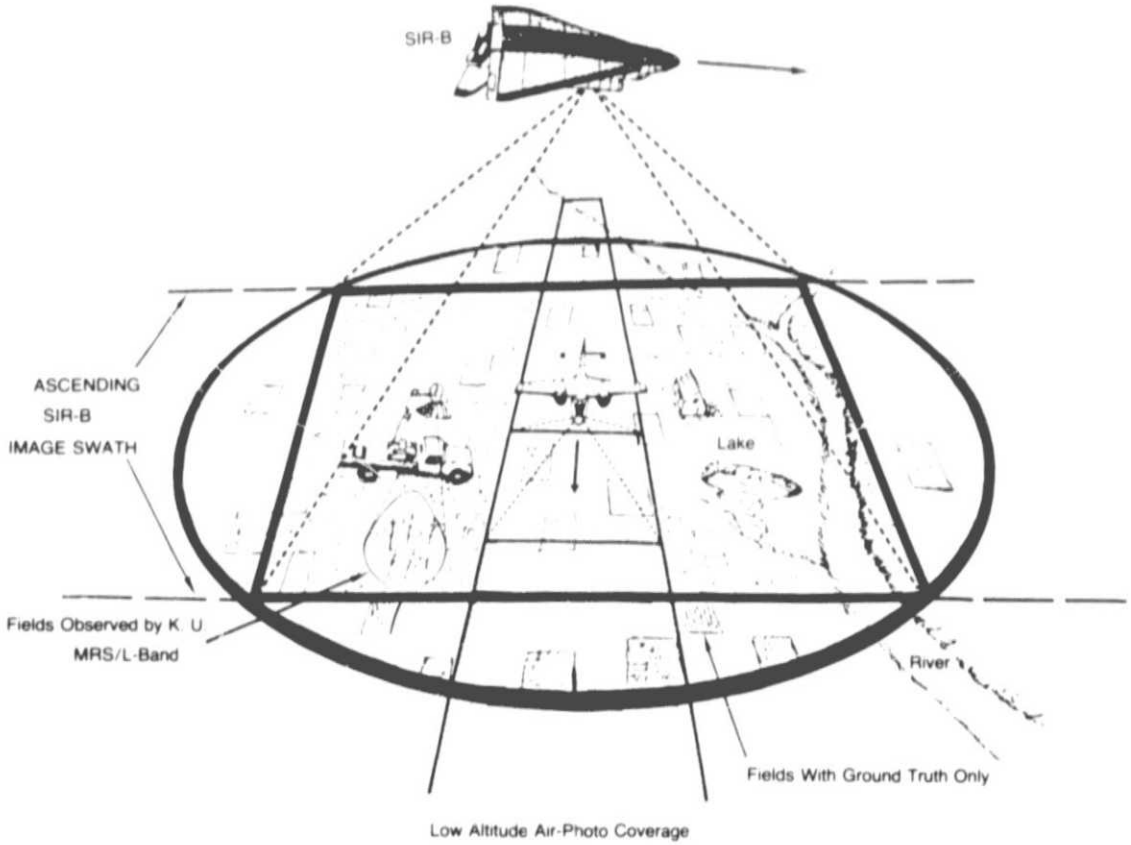

Fig. 2. Enlargement of the northeast Kansas site

Ground Truth for SIR-B Images Obtained by SIR System 8 Impulse Radar

Team Member:

P. Ulriksen
Lund University of Technology
Lund, Sweden

Collaborators:

H. Ottersten
National Defense Research Institute
Sweden

C. G. Borg
Swedish Space Corporation
Solna, Sweden

S. Axelsson
SAAB-Scania
Linkoping, Sweden

B. Ekengren
Ericsson Radic System
Molndal, Sweden

I. Objectives

The main objective of this investigation is to study the penetration capacity of SIR-B. Such results were presented after the SIR-A experiments, Refs. 1 and 2. It seems likely that a combination of a smooth surface and a material with small attenuation and little volume backscatter would make it possible to detect the presence of a contrasting second layer.

The target, a 150 km^2 limestone plain called the "Great Alvar" is situated at the southern part of the island Öland in the Baltic Sea. Although the latitude is N 56°, the island lies in the rain shadow of the elevated "Smålandska höglandet" on the mainland of Sweden. The annual precipitation is around 400 mm, Ref. 3 and Fig. 1, and the theoretical evaporation is 540 to 560 mm, Ref. 4. As a consequence, the plain is a very dry area in the end of the summer, when SIR-B is scheduled to fly.

The surface of the "Great Alvar" has a very thin (<10 cm) soil cover. Fracture zones frequently disappear under the soil; the SIR-B image may provide clues to their locations. The limestone plain is rich in archaeological remains, e.g., the ancient castle of Eketorp, dating back to the era of the Great Migration and the Middle Ages. This makes it probable that there are structures like building sites and ancient roads hidden in the soil layer. Furthermore, the limestone rock is likely to

contain numerous geological structures like fracture zones and coral reefs.

The size of the area makes it difficult to survey, in respect to the above structures, with any method other than remote sensing. Still, the remotely detected structures have to be verified and analyzed.

II. Description of the Experiment

The experiment consists basically of a comparison between visible photography and radar images that will reveal areas of possible penetration. When these areas have been located, they will be surveyed with a penetrating impulse radar system, the SIR-8 manufactured by GSSI. To get the strongest resemblance to SIR-B, an antenna with a center frequency of 0.9 GHz will be used. Parallel profiles across an area with suspected penetration will create an electromagnetic, three-dimensional picture of the existing structures. Correlating these to the SIR-B images will give information on penetration and resolution. The impulse radar system may be considered an electromagnetic magnifying glass.

Soil-moisture content will be determined at 100-m intervals along a north-south line across the target area.

Along these lines, three sensors will be operated continuously. They are a staring infrared radiometer (8 - 14 μm), an aircraft altimeter radar (4.3 GHz, pulse), and the impulse radar system. The latter will be operated with the antenna elevated 1.0 m in order to get a surface return. These sensor outputs will be calibrated with the soil-moisture samples to obtain a continuous profile of the soil-moisture content in the area. The impulse radar will also yield information on volume scattering (Fig. 2).

Image generating sensors will be operated from aircraft; they are airborne photography, real-aperture SLAR (X band), an IR-scanner, 30- and 90-GHz radiometers, and a 35-GHz radiometer. To get an image of soil moisture in the area, these sensors will be calibrated with the continuous line previously obtained. The soil-moisture image will be used to understand the penetration properties of SIR-B. The X-band SLAR is expected to provide information on surface roughness. These sensors will be operated by the Swedish Space Corporation, the Maritime Surveillance, and the National Defense Research Institute.

If possible, three areas will be irrigated for calibration purposes (SIR-B), and corner reflectors will be deployed for registration purposes.

III. Approach for Data Acquisition, Handling, and Analysis

The three sensors operated along the north-south lines will be installed in a lightweight terrain vehicle. This has an on-board HP 9826 computer, which will store the output from the sensors on a 10-Mbit hard disk. Sampling will be triggered at uniform intervals by a switch in the wheels. The signals stored will be infrared radiometer output, altimeter signal, and impulse radar surface return power. In addition, the impulse radar returns will be stored on an HP 3964A FM tape recorder for subsequent spectral analysis and extraction of surface roughness, volume scattering, and penetration along the lines.

All the airborne sensors produce computer-compatible tapes that will be processed by the National Defense Research Institute and the Swedish Space Corporation to produce a material that is registered pixel to pixel.

The infrared scanning radiometer will be flown both day and night. The transformation of IR-data to soil-moisture data will be performed at SAAB-Scania.

The postflight impulse radar survey of suspected subsurface features will be performed with the equipment installed in the terrain vehicle. At this occasion, it is expected that all information can be stored digitally to facilitate the processing and analysis of the data.

IV. Expected Results

This investigation is expected to give verification of suspected penetration by means of three-dimensional information on the features in the SIR-B images. The other imaging sensors will give a good opportunity to evaluate the SAR data. Many unforeseen effects will be amenable to analysis since the Great Alvar is a very well documented area, especially in geology and ecology.

References

1. Elachi, C., and Granger, J., "Spaceborne Imaging Radars Probe 'In Depth'," *IEEE Spectrum*, Nov. 1982.

2. Cauley, J. F., Schaber, G. G., Breed, C. S., Grolier, M. J., Haynes, C. V., Issawi, B., Elachi, C., Blom, R., "Subsurface Valleys and Geoarchaeology of the Eastern Sahara Revealed by Shuttle Radar," *Science*, Vol. 218, 3 Dec. 1982, pp. 1009-1019.

3. Granlund, E., "De Svenska Högmossarnas Geologi," *Sveriges Geologiska Undersökning*, Ser C, No. 373, 1932.

4. Rosen, E., "Vegetation Development and Sheep Grazing in Limestone Grasslands of South Öland, Sweden," *Acta Phytographica Suecia*, 72, Uppsala, Sweden.

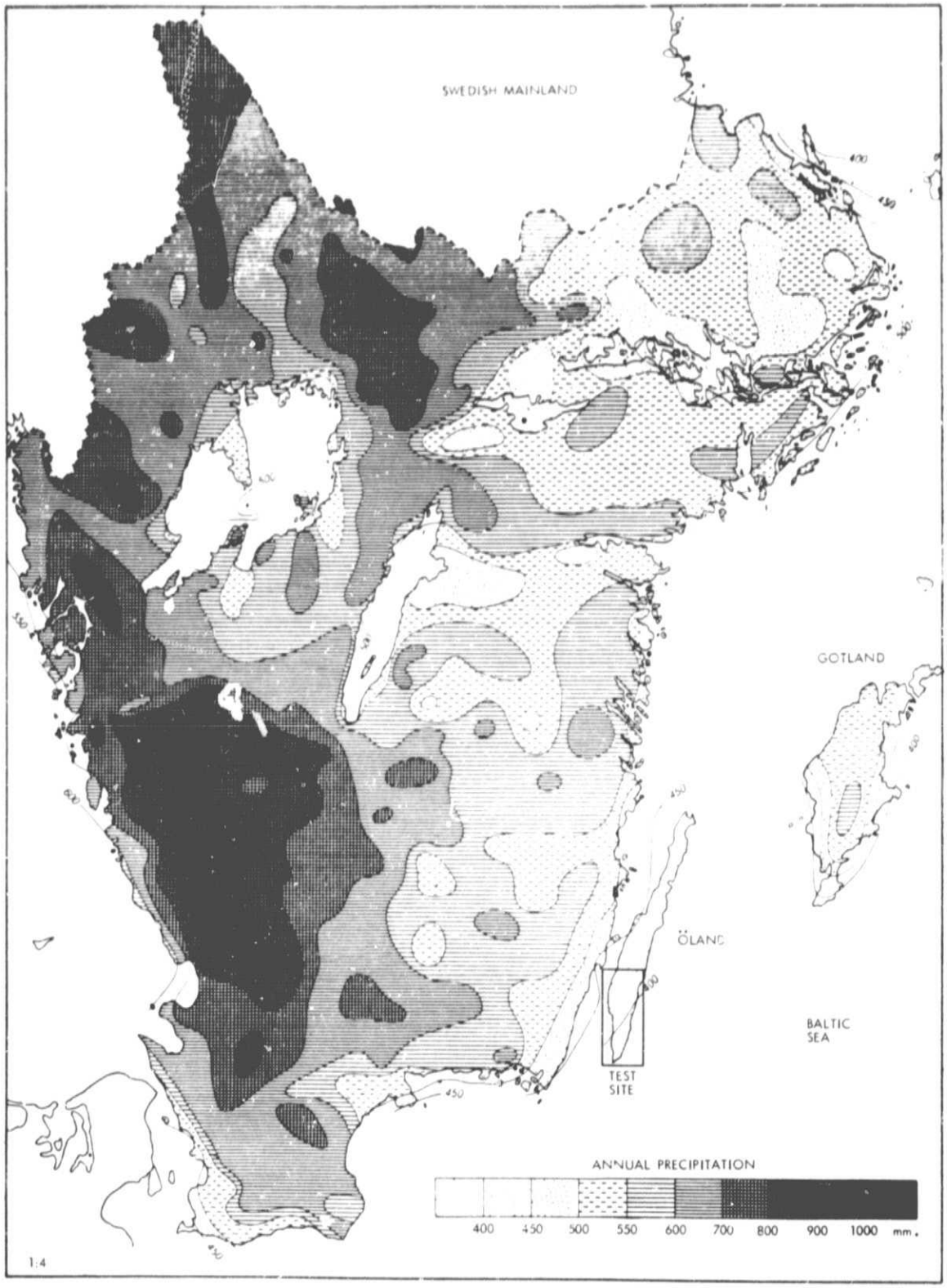

Fig. 1. Annual precipitation in southern Sweden (from S.G.U. Ser C. N:o 335)

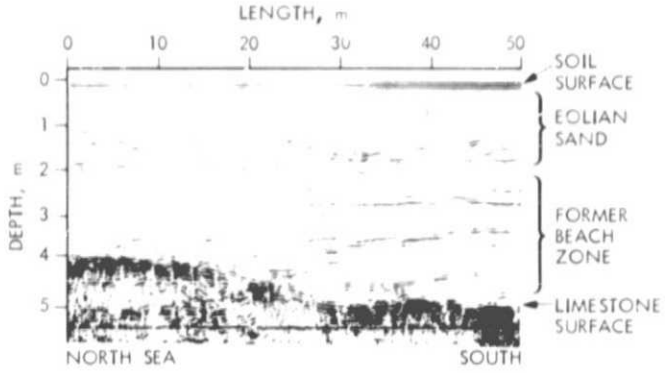

Fig. 2. An impulse radar record showing sand on limestone at the nearby island Gotland

Remote Sensing of Soil Moisture

Team Member:

J. R. Wang
Goddard Space Flight Center
Greenbelt, Maryland

Collaborators:

J. C. Shiue, T. J. Schmugge, and P. Cuddapah
Goddard Space Flight Center
Greenbelt, Maryland

T. J. Jackson
U.S. Department of Agriculture
Beltsville, Maryland

T. Mo
Computer Sciences Corporation
Silver Spring, Maryland

I. Objectives

There are four major objectives in our proposed investigations:

(1) To study the sensitivity of active and passive microwave remote sensing approaches to soil-moisture variations. Improvement in the estimation accuracy by the combination of both approaches will also be explored.

(2) To investigate the effect of vegetation cover on microwave backscatter and emission.

(3) To test theoretical models of microwave backscatter and emission from a natural terrain against the observations obtained from SIR-B and aircraft radiometer flights.

(4) To estimate vegetation biomass with airborne visible and infrared sensors. This will combine with the microwave measurements for estimating soil moisture in vegetated fields.

II. Approaches

A test site about 10 km × 10 km in size with its center located in the San Joaquin Valley, California, is selected for the experiment. The advantage of using this site is that the probability of rainfall in the August to September period is small, and the moisture content of soils can be controlled by irrigation. We plan to have some fields irrigated so that a wide range of soil-moisture variation in the test site is maintained for the SIR-B experiment.

Imaging of the test site by SIR-B at five incidence angles (θ) ranging from 15° to 57° will be made for this experiment. The multiangle measurements are needed for both theoretical-model verification and surface-property parametrization. The imaging data will primarily be in digital form, but copies of optical signal films recorded onboard the Shuttle will also be used for quick looks.

During each day that SIR-B overpasses the test site, aircraft underflights with an L-band microwave radiometer and a visible and infrared sensor (e.g., NS001) will also be conducted. Experiments in the past years have shown that surface soil-moisture estimates by microwave radiometry are best made at L-band when the effects of both surface roughness and vegetation cover are considered (Refs. 1 and 2). Measurements with both active and passive microwave sensors on the same test site will provide a comparison of soil-moisture estimation by two different techniques. These same measurements will also allow a sound test of theoretical models for microwave interaction in the vegetation/soil media. After all, a sound theoretical model should be able to describe simultaneously both microwave backscatter and emission from a natural terrain. The visible and infrared sensor provides a thermal infrared channel measuring the thermal temperature of a terrain surface, which can be used to remove the contribution of soil-temperature variation to the microwave radiometric respons. (Refs. 1 and 2). The visible and near-infrared data from this sensor will give an estimate of a terrain's vegetation biomass (Ref. 3). This information will be integrated with SIR-B and microwave radiometer data for estimating the moisture content of the vegetation-covered soils.

The ground truth of soil moisture and temperature will be acquired each day close to the time of SIR-B overpass. The measurements of these parameters will be made at two layers: 0 to 2.5 cm and 2.5 to 5.0 cm. Maps of soil-type distribution of the test site area will be acquired. In addition, mechanical analysis of soils will be performed to determine the texture of the major soil regimes in the test site. Soil density and vegetation biomass will be sampled. Some measure of surface roughness will be made for the study of the angular dependence of microwave backscatter and theoretical-model verification. This will be accomplished by a simple method of photographing the soil-surface profile with a scaled metal plate in the background, as previously made in the field measurements (Ref. 4). Most of the ground-truth data processing will be done at the USDA regional station near the test site. Processing of data related to surface roughness and soil texture will be performed at NASA Goddard Space Flight Center (GSFC) and USDA Beltsville Agricultural Research Center (BARC).

Processing and analysis of SIR-B and aircraft data will be done at GSFC. These data will be compiled in a suitable format for further analyses by the investigators. Presumably, there will be some 20 to 30 individual fields of various surface conditions in the test site. The compiled data set shall give average values of SIR-B backscatter, microwave radiometric response, visible and infrared intensities, as well as the ground-truth information for the individual fields. The studies of soil-moisture sensing, theoretical-model verification, and Sun-surface-parameter description will be based on the compiled data set.

Theoretical models of microwave backscatter from a natural terrain have also been developed in the past decade. The model developed by Fung and Eom (Ref. 5), based on the Kirchoff approximation method for bare rough fields, was recently modified by Mo (Ref. 6) to take into account the effect of vegetation cover. This modified model was used to match the data obtained on June 24, 1980, over one of the watersheds. This comparison is presented in Fig. 1a and b for both 1.6-GHz and 4.75-GHz frequencies. The parameters $K\sigma$ and KL in the figure are associated with surface roughness of the soil, whereas η and τ are associated with the vegetation cover. It is quite clear that, with proper selection of surface roughness and vegetation parameters, the observed variations of σ_0 with θ at both frequencies are described very well by the theoretical model. This same model can be used to match the data to be obtained at different θ from the SIR-B experiment on both bare and vegetated fields. Extension of the model to calculate microwave emission from a terrain surface can also be made as demonstrated by Fung and Eom (Ref. 5). This extended calculation can be compared with microwave radiometric measurements planned for the same test site chosen for the SIR-B experiment. In this way, the theoretical model for microwave backscatter and emission can be tested by both active and passive microwave measurements made over the same terrain at about the same time.

III. Anticipated Results

With multiangle measurements of microwave backscatter over the test site, we expect to make a proper assessment of an L-band SAR as a soil-moisture mapper. We realize the fact that the SIR-B microwave backscatter measurements of different incidence angles over a given field are made on different days with changing soil-moisture content may cause some difficulty in the experiment. But, with the aid of a reasonable theoretical model giving both microwave backscatter and emission, we can analyze both the active and passive microwave measurements over many fields in a coherent manner. In this process, we shall also be able to obtain a consistent result that gives both an evaluation of soil-moisture sensing by an active microwave approach and a thorough test of the theoretical model describing microwave interactions at the surface of the earth.

From both active and passive microwave measurements on the same test site with a good ground-truth data set, we shall also be able to compare soil-moisture estimates by active and passive microwave approaches. A study on the combination of active and passive microwave data to improve the soil-moisture sensing accuracy is only one step beyond. We anticipate no particular difficulty in carrying out such a study. Finally, the effect of vegetation cover is an important element in microwave soil-moisture sensing. With the addition of visible and infrared data, we expect to obtain a good estimate of surface biomass and deal with the problem of vegetation cover on soil-moisture sensing effectively.

References

1. Jackson, T.J., Schmugge, T.J., and Wang, J.R., "Passive Microwave Sensing of Soil Moisture under Vegetation Canopies," *Water Resources Res.*, Vol. 18, No. 4, pp. 1137-1142, 1982.

2. Wang, J.R., Schmugge, T.J., McMurtrey, J.E., Gould, W.I., Glazar, W.S., and Fuchs, J.E., "A Multi-Frequency Radiometric Measurement of Soil Moisture Content Over Bare and Vegetated Fields," *Geophys. Res. Letters*, Vol. 9, No. 4, pp. 416-419, 1982.

3. Tucker, C.J., Elgin, J.H., and McMurtrey, J.E., "Relationship of Crop Irradiance to Alfalfa Agronomic Values," *Int. J. Remote Sens.*, Vol. 1, pp. 69-76, 1980.

4. Wang, J.R., O'Neill, P.E., Jackson, T.J., and Engman, E.T., "Multi-Frequency Measurements of the Effects of Soil Moisture, Soil Texture, and Surface Roughness," *IEEE Trans. Geosci. Remote Sensing*, Vol. GE-21, No. 1, pp. 44-51, 1983.

5. Fung, A. K., and Eom, H. J., *An Approximate Model for Backscattering and Emission from Land and Sea*, AgRISTARS SM-K-04049, Remote Sensing Laboratory, University of Kansas Center for Research, Inc., March 1981.

6. Mo, T., personal communication.

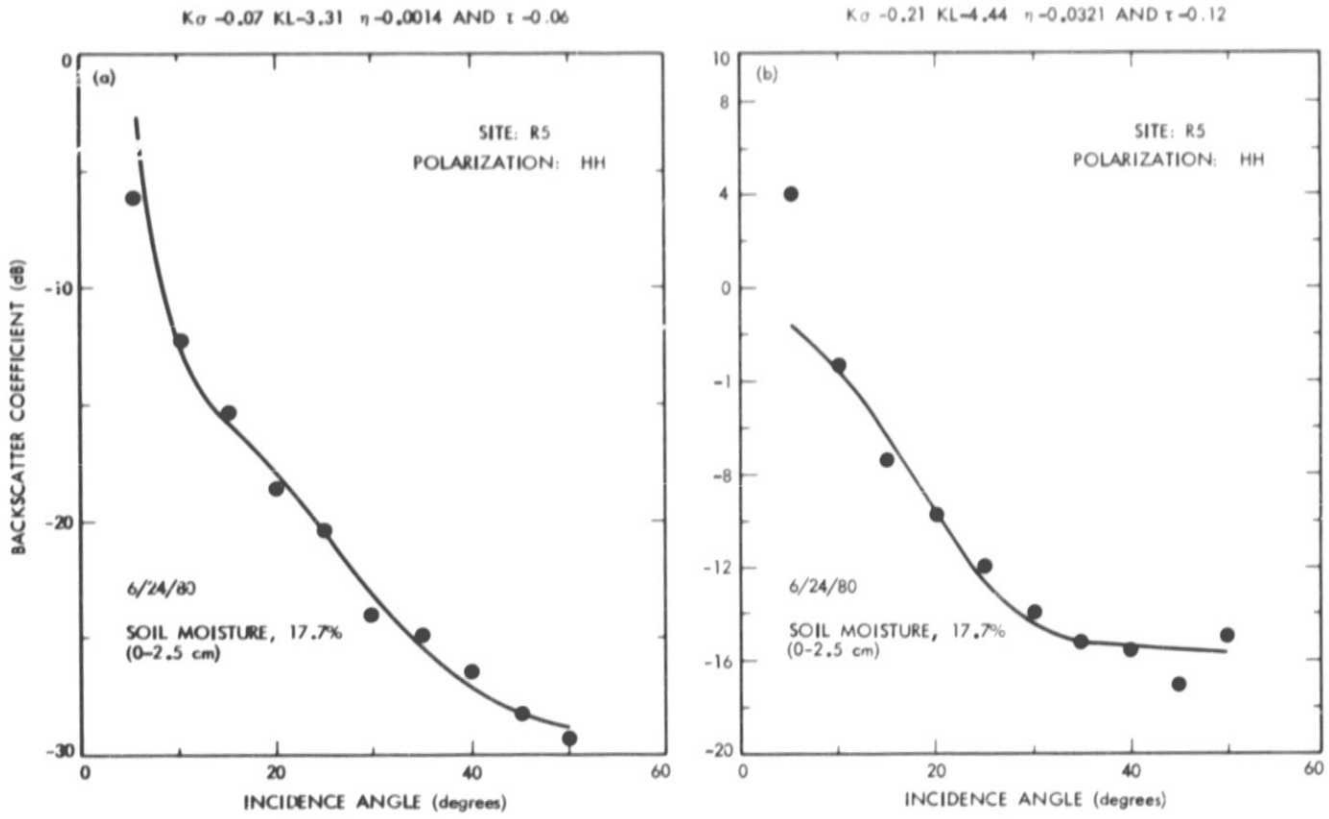

Fig. 1. Matching of theoretical-model calculations to data obtained from aircraft flight over a watershed in Chickasha, Oklahoma, at the frequencies of (a) 1.6 GHz and (b) 4.75 GHz

45

N85-17253

SAR Internal Wave Signature Experiment

Team Member:

R. S. Winokur
Office of Naval Research
Arlington, Virginia

Collaborators:

J. R. Apel and **R. F. Gasparovic**
The Johns Hopkins Applied Physics Laboratory
Laurel, Maryland

I. Introduction

Synthetic-aperture radar images from Seasat and the SIR-A experiment aboard the Space Shuttle Columbia include many examples of surface manifestations of oceanic internal waves (Refs. 1 through 5). These effects are due to surface currents modulating the structure of the short-wavelength surface waves, that in turn give rise to changes in the microwave backscatter. With the exception of the Hughes and Gower experiment (Ref. 4), the above cited SAR images of internal waves were obtained without benefit of coincident in-situ observations. As a result, there are numerous unresolved issues associated with the physics of internal wave-induced modulations of surface waves, the nature of electromagnetic scattering from the sea surface, and various SAR imaging phenomena.

To address these issues, the Office of Naval Research plans to conduct the SAR Internal Wave Signature Experiment (SARSEX) south of Long Island. During this experiment, research vessels will be deployed to the test site for internal wave and surface wave observations in conjunction with aircraft SAR images. SARSEX provides a unique opportunity to acquire aircraft and spacecraft SAR imagery of internal waves with appropriate sea-truth data.

II. SARSEX Objectives

The objectives of the SAR Internal Wave Signature Experiment are to:

(1) Investigate basic mechanisms, both hydrodynamic and electromagnetic, responsible for internal wave signatures in SAR images.

(2) Quantitatively test theories and models for predicting internal wave signatures from given oceanic and radar parameters.

III. Description of the Experiment

The site selected for SARSEX is approximately 100 km south of the eastern end of Long Island (Fig. 1). This area is known to contain large-amplitude, coherent internal wave trains during summer months when the near-surface water column becomes stratified (Ref. 6). The internal wave packets are generated twice daily by tidal flow over the shelf break and they propagate northward with a phase speed of about 0.35 m/s.

Figure 2 shows the experiment concept. Internal wave characteristics will be determined from three current-meter moorings and thermistor chain tows from the research vessel *Cape*. A second research vessel, the USNS *Bartlett*, will be used to measure vertical density profiles and the full set of in-situ observations will be used with nonlinear internal wave models to define the surface current field associated with the internal waves.

Measurements of surface wave slope modulations induced by the internal wave surface currents will be made using charge-coupled device television cameras mounted on the bow of the *Bartlett*. A wave buoy will be used to define the background surface wave spectrum. Radar backscatter measurements will also be made from the *Bartlett*.

SAR imagery at X-band and L-band wavelengths will be acquired from the Convair 580 aircraft operated by the Canada Centre for Remote Sensing. The aircraft will make repeated passes over the test area to obtain imagery at different viewing orientations relative to the internal wave propagation direction, as well as at varying incidence angles and polarizations.

During the SIR-B mission, attempts will be made to obtain near-coincident spacecraft and aircraft SAR imagery of the test site. The SIR-B SAR antenna will be adjusted appropriately to illuminate the test site; the natural progression of the Shuttle orbit will then allow us to examine the internal wave signature dependence on spatial resolution and viewing geometry.

IV. Analysis Approach

The analysis effort will be structured as an end-to-end examination of the process by which internal waves are imaged by synthetic-aperture radars. Signal tapes from SIR-B and the aircraft SAR will be processed using the digital SAR processor at the Applied Physics Laboratory to generate images for comparison with the sea-truth data. Internal wave signatures will be characterized by the change in backscatter cross section corresponding to the SAR image intensity variations. By correlating the observed changes in cross section with the measured surface roughness variations, we expect to be able to identify the dominant contributions to the SAR imaging process. The surface wave images will also be analyzed to extract changes in the surface wave slope spectrum as a function of position within the internal wave pattern in order to quantify the internal-wave/surface-wave interaction. With this approach, we expect to derive a substantial body of information that will advance the exploitation of synthetic-aperture radars for oceanic internal wave investigations.

References

1. Apel, J. R., and Gonzalez, F. I., "Nonlinear Features of Internal Waves off Baja California as Observed from the SEASAT Imaging Radar," *J. Geophys. Res.*, Vol. 88, pp. 4459-4466 (1983).

2. Alpers, W., and Salusti, E., "Scylla and Charybdis Observed from Space," *J. Geophys. Res.*, Vol. 88, pp. 1800-1808 (1983).

3. Ford, J. P., Cimino, J. B., and Elachi, C., *Space Shuttle Columbia Views the World with Imaging Radar: the SIR-A Experiment*. JPL Publication 82-95, Jet Propulsion Laboratory, Pasadena, Calif., January 1983.

4. Hughes, B. A., and Gower, J. F. R., "SAR Imagery and Surface Truth Comparisons of Internal Waves in Georgia Strait, British Columbia, Canada," *J. Geophys. Res.*, Vol. 88, pp. 1809-1824 (1983).

5. Trask, R. P., and Briscoe, M. G., "Detection of Massachusetts Bay Internal Waves by the Synthetic Aperture Radar (SAR) on SEASAT," *J. Geophys. Res.*, Vol. 88, pp. 1789-1799 (1983).

6. Apel, J. R., Byrne, H. M., Proni, J. R., and Charnell, R. L., 1975, "Observations of Oceanic Internal and Surface Waves from the Earth Resources Technology Satellite," *J. Geophys. Res.*, Vol. 80, pp. 865-881 (1975).

Fig. 1. Location of SARSEX Test Site

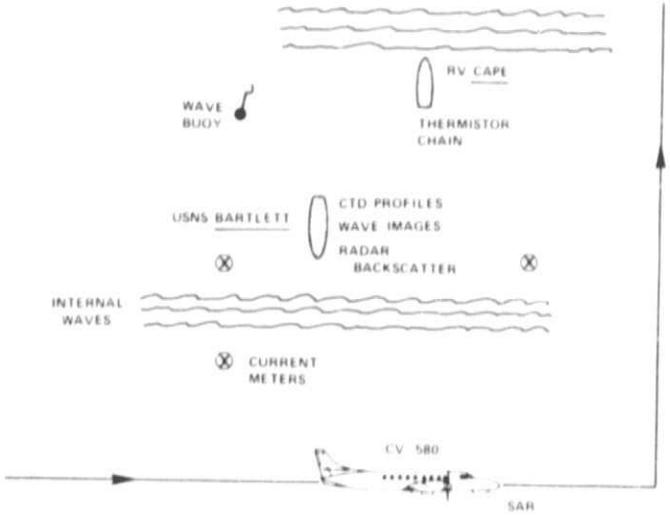

Fig. 2. SARSEX measurement concept

Section V
Data User's Manual

A. Data Products and Flow

The standard SIR-B data products will consist of both optical and digital output. These products are summarized in Table 5-1.

1. Optical Products

a. **True Optical.** All SIR-B true* optical products will be derived from the original signal history recorded on 70-mm film onboard the Shuttle. The cassette will be removed from the Shuttle as soon as possible after landing. It will be immediately transported to the JPL off-load facility, where the film will be removed under darkroom conditions. This film, when processed photographically, will be designated "signal-film original negative" (SFON). The SFON will be used to produce a one-to-one duplicate positive transparency designated the "signal-film master positive" (SFMP). The SFON will be the prime signal-history archival record of the optical recording and is not intended for use as a working data set. After generation of the positives, the SFON will be stored in the JPL Shuttle Imaging Radar (SIR) Data Center in a highly secure atmosphere; to limit further use, it will be accessible only with the permission of the Principal Investigator.

The SFMP will be transported to the correlator for the generation of a single set of image-film original negatives (IFON), and will then be stored in the SIR Data Center. The correlated imagery will be exposed on 12.7-cm-wide continuous-roll photographic transparency film. The processed IFON will be used to generate two sets of image-film master positives (IFMPs), which will be one-to-one duplications of the IFON.

One set of the IFMPs will be stored in the SIR Data Center; the second set will be stored in the JPL photographic laboratory until such time as a complete set of image-film duplicate negatives (IFDN) has been generated. The duplicate negatives will be one-to-one negative image renditions of the IFMP. Immediately upon complete processing of the IFDN, the second set of IFMP will also be returned to storage in the SIR Data Center. Both the duplicate negatives and the duplicate positives are intended to be working copies of the image data set. The positives can be used to produce negatives, and the negatives can be used to reproduce the data onto paper as prints or onto film as positive transparencies. Optical products of the entire mission will be produced during the first twelve months after landing.

b. **Survey Processing.** All digital data will be optically processed in a survey mode during the first six months. The high-density digital tape data will be converted to film through a digital-to-analog converter (laser-beam recorder) and optically correlated in a manner similar to that of the flight optical data. These images are intended primarily to afford the team members an early look at the data to verify coverage and assess image quality. The survey-mode images will also aid in determining which data will be processed to standard digital form.

2. Digital Products

All SIR-B digital products will be derived from two primary sources: HDDTs off-loaded from the Shuttle and HDDTs recorded on the ground at GSFC (Section II.A). These tapes

*True in the sense that the data are optically recorded. Survey data are digitally recorded, and it is only after a digital-to-analog conversion that these data can be optically correlated.

will be transferred to the JPL SIR-B ground processing facility and become the prime radar signal history in digital form. They will be treated as archival copies, and they will be transported, handled, and stored by only predesignated individuals and under the highest security conditions.

a. Quick-Look Digital Processing. Several frames (about one per day) of "quick-look" digital data will be processed during the mission from data relayed through the TDRS link. The signal data will be transferred to JPL from the ground station at the Johnson Space Center (JSC) via courier; at JPL, they will be processed by a quick-look low-resolution algorithm. These data will be placed on either film or video tape for viewing. The main purpose of these data is to determine the general condition of the radar and the general quality of the data. The goal is to produce completed images within 24 h after acquisition of the signal data in order to support any necessary changes to the radar for subsequent data acquisition.

b. Standard Digital Processing. The standard digital images will be processed at JPL from the HDDT data. Most of the team members will use these data. The standard products are 1600-bit/in. computer-compatible tapes (CCTs) and 20- × 25-cm negatives and prints. The current plan calls for the production of twelve images per week during the first year and 24 images per week subsequently. The priorities in the processing schedule will be determined by evaluation of each team member's requirements.

c. Menu Tapes. Computer-compatible tapes, consisting of the identifying information for the standard, digitally processed images, will be created by the processor and the information will be written into a database file. This information can then be converted into hard copy by using a query and report system. The hard copy will be supplied to users upon request. All processing parameters for the digitally correlated frame as well as the Shuttle orbit parameters necessary for the correlation will be stored in this file.

3. Product Distribution

a. JPL SIR Data Center. The JPL SIR Data Center is responsible for the logging and filing of all SIR-B data products from the receipt of signal data until the final processing of image data, and for the initial distribution of data (see Fig. 5-1). The latter includes, based on the decision of the Principal Investigator, the first data released publicly through the JPL Public Information Office (PIO). This release could occur within hours after the first data arrives at the JPL ground processing facility. Even though some data may be released to the public, SIR-B data is proprietary information for six months after the Shuttle landing. During this time, only team members have the right to use the data for scientific publications.

All SIR-B team members will receive copies of the data that cover their proposed study sites. Because of the vast amount of data expected and the required processing time, each team member will be limited to one product per month. Specially processed images are included in this limit.

After publication of a preliminary report, all SIR-B data products will be made available to the general public. At that time, the SIR Data Center can, at its discretion or on the advice of the Principal Investigator, distribute products to interested individuals or refer them to the National Space Science Data Center (NSSDC) (see Section 3.b), which will have received copies of all data from the SIR Data Center.

The SIR Data Center may be reached at:

JPL SIR Data Center
M.S. 183-701
Jet Propulsion Laboratory
California Institute of Technology
4800 Oak Grove Drive
Pasadena, California 91109
Telephone: (818) 354-2386

b. National Space Science Data Center. The NSSDC will be responsible for the general distribution of SIR-B data products to the public. Questions regarding specific product availability, costs, and turnaround times should be directed to:

National Space Science Data Center (NSSDC)
Request Coordination
NASA/Goddard Space Flight Center
Code 601.4
Greenbelt, Maryland 20771
Telephone: (301) 344-6695

B. Data Format

This section describes the format of the unprocessed echo data, optically processed image data, and digital image data. In addition, the header contents will be generally described as well as image annotation and supplementary image products.

1. Unprocessed Echo Data

The digital echo data will be recorded on HDDTs (Ampex 79a) at the Goddard Space Flight Center. These tapes will be transcribed onto CCTs (9-track, 1600 bits/in.) at JPL and made available to team members with accepted digital processing facilities. No optical film will be available. Digital data on HDDT will be available only in special cases.

The HDDT data layout is shown in Fig. 5-2. Each range line consists of a header (eight 32-bit words) and a data field. The

number of samples in the data field is dependent on the PRF (16 values), the bps (3, 4, 5, or 6), and the data rate (30.4 or 45.6 Mbits/s). A detailed description of the header format can be found in Ref. 5-1. The data will be packed at a density of 27 Kbits/in. and is expected to have a bit error rate (BER) $< 10^{-5}$.

These data will be transcribed to CCTs by JPL and distributed to approved users. In the transcription process, an additional three 32-bit status words will be added to each header; these words are applicable to the JPL processor only. In addition, the echo data will be packed into 32-bit words where two zeros precede the data in each word for the 3-, 5-, and 6-bit cases. The first bit in each sample is the most significant bit.

All users receiving raw data on CCTs will also receive supplementary information describing the data quality and header contents. Information such as BER, number of missing lines filled, and missing bits, as well as a histogram and range spectrum of the data, will be included in the package. The header will be decoded and printouts made available describing such radar parameters as PRF, look angle, bps, receiver gain, and data window position. In addition, Shuttle parameters for the center time of the image will be given. These include position, velocity, attitude, and attitude rate vectors.

2. Optical Imagery

The optical imagery will be printed on film strips 100 mm in width and up to 18 m in length. This would correspond to a data collection period of 20 min (approximately 9,000 km). As previously described, the imagery will be in slant-range format at an approximate 500,000-to-1 scale.

Each film strip will be annotated with a label at the beginning of the strip defining selected radar parameters and the GMT, including date of acquisition. At 10-s intervals, the time code (h, min, s) will be updated, and at 1-s intervals a time marker will appear on the image.

Table 5-2 lists the planned annotation on the optical products, a subset of the annotation on the digital tape (see Section B.3).

3. Digital Imagery

The digital imagery will be available either on 1600-bit/in. tapes or as photo products. The image tape will consist of records typically 8000 bytes in length. The first record is the header in ASCII format followed by 80 records of gray scale. The image data comprises approximately the next 4000 records (dependent on image mode). Each record contains a single range line of image data at one pixel per byte. The next 48 records are the distance scale followed by 136 records of annotation. The proposed image tape header is given in Table 5-3. The processing parameters to be included have not yet been finalized.

The digital photo product layout is shown in Figure 5-3. Each image will contain a gray scale and annotation as shown in the figure. The near swath will always be displayed at the top. The standard product will have 12.5-m spacing and a 25-μm raster size; this will result in a 500,000-to-1 scale, which is comparable to the SIR-A and SIR-B optical products. A supplementary information sheet listing the full set of processing and image parameters will be provided with all imagery.

Reference

5-1. *Functional Requirements: SIR-B SAR Processor Data Input Subsystem*. Internal report D-1435, Jet Propulsion Laboratory, Pasadena, California, December 1, 1983.

Table 5-1. Data products list

Product	Acronym
Quick-look data (digitally correlated from HDDR data)	
Quick-look high-density digital tape (from JSC)	Q-HDDT
Quick-look CCT	Q-CCT
Quick-look digital image-film original negative	Q-IFON
Quick-look digital image print	Q-IP
Survey data (optically correlated from HDDR data)	
Survey signal-film original negative	S-SFON
Survey signal-film master positive	S-SFMP
Survey image-film original negative	S-IFON
Survey image-film duplicate negative	S-IFDN
Survey image-strip contact print	S-SCP
Optical flight data (optically correlated from OR data)	
Optical signal-film original negative	O-SFON
Optical signal-film master positive	O-SFMP
Optical image-film original negative	O-IFON
Optical image-film master positive	O-IFMP
Optical image-film duplicate negative	O-IFDN
Optical image-strip contact print	O-SCP
Digital flight data (digitally correlated from HDDR data)	
High-density digital tape	D-HDDT
Digital computer compatible tape	D-CCT
Digital image-film original negative	D-IFON
Digital image-film master positive	D-IFMP
Digital image-film duplicate negative	D-IFDN
Digital image print	D-IP
Digital menu CCT	D-Menu

Table 5-2. Optical product annotation

Characters	Notation
	LINE 1
48	NASA JPL SIR-B digitally correlated SAR image
50	Site
26	Start time: ddd/hh:mm:ss
33	Center latitude: XX.XX deg (N)
32	Center longitude: XX.XX deg (W)
189 characters (220 maximum)	
	LINE 2
31	SIR-B ID:dddhhmmss/AC-56.2/D/4
40	Center resolution: XXm (R), XXm (AZ)
36	Pixel size: 12.5 m, 8 bps
16	PRI: XXXX.X Hz
30	Center look angle: XX.X deg
37	Track ← XXX.X deg (to true north)
190 characters (220 maximum)	

Table 5-3. Preliminary image tape header layout

Record No.	Item
1	Title
2	Identification
3	Start time
4	Processing date
5	Center latitude
6	Center longitude
7	Site name
8	Number of samples per AZ line
9	Total number of AZ line
10	Center resolution
11	Pixel size
12	PRI
13	Center look angle
14	Track
15	Blank
16	About 7480 bytes for selected processing parameters

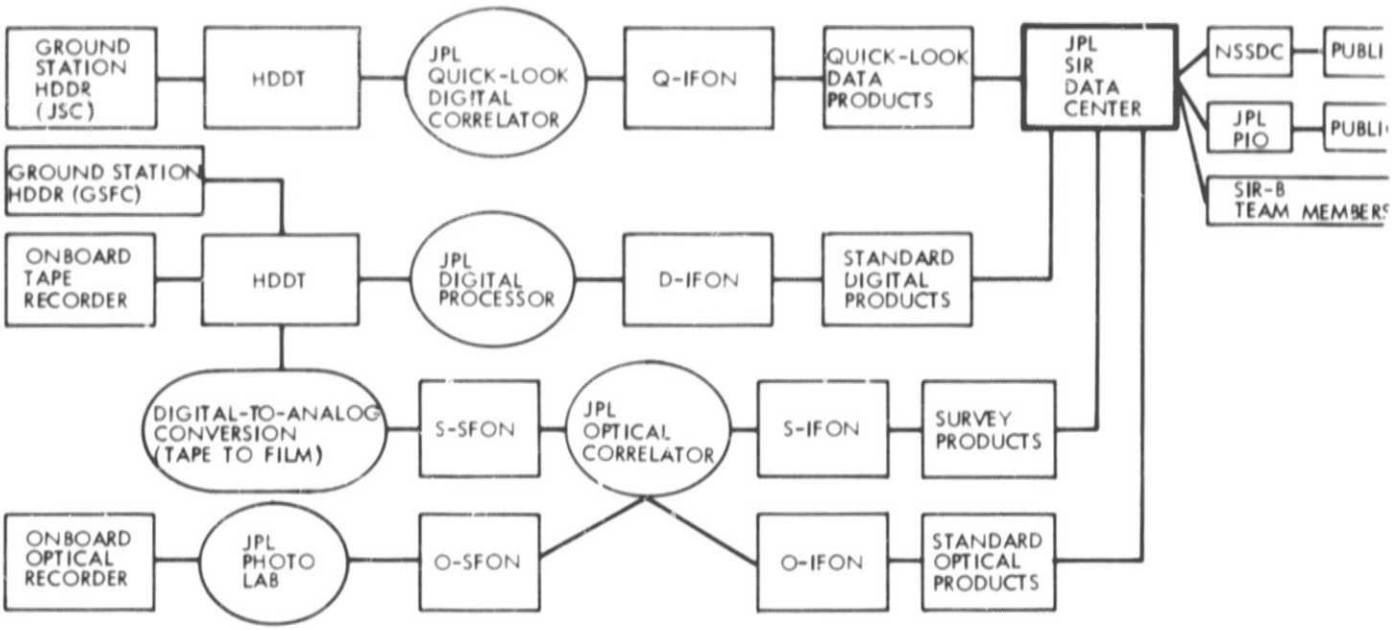

Fig. 5-1. Product flow diagram

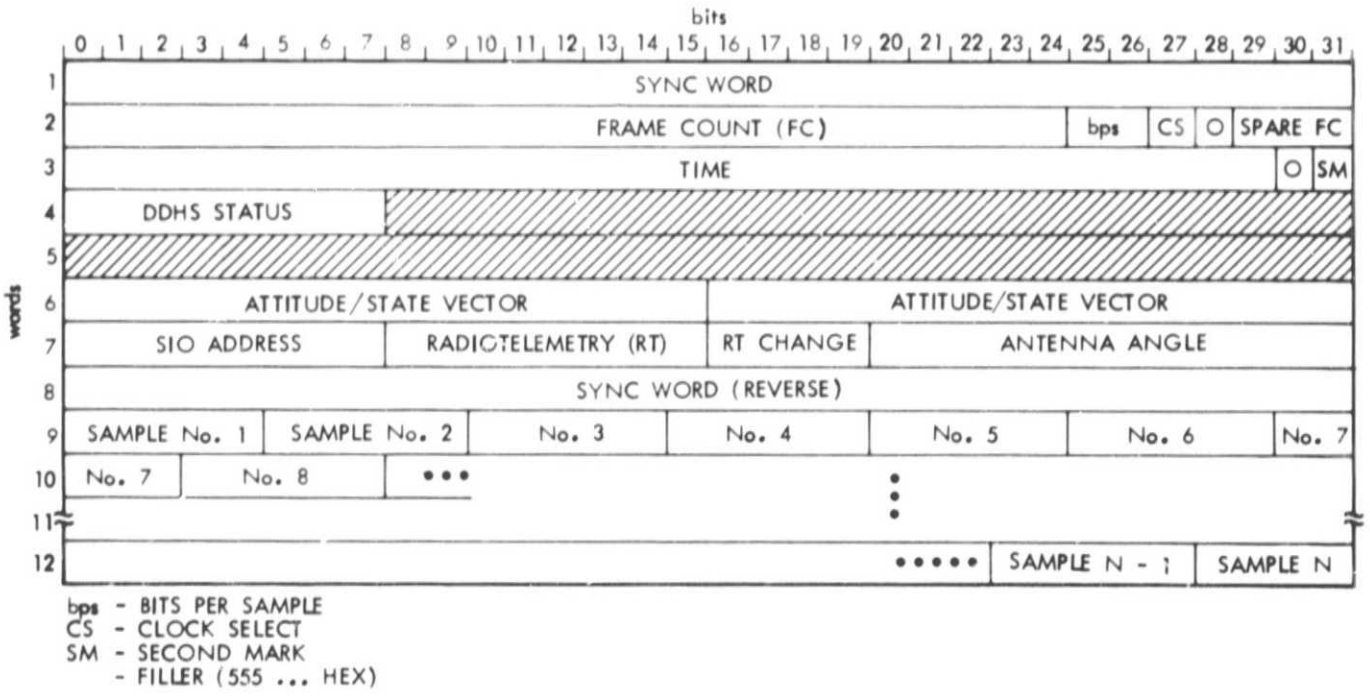

Fig. 5-2. HDDT data layout

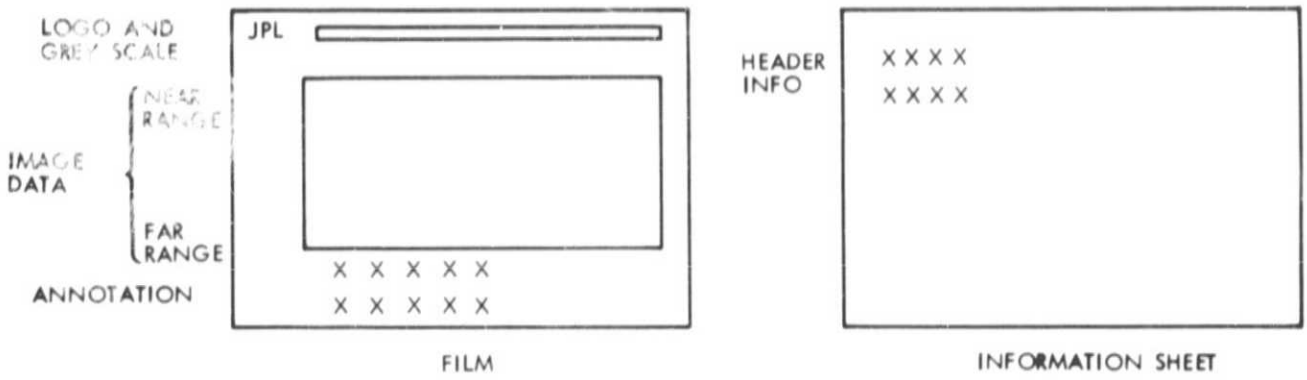

SIZE OF FILM	20 x 25 cm
SIZE OF PIXEL	25 μm
IMAGE COVERAGE	100 km x 50 km FRAME AT 1 FRAME PER FILM
No. OF PIXELS AT 12.5-m SPACING	8000 x 4000

Fig. 5-3. Digital photo product layout with supporting information sheet